Functional Characterization of Novel Human Gut Bacteria Involved in the Metabolism of Sulfur and Trimethylamine

Yuan Feng

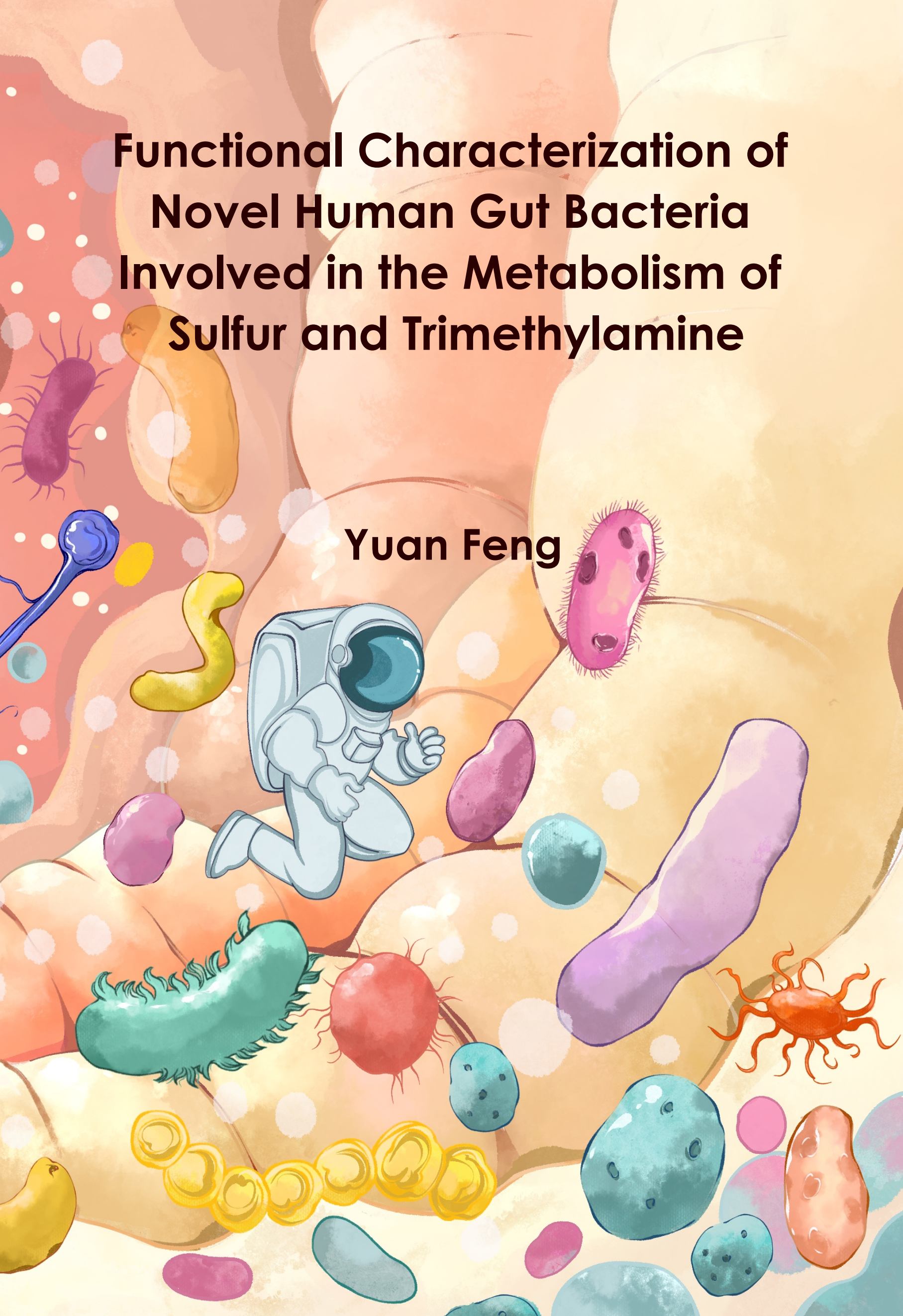

Propositions

1. The microcompartments of *Eubacterium maltosivorans* play a crucial role in linking the demethylation of trimethylamine to the one-carbon fixation pathway.
   (this thesis)
2. The impact of organic sulfur compounds on the bacterial sulfur metabolism in the human gut is underestimated.
   (this thesis)
3. The greatest value of plant-based meat analog products is offering ethical alternatives.
4. Using the term 'biome' to describe a person is a correct approach that embraces the evolving spectrum of individual identities.
5. Specialization within the education system promotes unawareness.
6. The fact that only ordinary Chinese individuals arrange their names in a Western manner is a sign of power disparity.
7. Diligence is a virtue that is overestimated in Chinese culture.

Propositions belonging to the thesis, entitled

Functional characterization of novel human gut bacteria involved in the metabolism of sulfur and trimethylamine

Yuan Feng

Wageningen, 20th March 2024

Functional characterization of novel human gut bacteria involved in the metabolism of sulfur and trimethylamine

Yuan Feng

Thesis committee

Promotors

Prof. Dr W.M. de Vos
Emeritus Professor of Microbiology
Wageningen University & Research

Prof. Dr A.J.M. Stams
Emeritus Personal chair at the Laboratory of Microbiology
Wageningen University & Research

Co-Promotor

Dr I. Sánchez-Andrea
Assistant professor at the Laboratory of Microbiology, Wageningen University & Research
Assistant Professor at Environmental Science & Sustainability Department, IE School of Science & Technology, Spain

Other members

Prof. Dr T. Abee, Wageningen University & Research
Dr H.J.M. Harmsen, University of Groningen
Prof. Dr A. Loy, University of Vienna, Austria
Dr H. Tytgat, Nestlé Research, Switzerland

This research was conducted under the auspices of the Graduate School for Socio-Economic and Natural Sciences of the Environment (SENSE)

Functional characterization of novel human gut bacteria involved in the metabolism of sulfur and trimethylamine

Yuan Feng

Thesis

submitted in fulfilment of the requirements for the degree of doctor
at Wageningen University
by the authority of the Rector Magnificus,
Prof. Dr C. Kroeze,
in the presence of the
Thesis Committee appointed by the Academic Board
to be defended in public
on Wednesday 20 March 2024
at 1:30 p.m. in the Omnia Auditorium.

Yuan Feng

Functional characterization of novel human gut bacteria involved in the metabolism of sulfur and trimethylamine

192 pages

PhD thesis, Wageningen University, Wageningen, The Netherlands (2024)

With references, with summary in English

DOI:10.18174/649727

Table of Contents

Chapter 1: General introduction and thesis outline

The human gut is colonized by large communities of mainly anaerobic bacteria that play a role in a myriad of metabolic conversions that contribute to health and disease. These include the metabolism of sulfur-containing components and trimethylamine (TMA) that have attracted considerable attention in recent years (de Vos *et al.*, 2022). Here an introduction is provided into the roles of anaerobic bacteria have in the metabolism of these compounds. Specific attention is given to gut bacteria and their potential impact on human health.

Sulfur and biological sulfur importance in a nutshell

Sulfur is a chemical element with the symbol S and atomic number 16. It has an average atomic mass 32.06 occurring in group 16 and period 3 of the periodic table. The availability of orbitals for bonding allows S to have eight different valences from +6 to -2. The range of oxidation states at which sulfur can exist also allows it to form numerous oxyanions, ranging from the most oxidized and stable forms (sulfate) to the most reduced state (sulfide) (Table 1). Furthermore, the ability of sulfur to concatenate and form oxyanion yields a series of acids, including bisulfite (HSO_3^-), pyrosulfite ($S_2O_5^{2-}$), trithionate ($S_3O_6^{2-}$), tetrathionite ($S_4O_4^{2-}$), tetrathionate ($S_4O_6^{2-}$), and beyond (Suzuki, 1999). Sulfur at oxidation states below +6 is unstable and the free energy from further oxidation is high. Thus, compounds at intermediate oxidation states can undergo both oxidation and reduction reactions.

Table 1. Oxidation states of example sulfur oxyanion compounds and their Gibbs free energies of formation values from elemental sulfur. Values are taken from [a] Kelly, 1999 and [b] Williamson and Rimstidt, 1992

Oxidation state	Example of compounds	Formula	Gibbs free energy of formation (ΔG_f^0 as kJ mol^{-1})
+6	Sulfate	SO_4^{2-}	-744.6[a]
+5	Dithionate	$S_2O_6^{2-}$	-596.7[b]
+4	Sulfite	SO_3^{2-}	-486.6[a]
+4	Pyrosulfite	$S_2O_5^{2-}$	-781.4[b]
+3	Dithionite	$S_2O_4^{2-}$	-600.3[b]
+2	Thiosulfate	$S_2O_3^{2-}$	-513.4[a]
0	Sulfur	S	
-2	Sulfide	S^{2-}	-85.8[a]

Sulfur is an essential element with biological importance across living species. In the chemistry of life, sulfur is one of the core elements needed for biochemical functioning as sulfur containing compounds play a major role in signal transduction and enzyme action (Janaky *et al.*, 1999; Sen, 2001; Richter, 2013). For instance, cysteine and methionine contribute to life as building blocks in proteins and they are the only two sulfur-containing amino acids in proteins.

The most distinctive role of cysteine in proteins lies in its ability to form a disulfide linkage with another cysteine residue, thus providing a stabilizing part of a folded protein (Brosnan and Brosnan, 2006). In bacteria, proteins with disulfide linkage are involved in important cellular activities such as cell division, transport of molecules, and assembly of the outer membrane of Gram-negative bacteria (Hiniker and Bardwell, 2004; Kadokura *et al.*, 2004). Methionine initiates protein synthesis as it is coded by a start codon in nuclear genes of eukaryotes and in *Archaea* (Schmitt *et al.*, 2019). In bacteria, protein synthesis is started by N-formylmethionine, which is a methionine derivative with a formyl group added to the amino group (Adams and Capecchi, 1966). Furthermore, methionine and cysteine serve as precursors for synthesis of glutathione (GSH), S-adenosyl-methionine (SAM), co-factors (e.g. coenzyme A, iron-sulfur proteins, heme, siroheme, molybdenum centers *etc.*), essential vitamins (biotin, thiamine), and beyond (Kessler, 2006).

Soluble sulfates in oceans, lakes, rivers and soil are readily available to plants, algae and microorganisms to assimilate organic sulfur compounds and used as precursors for anabolic processes. Inorganic sulfate is firstly converted to sulfide then incorporated into a nitrogen/carbon skeleton to form organic sulfur compounds, cysteine or homocysteine. In plants and microorganisms, methionine can be further biosynthesized from cysteine or homocysteine, while in vertebrates methionine *de novo* synthesis is absent (Finkelstein, 1990). Another vital sulfur-containing organic compound is taurine, especially for animals. It is virtually absent from plants and microorganisms, but is widely distributed in the animal kingdom, with relatively high concentrations in all mammalian and avian tissues (Chesney, 1985). Though commonly mentioned as a sulfur-containing amino acid (SAAs), strictly speaking taurine is not an amino acid but a sulfonic acid with an amino head, as indicated by its nomenclature name 2-aminoethanesulfonic acid. Chemical structures of the aforementioned SAAs and taurine are demonstrated in Figure 1.

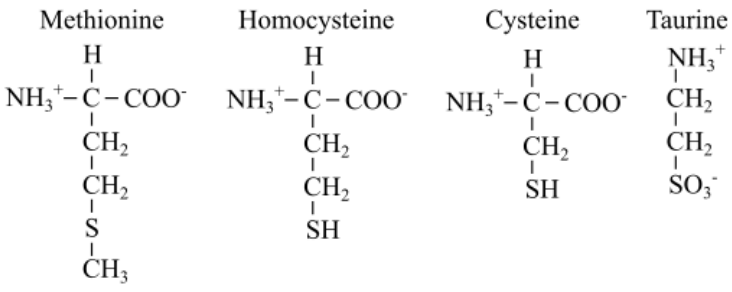

Figure 1. Chemical structures of the common sulfur-containing amino acids and taurine (Brosnan and Brosnan, 2006).

Importance of sulfur and sulfur-containing amino acids in the metabolism in human body

Sulfur is an essential element in human body. Following calcium and phosphorus, sulfur accounts for the third most abundant mineral in the human body, representing ~0.3% of total body mass and almost always is present in the form of organosulfur compounds or metal sulfides (Ziegler and Filer Jr, 1996; Parcell, 2002; Sundaravelu *et al.*, 2021). In healthy adults protein mass counts 14 to 16% of body mass (Wu, 2009); methionine and cysteine count 3 to 6% as the building blocks in proteins (Nimni *et al.*, 2007). Our outer skin and hair are rich in disulfide bonds formed by two cysteines, providing mechanical strength and insolubility of the protein keratin (Fraser *et al.*, 1988). The amino sulfonic acid taurine is also abundant in many human tissues and functions generally as an osmolyte. For instance, 15-20, 28-40, 20-35, and 20-35 mM taurine are found in human skeletal muscle, heart, retina, and placenta, respectively (Fukuda *et al.*, 1982; Schuller-Levis and Park, 2003; Wu, 2020). Furthermore, taurine plays critical roles in bile acid conjugation, central nervous system and muscle development, and are proposed to act as an antioxidant and neurotransmitter (Zachmann *et al.*, 1966; Burg and Ferraris, 2008; Wu and Prentice, 2010; Baliou *et al.*, 2021).

Like other higher animals, humans are unable to assimilate organic sulfur compounds from inorganic sulfur (Griffith, 1987; Francioso *et al.*, 2020). Thus, sulfur acquisition is crucial to humans via food. The gastrointestinal (GI) tract serves a key function in the digestion of dietary protein and absorption of amino acids. After methionine has been absorbed and transferred to different body tissues by blood stream, cysteine can be formed via the enzymatic processes of transmethylation and trans-sulfuration of methionine (Figure 2) (Finkelstein and Martin, 2000). This process requires an adequate source of methionine and serine precursors, and depends on the availability of vitamin B12 and B6 (Froese *et al.*, 2019; Stach *et al.*, 2021). The synthesis of taurine derives from the trans-sulfuration pathway, originating from methionine, and primarily takes place in the liver (Poloni *et al.*, 2015). The rate-limiting step in taurine biosynthesis is the decarboxylation of cysteine sulfinic acid by cysteine sulfinate decarboxylase, an enzyme whose activity varies considerably among species and probably with age (Sturman and Hayes, 1980; Worden and Stipanuk, 1985). This explains why taurine is also found in the milk of mammals (e.g., 0.4 mM in human, 0.8 mM in mouse, and 2.8 mM in cats), and is regarded as a physiologically essential nutrient for infants being therefore added in the infant formula (Sturman, 1993).

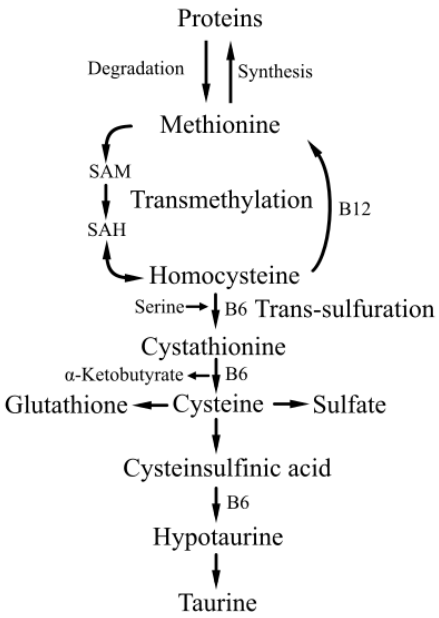

Figure 2. Simplified sulfur containing amino acids metabolite pathway in human. SAM: S-adenosylmethionine; SAH: SAH: s-adenosyl homocysteine. Adapted from Poloni *et al.*, 2015.

The human gut microbiome and health

A human being is never alone—since birth, we are colonized by microbes inside and outside, from head to toe that together with their genes and products constitute our microbiome. While all body sites are colonized, the majority of microbes are found in the gut that forms an exquisite ecosystem with predominantly (anaerobic), bacteria but also archaea, fungi and viruses (Figure 3). Together with daily food intake, millions of oral, saliva and food microbes are swallowed and then challenged by many factors to survive through each region of the gut, including the acidity of the stomach, the production of bile acids, digestive enzymes and antimicrobial proteins in the duodenum. After passing through the small intestine, digestible nutrients like simple carbohydrates, proteins and fat are broken down to sugar molecules, amino acids and lipids, and the majority of these is absorbed.

The complex carbohydrates, which are poorly degradable for human enzymes, are the major components arriving the colon. However, depending on the intake level, protein and fat can escape the ileal absorption and reach the colon as well. Due to the different physiological functions, microbial colonization in different regions of human gut varies considerably, with the highest density of microbes found in the colon that is highly anaerobic. Owing to the developments in molecular and sequencing technologies, considerable insight is accumulating on the gut microbial diversity that includes over 1000 species predominantly belonging to the

phyla *Firmicutes*, *Bacteroides*, *Actinobacteria*, *Proteobacteria*, and *Verrucomicrobiota*, (de Vos *et al.*, 2022).

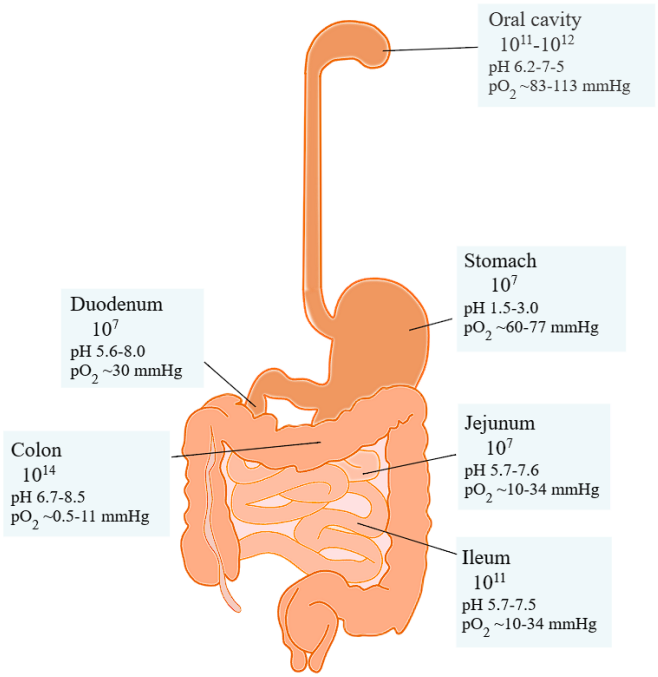

Figure 3. Luminal concentrations (cells/gram) of microbes, pH, and oxygen concentrations in various regions of the human gastrointestinal tract. Adapted from de Vos *et al.*, 2022.

In the colon, fermentation of complex carbohydrates into different SCFAs molecules (e.g. acetate, butyrate and propionate) is one of the most important microbial processes. The produced SCFAs can nourish the epithelium cells locally in the gut, furthermore, they can regulate metabolic pathways distantly in the liver, the adipose tissue, the muscles and the brain (Canfora *et al.*, 2015; Dalile *et al.*, 2019; Rastelli *et al.*, 2019). The health benefits brought out by administration of probiotics, prebiotics as well as symbiotics have been extensively studied in the past few decades and were summarized in several recent reviews (Calero *et al.*, 2020; Zommiti *et al.*, 2020; Pujari and Banerjee, 2021). The gut microbiome has been well recognized as one of the key elements influencing the health status of the host. It has significant roles in training host immunity, regulating gut endocrine function and neurological signaling, modifying drug action and metabolism, and producing numerous compounds that impact the host (de Vos *et al.*, 2022).

Many factors can influence the gut microbiome, including mode of birth, the genetics of the host, aging, medication, diet, lifestyle. Among others due to high level of urbanization and overeating of processed high-energy food, a considerable population in developed

countries has chronic metabolic disorders such as obesity, insulin resistance, type 2 diabetes, cardiovascular disease, inflammatory bowel diseases (IBDs) and irritable bowel syndrome (IBS). As urbanization and globalization continues, the evolution of the chronic metabolic disorders follows the advancement of society. From millennium, many such disorders were reported increasing in developing countries in Asia, the Middle East, and South America (Nugent, 2008; Ahuja and Tandon, 2010; Prideaux *et al.*, 2012; Malekzadeh *et al.*, 2016). Despite the differences in pathologies of chronic metabolic disorders, abnormalities in the composition and function of the intestinal microbiota are commonly observed (Vijay and Valdes, 2022). Microorganisms that are considered to contribute to intestinal disorders like IBDs and IBS, include sulfate-reducing bacteria (SRB) since these may be involved in the process of bowel inflammation due to the production of hydrogen sulfide (H_2S), which is a potent toxic gas (Jia *et al.*, 2012; Figliuolo *et al.*, 2017). Microbial sulfate reduction was described and studied a century ago (Beijerinck, 1895; Baars, 1930) and subsequently sulfate-reducing microorganisms have been recognized to play an important part in the sulfur cycle in nature (Bunker, 1936; Schouten, 1946; ZoBell, 1946). Yet SRB were only isolated from the human gut in the late 1970s (Moore *et al.*, 1976).

Compared to the luminal hydrolysis of undigested carbohydrates into monosugars and subsequent fermentation into SCFAs, the intestinal microbial sulfur metabolism has received less attention. This can be considered an omission since sulfur compounds are crucial for human health, and both organic and inorganic sulfur compounds are caron and energy sources for gut microbes. In the following sections, we will first discuss how sulfur compounds derive from both common daily food intakes and endogenous secreta (mucin and bile acids), and then illustrate the known microbial sulfur metabolic pathways with model bacteria.

Sulfur containing compounds intaking by daily food

Organic sulfur compounds

Food is an important source of sulfur-containing compounds that are mostly present in organic form, among which the SAAs (methionine and cysteine) and taurine are the most abundant. In general, the number of SAAs in dietary proteins does not exceed 5% of the total amino acids. Among plant proteins, cereals contains 3% to 5% SAAs of the total protein, while for legumes the SAAs contents amounts to 2% to 3.5% (Bos *et al.*, 2009). Food from animal sources generally bring slightly higher amounts of SAAs compared to that from vegetable origin. For instance, milk proteins contain 3.6% SAAs and egg protein is over 5% (Bos *et al.*, 2009). Beef and fish protein contain around 4% SAAs while poultry protein contains approximately 2.9% (Bos *et al.*, 2009). The up-to-date SAAs of common foodstuffs are provided on the FoodData Central webpage of the US Department of Agriculture for agricultural research service (https://fdc.nal.usda.gov/index.html).

Published reports on dietary taurine content were limited before 1970s, as the physiological and nutritional importance of taurine was not revealed till the late 1960s (Jacobsen and Smith, 1968). Moreover, there was a limitation in the measuring method, as the amino acid content in foods was generally determined by measuring methionine and cysteine in their hydrolysates. Afterwards, dietary taurine contents were measured and published in a few studies but there was a significant amount of variability between similar samples mainly due to differences in sample preparation methods (Roe and Weston, 1965; Laidlaw *et al.*, 1990; Spitze *et al.*, 2003). However, a few important trends could be noticed. First, most plant-derived proteins, including fruits, grains, legumes, nuts, seeds and vegetables do not contain taurine. Interestingly, taurine was found in seaweeds, some fungi and yeasts (Spitze *et al.*, 2003). Second, seafoods in general have higher amount of taurine comparing to meat of terrestrial animals, especially shellfish (oyster, clam, scallop and mussel), squid and white fish that contain up to 8 g taurine per kilogram of wet weight (Spitze *et al.*, 2003). Among the food from terrestrial animals, poultry including turkey and chicken have the highest taurine content compared to pork and beef. Perhaps not used by everyone, but an energy drink is an highly important source of taurine for certain populations, such as teenagers and sport enthusiasts. One bottle (250 ml) of common commercial energy drink (e.g. Red Bull, Monster, Rockstar) contains 1g of taurine.

Another type of organic sulfur compound that caught the attention of gut microbiologists in the recent years is sulfoquinovosyl diacylglycerol (SQDG) that was first described in 1959 (Benson *et al.* 1959). SQDG constitutes a class of compounds with a high diversity of the diacylglycerol backbone but shares a sulfonic acid head group referred to as sulfoquinovose (6-deoxy-6-sulfoglucose, SQ). SQDG is one of the three non-phosphorous glycolipids that form the main part of the structural lipids in the thylakoid membranes of photosynthetic organisms of all land plants, algae, dinoflagellates, and cyanobacteria (Benning, 1998). SQDG can comprise greater than 25% of the total lipids in common leafy green vegetables (Benning, 1998). Owing to its distribution in plants, a diet rich in leafy vegetables like kale, cabbage, spinach, lettuce and beet greens can increase of the amount of SQDG in the GI tract of humans. Besides, there is a growing demand for vegan nutrition and functional food nowadays. Edible algae and cyanobacterium are used as alternative nutrition sources worldwide, in which sulfolipids can count up to 33% of the total algal lipids (Antonelli *et al.*, 2019). Furthermore, it has been estimated that the worldwide market of Spirulina and Spirulina-based product is expected to show continued and rapid growth until 2028 (Masten Rutar *et al.*, 2022).

Lastly, although present in trace amounts, volatile sulfur compounds (VSC) are also a group of sulfur compounds we receive via food intake. The VSCs provide special aroma and flavors to foodstuffs and beverages, which make people either excited for or keep distance to. Some fruits and vegetables naturally contain higher volatile sulfur compounds, especially tropical fruits like dourine, mango, passion fruits (Cannon and Ho, 2018). Vegetables like cauliflower, cabbage, garlic and onions are known to have strong odors and aromas that not everyone is a fan of. This is also due to VSCs such as methionol, dimethyl sulfide (DMS), dimethyl disulfide (DMDS), dimethyl trisulfide (DMTS), allyl (poly)sulfides, ajoenes (McGorrin, 2011). The VSCs are especially important for fermented foods like cheese and beverages like wine and beer, as the composition and concentration of VSCs impart essential sensorial properties to the final product. For instance, both DMS and DMTS could contribute to the distinctive taste of several beers (Gijs *et al.*, 2000; Hansen *et al.*, 2002). When present at higher concentration than their perception thresholds, sulfide, ethanethiol, and methanethiol have a major negative impact on the wine aroma, while DMS and methionol contribute positively the wine aroma (Smith *et al.*, 2015).

Inorganic sulfur compounds

As industrialization is spreading over the world, packaged food and beverage products have potentially unwittingly become an essential part of everyone's life. To extend the shelf-life and to maintain the nutritional characteristics of the products, different preservation techniques are applied, including pasteurization, freezing, drying, lactic acid and other fermentations and adding preservatives. Preservatives can be mainly divided into two groups based on their purpose of their usage, one group has antimicrobial function such as lactic, propionic and other acids while the other group includes antioxidants. Sulfur oxides, which have multifunctional effects due to their chemical reactivity, have a long history of being employed as a food preservatives. It was documented that the ancient Romans knew "vapor of sulfur" as an improving agent for wine (Lück and Jager, 1997, from Plinius, Naturalis historia XlV). Nowadays, salts of sulfur oxides are still commonly used in food and beverages industries. This group of compounds is recognized as common food additive by European Food Safety Authority (EFSA) and have received E-numbers including gaseous sulfur dioxide, E220; sodium sulfite, E221; sodium bisulfate, E222; sodium metabisulphite, E223; potassium metabisulphite, E224; calcium sulfite, E226; calcium bisulfate, E227; potassium bisulfate, E228 (EFSA, 2016). Because of their antimicrobial and antimycotic effects, sulfites are among the most used food additives for the control of spoilage microorganisms in fruits, vegetables and meat products resulting in an extended shelf-life (D'Amore *et al.*, 2020; Bensid *et al.*, 2022). Sulfites are also added in beverages and some other low pH products, to prevent the growth of yeasts and molds rather than bacteria without introducing food-poisoning risks (Rhem, 1964). Besides, sulfite is also employed to prevent enzymatic and non-enzymatic oxidative browning reactions. Its various functions as a food additive makes it also an excellent bleaching agent, color stabilizer, vitamin C satabilizer, and an improvement agent for flour (Gould and Russell, 2003). Sulfites and sulfur dioxides (E 220–228) are authorized in over 40 food categories in the EFSA Regulation (EC) No 1333/2008 with maximum permitted level ranging from 20 to 2,000 mg/kg. Dried fruits such as apricots, peaches, grapes, prunes and figs and concentrated grape juice for home wine making have the highest added sulfites of 2 g/kg, followed by sausages and burger meat of 450 mg/kg.

Endogenous sulfur sources

Mucus layer and mucus derived sulfate

The entire gut epithelium is covered by mucus as a protection barrier for the damage caused by food, digestive proteases, pathogens, toxins and beyond (Deplancke and Gaskins, 2001). Additionally, the mucus layer also functions as a lubricant for passing food particles, as a selective barrier for nutrients passage to epithelial cells, and as a niche for commensal bacteria. It is now established that the ability to graze on mucin glycans as a carbon source gives bacteria a competitive advantage to colonize the mucus layer (Schroeder, 2019).

The colon is covered by the thickest mucus layer composed dominantly by mucin 2 (MUC2), with an inner layer that is dense and firmly attached to the epithelium and a loose, viscous, and hydrated outer layer. MUC2 is a high-molecular-weight glycoprotein containing up to 80% glycans by mass, with more than 100 different glycan structures linked to serine or threonine by O-glycosidic linkages (Holmén Larsson *et al.*, 2009) (Figure 4). Moreover, the N- and C-terminal of MUC2 structures are less glycosylated and rich of cysteine domains, which are involved in mucin polymerization by forming disulfide bonds (Gum *et al.*, 1992).

Mucin glycosylation is variable along the GI tract, with an increase in sulfation in the colon especially in the distal colon (can reach up to 100% sulfation), and then slightly diminished (75% sulfation) moving further to the rectum (Croix *et al.*, 2011). A level of 2.0 to 6.5 g of sulfate per 100 g of mucin in the distal colon has been recorded (Podolsky and Isselbacher, 1983; Irimura *et al.*, 1991). Sulfation of mucins makes them less feasible to degradation by bacterial glycosidases, and thus the protective fence is thought to remain more intact. The O-linked sulfate may be attached to the 3-hydroxyl and 6-hydroxyl of N-acetyl-glucosamine(GlcNAc), and terminal galactose (Gal) sugars at hydroxyl positions 3, 4 or 6 of the glycan sugars, leading to the formation of GlcNAc-3-sulfate, GlcNAc-6-sulfate, Gal-3-sulfate, Gal-4-sulfate and Gal-6-sulfate, respectively (Robbe *et al.*, 2003; Holmén Larsson *et al.*, 2009) (Figure 4). Degradation of sulfated mucins requires members of the human gut microbiome to express appropriate sulfatases, which are also termed as carbohydrate sulfatases, glycolsulfatases or mucin sulfatases, to remove sulfation caps allowing further access to O-glycan sugars (Wright *et al.*, 2000; Rho *et al.*, 2005). An alternative strategy has been found in *Bifidobacterium bifidum*, one of the mucin degrading specialists, in which a sulfoglycosidase removes sugars with sulfate attached (Katoh *et al.*, 2017).

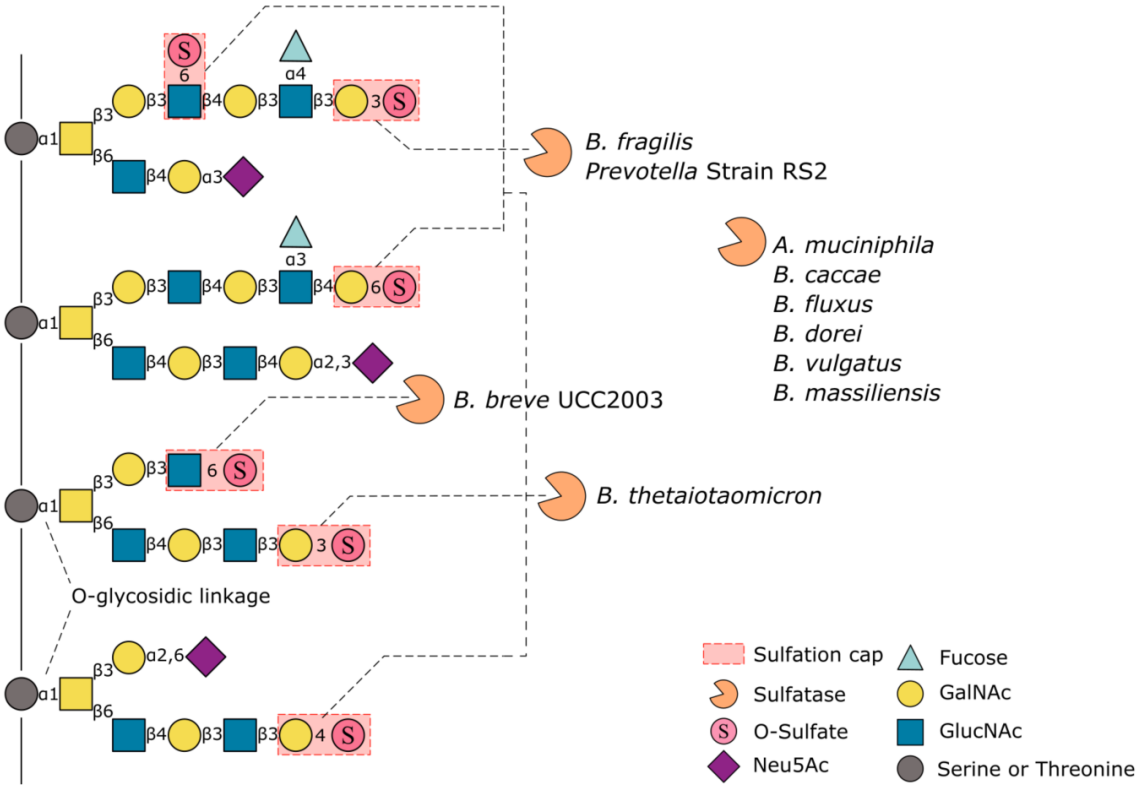

Figure 4. The main structural features of a model mucin O-glycan chain with O-sulfate terminal epitopes highlighted (pink dashed box). Bacterial sulfatases have been found to release sulfate from their specific substrates and are indicated. Bacteria listed in the figure belong to genera *Bacteroides*, *Akkermansia*, *Bifidobacterium* (for *B. breve*) and *Prevotella* strain RS2. GalNAc: N-acetyl-D-galactosamine, GlcNAc: N-acetyl-glucosamine; Neu5Ac: N-acetylneuraminic acid. Adapted from Luis *et al.*, (2021).

Many mucin degraders possess abundant sulfatases in their genomes. *Akkermansia muciniphila* is a mucin glycan degradation specialist and therefore considered as a keystone member of the mucus-associated microbiome. There are 12 sulfatases encoded in its genome and in a comparative proteomic study it was shown that 6 of these were significantly upregulated when grown with mucin in comparison with glucose (Ottman *et al.*, 2017). Colonic O-glycan degraders with a rich reservoir of sulfatases also include *Bacteroides fragilis*, *B. thetaiotaomicron*, *B. caccae*, *B. fluxus*, *B. vulgatus*, *B. dorei*, *B. massiliensis*, *Bifidobacterium breve*, and beyond (Luis *et al.*, 2021). Noteworthy to mention is that sulfatases are substrate specific, as revealed from the sulfatases of a few bacteria that were studied. It was discovered that sulfatases in *Prevotella* sp. strain RS2 and *B. fragilis* can release sulfate from GlcNAc-6-sulfate, Gal-3-sulfate and Gal-6-sulfate, but neither from GlcNAc-3-sulfate or Gal-4-sulfate (Wright *et al.*, 2000). On the other hand, *B. breve* UCC2003 can only release sulfate from GlcNAc-6-sulfate (Egan *et al.*, 2016). Previous reports have shown that *B. thetaiotaomicron* has a strong ability to grow on highly sulfated mucin oligosaccharides and recently it was

shown that the active sulfatases in *B. thetaiotaomicron* are capable of removing sulfates from all the above mentioned sulfation points of the glycan sugars in mucins (Luis *et al.*, 2021).

Bile acids and bile derived taurine and sulfate

Another important endogenous source of sulfur is derived from conjugated bile acids, predominantly in the form of bound taurine and in small amounts of sulfate. Bile acids are the major organic compounds in bile juice, which is a digestive fluid that facilitates digestion and absorption of lipids and fats nutrients. In brief, the human primary bile acids, cholic acid and chenodeoxycholic acid are synthesized in the liver from cholesterol (Figure 6). Then, primary bile acids are conjugated with either glycine or taurine with the ratio about 3:1 to form bile acids, and are further stored and concentrated in the gallbladder (Camilleri, 2022). After consumption of a meal, bile acids are released into the duodenum and form micelles which help dissolving and transporting fat soluble nutrients to the mucosa of the small intestine. About 90% to 95% of total bile acids are reabsorbed in the ileum and are transported back to the liver via portal blood circulation. The escaped bile acids (400 to 800 mg daily), leading to 2-10 mM bile acids concentrations in colon, are modified intensively by gut microbes via deconjugation and subsequent dehydroxylation reactions, resulting in a broad range of secondary bile acids (Northfield and McColl, 1973; Guzior and Quinn, 2021).

Biotransformation of bile acids in the gut occurs in distal ileum, starting with bacterial bile salt hydrolases which hydrolyze the amide bond between the bile acids and taurine or glycine (Jones *et al.*, 2008). The released taurine is further metabolized predominantly by *Bilophila wadsworthia*, for which the taurine degradation pathway will be explained later in detail. The bile salt hydrolase can be found in numerous commensal human intestinal bacteria and archaea. For instance, Gram-positive intestinal bacteria including *Clostridium*, *Enterococcus* and *Bifidobacterium*, *Lactobacillus*, Gram-negative *Bacteroides, Stenotrophomonas* and *Brucella*, and Archaea *Methanobrevibacter* and *Methanosphera* were found to encode BSH (Guzior and Quinn, 2021). The generated free bile acids are then converted by bacterial 7α-dehydroxylase to secondary bile acids, including deoxycholic acid (DCA) and lithocholic acid (LCA) (Funabashi *et al.*, 2020).

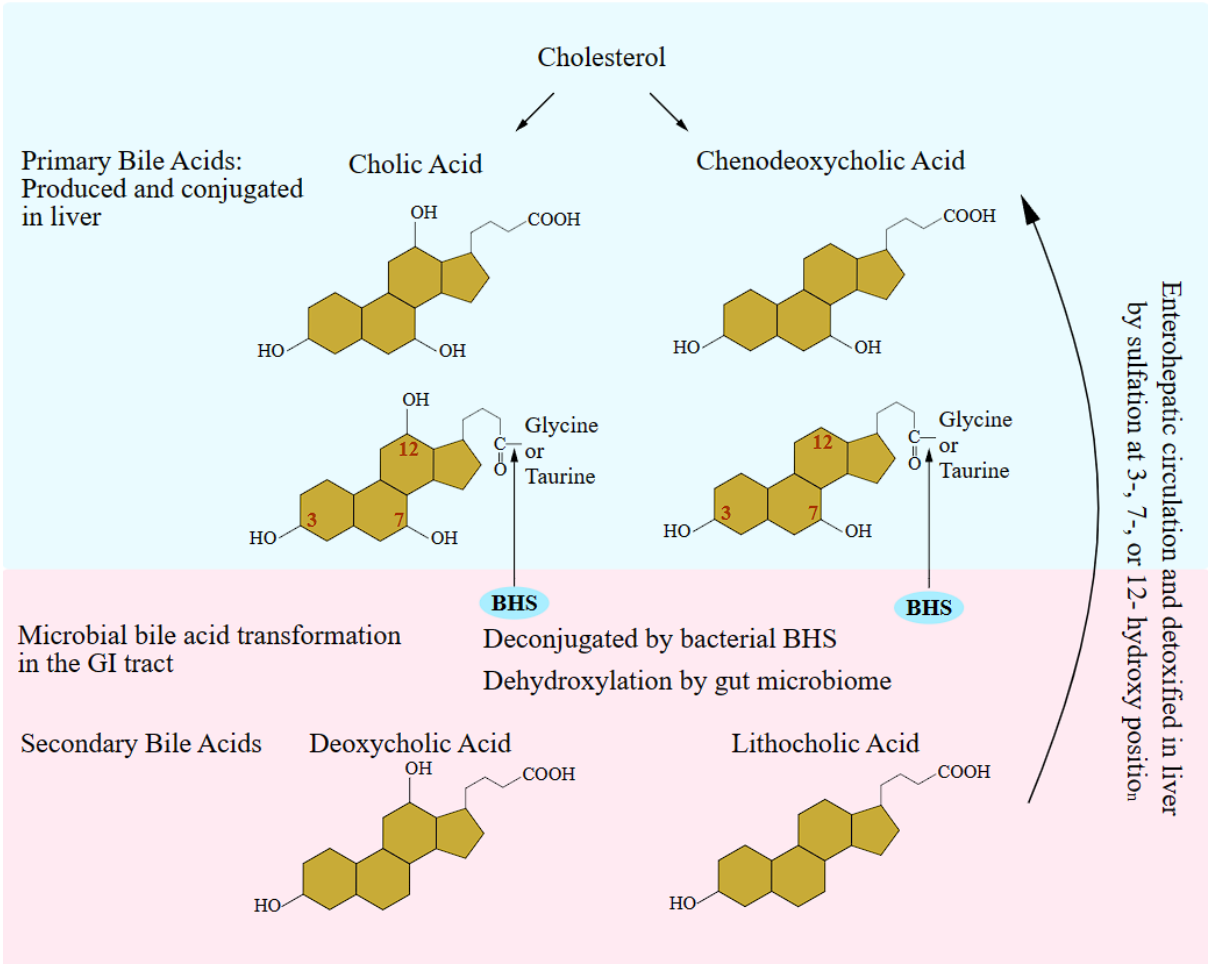

Figure 5. Simplified bile acids metabolism including bile acids production, microbial bile acid transformation, and enterohepatic circulation in human. BSH: bile salt hydrolases.

The enterohepatic circulation in human is highly efficient and a high concentration of bile acids might be hepatotoxic. Consequently, these are detoxified predominantly by liver cytosolic bile acid sulfotransferase with an addition of sulfonate group ($-SO_3^-$). The sulfation can occur at three different positions (3-, 7-, or 12- hydroxy position) of the bile acid structure (Figure 6) (Alnouti, 2009). Afterwards, the sulfated bile acids are excreted into gallbladder, duodenum and ileum as described previously. In general it is believed that the sulfated bile acids are poorly reabsorbed from the gut, as most of them are excreted through feces and urine (Camilleri, 2022). Nevertheless, it was reported in the early 80s that human gut microbes can de-sulfate sulfated bile acids with the formation of a variety of metabolites (Huijghebaert *et al.*, 1984). In this study, fecal samples of healthy volunteers on a Western diet were collected and incubated both anaerobically and aerobically with bile acid 3-, 7- and 12- monosulfate. Anaerobic fecal incubation lead to desulfation of 3-sulfate esters of chenodeoxycholic acid, cholic acid and allochenodeoxycholic acid, and in contrast, the 7- and 12-sulfate isomers were not desulfated and were not transformed into secondary bile acids (Huijghebaert *et al.*, 1984).

However, no molecular analysis were involved to indicate the enriched fecal bacteria, but earlier studies from Borriello and Owen (1982) reported that several *Clostridium* species have bile salt sulfatase activity on 3-sulfate lithocholic acid.

Gut microbiome sulfur metabolism

Whereas the gut is highly efficient in digesting dietary and endogenous proteins, still a significant proportion of luminal undigested and partially digested proteins undigested proteins and peptides (~12 g/d) can reach the colon which are transferred from small intestine to the large intestine (Gibson *et al.*, 1976). It was also estimated that 20% and 25% of dietary methionine and cysteine is metabolized in the gut (Bauchart-Thevret *et al.*, 2009), but due to the high metabolic activity of the intestinal ecosystem, the concentration of free methionine in the colon is rather low (Ahlman, 1993). Daily dietary inorganic sulfur intake is estimated to range from 2 to 9 mmol approximately (Dordević *et al.*, 2021). Hydrogen sulfide, the end product of many microbial metabolic pathways of sulfur compound, commonly present in the gut with a concentration of 1.0 to 2.4 mM (Blachier *et al.*, 2010). Moreover, according to a review summarized the Human Metabolome Database (HMDB) results, 620 different sulfur-containing metabolites were detected in serum, urine, cerebrospinal fluid, saliva and feces of the healthy donors (Karu *et al.*, 2018; Wishart *et al.*, 2018). Collectively, there is solid evidence that gut microbiomes have a pivotal role in sulfur metabolism. The major metabolic pathways and the representative bacteria genera are briefly shown in Figure 6, with detailed illustrations of each pathway in the following sections.

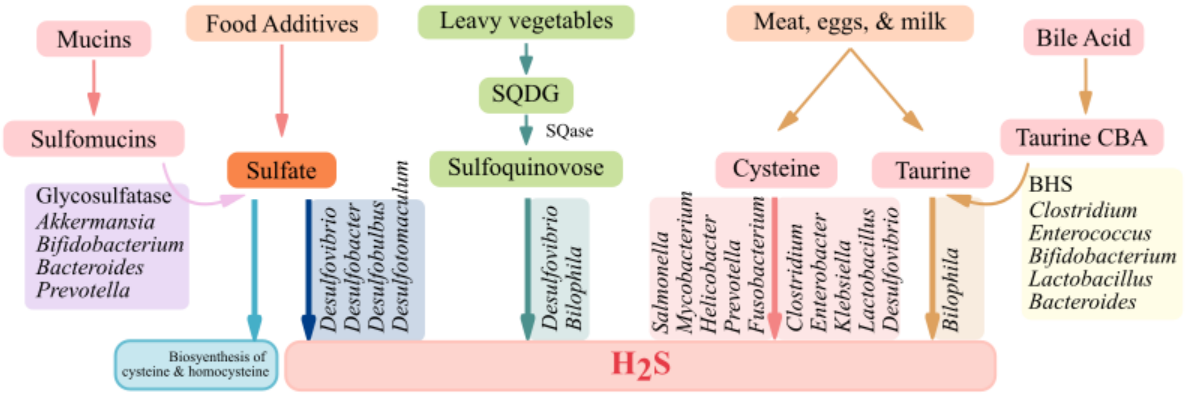

Figure 6.Human gut microbiome sulfur metabolic pathways and the corresponding bacteria. CBA: conjugated bile acids. Data summarized from Peck *et al.* (2019), Kushkevych *et al.*, (2020) and Luis *et al.*, (2021).

Sulfate reduction: Assimilatory and Dissimilatory Pathway

Colonic sulfate can be used by the gut microbiome in two pathways: assimilatory and dissimilatory sulfate reduction. Assimilatory sulfate reduction is widespread in microorganisms and this pathway provides a mechanism by which microorganisms can reduce sulfate to satisfy assimilatory requirements (Schiff and Fankhauser, 1981). Not as common as assimilatory sulfate reduction and only restricted to a single microbial group, the SRB are capable of conducting dissimilatory sulfate reduction to conserve energy for growth with a release of a great quantity of sulfide. Nevertheless, the activation of sulfate is the same in both pathways. In this step, sulfate adenylyltransferase (Sat, also known as ATP sulfurylase) catalyzes the attachment of sulfate to a phosphate of ATP forming adenosine phosphosulfate (APS). In assimilatory sulfate reduction, APS is then phosphorylated by APS kinase to 3′-phosphoadenosine-5′-phosphosulfate (PAPS, Figure 7). Subsequently, PAPS is reduced to sulfite by PAPS reductase (CysH), and sulfite is consequently reduced by sulfite reductase (CysJI) to sulfide. The reduced sulfide is incorporated into carbon skeletons of amino acids to form cysteine or homocysteine (Brunold, 1993). Assimilatory sulfate reduction likely represents a crucial step in sulfur cycling by gut microbiome as it allows for disposal of sulfate and conversion to necessary organic sulfur compounds. However, the fraction of sulfate used for biosynthesis has not been reported yet, neither do we know the dominant microbial species which are responsible for this step.

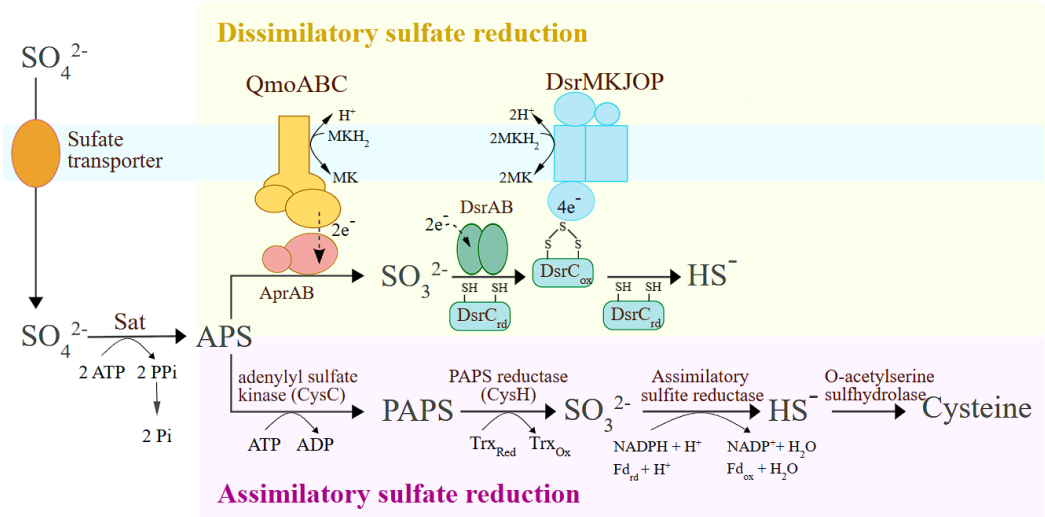

Figure 7. The dissimilatory and assimilatory sulfate reduction (DSR and ASR) pathways. After being transported into the cytoplasm, sulfate is activated by sulfate adenylyl transferase (Sat) to adenosine 5′-phosphosulfate (APS). In DSR, the APS is reduced to sulfite by APS reductase (AprAB), then to DsrC trisulfide by DsrAB/DsrC and lastly, DsrC trisulfide is reduced to sulfide by the DsrMKJOP transmembrane complex. In ASR, 3′ -phosphoadenosine-5′ -phosphosulfate (PAPS) is generated from APS with a final product of cysteine. Trx: Thioredoxin; Fd: ferredoxin. After Santos *et al.* (2015).

In dissimilatory sulfate reduction pathway, APS is reduced to sulfite and adenosine monophosphate by APS reductase (Apr) (Lampreia *et al.*, 1994) (Figure 7). The Apr (AprAB) is composed by 2 subunits, of which the α subunit is the catalytic subunit with the FAD-binding region and the β subunit is involved in electron transfer with a ferredoxin domain (Fritz *et al.*, 2000). The Apr is a cytoplasmic enzyme, thus is not directly involved in membrane-linked electron transport. It was proposed by Pires *et al.*, (2003) that a Qmo (quinone-interacting membrane-bound oxidoreductase) ABC membrane complex participates in electron flow between the quinone pool and the cytoplasm and transfers the electron donor to AprAB. Later it was shown by a comparative genomic analysis that a gene cluster containing *sat*, *aprAB* and the *qmoABC* genes is present in the majority of SRB analyzed, with the exception of the Gram-positive SRB where the *qmoC* gene is absent (Pereira *et al.*, 2011). Lastly, sulfite is reduced to sulfide by dissimilatory sulfite reductase (DsrAB) and DsrC, coupling two and four electrons reduction, respectively. Similar to AprAB, DsrAB is not a membrane-associated protein; thus the mechanism of energy conservation during sulfite reduction needed to be addressed and a transmembrane complex DsrMKJOP was subsequently discovered and proposed to be involved in the energy conservation of DsrAB reduction from *D. desulfuricans* ATCC 27774 (Pires *et al.*, 2006). With a few exceptions, the *dsrMKJOP* genes are present in Gram-negative SRB, while in Gram-positive SRB, mainly just *dsrMK* genes are present (Junier *et al.*, 2010).

Culture-based methods conducted in the early 1980s using human fecal slurries revealed that SRB belonging to the genera *Desulfotomaculum*, *Desulfobacter*, *Desulfomonas* and *Desulfobulbus* were present in the human gut, and *Desulfovibrio* types always predominated (Gibson *et al.*, 1988). These findings were confirmed later by molecular methods e.g. 16S rRNA targeted PCR, qPCR and sequencing (Stewart *et al.*, 2006; Rey *et al.*, 2013). Cultivating experiments aimed to isolate SRB from the human gut were performed mainly since the early 2000 and led to isolation of *Desulfovibrio vibrio*, *D. piger*, *D. fairfieldensis*. *D. desulfuricans* and *D. legallii* (Loubinoux *et al.*, 2003; Vasoo *et al.*, 2014).

Taurine metabolism

The best known taurine degradation pathway in the human gut microbiome is carried out by *B. wadsworthia* (Baron *et al.*, 1989). In *B. wadsworthia* taurine is first deaminated to sulfoacetaldehyde by a taurine-pyruvate aminotransferase (Tpa) with the presence of pyruvate leading to production of alanine (Figure 8). Then, sulfoacetaldehyde is reduced to isethionate by a NADH-dependent sulfoacetaldehyde reductase (SarD, or TauF). The process of releasing

sulfonate from isethionate was fully elucidated recently and shown to be catalyzed by a new class of glycyl radical enzymes, isethionate-sulfite lyase (IslAB, also known as isethionate sulfo-lyase IseGH) (Peck *et al.*, 2019; Xing, Wei, Zhou, *et al.*, 2019). With the presence of cofactor SAM, IslAB cleaves the radical-mediated C-S bond of isethionate so that sulfite is released, and the carbon moiety becomes acetaldehyde. Sulfite is then reduced by the Dsr complex of *B. wadsworthia* to sulfide with an additional electron donor such as lactate, formate or H_2 (da Silva *et al.*, 2008). Acetaldehyde on the other hand, is oxidized to acetate via acetyl-CoA and acetylphosphate, yielding one ATP in the process. It was found that bacterial microcompartments (BMC) are formed in the cells of *B. wadsworthia* during this process as acetaldehyde is toxic (Burrichter *et al.*, 2021). A similar pathway was found in some other human gut isolates such as *Clostridium butyricum* and *Anaerostipes hadrus* (Xing, *et al.*, 2019). Taurine is deaminated by Tpa to produce sulfoacetaldehyde, which is then reduced to isethionate by TauF. Isethionate is desulfonated to sulfite and acetaldehyde by IseGH. However, *C. butyricum* is not a sulfate or sulfite reducer and accordingly Dsr cluster is absent. It was proposed that in this bacterium the released sulfite is used for assimilation (Xing, *et al.*, 2019).

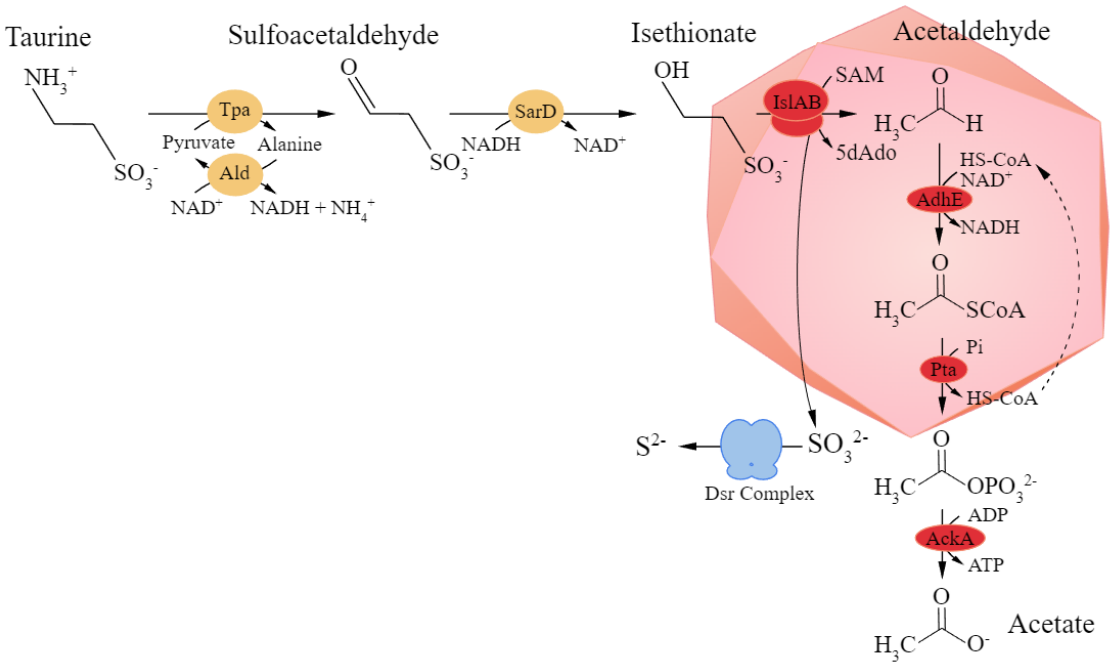

Figure 8. Illustration of the taurine degradation pathway via isethionate desulfonation by a glycyl radical enzyme IslA and the subsequent conversion of the acetaldehyde released from isethionate to acetate, and the reduction of the sulfite released to H_2S by the dissimilatory sulfite reductase complex. Tpa: taurine-pyruvate aminotransferase; Ald: alanine dehydrogenase SarD: sulfoacetaldehyde reductase; IslAB: isethionate-sulfite lyase; SAM: S-adenoslymethionine; 5dAdo: methionine 5-Deoxyadenosine; AdhE: acetylating acetaldehyde dehydrogenase; Pta: phosphotransacetylase; AckA: acetate kinase; Dsr: dissimilatory sulfite reductase. After Burrichter *et al.* (2021).

Sulfoquinovose metabolism

A novel organic sulfur compounds SQDG, considered as a great dietary sulfur source from leavy plants like lettuce, spinach and novel food supplements like algae, has taken the research spotlight of microbiologists in the recent years (Kalisch *et al.*, 2016; Körber *et al.*, 2022). SQ is released from SQDG by sulfoquinovosidases (SQases) (Figure 9). This gateway enzyme for further metabolism SQDG was first unveiled in *E. coli* (Speciale *et al.*, 2016) and then predicted to be spread in other enteric bacteria such as *Salmonella*, *Klebsiella*, *Citrobacter*, *Bacillus*, *Lactobacillus*, *Eubacterium* and *Clostridium* (Burrichter *et al.*, 2018; Frommeyer *et al.*, 2020).

The further degradation of SQ has been illustrated in three pathways: sulfo-Embden–Meyerhof–Parnas pathway (sulfo-EMP), sulfo-Entner–Doudoroff pathway (sulfo-ED), and 6-deoxy-6-sulfofructose transaldolase (SFT) pathway, which all lead to production of three-carbon organosulfonates, 2,3-dihydroxypropane-1-sulfonate (DHPS) or 3-sulfolactate (SL) (Denger *et al.*, 2014; Felux *et al.*, 2015; Abayakoon *et al.*, 2018; Frommeyer *et al.*, 2020). Denger and colleagues (2014) first reported that *E. coli* strain K12 possesses the sulfo-EMP pathway and produces DHPS under aerobic growth conditions with SQ. Later, intestinal strains *Enterococcus gilvus*, *Clostridium symbiosum*, and *Eubacterium rectale* were tested under anaerobic condition and proved to express SFT pathway for fermentative growth with SQ (Frommeyer *et al.*, 2020). The end products of *E. gilvus* is SL, while in *C. symbiosum* and *E. rectale* DHPS was formed. The further bacterial degradation of DHPS or SL can serve as sources of sulfite via diverse catabolic pathways of specialized sulfite-respiring and sulfide-producing *Desulfovibrionaceae* species. Co-cultures of *E. coli* with *Desulfovibrio* strain DF1, and *E. rectale* with *B. wadsworthia* demonstrated this collaborative anaerobic degradation feature (Burrichter *et al.*, 2018; Hanson *et al.*, 2021).

In *Desulfovibrio* strain DF1, DHPS is oxidized to SL via 3-sulfolactaldehyde (SLA) by two NAD^+-dependent dehydrogenases (DhpA, SlaB). Then, SL is cleaved by an SL sulfite-lyase (SuyAB) to pyruvate and sulfite, with SuyB being catalytically active (Burrichter *et al.*, 2018). The pyruvate is oxidized to acetate, while the sulfite is used as electron acceptor in respiration and reduced to sulfide (Figure 9) as explained in sulfite respiration pathway. Candidates of DHPS degradation gene set were reported to be present in another human gut SBR *D. desulfuricans* DSM 642 (Burrichter *et al.*, 2018).

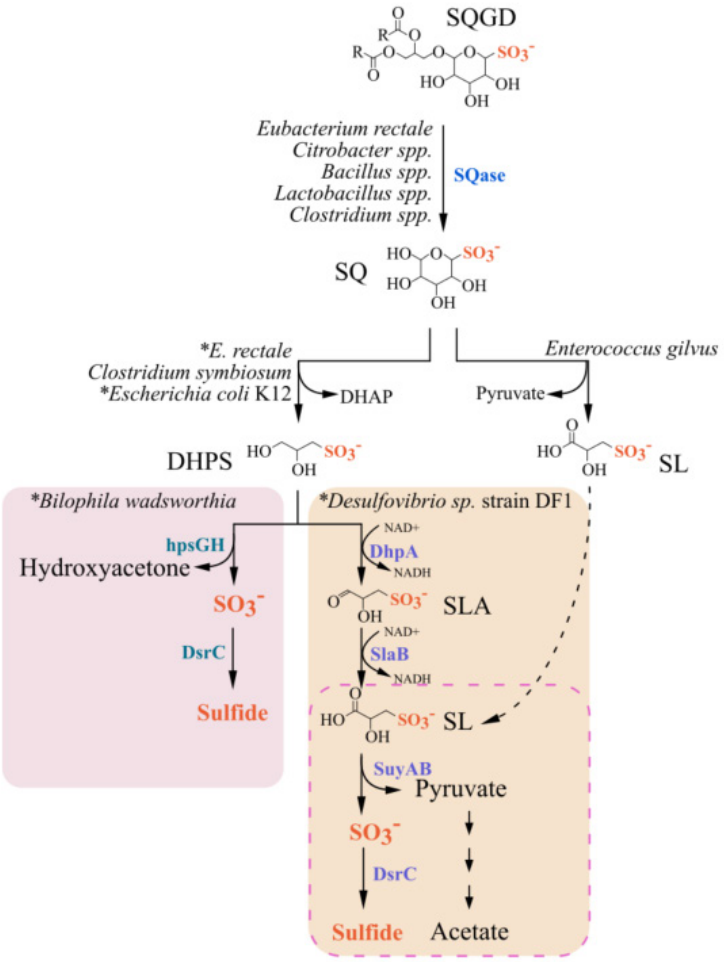

Figure 9. Sulfoquinovosyl diacylglycerol (SQGD) collaborative degradation by human gut microbiome. Genomic analysis indicated that numerous gut microbiome encode sulfoquinovosidases (SQase), which release sulfoquinovose (SQ) for further degradation to either 3-dihydroxypropane-1-sulfonate (DHPS) or 3-sulfolactate (SL). The intestinal strains of the *Firmicutes* species *E. rectale*, *C. symbiosum* and *E. gilvus* degrade SQ via 6-deoxy-6-sulfofructose transaldolase pathway (Frommeyer *et al.*, 2020), while *E. coli* K12 degrades SQ via Embden-Meyerhof-Parnas pathway (Denger *et al.*, 2014). * indicates that co-cultures of *E. rectale* with *B. wadsworthia* (Hanson *et al.*, 2021), and *E. coli* with *Desulfovibrio* strain DF1 (Burrichter *et al.*, 2018) to degrade SQ with a sulfidogenic growth have been tested *in vitro*. Dashed box shows that *B. wadsworthia* possesses the same SL degradation pathway as in *Desulfovibrio* strain DF1. DHAP: dihydroxyacetone phosphate; DHPS: 2,3-dihydroxypropane sulfonate; SLA: 3-sulfolactaldehyde; hspGH: glycyl radical DHPS sulfite-lyase system; DhpA: DHPS dehydrogenase; SlaB: 3-sulfolactaldehyde dehydrogenases; SuyAB: 3-sulfolactate sulfite-lyase; DsrC: dissimilatory sulfite reductase subunit C.

Interestingly, as a close relative to *Desulfovibrio* spp. in the same *Desulfovibrionaceae* family, *B. wadsworthia* displayed sulfidogenic growth on DHPS, whereas DhpA and SlaB are both absent. Through comparative proteomes study, a novel DHPS degradation pathway was discovered (Hanson *et al.*, 2021). In *B. wadsworthia*, DHPS is directly cleaved by a recently identified and characterized glycyl radical DHPS sulfite-lyase system (HpsHG) to sulfite and hydroxyacetone (Figure 9) (Liu *et al.*, 2020). Hydroxyacetone is not further utilized and thus

excreted, while sulfite is reduced by the DsrC to sulfide. Moreover, *B. wadsworthia* also possesses the same SuyAB cluster to degrade SL and indeed showed sulfidogenic growth with SL as a sole carbon source (Hanson *et al.*, 2021).

Cysteine degradation

One of the important SAAs in the gut ecosystem is cysteine. Bacterial cysteine degradation has been reported as connecting sulfidogenic bacteria and health in several diseases including intestinal disorders, inflammatory bowel diseases, and colorectal cancer (Carbonero *et al.*, 2012; Blachier *et al.*, 2019; Teigen *et al.*, 2019; Walker and Schmitt-Kopplin, 2021). Cysteine can be degraded to H_2S by L-cysteine desulfhydrase and was first discovered in *E. coli* (Metaxas and Delwiche, 1955). Since then, this enzyme was also detected in other intestinal pathogens such as *Salmonella thyphimurium* (Kredich *et al.*, 1972), *Mycobacterium tuberculosis* (Wheeler *et al.*, 2005) and *Helicobacter pylori* (Lee *et al.*, 2006) and commensal gut bacteria such as *Prevotella*, *Fusobacterium*, *Clostridium*, *Enterobacter*, *Klebsiella* and the SRB genus *Desulfovibrio* (Carbonero *et al.*, 2012). Unlike the dedicated dissimilatory sulfate reduction pathway, sulfidogenic cysteine metabolic pathway can be conducted via different enzymes. For example, beta C-S lyases and cystathionine-γ-lyase that can carry out reactions similar to desulfhydrases have been described in bacteria such as *E. coli*, *Lactobacillus* spp. and SRB *D. desulfuricans* (Zdych *et al.*, 1995; De Angelis *et al.*, 2002; Irmler *et al.*, 2008). In addition, while species that perform dissimilatory sulfate reduction are well known, those involved in intestinal cysteine degradation have not been well-characterized.

H_2S effects on human health and clearance

Sulfide toxicity

Sulfate reduction in the human gut has primarily been studied in the perspective of the toxicity of its end product, hydrogen sulfide (Nakamura *et al.*, 2010; Fava and Danese, 2011; Medani *et al.*, 2011). In the gut ecosystem specially, the toxicity of sulfide is reflected mainly in three aspects. First, it damages the colonic epithelium cells. Attene-Ramos *et al.* (2010) revealed that exposing non-transformed human intestinal epithelial cells (FHs 74 Int) to sulfide for 4 hours generated a genotoxic effect as sulfide modulates the expression of genes involved in cell-cycle progression and triggers both inflammatory and DNA repair responses. The tested sulfide concentration had a range from 0.25 to 2 mM, which is like the normal colonic luminal

sulfide concentration. Besides, at higher concentration, sulfide becomes toxic by binding to and inhibiting cytochrome C oxidase, which induces oxidative stress and supresses ATP synthesis in a fashion similar as cyanide (Módis *et al.*, 2013; Szabo *et al.*, 2014; Jiang *et al.*, 2016). Secondly, sulfide can impair the metabolic function of colonocytes, especially it inhibits butyrate oxidation. It was found by Roediger *et al*. (1993) that with 2 mM sulfide present, colonocytes butyrate oxidation in ascending colon was decreased by ~40% and in descending colon by ~58%. It was later discovered that acyl-CoA dehydrogenase, which is crucial in regulating the oxidation of butyrate in colonocytes, is severely inhibited in the presence of sulfide (Moore *et al.*, 1997). In summary, oxidative stress and energy starvation caused by excessive sulfide concentrations may lead to colonocyte death, penetration of the epithelial barrier by the intestinal microbes and their direct interaction with the mucosal immune system. Lastly, another mechanism of sulfide toxic effect to the gut was proposed more recently and linked to mucus integrity. Cysteine domains in MUC2 mucin mediate its multimerization through disulfide bonds, but sulfide can directly break these disulfide bonds, leading to a disruption of the MUC2 network, and promote an increased gut permeability (Ijssennagger *et al.*, 2016).

Beneficial effects of sulfide and SRB

Nearly 500 years ago, Paracelsus addressed the principle of toxicology as “the dose makes the poison”, which applies to sulfide unexceptionally. There are numerous observations in support of the hypothesis that sulfide confers a broad range of health benefits. Instead of above-stated inhibition of ATP synthesis, at a low concentration (tested range from 0.01 to 1 μM) sulfide donates electrons to complex II of the mitochondrial electron transport chain, thereby stimulating ATP production (Mustafa *et al.*, 2009). Moreover, human cells are able to use H_2S as a biological signaling molecule in the nervous and vascular systems, and additionally H_2S was found to have a role as a cytoprotectant in the nervous system (Kimura *et al.*, 2012; Shefa *et al.*, 2018). Furthermore, as sulfate is a natural electron acceptor in the gut, SRB can perform anaerobic metabolic conversions that other gut bacteria lack, such as the capacity to efficiently use lactate or ethanol as electron donor. Additionally, *D. piger* as an abundant gut SRB has been studied as part of synthetic communities in germ-free mice and found to be producing sulfide without affecting the mice health or gut integrity (Rey *et al.*, 2013).

Detoxification of sulfide by colonocytes

The colonic epithelium is a monolayer of cells in rapid renewal with specialized functions, which include absorbing colonocytes, enteroendocrine cells, goblet cells and tuft cells. Among these, the absorbing colonocytes are responsible for transporting water and electrolytes, thus making the epithelial colonocytes high energy consumers (Bachmann *et al.*, 2011). At an extracellular concentration of around 50 μM sulfide, the colonocytes are capable of oxidizing sulfide to thiosulfate to obtain ATP with their equipped mitochondrial multi-enzymatic sulfide-oxidizing unit (SOU) (Mimoun *et al.*, 2012). This SOU is composed by sulfide quinone reductase (also known as sulfide:quinone oxidoreductase), persulfide dioxygenase, and sulfur transferase rhodanese, which oxidize sulfide in three steps through persulfide, sulfite and finally to thiosulfate (Figure 10, Hildebrandt and Grieshaber, 2008). The sulfide oxidation pathway is mainly localized in human colonic crypts (Libiad *et al.*, 2019). Endogenous detoxification of free sulfide in the lumen has also been suggested to occur via methylation by S-methyltransferase of sulfide to aliphatic sulfur compound methanethiol and then to dimethyl sulfide (DMS) (Weiseger *et al.*, 1980), or by conversion of sulfide to thiocyanate by rhodanese in the presence of cyanide (Picton *et al.*, 2002; Wilson *et al.*, 2008).

When under inflammatory stress conditions, cytokine and interferon-γ are produced and lead to an increased amount of free radicals in reactive oxygen species (ROS) (Marciano and Vajro, 2017; Singh *et al.*, 2022). The elevated level of radicals in ROS then causes oxidation of common gut lumen metabolites like thiosulfate, DMS and TMA to tetrathionate, dimethyl sulfoxide (DMSO) and trimethylamine N-oxide (TMAO), correspondingly (Winter *et al.*, 2013). It was reported that pathogens like *E.coli* and *S. typhimurium* can use some of these compounds as electron acceptor to promote its outgrowth leading a dysbiosis of gut microbiome (Winter and Bäumler, 2011; Adsit Jr *et al.*, 2022).

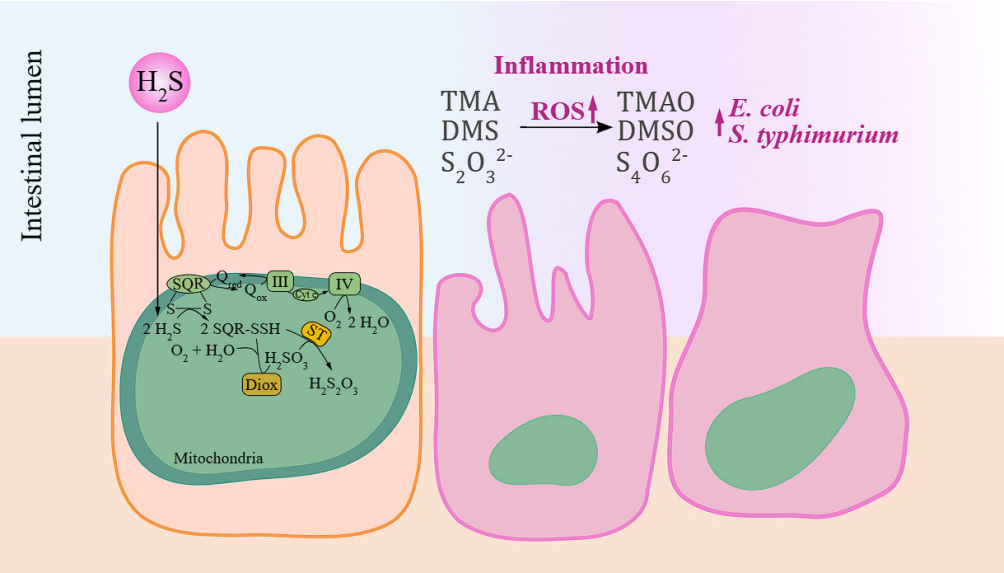

Figure 10. Schematic illustration of mitochondrial oxidation of sulfide to thiosulfate (H2S2O3) in gut epithelium cells. Sulfide is oxidized by a membrane-bound sulfide quinone reductase (SQR) with the electrons fed into the respiratory chain via the quinone pool (Q_{ox} / Q_{red}), and finally transferred to oxygen by cytochrome oxidase (complex III and IV). Diox: sulfur dioxygenase; ST: sulfur transferase. Under inflammatory stress, ROS (reactive oxygen species) can oxidise normal bacterial metablites including TMA (trimethylamine), DMS (dimethyl sulfide) and thiosulfate to TMAO (trimethylamine N-oxide), DMSO (dimethyl sulfoxide) and tetrathionate, which serve as electron respiratory electron acceptors for the out growth of *E. coli* and *S. typhimurium*. Adapted from Hildebrandt and Grieshaber (2008) and Adsit Jr *et al.*, (2022).

TMA metabolism in human gut and its effects to health

Recently another microbial metabolite, trimethylamine (TMA), has been proposed to have negative impacts to human health. The microbial derived TMA can enter the bloodstream, and then is converted to TMAO by the hepatic enzyme flavin monooxygenase 3 (Schugar and Brown, 2015). Higher level of serum TMAO correlates with the onset of atherosclerosis and increased occurrence of adverse cardiovascular events, vascular inflammation, colorectal and liver cancers, and increased risk of mortality in patients with kidney disease (Figure 10) (Janeiro *et al.*, 2018; Subramaniam and Fletcher, 2018).

TMA is produced via different microbial degradations on dietary quaternary amines including betaine, choline and L-carnitine, which are commonly found in vegetables, fruits, seafood and meat. Several key TMA-producing enzymes have been identified in human gut microbiome, including choline-TMA lyase (CutC) and its activating enzyme (CutD) in the SRB *D. desulfuricans* (Craciun and Balskus, 2012), a two-component carnitine oxygenase/reductase (CntAB) in *Acinetobacter calcoaceticus* (Zhu *et al.*, 2014), and another enzyme complex termed YeaW/X which acts on γ-butyrobetaine (Koeth *et al.*, 2014), and betaine reductase

(GrdH) for bacterial degradation of glycine betaine (Andreesen, 1994). Yet the main TMA producing bacteria need to be uncovered and studied *in vitro*, many *in silico* studies have screened both human-associated bacterial isolate genomes and whole gut metagenomes with the aforementioned TMA-producing enzymes to determine which bacteria are responsible for TMA formation in the human gut. For instance, CutC homologs were detected in SRB including *Desulfotomaculum*, *Desulfosporosinus*, *Desulfitobacterium*, and sulfite-reducer *Bilophila*, and were also found in other common human gut taxa like *Clostridium* XIVa strains, *Streptococcus*, *Klebsiella*, and *Proteus* (Figure 10) (Craciun and Balskus, 2012; Rath *et al.*, 2017; Kivenson and Giovannoni, 2020). On the other hand, CntA and GrdH homologs were revealed to present primarily in *Klebsiella*, *Escherichia* and *Clostridium* XIVa, respectively (Rath *et al.*, 2018).

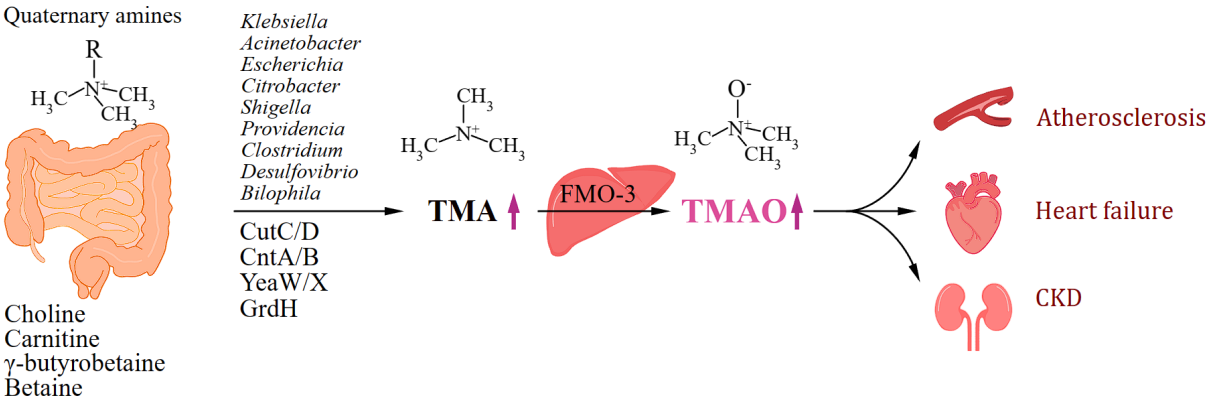

Figure 11. Simplified schematic diagram of TMA metabolism in human body. Dietary quaternary amines (QAs, e.g. L-carnitine, choline, betaine, γ-butyrobetaine) reached in the intestine are converted by the gut microbiota into TMA by CutC/D (choline utilization gene cluster), CntA/B (carnitine oxygenase/reductase) and its similar enzyme complex YeaW/X, and GrdH (betaine reductase). TMA is transferred to liver and then converted to TMAO by a hepatic flavin monooxygenase 3 (FMO-3). High TMAO concentration in blood leads to increased risk of cardiovascular disease, atherosclerosis, and chronic kidney disease (CKD).

Research aims and thesis outline

The research reported in this thesis aimed to investigate the anaerobic metabolism of sulfur-containing compounds in the human gut because of their potential health impact. The approach taken included the isolation and characterization of novel anaerobes from the human gut. A combination of physiological, biochemical and genomic methodologies was used for their characterization. A review of the literature of the state of the art in the knowledge of human gut bacteria and their role in sulfur metabolism is provided in **Chapter 1**. This also

includes a short description of the TMA metabolism since this was discovered to be an important feature of the newly isolated gut anaerobe.

Chapter 2 describes the identification and isolation of bacteria involved in sulfide formation by anaerobically enriching human gut microbiome with different sulfur compounds. Fresh fecal samples of two adult donors were used as inocula for enrichments. Sulfate or sulfite were used as electron acceptors in combination with different electron donors, and organic sulfur compounds e.g. ox-bile, taurine and cysteine were included as substrates for respiration and fermentation. Cultures showing high sulfidogenic conversions were selected for phylogenetic analysis of the enriched microbial communities. Sulfite reduction and cysteine degradation were the dominant sulfidogenic processes in the gut microbiome of both subjects, and the most abundantly enriched bacteria belonged to *Bilophila* and genera within *Clostridium* cluster XIVa. Further analysis of the selected cultures led to two novel and pure isolates, strain YI and strain 2C. Strain 2C is a novel sulfite reducer and belongs to the *Veillonellaceae* family of *Firmicutes* phylum and showed limited (91%) 16S rRNA gene sequence similarity with that of known *Sporomusa* species and hence may represent a novel genus. The other isolate strain YI isolate, was found not to be capable of sulfidogenic growth but survived high sulfite and sulfide (both at 5 mM) concentrations during the enrichment.

Strain YI is described in **Chapter 3** including its morphological, biochemical and physiological characterization. This novel isolate *Eubacterium maltosivorans* YI^T is affiliated to the *Eubacteriaceae* family of Clostridium cluster II showing less than 97.5% of 16S rRNA gene identity to the four most related species described in the *Eubacterium* genus. Strain YI^T converts H_2 and CO_2, as well as methanol and formate with weak growth, into acetate. Besides homoacetogenic growth, it was able to ferment a range of monomeric sugars and disaccharides, including maltose, with acetate and butyrate as the main end products. More specifically, it can generate beneficial butyrate and propionate from low energy compounds, as it shows butyrogenic growth from lactate and acetate and propionogenic growth from 1,2-propanediol. Lastly, and it can deaminate the quaternary amines, e.g. betaine, carnitine and choline resulting in acetate and butyrate production and limiting the formation of the undesired trimethylamine.

Chapter 4 provides a further detailed comparative genomic and proteomic studies on *E. maltosivorans* YI^T, who possesses homoacetogenesis, propionigenesis and butyrogenesis in one single human gut bacteria. Its complete genome was sequenced, annotated, and compared with closely related *Eubacterium limosum* species. An unusual feature shared with these *E.*

maltosivorans and *E. limosum* related species is the presence of abundant genes (41 in strain YI^T) encoding TMA methyltransferase family proteins. Comparative proteomics of strain YI^T showed upregulated production of proteins encoded by the *lctABCDEF* cluster and accessory proteins, while the Wood–Ljungdahl pathway proteins was actively produced during homoacetogenic growth on H_2 and CO_2 with unexpectedly highly induced the production of two related TMA methyltransferases. Moreover, a set of 16 different TMA methyltransferases together with proteins for bacterial microcompartments were produced during growth and vitamin B12-dependent deamination of the quaternary amines, (betaine, carnitine and choline). Bacterial microcompartments were prominently visible in both betaine-grown and 1,2-propanediol-grown cells.

The forementioned sulfite reducer strain 2C is described and characterized in **Chapter 5** by a comparative genomic and proteomic analysis. Strain 2C is allocated in *Sporomusaceae* family (*Selenomonadales* order, *Negativicutes* class, *Bacillota* phylum). Its 16S rRNA genes showed less than 93% identity to 9 type species described in *Sporomusaceae* family, indicating a novel species in a new genus for which the name *Sporobaculum desulfitilongum* is proposed. This new isolate reduces sulfite, DMSO, and likely tetrathionate, and TMAO, but not sulfate, thiosulfate and sulfur. Comparative genomic analysis of strain 2C with other human gut sulfate or sulfite reducers indicated that strain 2C and other sulfite reducers in *Sporomusaceae* family have a Gram-positive type membrane electron transfer chain. Proteome studies comparing strain 2C grown with sulfite reduction and pyruvate showed an active sulfite reduction pathway with an upregulated production of thioredoxin, which might be involved in controlling the redox state of strain $2C^T$ when growing with sulfite.

Chapter 6 summarizes the findings of this thesis, discusses the outcome in a broader context and provides perspectives and directions for future research. The role of the newly isolated anaerobes in sulfur metabolism is discussed and specific attention is given to the generated insight in the metabolism of trimethylamines and preventing the formation of its oxide TMAO, which has been recognized as a cardiometabolic risk factor.

Chapter 2: Fecal enrichments reveal novel sulfite reducers in the human intestinal tract

This chapter has been published as:

Feng, Y., Stams, A. J., De Vos, W. M., & Sánchez-Andrea, I. (2017). "Enrichment of sulfidogenic bacteria from the human intestinal tract." FEMS Microbiology Letters, **364**(4), fnx028.

Abstract

Hydrogen sulfide is formed in the human intestinal tract as the end product of the anaerobic microbial degradation of sulfur-compounds present in mucus, bile or proteins. Since human gut microbial sulfur metabolism has been poorly characterized, we aimed to identify and isolate the microorganisms involved in sulfide formation. Fresh faecal samples from one healthy donor and one diagnosed with irritable bowel syndrome were used as inocula for enrichments that were supplemented with sulfate or sulfite as electron acceptors in combination with different electron donors. After two transfers, cultures with high sulfide production were selected and the phylogenetic composition of the enriched microbial communities was determined. Sulfite respiration and cysteine degradation were the dominant sulfidogenic processes, and the most abundant bacteria enriched belonged to *Bilophila* and *Clostridium* cluster XIVa. Different isolates were obtained and remarkably, included a novel sulfite reducer, designated strain 2C. Strain 2C belongs to the *Veillonellaceae* family of *Firmicutes* phylum and showed limited (91%) 16S rRNA gene sequence similarity with that of known *Sporomusa* species and hence may represent a novel genus. This study indicates that bacteria that utilize sulfite and organic sulfur-compounds rather than merely sulfate are relevant for human intestinal sulfur metabolism.

Introduction

The human gastrointestinal (GI) tract is colonized by billions of commensal microbes, which constitute a complex and diverse community known as the gut microbiota (Qin, Li, *et al.*, 2010; Flint *et al.*, 2012). The luminal hydrolysis of undigested carbohydrates into mono-sugars and fermentation to short chain fatty acids has been extensively studied, whereas the intestinal microbial sulfur metabolism has received less attention (den Besten *et al.* 2013).

Sulfur is the third most abundant trace element in humans by percent of mass (Parcell, 2002). Humans require intake of organic sulfur sources such as methionine, cysteine/cystine, and taurine, present in meat, eggs and dairy products (Magee *et al.* 2000). Organic sulfur compounds can be used by mammalian cells as building blocks for tissues, or to form secreta such as mucin and bile acids (Wu 2009). Inorganic sulfur, such as sulfate and sulfite, which mainly derives from food preservation, cannot be used by the mammalian cells for energy conservation (Florin *et al.* 1993; Gibson *et al.* 1993). Whereas in the GI tract, both organic and inorganic sulfur-compounds are sources for microbiota to grow and are used, either assimilatory to synthesize cysteine or methionine, or dissimilatory and fermentatively to release sulfide. To date the sulfide levels in the human intestine are not measured, but in human feces a range of 0.3 to 3.4 mmol L^{-1} was detected (Magee *et al.*, 2000). Although low concentrations of sulfide (37 to 462.5 μmol L^{-1}) may act as neuromodulator (Schicho *et al.*, 2006; Krueger *et al.*, 2010), higher concentrations of sulfide can cause DNA damage of epithelium cells (Attene-Ramos *et al.* 2007) and impair metabolic functions such as butyrate oxidation in colonic epithelial cells (Hamer *et al.* 2008). Consequently, it has been suggested that sulfide could be involved in intestinal disorders such as inflammatory bowel disease and irritable bowel syndrome (IBS) (Nakamura *et al.*, 2010; Medani *et al.*, 2011). However, such a link between sulfur biotransformation and diseases has not yet been convincingly shown (Ijssennagger *et al.* 2016) and needs to be investigated. Sulfate reduction in the human GI tract has primarily been studied related to sulfide toxicity. Sulfate-reducing bacteria (SRB) in the GI tract of animals and humans have been detected (Hilton and Oleszkiewicz, 1988; Qin, Li, *et*

al., 2010). The genus *Desulfovibrio* is generally the most abundant (Scanlan *et al.* 2009), while *Desulfobacter*, *Desulfobulbus*, and *Desulfotomaculum* were also present (Nava *et al.* 2011). *In vitro* incubation studies of Levine *et al.* (1998) using human feces suggested that sulfate was a less efficient source for sulfide production than organic sulfur-containing compounds. Unfortunately, this study did not include a microbial characterization to reveal the involved microbes. Hence, the aim of our research was to determine the microbial communities involved in the degradation of sulfur compounds leading to sulfide formation and to isolate novel microbial players.

Material and methods

Samples, media and cultivation

To increase the diversity of the inocula source, fresh faecal samples from one healthy subject and one suffering from IBS were collected and inoculated separately. The study was approved by CCMO Netherlands (project ID: NL2907008109). One milliliter of an 1% (w/v) diluted faecal sample from each donor was inoculated into a 120 mL serum bottle containing 50 mL of O_2-free basal medium as described by Stams *et al.* (1993). The enrichments were supplemented with 0.1 g L^{-1} of yeast extract and either sulfate (20 mM) or sulfite (5 mM) as electron acceptor. Nine different electron donors were tested due to their significance in sulfur cycle and in the human GI tract: acetate, butyrate, propionate, lactate, pyruvate, L-cysteine, taurine at a concentration of 10 mM; ox-bile at 0.75 g L^{-1} and H_2 at 1.7 atm of H_2/CO_2 (80:20, v/v). Commonly, 1 M stock solutions of electron acceptors and donors were prepared in sodium salt form and autoclaved. 250 mM sodium sulfite, 280 mM L-cysteine, 400 mM taurine and 37.5 g L^{-1} ox-bile stock solutions were dissolved in O_2-free demi water and filter-sterilized into each 120 mL autoclaved serum bottle. Cultures were incubated under 1.7 atm of N_2/CO_2 (80:20, v/v) at 37°C and pH 7.2. Negative controls without electron donor or acceptor were included.

Both sets of enrichments with healthy donor (HEA) and IBS-diagnosed donor faecal samples were first incubated for 14 days (primary incubation). On day 15, cultures with higher

sulfide production than the control group were selected and 1 mL of culture was transferred to a fresh medium to perform a secondary incubation for another 9 days under the same condition. Sulfide (1 mM) and cysteine (4 mM) were used as reducing agents for both primary and secondary enrichment in HEA enrichments. Since a background sulfide production was observed from the cysteine, titanium citrate was used as reducing agent for IBS enrichments.

Analytical methods

Sulfide was fixed immediately by adding 50 µL of 5% (w/v) $ZnCl_2$ to 1 mL of each sample and measured by methylene-blue method (Cline 1969). Samples were also fixed with 5% (v/v) of methanol to stabilize sulfite (Michigami and Ueda, 1994). Sulfate and sulfite were analyzed using a Dionex 1000 ion chromatograph unit (Dionex, USA) equipped with an IonPac AS17 Anion-Exchange column operating with a 0.1 mL min^{-1} flow rate at 30°C. Organic compounds were quantified by high-performance liquid chromatograph (HPLC) with a Varian Metacarb 67H 300 mm column and sulfuric acid (0.01 N) eluent at a flow rate of 0.8 mL min^{-1}. Gases such as methane and H_2 were measured using a gas chromatograph (Shimadzu, Kyoto, Japan) as described by Florentino *et al.* 2015.

Bacterial community analysis

An aliquot (1-5 mL) of well-homogenized liquid culture was concentrated by centrifuging at 13400 g for 10 min and DNA was extracted from the pellet by FastDNA SPIN Kit for Soil (MP Biomedicals, OH) according to the manufacturer's instructions. PCR was performed and purified in the same procedure of Timmers *et al.* (2015) for both bacterial and archaeal 16S rRNA genes. The purified PCR products were then cloned into *Escherichia coli* XL1-Blue Competent Cells (Agilent Technologies, Santa Clara, CA) by using the pGEM Easy Vector Systems (Promega, Madison, WI). All steps mentioned above were done following the manufacturers' instructions. Sanger sequencing was performed by GATC Biotech (Konstanz, Germany) using SP6 (5'-ATTTAGGTGACACTATAGAA-3') as sequencing primer. The sequences were trimmed with DNA Baser software (version 4.20.0. Heracle BioSoft SRL,

Pitesti, Romania) to remove vector contamination and manually checked. Later they were aligned with the multiple sequence aligner SINA (Pruesse *et al.* 2012) and merged with the Silva SSU Ref database (release 111). Phylogenetic trees were constructed in the ARB software package (v. 6) by the same algorithm (Ludwig *et al.* 2004) described previously (Timmers *et al.* 2015). Sequences were deposited in ENA under the accession numbers LT623288 to LT623571.

Genomic and metagenomic datamining

Blast search (Gish and States, 1993) of the enzymes of the sulfite reduction pathway of *Desulfovibrio desulfuricans* strain ATCC 27774 (NC_011883) was performed against the genome of *B. wadsworthia* strain 3_1_6 (NZ_KE150238).

For metagenomic datamining, 50 assembled and reviewed metagenome datasets of human stool microbial communities were selected from IMG/MER of JGI database (see Table S3). “Dissimilatory sulfite reductase”, “cysteine desulfhydrase” and “taurine dehydrogenase” were used as query for the search. Scaffolds containing the target genes were selected and their phylogeny was analyzed by IMG/MER database.

Isolation and sulfur metabolism of the isolate

Enrichments were selected for further isolation when they showed highly enriched (abundance >50%) of novel strains (16S rRNA gene sequence similarity <98.7%), according to Stackebrandt (2006). Isolation strategies combined pasteurization in liquid media at 80°C for 15 min, repeated serial dilution, antibiotic treatments and streaking on agar plates. After pure cultures were obtained, cloning and phylogenetic reconstruction were conducted as described in the bacterial community analysis section in addition of extra sequencing of the 16S rRNA gene with T7 primer (5′-TAATACGACTCACTATAGGG-3′). Sequences amplified with both SP6 and T7 primers were then trimmed, combined and deposited in ENA under the accession numbers LT623572 and LT623573.

Both strains 2C and YI were tested with API® 50 CH, 20 A and ZYM (bioMérieux SA, Lyon, France) according to the manufacturer's instructions. Using the same O_2-free basal medium supplied with trace elements, vitamins solution and a final concentration of 0.5% yeast extract, the isolates were tested in different relevant substrates. Sulfate (20 mM), sulfite (5 mM), and taurine (10 mM) were tested separately as an electron acceptor in combination of 20 mM of either butyrate, pyruvate, lactate or L-cysteine (10 mM). Negative control of both electron donor and acceptor were included as well. Compounds consumption and production were monitored in the same way as described in the analytical methods section.

Results and Discussion

Enrichment experiments

Methane and H_2 were never detected, neither in the primary nor in the secondary enrichments. None of the enrichments showed sulfide production coupled to sulfate reduction either (Table S1 & S2). In both HEA and IBS enrichments provided with sulfite, higher sulfide production was detected after the first transfer when H_2, lactate, or pyruvate served as electron donor (Figure 1 A & C). In the absence of any electron acceptor, higher sulfide production was observed when cysteine was added as a substrate in both HEA and IBS enrichments (Figure 1 B & D). When using ox-bile as substrate, higher sulfide production occurred in the HEA enrichment, in the presence of sulfite, whereas for IBS enrichment, maximum production of sulfide was observed in the enrichment without sulfite (Figure 1 A & D). Hence for both HEA and IBS enrichments, sulfite reduction and cysteine utilization were the dominant sulfidogenic processes. These results are in line with those from Levine *et al.* (1998) who pointed out that sulfate was a less efficient source for sulfide production than cysteine, taurocholate and mucin when incubating human faecal samples *in vitro*.

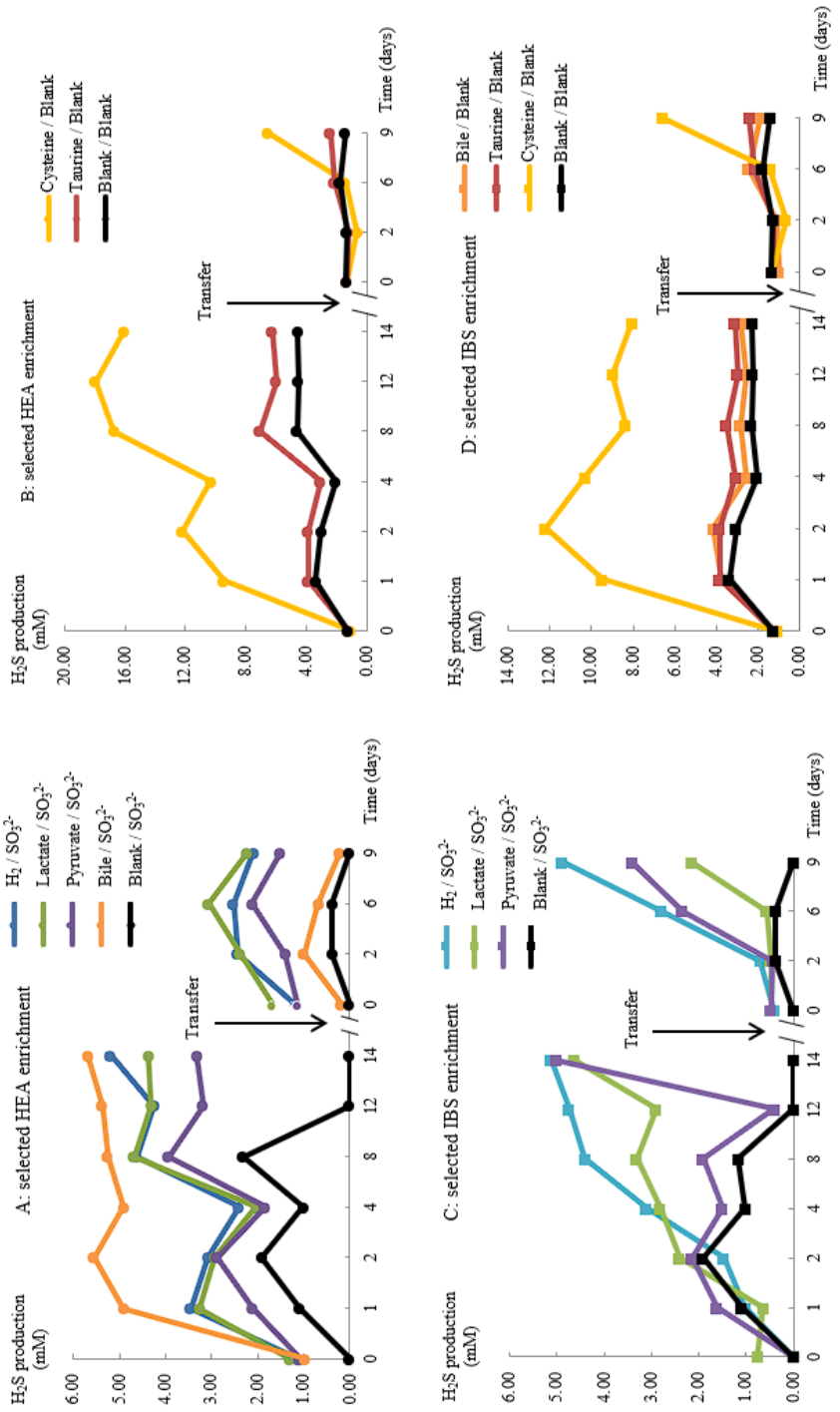

Figure 1: Sulfide production of selected healthy (A and B) and IBS-diagnosed (C and D) donor fecal enrichments within primary (before transfer) and secondary incubation (after transfer). " Black" represents no electron acceptor or donor was added in the enrichment culture to serve as the control. Measurements were performed in duplicates and the standard error is within 10% of the values obtained

Phylogenetic analysis of selected enrichments based on 16S rRNA gene clone libraries

Bilophila was the most commonly enriched genus in all selected cultures for both HEA and IBS enrichments (Figure 2, see Fig. S1 & S2 for rarefaction curves) except for those with cysteine as sole substrate. It was especially abundant in the enrichment with H_2 and sulfite of the HEA enrichment (up to 90% of the sequences). The closest cultured relative to the obtained sequences is *Bilophila wadsworthia* (average 16S rRNA gene identity 99%, Fig. S3), which is the only cultured species within the genus (da Silva *et al.*, 2008). *B. wadsworthia* is a commensal human GI tract microbiota, which is phylogenetically related to *Desulfovibrio desulfuricans* with a 91.4% 16S rRNA gene similarity. *B. wadsworthia* is not able to reduce sulfate, instead it can conserve energy by performing dissimilatory sulfite reduction; it can use taurine as a source of sulfite (Laue *et al.*, 2001). The enzymes involved in sulfite reduction were found in the genome of *B. wadsworthia* (Figure 3): DsrA, DsrB, DsrC and the membrane complex involved in electron transport (complex DsrMKJOP) from the membrane to the DsrC trisulfide (Leavitt *et al.*, 2016). The growth rate of *B. wadsworthia* was higher with H_2/taurine than with lactate/taurine and pyruvate/taurine (da Silva *et al.*2008). This may explain that in our experiment under H_2/sulfite condition for both HEA and IBS enrichments, the abundance of *Bilophila* was largely promoted. When bile served as the only substrate, *Bilophila spp.* were also highly enriched in IBS enrichment, representing 84% of the sequences (Figure 2). This is explained by the ability of *B. wadsworthia* to ferment taurine leading to sulfide production (da Silva *et al.*, 2008). Under this condition, *Escherichia/Shigella* represented 10% of the cloned sequences. The related species was *Escherichia coli* (~ 99% average 16S rRNA gene identity, Fig. S3). The antimicrobial activity of bile can select or exclude certain microbes in the human GI ecosystem (Ridlon *et al.*, 2014). Several intestinal pathogens are bile-resistant and therefore highly favored when bile is present (Ananieva *et al.* 2002).

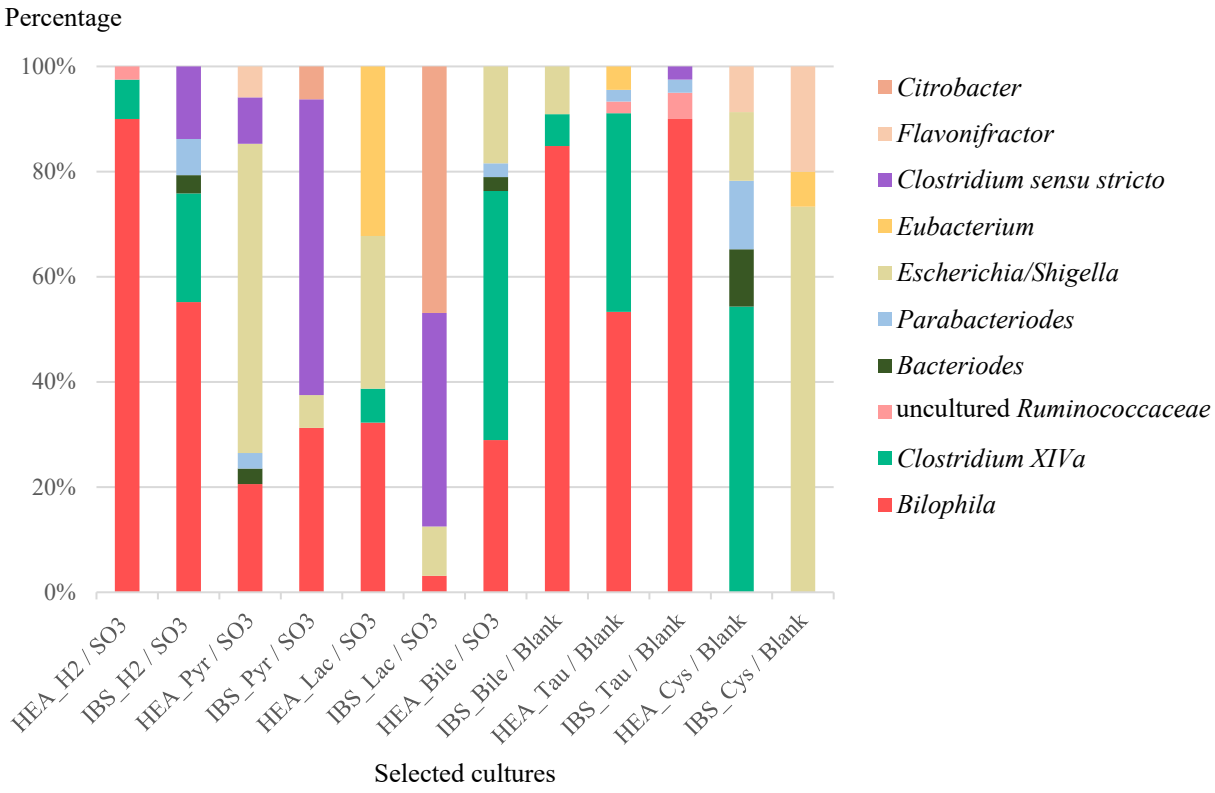

Figure 2. Microbial communities of selected enrichments based on SILVA classification at the genera level. HEA: healthy donor fecal sample enrichment; IBS: IBS-diagnosed donor fecal sample enrichments; H2: hydrogen as electron donor; Pyr: pyruvate; Lac: lactate; Cys: cysteine; Tau: taurine; SO3: sulfite as electron acceptor; Blank: no electron acceptor.

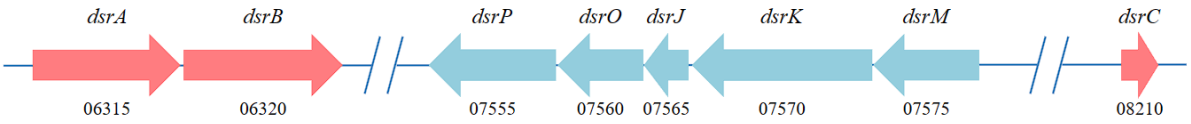

Figure 3. Relative position of the dissimilatory sulfite reductase operons and genes involved in the dissimilatory sulfite reduction pathway of *Bilophila wadsworthia* strain 3_1_6. Locus tag (all begin with identifier HMPREF0179_RS) is indicated below each gene. *dsrA*: dissimilatory sulfite reductase alpha subunit; *dsrB*: dissimilatory sulfite reductase beta subunit; *dsrC*: dissimilatory sulfite reductase C; *dsrMKJOP* complex.

There has been a shift from traditional diet habits- high in vegetables and low meat content- to modern diet habits more based on processed foods, high in protein and saturated fats (Jew *et al.* 2009). After taking a high fat diet, bile formation is promoted since bile improves the digestion of fat (Lefebvre *et al.*, 2009). Devkota *et al.* (2012) correlated consumption of a high saturated fat with increased taurocholic acid, which promoted *B. wadsworthia* abundance and colitis in a mouse model. Hence, the role of bile and *B. wadsworthia* in the sulfur cycle in the human GI tract needs to receive more attention.

Clostridium cluster XIVa was the second most abundant group enriched, and was especially abundant (51% of the total sequences) in the HEA enrichment where cysteine was utilized as substrate (Figure 2). The enriched *Clostridium* species from this culture were mainly related with three species: *Clostridium aldenense* (~ 97% average 16S rRNA gene identity), *Clostridium citroniae* (~ 98% average identity) and *Clostridium bolteae* (98% identity) (Fig. S3). All three species were isolated from human clinical samples and were detected in human faecal samples as well (Warren *et al.*, 2006; Pequegnat *et al.*, 2013). Taking up a substantial part (10-40%) of the total human GI tract bacteria, *Clostridium* spp. have important roles in the maintenance of overall gut function and were suggested to be leading players in the maintenance of gut homeostasis (Lopetuso *et al.*, 2013).

Isolation and characterization

The different isolation strategies applied led to the isolation of two novel isolates: strain YI (97% 16S rRNA gene similarity to *Eubacterium limosum*) and strain 2C (91% 16S rRNA gene similarity to that of representatives of the *Sporomusa* cluster and to *Anaeroarcus* cluster) (Figure 4). The carbohydrates utilization patterns of both strains are listed in Table 1. Strain 2C utilizes a broader range of substrates for fermentation than strain YI. Moreover, Strain YI did not form sulfide from sulfate or sulfite.

Table 1. API® 50 CH test for Strain 2C and Strain YI. "+" indicates that the tested bacteria could ferment the substrate, "-" indicates not.

	Strain 2C	Strain YI		Strain 2C	Strain YI
Control	-	-	Esculin ferric citrate	+	-
Glycerol	-	-	Salicin	+	-
Erythritol	+	+	D-cellobiose	+	-
D-arabinose	-	-	D-maltose	+	-
L-arabinose	+	-	D-lactose	+	-
D-ribose	+	-	D-melibiose	-	-
D-xylose	+	-	D-saccarose	+	-
L-xylose	-	-	D-trehalose	+	-
D-adonitol	-	+	Inulin	-	-
Mthyl-βD-xylopyranoside	-	-	D-melezitose	-	-
D-galactose	+	-	D-raffinose	-	-
D-glucose	+	+	Amidon	+	-
D-fructose	+	+	Glycogen	+	-
D-manose	+	-	Xylitol	-	-
L-sorbose	-	-	Gentiobiose	+	-
L-rhamnose	-	-	D-turanose	+	-
Dulcitol	-	-	D-lyxose	+	-
Inositol	-	-	D-tagatose	-	-
D-mannitol	+	-	D-fucose	-	-
D-sorbitol	-	-	L-fucose	-	-
Mehtyl-αD-mannopyranoside	-	-	D-arabitol	-	+
Mehtyl-αD-glucopyranoside	-	-	L-arabitol	+	+
N-acetylglucosamine	+	-	potassium gluconate	+	-
Amygdalin	+	-	potassium 2-ketogluconate	-	-
Arbutin	+	-	potassium 5-ketogluconate	-	-

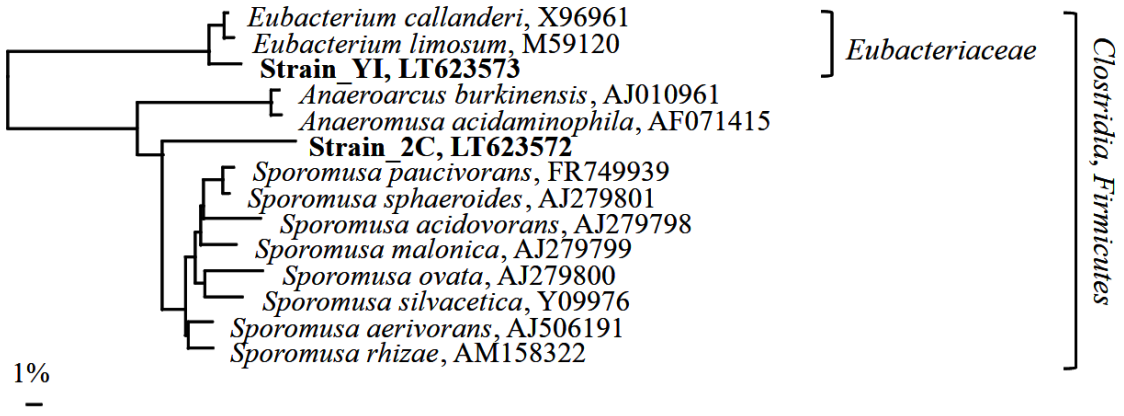

Figure 4. Phylogenetic reconstruction of 16S rRNA gene sequences of the isolated strain 2C and strain YI (in bold) and the closest representative species. The tree was rooted with *Escherichia coli* as outgroup but removed after tree construction. The scale bar represents the percentage of changes per nucleotide position.

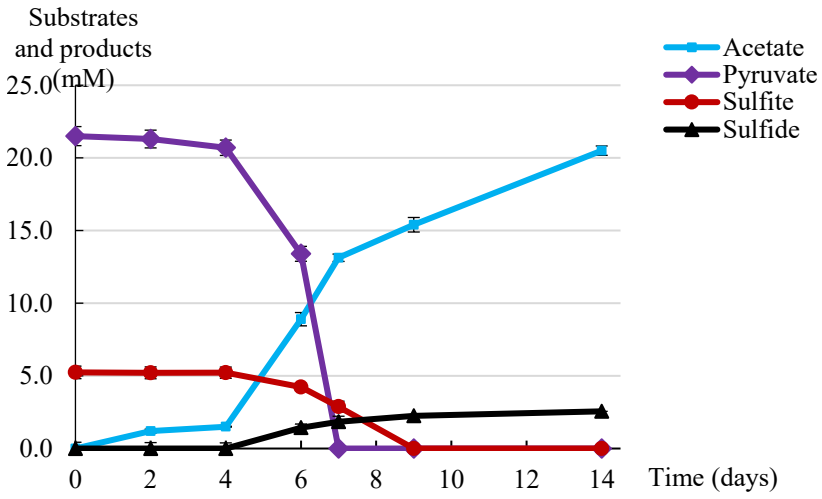

Figure 5. Growth of strain 2C on pyruvate and sulfite to yield sulfide and acetate. On all data series, a standard deviation is displayed over triplicate experiments.

Remarkably, strain 2C shows sulfite reduction with pyruvate resulting in acetate and sulfide production (Figure 5, Eq. 1 and 3). Pyruvate also supports fermentative growth with acetate accumulation (Eq. 1 and 4). Sulfate was not reduced when tested with butyrate, pyruvate or lactate. Strain 2C ferments cysteine to sulfide and acetate (Eq. 1, 3 and 4). Besides, it can also assimilate taurine while releasing sulfide and acetate. Taurine fermentation was described for *Desulforhopalus singaporensis* and *Desulfonispora thiosulfatigenes* leading to either sulfide or to thiosulfate (Denger *et al.* 1999; Lie *et al.* 1999). *D. singaporensis* is a

sulfate/sulfite-reducing bacterium while *D. thiosulfatigenes* cannot reduce sulfate nor sulfite. These two species were isolated from marsh and fresh water. The strain is currently characterized to broaden the knowledge of its involvement of the sulfur cycle in the human gut.

$C_3H_4O_3 + H_2O \rightarrow CH_3COOH + CO_2 + 2H^+ + 2e^-$ (Eq. 1 pyruvate)

$C_3H_7NO_2S + H_2O \rightarrow C_3H_4O_3 + NH_3 + H_2S$ (Eq. 2 cysteine)

$SO_3^{2-} + 6H^+ + 6e^- \rightarrow S^{2-} + 3H_2O$ (Eq. 3 sulfite)

$2H^+ + 2e^- \rightarrow H_2$ (Eq. 4 H_2)

Datamining

Datamining of the available metagenomic datasets can give us a guidance of the unrevealed sulfidogenic potential in the human gut system. Our search for dissimilatory sulfite reductase in the selected metagenomes showed hits in *Desulfovibrio*, *Bilophila*, *Eubacterium*, *Ruminococcus*, *Clostridium*, *Citrobacter* and *Escherichia* etc. (Table S4). The reversibility of this pathway for sulfide oxidation must be considered before drawing conclusions but surely it implies an active sulfur cycle in the human gut system. The search for taurine dehydrogenase gave no hit. Cysteine desulfhydrase is the key enzyme of bacterial cysteine fermentation, which releases sulfide, pyruvate and ammonia as products and is reported to be present in *Clostridium* spp. (Carbonero, Benefiel, and Gaskins, 2012). In the current datamining search, D-cysteine desulfhydrase was present in *C. citroniae*, *Clostridium hathewayi*, unclassified *Clostridiales*, *E. coli, Oscillibacter* spp. and *B. wadsworthia* in the selected database (Table S5).

Conclusion

The current *in vitro* work showed that sulfite and organic sulfur-containing compounds such as taurine, bile and cysteine, are potentially important sources of sulfide production. Sulfite-reducing bacteria belonging to *Bilophila* and cysteine-fermenting bacteria belonging to *Clostridium* cluster XIVa were highly predominant in the enrichments. Furthermore, we isolated two strains, from which strain 2C represents a novel genus, and it is able to produce sulfide by cysteine fermentation as well as by sulfite reduction. In this work, sulfate did not

promote growth of sulfate-reducing bacteria, suggesting that more attention should be given to sulfite reduction and anaerobic conversions of organic sulfur compounds to expand our knowledge of sulfide formation in the human GI tract.

Acknowledgements

This work was supported by Gravitation grant The Soehngen Institute of Anaerobic Microbiology (project 24002002) of the Netherlands Ministry of Education, Culture and Science and the Netherlands Science Foundation (NWO). We also thank the technical supports from Ton van Gelder and Bastian Hornung.

Supplementary data

Table S1: Maximum sulfide production (mM) of 24-day enrichment in different combinations of electron donor and acceptors of healthy donor's faecal sample. Cultures showed higher sulfide production compared to control setup were indicated in red cells. "Blank" represents no electron acceptor or donor was added in the enrichment culture to serve as the control.

Maximum sulfide production (mM) during 24 days enrichment		Electron acceptors		
		SO_4^{2-}	SO_3^{2-}	Blank
Electron donors	H_2	3.45	5.19	3.45
	Acetate	3.64	1.76	3.30
	Bile	3.56	5.69	4.16
	Butyrate	3.19	1.61	3.64
	Cysteine	10.22	9.94	17.97
	Lactate	3.26	5.00	4.13
	Propionate	3.11	1.84	3.71
	Pyruvate	2.89	4.63	2.63
	Taurine	3.49	5.32	7.06
	Blank	3.60	4.63	3.38

Table S2: Maximum sulfide production (mM) of 24-day enrichment of the faecal sample from Irritable Bowel Syndrome donor in different combinations of electron donor and acceptors. Cultures showed higher sulfide production compared to control setup were indicated in red cells. "Blank" represents no electron acceptor or donor was added in the enrichment culture to serve as the control.

Maximum sulfide production(mM) during 24 days enrichment		Electron acceptors		
		SO_4^{2-}	SO_3^{2-}	Blank
Electron donors	H_2	2.53	5.12	2.03
	Acetate	1.91	0.47	2.00
	Bile	2.94	1.00	2.56
	Butyrate	2.91	0.38	1.91
	Cysteine	6.33	6.56	7.34
	Lactate	3.06	5.00	1.94
	Propionate	2.84	0.40	2.00
	Pyruvate	2.13	3.31	1.59
	Taurine	2.09	2.15	3.86
	Blank	3.88	1.91	2.16

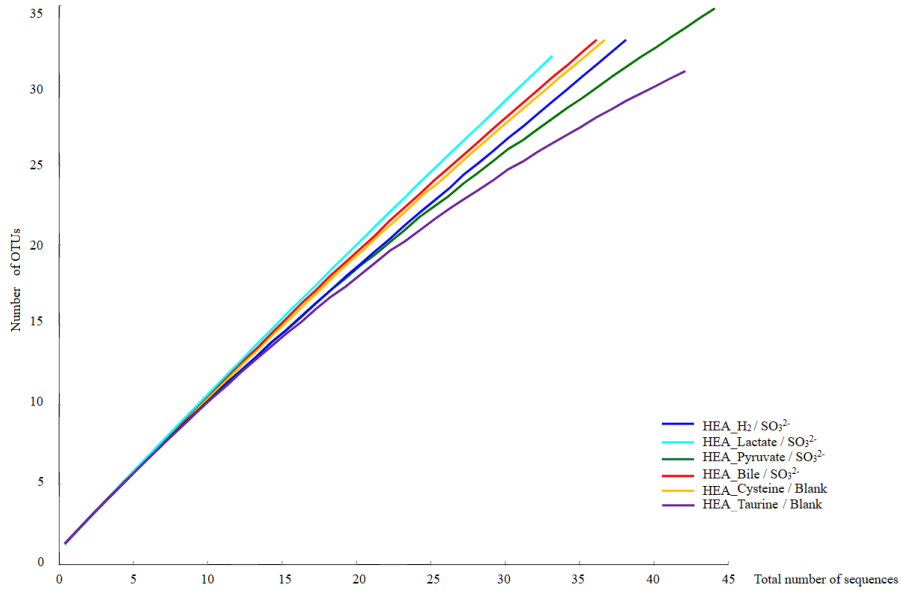

Fig. S1: Rarefaction curves of the 16S rRNA gene libraries of the healthy (HEA) donor selected enrichments.

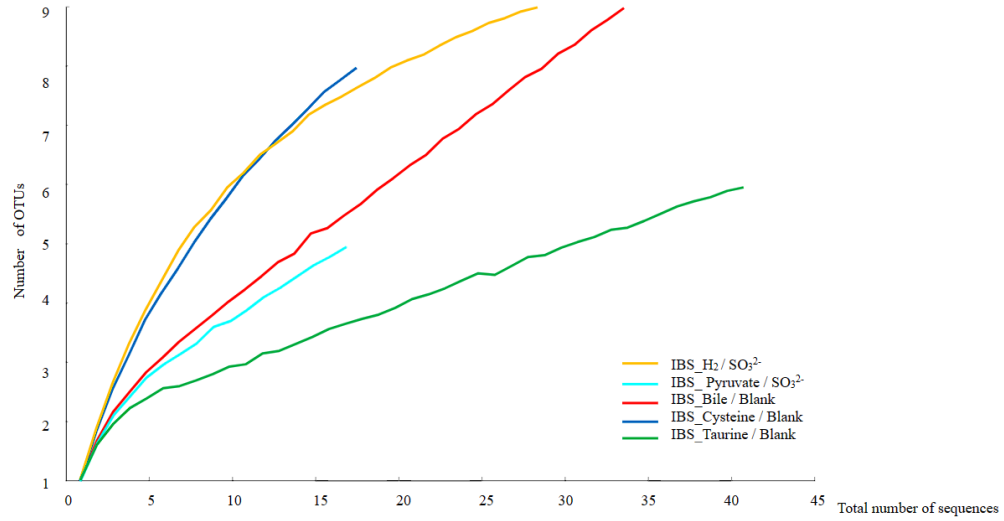

Fig. S2: Rarefaction curves of the 16S rRNA gene libraries of the Irritable bowel syndrome - diagnosed (IBS) donor selected enrichments.

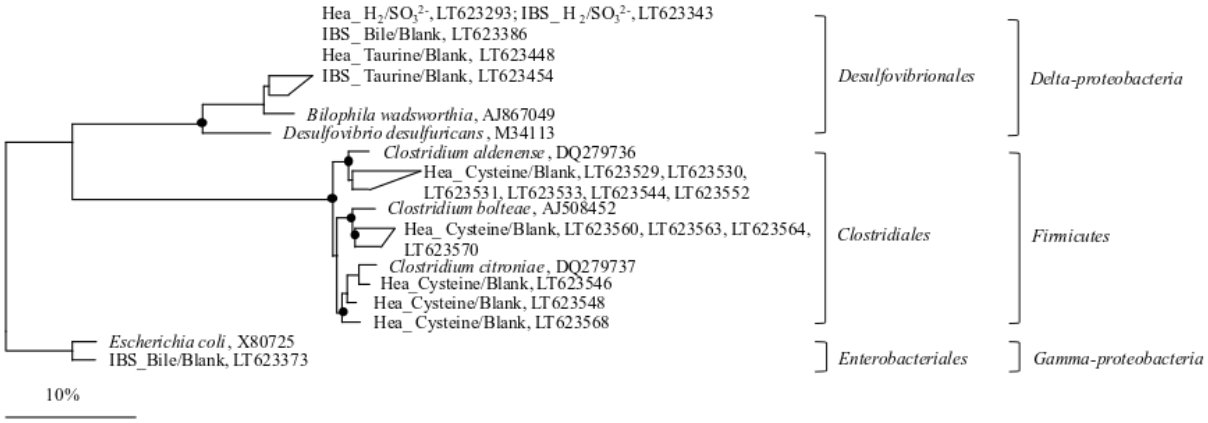

Fig S3. Phylogenetic reconstruction of 16S rRNA gene sequences of the enriched *Bilophila spp.* in HEA and IBS enrichments. Circles indicate bootstrap values higher than 70% (1,000 replicates). The scale bar represents the percentage of changes per nucleotide position.

Table S3: Selected metagenomes from IMG/MER of JGI database for datamining. HMC: human microbial communities; JCVI: J. Craig Venter Institute.

Study Name	**Genome Name / Sample Name**	**Sequencing Center**	**IMG Genome ID**
HMC from the National Institute of Health, USA, HMP production phase	Human stool microbial communities from NIH, USA - visit 2, subject 159247771	Washington University in St. Louis, Baylor College of Medicine, JCVI	7000000296
HMC from the National Institute of Health, USA, HMP production phase	Human stool microbial communities from NIH, USA - visit 1, subject 764224817	Washington University in St. Louis, Baylor College of Medicine, JCVI	7000000628
HMC from the National Institute of Health, USA, HMP production phase	Human stool microbial communities from NIH, USA - visit 2, subject 158337416	Washington University in St. Louis, Baylor College of Medicine, JCVI	7000000191
HMC from the National Institute of Health, USA, HMP production phase	Human stool microbial communities from NIH, USA - visit 1, subject 823052294	Baylor College of Medicine, Washington University in St. Louis, JCVI	7000000083
Human fecal microbial communities from Washington University at St. Louis, Missouri, USA, of twins	Human fecal microbial communities from Washington University at St. Louis, Missouri, USA, of twins - TS29	Washington University in St. Louis	3300003140
HMC from the National Institute of Health, USA, HMP production phase	Human stool microbial communities from NIH, USA - visit 1, subject 763860675	Baylor College of Medicine, Washington University in St. Louis, JCVI	7000000352
HMC from the National Institute of Health, USA, HMP production phase	Human stool microbial communities from the National Institute of Health, USA - subject 158499257, visit 2	Baylor College of Medicine, JCVI , Washington University in St. Louis	7000000187
HMC from the National Institute of Health, USA, HMP production phase	Human stool microbial communities from NIH, USA - visit 2, subject 809635352	Baylor College of Medicine, Washington University in St. Louis, JCVI	7000000320
HMC from the National Institute of Health, USA, HMP production phase	Human stool microbial communities from NIH, USA - visit 1, subject 158458797	Baylor College of Medicine, JCVI , Washington University in St. Louis	7000000693
HMC from the National Institute of Health, USA, HMP production phase	Human stool microbial communities from NIH, USA - visit 1, subject 675950834	Baylor College of Medicine, Washington University in St. Louis, JCVI	7000000188

HMC from the National Institute of Health, USA, HMP production phase	Human stool microbial communities from NIH, USA - visit 1, subject 764649650	Baylor College of Medicine, Washington University in St. Louis, JCVI	7000000272
HMC from the National Institute of Health, USA, HMP production phase	Human stool microbial communities from NIH, USA - visit 2, subject 159369152	Baylor College of Medicine, Washington University in St. Louis, JCVI	7000000587
Premature infant stool microbial communities from Comer Children's Hospital, University of Chicago, Illinois, USA	Premature infant stool microbial communities from Comer Children's Hospital, University of Chicago, Illinois, USA	University of California, Berkeley	3300003122
HMC from the National Institute of Health, USA, HMP production phase	Human stool microbial communities from NIH, USA - visit 2, subject 763597684	Baylor College of Medicine, JCVI , Washington University in St. Louis	7000000684
Human fecal microbial communities from Valencia, Spain, of healthy infants and adults	Gut Microbiota of 1 Month Old Human Infant	DOE Joint Genome Institute (JGI)	2018322000
HMC from the National Institute of Health, USA, HMP production phase	Human stool microbial communities from NIH, USA - visit 1, subject 404239096	Baylor College of Medicine, Washington University in St. Louis, JCVI	7000000372
HMC from the National Institute of Health, USA, HMP production phase	Human stool microbial communities from NIH, USA - visit 2, subject 764669880	JCVI , Washington University in St. Louis, Baylor College of Medicine	7000000582
HMC from the National Institute of Health, USA, HMP production phase	Human stool microbial communities from NIH, USA - visit 1, subject 765034022	Baylor College of Medicine, JCVI , Washington University in St. Louis	7000000407
HMC from the National Institute of Health, USA, HMP production phase	Human stool microbial communities from NIH, USA - visit 2, subject 764325968	JCVI , Baylor College of Medicine, Washington University in St. Louis	7000000297
HMC from the National Institute of Health, USA, HMP production phase	Human stool microbial communities from NIH, USA - visit number 3 of subject 763536994	Baylor College of Medicine, Washington University in St. Louis, JCVI	7000000630
HMC from the National Institute of Health, USA, HMP production phase	Human stool microbial communities from NIH, USA - visit 1, subject 763901136	Baylor College of Medicine, Washington University in St. Louis, JCVI	7000000332
HMC from the National Institute of Health, USA, HMP production phase	Human stool microbial communities from NIH, USA - visit 1, subject 764508039	Washington University in St. Louis, JCVI , Baylor College of Medicine	7000000075
HMC from the National Institute of Health, USA, HMP production phase	Human stool microbial communities from NIH, USA - visit 2, subject 763536994	Washington University in St. Louis, Baylor College of Medicine, JCVI	7000000145
HMC from the National Institute of Health, USA, HMP production phase	Human stool microbial communities from NIH, USA - visit 1, subject 159247771	Washington University in St. Louis, JCVI , Baylor College of Medicine	7000000213
HMC from the National Institute of Health, USA, HMP production phase	Human stool microbial communities from NIH, USA - visit 2, subject 763496533	JCVI , Washington University in St. Louis, Baylor College of Medicine	7000000516
HMC from the National Institute of Health, USA, HMP production phase	Human stool microbial communities from NIH, USA - visit 1, subject 763961826	Baylor College of Medicine, JCVI , Washington University in St. Louis	7000000715
HMC from the National Institute of Health, USA, HMP production phase	Human stool microbial communities from NIH, USA - visit 1, subject 765560005	Washington University in St. Louis, Baylor College of Medicine, JCVI	7000000526
HMC from the National Institute of Health, USA, HMP production phase	Human stool microbial communities from NIH, USA - visit 1, subject 159268001	Baylor College of Medicine, JCVI , Washington University in St. Louis	7000000045

HMC from the National Institute of Health, USA, HMP production phase	Human stool microbial communities from NIH, USA - visit 2 of subject 763759525	JCVI , Washington University in St. Louis, Baylor College of Medicine	7000000040
HMC from the National Institute of Health, USA, HMP production phase	Human stool microbial communities from NIH, USA - visit 2, subject 159510762	Baylor College of Medicine, JCVI , Washington University in St. Louis	7000000538
HMC from the National Institute of Health, USA, HMP production phase	Human stool microbial communities from NIH, USA - visit 2, subject 763435843	Baylor College of Medicine, JCVI , Washington University in St. Louis	7000000441
HMC from the National Institute of Health, USA, HMP production phase	Human stool microbial communities from NIH, USA - visit 1, subject 764325968	Washington University in St. Louis, JCVI , Baylor College of Medicine	7000000646
HMC from the National Institute of Health, USA, HMP production phase	Human stool microbial communities from NIH, USA - visit 2, subject 159005010	Washington University in St. Louis, JCVI , Baylor College of Medicine	7000000521
HMC from the National Institute of Health, USA, HMP production phase	Human stool microbial communities from NIH, USA - visit 1, subject 159146620	JCVI , Baylor College of Medicine, Washington University in St. Louis	7000000022
HMC from the National Institute of Health, USA, HMP production phase	Human stool microbial communities from NIH, USA - visit 1, subject 160603188	JCVI , Washington University in St. Louis, Baylor College of Medicine	7000000192
HMC from the National Institute of Health, USA, HMP production phase	Human stool microbial communities from NIH, USA - visit 2, subject 158924089	JCVI , Washington University in St. Louis, Baylor College of Medicine	7000000098
HMC from the National Institute of Health, USA, HMP production phase	Human stool microbial communities from NIH, USA - visit 2, subject 765094712	Washington University in St. Louis, Baylor College of Medicine, JCVI	7000000609
HMC from the National Institute of Health, USA, HMP production phase	Human stool microbial communities from NIH, USA - visit 1, subject 159369152	Washington University in St. Louis, Baylor College of Medicine, JCVI	7000000431
HMC from the National Institute of Health, USA, HMP production phase	Human stool microbial communities from NIH, USA - visit 1, subject 159510762	Washington University in St. Louis, JCVI , Baylor College of Medicine	7000000178
HMC from the National Institute of Health, USA, HMP production phase	Human stool microbial communities from NIH, USA - visit 1, subject 764487809	Washington University in St. Louis, Baylor College of Medicine, JCVI	7000000380
HMC from the National Institute of Health, USA, HMP production phase	Human stool microbial communities from NIH, USA - visit 2, subject 604812005	Baylor College of Medicine, JCVI , Washington University in St. Louis	7000000429
HMC from the National Institute of Health, USA, HMP production phase	Human stool microbial communities from NIH, USA - visit 2, subject 763982056	Baylor College of Medicine, JCVI , Washington University in St. Louis	7000000632
HMC from the National Institute of Health, USA, HMP production phase	Human stool microbial communities from NIH, USA - visit 2, subject 158944319	JCVI , Washington University in St. Louis, Baylor College of Medicine	7000000543
HMC from the National Institute of Health, USA, HMP production phase	Human stool microbial communities from NIH, USA - visit 2, subject 764487809	Baylor College of Medicine, JCVI , Washington University in St. Louis	7000000460
HMC from the National Institute of Health, USA, HMP production phase	Human stool microbial communities from NIH, USA - visit 2, subject 159268001	Baylor College of Medicine, JCVI , Washington University in St. Louis	7000000302
HMC from the National Institute of Health, USA, HMP production phase	Human stool microbial communities from NIH, USA - visit 1, subject 160158126	JCVI , Baylor College of Medicine, Washington University in St. Louis	7000000278
HMC from the National Institute of Health, USA, HMP production phase	Human stool microbial communities from NIH, USA - visit 2, subject 763678604	Baylor College of Medicine, Washington University in St. Louis, JCVI	7000000282

HMC from the National Institute of Health, USA, HMP production phase	Human stool microbial communities from NIH, USA - visit 1, subject 763982056	Baylor College of Medicine, Washington University in St. Louis, JCVI	7000000486
HMC from the National Institute of Health, USA, HMP production phase	Human stool microbial communities from NIH, USA - visit 2, subject 764184357	JCVI , Washington University in St. Louis, Baylor College of Medicine	7000000193

Table S4. Datamining of dissimilatory sulfite reductase in the selected metagenomes with scaffold ID and the phylogeny of the scaffolds analysed by IMG/MER database.

Scaffold ID	**Genome name**	**Scaffold ID**	**Genome name**
2018322000 assembled umic_TS1_000455_0273_2900	*Eubacterium siraeum*	2018322000 assembled umic_TS1_116366_0986_2558	*Clostridium novyi*
2018322000 assembled umic_TS1_001538_0804_2817	*Ruminococcus bromii*	2018322000 assembled umic_TS1_120538_1223_1860	*Anaerotruncus colihominis*
2018322000 assembled umic_TS1_002727_0608_3264	*Marvinbryantia formatexigens*	2018322000 assembled umic_TS1_129283_3465_1791	*Eubacterium biforme*
2018322000 assembled umic_TS1_004788_0515_2295	*Eubacterium eligens*	2018322000 assembled umic_TS1_135124_2604_2760	*Ruminococcus bromii*
2018322000 assembled umic_TS1_008067_0621_3154	*Eubacterium eligens*	2018322000 assembled umic_TS1_139862_3841_2353	*Desulfovibrio desulfuricans*
2018322000 assembled umic_TS1_011704_0668_0773	*Clostridium leptum*	2018322000 assembled umic_TS1_149725_2512_0709	*Collinsella stercoris*
2018322000 assembled umic_TS1_016180_2785_0475	*Clostridium bolteae*	2018322000 assembled umic_TS1_168091_2954_2571	*Bacteroides sp. D1*
2018322000 assembled umic_TS1_020153_1324_3035	*Prevotella bryantii*	2018322000 assembled umic_TS1_175498_0772_0765	*Alistipes shahii*
2018322000 assembled umic_TS1_039846_1341_0138	*Pseudoflavonifractor capillosus*	2018322000 assembled umic_TS1_176297_0457_0902	*Bacteroides sp. 20_3*
2018322000 assembled umic_TS1_064315_1663_1942	*Alkaliphilus metalliredigens*	2018322000 assembled umic_TS1_184962_2262_1237	*Faecalibacterium prausnitzii*
2018322000 assembled umic_TS1_071749_1776_0589	*Pyramidobacter piscolens*	2018322000 assembled umic_TS1_187937_1582_0804	*Faecalibacterium prausnitzii*
2018322000 assembled umic_TS1_084701_0400_1202	*Eubacterium eligens*	2018322000 assembled umic_TS1_225291_2573_1653	*Ruminococcus obeum*
2018322000 assembled umic_TS1_087367_0890_1850	*Faecalibacterium prausnitzii*	2018322000 assembled umic_TS1_227875_0508_2104	*Anaerococcus hydrogenalis*
2018322000 assembled umic_TS1_099574_2094_1421	*Eubacterium siraeum*	2018322000 assembled umic_TS1_245936_1189_2305	*Anaerotruncus colihominis*
2018322000 assembled umic_TS1_108211_1435_0923	*Pyramidobacter piscolens*	2018322000 assembled umic_TS1_259717_1724_3474	*Subdoligranulum variabile*
2018322000 assembled umic_TS1_109505_3591_0759	*Thermosinus carboxydivorans*	2018322000 assembled umic_TS1_270728_0835_1248	*Blautia hydrogenotrophica*
2018322000 assembled umic_TS1_113232_0239_2613	*Faecalibacterium prausnitzii*	2018322000 assembled umic_TS1_277490_1401_3076	*Clostridium methylpentosum*
2018322000 assembled umic_TS1_000455_0273_2900	*Eubacterium siraeum*	2018322000 assembled umic_TS1_116366_0986_2558	*Clostridium novyi*
2018322000 assembled umic_TS1_001538_0804_2817	*Ruminococcus bromii*	2018322000 assembled umic_TS1_120538_1223_1860	*Anaerotruncus colihominis*
2018322000 assembled umic_TS1_002727_0608_3264	*Marvinbryantia formatexigens*	2018322000 assembled umic_TS1_129283_3465_1791	*Eubacterium biforme*

2018322000 assembled umic_TS1_004788_0515_2295	*Eubacterium eligens*	2018322000 assembled umic_TS1_135124_2604_2760	*Ruminococcus bromii*
2018322000 assembled umic_TS1_008067_0621_3154	*Eubacterium eligens*	2018322000 assembled umic_TS1_139862_3841_2353	*Desulfovibrio desulfuricans*
2018322000 assembled umic_TS1_011704_0668_0773	*Clostridium leptum*	2018322000 assembled umic_TS1_149725_2512_0709	*Collinsella stercoris*
2018322000 assembled umic_TS1_016180_2785_0475	*Clostridium bolteae*	2018322000 assembled umic_TS1_168091_2954_2571	*Bacteroides sp. D1*
2018322000 assembled umic_TS1_114499_3176_0885	*Thermoanaerobacter italicus*	2018322000 assembled umic_TS1_277645_1195_1112	*Faecalibacterium prausnitzii*
2018322000 assembled umic_TS1_302474_3035_3276	*Clostridium phytofermentans*	2018322000 assembled umic_TS1_284403_1010_2205	*Akkermansia muciniphila*
2018322000 assembled umic_TS1_304619_0266_3345	*Desulfovibrio desulfuricans*	3300003109 assembled Ga0051163_100005	*Citrobacter freundii*
2018322000 assembled umic_TS1_330939_3154_3712	*Clostridium methylpentosum*	3300003122 assembled Ga0052257_104791	*Escherichia coli*
2018322000 assembled umic_TS1_331107_0246_2062	*Ruminococcaceae bacterium D16*	3300003122 assembled Ga0052257_107807	*Escherichia coli*
2018322000 assembled umic_TS1_341040_1802_3389	*Desulfovibrio desulfuricans*	3300003122 assembled Ga0052257_116006	*Clostridium bartlettii*
2018322000 assembled umic_TS1_344529_3103_0445	*Desulfovibrio piger*	3300003140 assembled Ga0051081_1002631	*[Clostridium] leptum*
2018322000 assembled umic_TS1_346558_3746_1393	*Heliobacterium modesticaldum*	3300003140 assembled Ga0051081_1012999	*Ruminococcus sp.*
2018322000 assembled umic_TS1_357275_0783_0394	*Parabacteroides distasonis*	3300003140 assembled Ga0051081_1013280	*Ruminococcus sp.*
2018322000 assembled umic_TS1_363782_2361_2202	*Eubacterium eligens*	7000000022 assembled C852947	*Eubacterium hallii*
2018322000 assembled umic_TS1_367941_1120_2290	*Ruminococcus obeum*	7000000022 assembled C859441	*Fibrobacter succinogenes*
2018322000 assembled umic_TS1_374759_3033_1565	*Pseudoflavonifractor capillosus*	7000000022 assembled C861958	*Eubacterium rectale*
2018322000 assembled umic_TS1_394171_0612_1732	*Bilophila wadsworthia*	7000000022 assembled C891096	*Eubacterium eligens*
2018322000 assembled umic_TS1_421085_2533_0852	*Clostridium cf. saccharolyticum*	7000000022 assembled C893774	*Eubacterium rectale*
2018322000 assembled umic_TS1_431017_2978_2633	*Clostridium bolteae*	7000000022 assembled SRS011452_WUGC_scaffold_12720	*Fibrobacter succinogenes*
7000000075 assembled C1074123	*Eubacterium rectale*	7000000045 assembled C2374690	*Fibrobacter succinogenes*
7000000075 assembled C1154792	*Clostridium perfringens*	7000000045 assembled C2388278	*Anaerofustis stercorihominis*
7000000083 assembled C15394891	*Roseburia intestinalis*	7000000045 assembled C2394400	*Roseburia intestinalis*
7000000083 assembled C15444658	*Ruminococcus obeum*	7000000045 assembled C2577036	*Fibrobacter succinogenes*
2018322000 assembled umic_TS1_114499_3176_0885	*Thermoanaerobacter italicus*	2018322000 assembled umic_TS1_277645_1195_1112	*Faecalibacterium prausnitzii*
2018322000 assembled umic_TS1_302474_3035_3276	*Clostridium phytofermentans*	2018322000 assembled umic_TS1_284403_1010_2205	*Akkermansia muciniphila*
2018322000 assembled umic_TS1_304619_0266_3345	*Desulfovibrio desulfuricans*	3300003109 assembled Ga0051163_100005	*Citrobacter freundii*

7000000083 assembled C15490576	*Meiothermus silvanus*	7000000045 assembled C2631239	*Eubacterium rectale*
7000000083 assembled C15580659	*Eubacterium rectale*	7000000187 assembled SRS022609_Baylor_scaffold_2 2472	*Roseburia intestinalis*
7000000083 assembled SRS049712_WUGC_scaffold_ 10550	*Fibrobacter succinogenes*	7000000191 assembled C2786512	*Eubacterium hallii*
7000000093 assembled C1631516	*Blautia hansenii*	7000000191 assembled C2904094	*Desulfovibrio desulfuricans*
7000000093 assembled C1648424	*Eubacterium hallii*	7000000191 assembled C3055394	*Coprococcus eutactus*
7000000093 assembled C1720582	*Clostridium sp. 7_2_43FAA*	7000000191 assembled C3060228	*Fibrobacter succinogenes*
7000000093 assembled SRS022137_LANL_scaffold_1 1642	*Eubacterium rectale*	7000000193 assembled SRS048870_WUGC_scaffold_2 9029	*Eubacterium rectale*
7000000093 assembled SRS022137_LANL_scaffold_2 7719	*Roseburia intestinalis*	7000000200 assembled C2911461	*Ruminococcus obeum*
7000000098 assembled C898737	*Clostridium perfringens*	7000000200 assembled C2982154	*Fibrobacter succinogenes*
7000000145 assembled C2652125	*Ruminococcus obeum*	7000000200 assembled C2988834	*Clostridium scindens*
7000000145 assembled C2731597	*Ruminococcus obeum*	7000000200 assembled C3228089	*Fibrobacter succinogenes*
7000000145 assembled SRS050422_LANL_scaffold_3 2893	*Ruminococcus obeum*	7000000213 assembled C3519879	*Eubacterium eligens*
7000000145 assembled SRS050422_LANL_scaffold_8 0494	*Roseburia intestinalis*		

Table S5. Datamining of cysteine desulfhydrase in the selected metagenomes with scaffold ID and the phylogeny of the scaffolds analysed by IMG/MER database.

Scaffold ID	**Genome name**	**Scaffold ID**	**Genome name**
7000000045 assembled SRS013687_Baylor_scaffold_4 3105__gene_78161	*Oscillibacter* sp. PC13	7000000380 assembled C3048042__gene_225462	*Blautia producta* DSM 2950
7000000045 assembled SRS013687_Baylor_scaffold_4 7459__gene_88290	*Oscillibacter* sp. PC13	7000000380 assembled C3100542__gene_251215	*Acholeplasma brassicae* 0502, ATCC 49388
7000000083 assembled C15421147__gene_71545	*Clostridiales bacterium* VE202-28	7000000380 assembled SRS015663_WUGC_scaffold_1 2335__gene_27384	*Oscillibacter* sp. PC13
7000000083 assembled C15430985__gene_76984	*Clostridium citroniae* WAL-19142	7000000380 assembled SRS015663_WUGC_scaffold_3 7405__gene_84955	*Oscillibacter* sp. PC13
7000000093 assembled C1770295__gene_138951	*Oscillibacter* sp. PC13	7000000380 assembled SRS015663_WUGC_scaffold_3 7445__gene_85053	*Oscillibacter* sp. PC13
7000000093 assembled SRS022137_LANL_scaffold_2 3862__gene_54640	*Oscillibacter* sp. PC13	7000000429 assembled C1888561__gene_72758	*Blautia producta* DSM 2950

7000000145 assembled C2528668__gene_185320	*Clostridium hathewayi* DSM 13479	7000000443 assembled C2873542__gene_225561	*Prevotella nigrescens* F0103
7000000145 assembled C2565700__gene_196902	*Clostridium citroniae* WAL-19142	7000000443 assembled C2885665__gene_231312	*Johnsonella ignava* ATCC 51276
7000000145 assembled C2626701__gene_215696	*Bilophila wadsworthia* ATCC 49260	7000000443 assembled SRS058808_LANL_scaffold_51626__gene_65124	*Streptococcus sanguinis* SK330
7000000145 assembled C2651217__gene_223244	*Oscillibacter* sp. PC13	7000000526 assembled C1354625__gene_113590	*Rhodocyclaceae bacterium* EBPR_Bin_590
7000000145 assembled SRS050422_LANL_scaffold_44221__gene_68069	*Bilophila wadsworthia* 3_1_6	7000000526 assembled C1358430__gene_114740	*Oscillibacter* sp. PC13
7000000187 assembled C3320934__gene_307708	*Clostridia bacterium* UC5.1-1A9	7000000526 assembled C1453488__gene_139311	*Clostridium hathewayi* DSM 13479
7000000187 assembled SRS022609_Baylor_scaffold_47539__gene_74120	*Oscillibacter* sp. PC13	7000000526 assembled SRS019397_WUGC_scaffold_19568__gene_56571	*Faecalibacterium cf. prausnitzii* KLE1255
7000000187 assembled SRS022609_Baylor_scaffold_79510__gene_136601	*Oscillibacter* sp. PC13	7000000538 assembled C1517792__gene_112346	*Clostridium symbiosum* WAL-14673
7000000188 assembled C2281974__gene_181773	*Blautia producta* DSM 2950	7000000538 assembled C1521723__gene_113746	*Clostridiales bacterium* VE202-16
7000000191 assembled C2956454__gene_131948	*Oscillibacter* sp. KLE 1745	7000000538 assembled C1532025__gene_117414	*Blautia producta* DSM 2950
7000000193 assembled C1790019__gene_153486	*Dickeya paradisiaca* NCPPB 2511	7000000628 assembled C3235750__gene_166640	*Blautia producta* DSM 2950
7000000193 assembled SRS048870_WUGC_scaffold_13672__gene_22170	*Oscillibacter* sp. PC13	7000000628 assembled C3364509__gene_226405	*Oscillibacter* sp. KLE 1745
7000000200 assembled C2986268__gene_132318	*Oscillibacter* sp. PC13	7000000633 assembled C2256074__gene_169844	*Oscillibacter* sp. PC13
7000000200 assembled C3069310__gene_169609	*Candidatus Bathyarchaeota archaeon* BA1 Ga0136912	7000000633 assembled C2256480__gene_170010	*Clostridium citroniae* WAL-19142
7000000278 assembled C4637617__gene_88993	*Clostridiales bacterium* VE202-16	7000000633 assembled C2373771__gene_221258	*Oscillibacter* sp. PC13
7000000282 assembled C8104706__gene_69405	*Clostridium citroniae* WAL-19142	7000000684 assembled C2996794__gene_216569	*Oscillibacter* sp. PC13
7000000282 assembled C8215981__gene_117774	*Fusobacterium* sp. 12_1B	7000000684 assembled C3020466__gene_224139	*Oscillibacter* sp. PC13
7000000282 assembled C8265087__gene_140157	*Oscillibacter* sp. PC13	7000000684 assembled C3059850__gene_236554	*Oscillibacter* sp. KLE 1745
7000000740 assembled C2525226__gene_260093	*Caminicella sporogenes* DSM 14501	7000000684 assembled C3140651__gene_261016	*Clostridium symbiosum* WAL-14673
7000000740 assembled SRS064276_LANL_scaffold_26155__gene_53887	*Clostridium hathewayi* DSM 13479	7000000684 assembled SRS019582_WUGC_scaffold_41912__gene_52385	*Clostridiales bacterium* VE202-16

7000000740 assembled SRS064276_LANL_scaffold_26155__gene_53888	*Clostridium citroniae* WAL-19142	7000000684 assembled SRS019582_WUGC_scaffold_58990__gene_79608	*Clostridiales bacterium* VE202-16
7000000715 assembled SRS014683_WUGC_scaffold_23284__gene_33239	*Blautia producta* DSM 2950	7000000684 assembled SRS019582_WUGC_scaffold_91014__gene_143205	*Oscillibacter* sp. PC13
7000000740 assembled C2275846__gene_171230	*Ruminococcaceae* bacterium 585-1	7000000715 assembled SRS014683_WUGC_scaffold_10626__gene_14997	*Escherichia coli* 907357
7000000740 assembled C2308799__gene_183087	*Escherichia coli* 907357	7000000715 assembled SRS014683_WUGC_scaffold_15048__gene_21737	*Megasphaera elsdenii* 14-14
7000000740 assembled C2326003__gene_189179	*Oscillibacter* sp. PC13	7000000740 assembled C2518184__gene_257521	*Blautia producta* DSM 2950
7000000740 assembled C2362048__gene_202025	*Clostridium citroniae* WAL-19142		

Chapter 3: *Eubacterium maltosivorans* sp. nov., a novel human intestinal acetogenic and butyrogenic bacterium with a versatile metabolism

This chapter has been published as:

Feng, Y., Stams, A. J., Sánchez-Andrea, I., & De Vos, W. M. (2018). "*Eubacterium maltosivorans* sp. nov., a novel human intestinal acetogenic and butyrogenic bacterium with a versatile metabolism." International Journal of Systematic and Evolutionary Microbiology, **68**(11), 3546-3550.

Abstract

A novel anaerobic, non-spore-forming bacterium was isolated from a fecal sample of a healthy adult. The isolate, designated strain YI^T, was cultured in a basal liquid media under the gas phase of H_2/CO_2 supplemented with 0.1 g/L yeast extract. Cells of strain YI^T were short rods (0.4–0.7 x 2.0–2.5 μm), appearing singly or in pairs and stained Gram-positive. Catalase activity and gelatin hydrolysis were positive while oxidase activity, indole formation, urease activity and esculin hydrolysis were negative. Growth was observed within a range of 20 to 45 °C (optimum, 35-37 °C), and a pH range of 5.0 to 8.0 (optimum 7.0-7.5). Doubling time was 2.3 h when grown with glucose at pH 7.2, 37 °C. Besides acetogenic growth, the isolate can ferment a large range of monomeric sugars with acetate and butyrate as the main end products. Strain YI^T did not show respiratory growth with sulfate, sulfite, thiosulfate or nitrate as electron acceptors. The major cellular fatty acids of the isolate were $C_{16:0}$ (44.5%) and $C_{18:0}$ (10.4%). The genomic DNA G+C content was 47.8 mol%. Strain YI^T is affiliated to the genus *Eubacterium*, sharing highest levels of 16S rRNA gene similarity with *Eubacterium limosum* ATCC 8486^T (97.3%), *Eubacterium callanderi* DSM 3662^T (97.5%), *Eubacterium aggregans* DSM 12183^T (94.4%) and *Eubacterium barkeri* DSM 1223^T (94.8%). Considering the physiological and phylogenetic characteristics, strain YI^T represents a novel species within the genus *Eubacterium*, for which the name *Eubacterium maltosivorans* sp. nov. is proposed. The type strain is YI^T (=DSM 105863^T =JCM 32297^T).

The human intestinal tract is colonized by billions of commensal microorganisms that represent over a thousand species contributing to either health or disease. Among others, intestinal microbes convert undigested carbohydrates mainly into short chain fatty acids, such as butyrate, propionate and acetate (Qin, Li, *et al.*, 2010; Flint *et al.*, 2012; Rajilić-Stojanović and de Vos, 2014). As the colonic fermentations are generally anaerobic, redox balancing often involves the production of hydrogen, which can also be consumed by methanogens, sulfur compounds respirers or homoacetogenic bacteria (Gibson *et al.*, 1993)

In the course of a study to enrich sulfidogenic bacteria from the human gut (approved by CCMO Netherlands, project ID: NL2907008109), we isolated a novel acetogenic bacterial strain (strain YI^T) showing 97.3% 16S rRNA gene similarity with that of *Eubacterium limosum* ATCC 8486^T (Y. Feng *et al.*, 2017). Strain YI^T was enriched under anaerobic conditions in a basal liquid medium prepared according to Stams *et al.* (1993) supplemented with 5 mM Na_2SO_3, 0.1 g/L yeast extract (BD BBL™) and H_2/CO_2 (80:20, v/v, 1.7 atm) in the gas phase. Throughout the enrichment, sulfite was not reduced but H_2 and CO_2 were consumed, and acetate was produced. Subsequently, a pure culture was obtained by a combination of serial dilution and plating on solidified media, with 1% Noble agar (Sigma-Aldrich), under 1.7 atm of H_2/CO_2 (80:20, v/v).

Cell morphology, motility, Gram-staining and spore formation were studied using phase-contrast microscopy using a ZEISS AXIO Scope A1. Gram-staining was performed according to standard procedures (Doetsch, 1981). Survival due to spore formation was checked by placing the cultivation bottle in 80 °C water bath for 20 min. The oxidase and catalase activities were tested as described by Florentino *et al.* (2016). Indole and urease formation, as well as gelatin and esculin hydrolysis were examined in duplicate by the API® 20 A test (bioMérieux) according to the manufacturer's instructions.

To determine temperature range and optimum, strain YI^T was grown in the basal medium supplemented with 20 mM glucose under 1.7 atm of N_2/CO_2 (80:20, v/v) gas phase without yeast extract and incubated up to 6 weeks with the temperature range from 15 to 60 °C

(in 5 °C intervals, 37 °C was tested as well) at pH 7.2. The optimum pH was tested in the same medium at 37 °C but bicarbonate and N_2/CO_2 was omitted. Different buffer systems were employed at different pH range and gas phase contained only N_2. For pH higher than 7.0, 20 mM TRIS was used; for pH 6 to 7.5, 20 mM PIPES was added; and for pH 6 to 4, 20 mM citrate/phosphate was employed. Hence, the pH ranging from 4.0 to 8.5 was tested with 0.5 intervals, incubated at 37 °C up to 6 weeks. Both temperature and pH tests were run in triplicate.

To explore the physiological properties of strain YI^T, a variety of substrates including sugars, organic acids, amino acids and sugar alcohols (see Table 1) were added to the basal medium to a final concentration of 20 mM without yeast extract, unless mentioned otherwise. Cultures were incubated under 1.7 atm of N_2/CO_2 (80:20, v/v) at 37 °C and pH 7.2. Each incubation was performed in triplicate. Soluble corn starch and betaine were tested at a final concentration of 5 g/L supplied with 0.1 g/L yeast extract in the basal medium. When hydrogen was used as a substrate, the headspace was at 1.7 atm with H_2/CO_2 (80:20, v/v) and the medium was supplemented with 0.5 g/L yeast extract. Carbon monoxide (40%) was tested as an energy source by exchanging the N_2/CO_2 in the headspace with filter sterilized CO. The headspace was kept at 1.7 atm and the medium was supplemented with 0.5 g/L yeast extract. Negative controls without substrate were included and showed no growth. Sulfate (20 mM), thiosulfate (20 mM), sulfite (5 mM) and nitrate (10 mM) were tested as electron acceptors. For this, six different electron donors were tested due to their relevance for the human intestinal tract: acetate, butyrate, propionate, lactate, pyruvate at a concentration of 10 mM, and H_2 at 1.7 atm of H_2/CO_2 (80:20, v/v). For all physiological tests, products were quantified by high-performance liquid chromatograph (HPLC) with a Varian Metacarb 67H 300 mm column and sulfuric acid (0.01 N) eluent at a flow rate of 0.8 mL min^{-1}. Hydrogen was measured by a gas chromatograph (Shimadzu, Kyoto, Japan) as described by Florentino *et al.* (2015). Sulfate, thiosulfate and sulfite were analyzed using a Dionex 1000 ion chromatograph unit (Dionex, Waltham, USA) equipped with an IonPac AS17 Anion-Exchange column operating with a 0.1 mL min^{-1} flow rate at 30 °C. Hydrogen sulfide was measured by a methylene blue method (Cline, 1969). First, H_2S, HS^- and S^{2-} were fixed by a 5% (w/v) $ZnCl_2$ solution. Then, ZnS

deposition was re-dissolved by an acid N, N-dimethyl-p-phenylenediamine solution, and simultaneously a ferriammonium sulfate solution was added to generate methylene blue. Reagents were prepared according to Cline (1969).The amount of sulfide was determined by a spectrophotometer after the reaction was fully developed.

To study the differences of the cellular fatty acid composition, strain YI^T and *E. limosum* ATCC 8486^T were incubated under the same condition (20 mM fructose with 0.5 g/L yeast extract) for 2 days. Cells were harvested and analysis was performed at the Identification Service of the Deutsche Sammlung von Mikroorganismen und Zellkulturen (DSMZ).

To obtain the genomic DNA, strain YI^T was grown in the aforementioned basal medium containing 20 mM glucose under 1.7 atm of N_2/CO_2 (80:20, v/v) for 48 hours at 37 °C. The biomass was harvested by centrifugation at 13000 g for 5 min at 4 °C. Genomic DNA was isolated by MasterPure™ (Epicentre) and purified by Wizard® Genomic DNA Purification Kit (Promega) following the manufacturers' instructions. Illumina MiSeq sequencing was performed at GATC Biotech and assembled using the Edena v3.130110 and IDBA-UD v1.1.1 assemblers and merged (Peng *et al.*, 2012; Chun *et al.*, 2018). The assembled draft genome had a size of 4.5 Mbp and the sequence has been deposited at GenBank under the accession GCA_002441855.1. The 16S rRNA gene sequence (1,512 bp) was obtained from the draft genome and deposited at GenBank under the accession number MG015881. To check whether was any heterogeneity between 16S rRNA genes operons, a PCR amplicon of the 16S rRNA genes was sequenced by Sanger sequencing (performed by GATC Biotech, Germany). This 1288-bp sequence (deposited at NCBI with accession number MH400075) was found to be identical except for 1 mismatch with that obtained by the Illumina sequencing. Later, the whole 16S rRNA sequence of strain YI^T was aligned using the SINA online alignment tool (version 1.2.11) (Pruesse *et al.*, 2012; Quast *et al.*, 2012) and then merged with the Silva SSU Ref database (release 111) (Quast *et al.*, 2012). The phylogenetic tree was constructed in the ARB software package (v. 6) using the neighbor-joining algorithm (Ludwig *et al.*, 2004). The G+C content of the DNA was determined based on the draft genome obtained by Illumina

sequencing. The average nucleotide identity (ANI) and the *in-silico* DNA-DNA hybridization (DDH) data were calculated by the online tools developed by Environmental Microbial Genomics Laboratory (Rodriguez-R and Konstantinidis, 2016) and DSMZ (Auch *et al.*, 2010), respectively. The draft or complete genomes of *E. limosum* ATCC 8486^T, strain KIST 612, strain SA11 and *E. callanderi* DSM 3662^T as deposited at NCBI under numbers GCA_000807675.2, NC_014624.2, GCA_001481725.1 and GCA_900142645.1 were used for the ANI and *in-silico* DDH analysis.

Cells of strain YI^T were short rods, 0.4–0.7 x 2–2.5 μm in size, non-motile, appearing singly or in pairs, rarely in chains [Fig. S1(a)]. Spores were never detected by phase contrast microscope in growing or stationary cultures, or in cultures that had been heated at 80 °C for 20 min. Cells stained Gram-positive [Fig. S1(b)]. Catalase activity was positive. Oxidase and urease activities were negative, indole formation and esculin hydrolysis were absent, but gelatin hydrolysis occurred. The predominant components of the cellular fatty acids of the isolate were $C_{16:0}$ (44.5%) and $C_{18:0}$ (10.4%). The main differences compared to that of the *E. limosum* type strain were the different proportional abundancies of $C_{18:0}$ (4.6%) and $C_{14:0}$ (16.8%) (Table 1).

Strain YI^T grew from 20-45 °C, with an optimum at 35-37 °C. It can grow from pH 5.0-8.0, but best at pH 7.0-7.5. The doubling time when grown at optimal pH and temperature with glucose was 2.3 h, and 2.5 h with fructose. Strain YI^T fermented a large range of monomeric sugars besides acetogenic growth with H_2/CO_2 (Table 1). When sugars were fermented, acetate, butyrate and H_2 were the principle end products, while growing with H_2/CO_2 and CO, acetate was the only product. Strain YI^T was also capable of fermenting cysteine releasing acetate and hydrogen sulfide. The strain was not able to reduce sulfate, thiosulfate, sulfite and nitrate. Physiologically, strain YI^T can be distinguished from the type strain of *E. limosum* by its ability to ferment maltose, sucrose, mannose and raffinose.

Table 1. Selected physiological and biochemical characteristics that differentiate strain YI^T from its closest described relatives. The major fatty acids are shown in bold. *, data for *E. limosum* ATCC 8486^T were from reported previously (Moore and Cato, 1965) (except otherwise indicated). §, data from this study; +, positive; -, negative; w, weak (after 5 days less than 3 mM of substrates were consumed). Both strains stained Gram-positive, and were non-motile, non-spore-formers. Both strains were able to use H_2/CO_2, CO, glucose, fructose, ribose, lactate, pyruvate, mannitol, erythritol, vanillate, cysteine, betaine and showed weak growth on soluble starch, but not lactose, arabinose, cellobiose, galactose, rhamnose, melibiose, succinate, glycine, serine, glycerol and ethanol.

Characteristics	***E. limosum* ATCC 8486^T***	**Strain YI^{T§}**
Growth Temperature	25-45	20-45
(optimal, °C)	(30-37)	(35-37)
pH range	5.0-8.0	5.0-8.0
(optimal)	(7.0-7.2)	(7-7.5)
DNA G+C content (mol%)	47.2	47.8
Genome size (Mbp)	4.37	4.58
Sugars		
D-xylose	w§	-
Maltose	-§	+
Mannose	-§	+
Sucrose	-§	+
Raffinose	-	+
Acids		
Formate	w	w
Vanillate	+§	+
Alcohol		
Methanol	+	w
Cellular fatty acids (%)	***E. limosum* ATCC 8486^{T§}**	**Strain YI^{T§}**
Saturated straight-chain		
12:0	0.3	0.2
14:0	**16.8**	6.3
14:0 DMA	1.1	0.1
16:0	**38.6**	**44.5**
16:0 aldehyde	3.8	3.0
16:0 DMA	**9.6**	**9.1**
18:0	4.6	**10.5**
18:0 aldehyde	0.6	1.5
18:0 DMA	1.0	3.3
20:0	0.3	1.1
Unsaturated straight-chain		
16:1 w5c	0.2	0.7
16:1 w7c	1.7	1.2
16:1 w7c DMA	0.8	0.2
18:1 w7c	**8.1**	**7.7**

18:1 w7c DMA	1.3	0.9
Saturated branched-chain		
15:0	0.3	0.2
15:0 anteiso	0.2	-
15:0 iso	0.2	-
17:0 cyclopropane	1.4	0.8
17:0 cyclo DMA	0.2	0.1
19 cycloprop-11,12	**6.1**	**7.2**
19 cyclo 11,12 DMA	1.2	1.7

Phylogenetic analysis showed that strain YI^T is located in the *Eubacterium* genus of the *Eubacteriaceae* family (order *Clostridiales*, *Clostridia* class, *Firmicutes* phylum), sharing highest levels of 16S rRNA gene similarity with *Eubacterium limosum* KIST 612 (98.3%) (Chang *et al.*, 1997), *Eubacterium limosum* ATCC 8486^T (97.3%), *Eubacterium callanderi* DSM 3662^T (97.5%), *Eubacterium aggregans* DSM 12183^T (94.4%) and *Eubacterium barkeri* DSM 1223^T (94.8%) (Figure 1). The *Eubacteriaceae* family also includes *Acetobacterium* spp., that are well known for their ability to grow on C1 compounds. However, species of the *Eubacterium* genus can utilize a larger range of substrates, including hexoses, pentoses, alcohols, and some amino acids. Moreover, the fermentative growth leads to acetate and butyrate as products. The type species of the genus *Eubacterium* was first designated as *Eubacterium foedans* (Skerman *et al.*, 1980), which was isolated by Klein (1908) from spoiled hams. Later, Cato *et al*. (1981) proposed *E. limosum* as the type species because no cultures of *E. foedans* were extant, and this request was approved in 1983. The type strain of *E. limosum* was first isolated from human feces (Eggerth, 1935). Later this bacterium was commonly found in many other ecosystems (Eggerth, 1935). *E. limosum* is known for its capability of converting C1 compounds like CO, H_2/CO_2, formate and methanol, as well lactate, hexoses, pentoses and some more complex carbohydrates into acetate, ethanol or butyrate (Genthner *et al.*, 1981). The closest relative of *E. limosum* is *E. callanderi*, sharing 99.5% 16S rRNA gene sequence similarity. *E. callanderi* differs from *E. limosum* in that it cannot utilize H_2/CO_2, CO, methanol, or other one-carbon compounds. Moreover, *E. callanderi* cannot grow on glucose without a

supply of acetate in a defined medium, whereas this is not the case for *E. limosum* (Mountfort *et al.*, 1988).

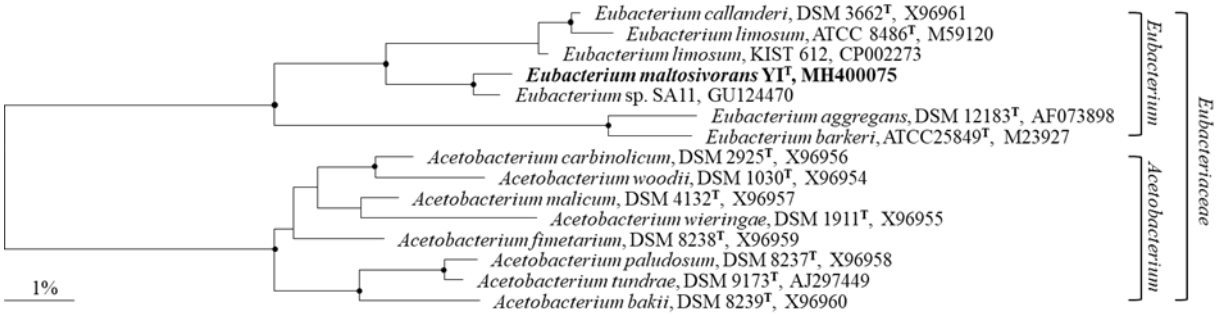

Figure 1. Neighbor-joining tree showing the phylogenetic affiliation of strain YI^T to other representatives of the family *Eubacteriaceae* based on 16S rRNA gene sequence calculated with Jukes-Cantor correction in ARB. Phylogenetic tree was rooted with *Escherichia coli*, which was removed afterwards. The bar indicates 1% sequence divergence. Bootstrap values greater than 90% (1000 replicates) are indicated by filled circles.

Because of the phylogenetic similarity and acetogenic growth characteristics of the new strain YI^T and *E. limosum,* we compared the physiological and biochemical properties of strain YI^T with that of *E. limosum* ATCC 8486^T (Table 1). The substrate utilization of strain YI^T included maltose, sucrose, mannose as well as raffinose, which all could not be used by *E. limosum*. However, *E. limosum* could use xylose in contrast to strain YI^T. The *in-silico* ANI and DDH values of the genomes of strain YI^T and the *E. limosum* ATCC 8486^T were considerably different, calculated to be 89.2% and 38.6% respectively. Both values are well below the cut-off values for novel species [< 95-96% and < 70 %, respectively, (Richter and Rosselló-Móra, 2009; Tindall *et al.*, 2010)] (Table S1). Similarly, the same applied for the *in-silico* ANI and DDH values of the genomes of strain YI^T and the *E. callanderi* DSM 3662^T (89.7% and 39.7% respectively. See Table S1). Hence, we conclude that strain YI^T differs genotypically and physiologically from the type strain of *E. limosum* ATCC 8486^T and hence belongs to a novel species. The genome of strain YI^T shares approximately 86% sequence similarity (Table S1) with that of the recently reported but not publicly deposited strain SA11, isolated from the rumen of a New Zealand sheep (Kelly *et al.*, 2016). Based on these considerations, we propose that strain YI^T represents a novel species *Eubacterium maltosivorans* sp. nov., within the genus of *Eubacterium*.

Description of *Eubacterium maltosivorans* sp. nov.

Eubacterium maltosivorans (mal.to.si.vo'rans. N.L. neut. n. *maltosum* maltose; L. pres. part. *vorans* eating; N.L. part. adj. *maltosivorans* maltose eating).

Cells are non-motile, non-spore forming, and stained Gram-positive. Short rods (0.4–0.7 x 2.0–2.5 μm) appearing singly and in pairs, rarely in chains when grown with glucose. Catalase activity and gelatin hydrolysis were positive. Oxidase and urease activity, indole formation and esculin hydrolysis were negative. The temperature range is 20-45 °C, with optimum 35-37 °C. The pH range is 5.0-8.0, with optimum 7.0-7.5. Yeast extract was only essential when strain YI^T grew with H_2/CO_2. It utilizes glucose, fructose, ribose, maltose, mannose, sucrose, raffinose, lactate, pyruvate, sorbitol, erythritol and betaine. Fermentative growth with sugars occurs leading to production of acetate, butyrate and hydrogen. It ferments cysteine releasing sulfide and acetate. It does not use xylose, lactose, arabinose, cellobiose, galactose, rhamnose, melibiose, formate, succinate, glycine, serine, glycerol or ethanol. No respiratory metabolism was detected. The G+C content of the genomic DNA is 47.8 mol%. The type strain is YI^T (=DSM 105863^T=JCM 32297^T), isolated from human feces.

Acknowledgements

We would like to thank Steven Aalvink for his valuable tips on genomic DNA extraction, and Bastian Hornung and Benoit Carreres for their help with the genome assembly.

Supplementary data

Fig. S1. Images of strain YI^T. a) Obtained by scanning electron microscopy. Bar represents 1 µm; b) Gram-staining cells by bright field microscopy. Bar represents 10 µm.

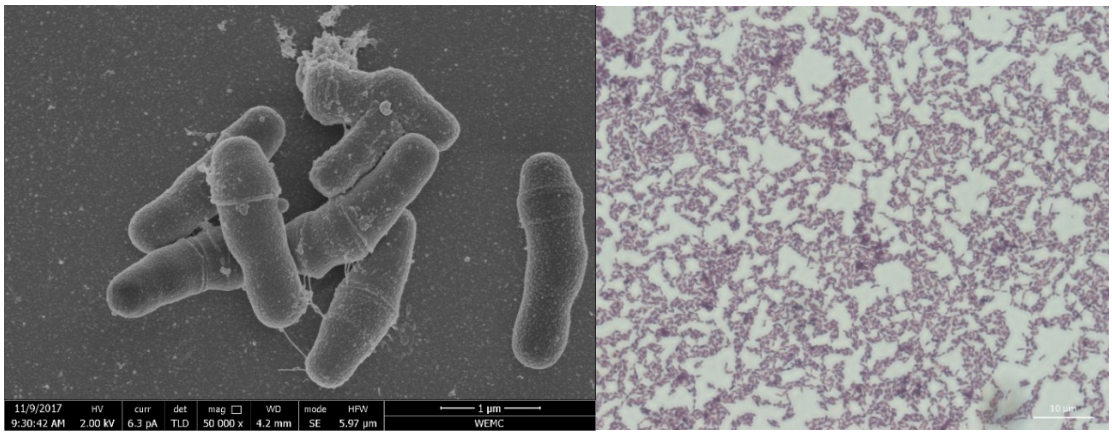

Table S1. Phylogenetic and genomic comparisons of strain YI^T, strain SA11, *E. limosum* ATCC 8486^T, *E. limosum* KIST 612 and *E. callanderi* DSM 3662^T.

16S rRNA gene sequence similarity %	strain YI^T	strain SA11	*E. limosum* ATCC 8486^T	*E. limosum* KIST 612	*E. callanderi* DSM 3662^T
strain YI^T	100	99.7	97.3	98.1	97.5
strain SA11		100	96.8	98.4	97.0
E. limosum ATCC 8486^T			100	99.7	99.5
E. limosum KIST 612				100	99.7
E. callanderi DSM 3662^T					100
ANI %	strain YI^T	strain SA11	*E. limosum* ATCC 8486^T	*E. limosum* KIST 612	*E. callanderi* DSM 3662^T
strain YI^T	100	98.5	89.2	89.9	89.7
strain SA11		100	89.4	89.9	89.9
E. limosum ATCC 8486^T			100	94.5	94.6
E. limosum KIST 612				100	99.8
E. callanderi DSM 3662^T					100
in silico DDH %	strain YI^T	strain SA11	*E. limosum* ATCC 8486^T	*E. limosum* KIST 612	*E. callanderi* DSM 3662^T
strain YI^T	100	86.4	38.6	39.5	39.7
strain SA11		100	39.9	39.9	39.8
E. limosum ATCC 8486^T			100	57.8	58.1
E. limosum KIST 612				100	98.4
E. callanderi DSM 3662^T					100

Chapter 4: Comparative genomics and proteomics of *Eubacterium maltosivorans*: Functional identification of trimethylamine methyltransferases and bacterial microcompartments in a human intestinal bacterium with a versatile lifestyle

This chapter has been published as:

Feng, Y., Bui, P. T. N., Stams, A. J., Boeren, S., Sánchez-Andrea, I., & de Vos, W. M. (2018). "Comparative genomics and proteomics of *Eubacterium maltosivorans*: Functional identification of trimethylamine methyltransferases and bacterial microcompartments in a human intestinal bacterium with a versatile lifestyle" Environmental Microbiology, **24**(1), 517-534.

Abstract

Eubacterium maltosivorans YI^T is an intestinal isolate capable of acetogenic, propionogenic and butyrogenic growth. Its 4.3-Mb genome sequence contains coding sequences for 4,227 proteins, including 41 different methyltransferases. Comparative proteomics of strain YI^T showed the Wood-Ljungdahl pathway proteins to be actively produced during homoacetogenic growth on H_2 and CO_2 while butyrogenic growth on a mixture of lactate and acetate significantly upregulated the production of proteins encoded by the recently identified *lctABCDEF* cluster and accessory proteins. Growth on H_2 and CO_2 unexpectedly induced the production of two related trimethylamine methyltransferases. Moreover, a set of 16 different trimethylamine methyltransferases together with proteins for bacterial microcompartments were produced during growth and deamination of the quaternary amines, betaine, carnitine, and choline. Growth of strain YI^T on 1,2-propanediol generated propionate with propanol and induced the formation of bacterial microcompartments that were also prominently visible in betaine-grown cells. The present study demonstrates that *E. maltosivorans* is highly versatile in converting low-energy fermentation end-products in the human gut into butyrate and propionate whilst being capable of preventing the formation of the undesired trimethylamine by converting betaine and other quaternary amines in bacterial microcompartments into acetate and butyrate.

Introduction

The human intestinal tract is a natural reservoir of dynamic and diverse microbial communities with important developmental, nutritional and protective functions that are tightly linked to health and disease. The vast majority of the intestinal species are anaerobic bacteria which salvage nutrients and energy by fermenting complex carbohydrates into short chain fatty acids (SCFAs), other organic acids such as formate and lactate, and gases, including H_2 and CO_2 (Rajilić-Stojanović and de Vos, 2014; Louis and Flint, 2017).

Lactate is another intermediate of carbon metabolism, produced by lactic acid and other abundant bacteria in the human intestinal tract (Smith and Macfarlane, 1997; Barcenilla *et al.*, 2000). Lactate accumulation could lead to detrimental consequences, such as acidosis and neurotoxicity whilst increased colonic levels are associated with colitis in patients with inflammatory bowel disease (Hove *et al.*, 1994; Hove and Mortensen, 1995; Mortensen and Clausen, 1996; Kowlgi and Chhabra, 2015). Therefore, both isomers of lactate must be efficiently depleted by intestinal microbes. Lactate can be utilized by sulfate- or sulfite-reducing bacteria like *Desulfovibrio*, *Bilophila* and *Clostridium* sp. resulting in elevated hydrogen sulfide levels, which could potentially cause colonic pain and gastrointestinal discomfort in both infants and adults (Chassard *et al.*, 2012; Y. Feng *et al.*, 2017; Pham *et al.*, 2017). Lactate can also be consumed by butyrate-producing bacteria in presence of acetate as isotope labelling studies have identified lactate and acetate as important precursors of butyrate production in mixed gut communities (Bourriaud *et al.*, 2005; Muñoz-Tamayo *et al.*, 2011). Intestinal bacteria that can perform this low energy metabolic conversion mostly belong to *Clostridium* cluster XIVa, including *Anaerostipes* spp. and *Anaerobutyricum* spp. (previously known as *Eubacterium hallii*) (Duncan *et al.*, 2004; Shetty *et al.*, 2020). The pathway of butyrate production from lactate and acetate has been recently elucidated in *Anaerobutyricum* and *Anaerostipes* spp. (Shetty *et al.*, 2020).

Acetate, propionate and butyrate- the most abundant SCFAs -can fuel the intestinal epithelium cells and confer health benefits via a variety of pathways (Tremaroli and Bäckhed, 2012; Fan and Pedersen, 2021). Moreover, all intestinal SCFAs are known to signal to G-protein coupled receptors, such as FFAR2, and have specific health-promoting effects, among others via the production of anorectic gut hormones (Deleu *et al.*, 2021). Notably, butyrate-producing bacteria have gained increasing attention as butyrate plays an important role in maintaining gut homeostasis and intestinal epithelial integrity (Hamer *et al.*, 2008). Butyrate is

also the major substrate for colonocytes and is reported to have anti-carcinogenic, anti-inflammatory, and anti-oxidative effects (Hinnebusch *et al.*, 2002; Klampfer *et al.*, 2003). Interestingly, decreased amounts of butyrogenic bacteria have been observed in inflammatory bowel diseases, colon cancer, and type 2 diabetes (Qin, Ruiqiang Li1, *et al.*, 2010; Flint *et al.*, 2012; De Vos and Nieuwdorp, 2013; Rajilić-Stojanović *et al.*, 2013).

Propionate has high affinity for FFAR2 of all SCFAs and its role in promoting health effects as well as increasing satiety has been described (Chambers *et al.*, 2015). Propionate can be produced from sugars via various pathways, but several intestinal species can produce this C3 compound from 1,2-propanediol (1,2-PDO), generated from methylpentoses such as fucose or rhamnose (Louis and Flint, 2017). The conversion of 1,2-PDO proceeds through a pathway that generates toxic intermediates that are encapsulated in self-assembling organelles termed bacterial microcompartments (BMCs) that are separated from the cytosol (Kerfeld *et al.*, 2018). These BMCs are typically produced when needed and are thought to include a respiratory electron acceptor and a vitamin B12 cofactor. (Cheng *et al.*, 2011; Thompson *et al.*, 2014).

Besides carbohydrate fermentation in the human intestinal tract the metabolism of many other compounds present in our diet is highly relevant since some may generate undesired products (Fan and Pedersen, 2021). These include quaternary amines such as betaine, choline and L-carnitine, which are commonly found in vegetables, fruits, meat and seafood and are well-known bacterial osmoprotectants (Sleator and Hill, 2002; Zeisel *et al.*, 2003; Demarquoy *et al.*, 2004). Several gut bacteria can convert these quaternary ammonium ions into trimethylamine (TMA), which is converted in the liver into trimethylamine-N-oxide (TMAO) that has been implied in artherosclerosis and cardiovascular risks (Brown and Hazen, 2014). Hence there is considerable interest in understanding the metabolism of these quaternary ammonium ions into compounds that do not lead to TMA or other TMAO precursors.

Recently, we isolated and described a novel human intestinal species *Eubacterium maltosivorans* YI^T affiliated the *Clostridium* cluster II, that is capable of converting H_2 and CO_2, as well as methanol and formate with weak growth, into acetate (Feng *et al.*, 2018). Besides homoacetogenic growth, it was able to ferment a range of monomeric sugars and disaccharides, including maltose, with acetate and butyrate as the main end products. Moreover, *E. maltosivorans* can also convert lactate and acetate into butyrate and 1,2-propanediol (1,2-PDO) into propionate. These properties are unique for the gut ecosystem and link three important metabolic processes, homoacetogenesis, propionigenesis and butyrogenesis in a

single human species. Some of these features were predicted by genomic characterization of the phylogenetically closely related *Eubacterium limosum* strain ATCC 8486 isolated from human colon (Song *et al.*, 2017), strain KIST612 isolated from an anerobic digestor (Roh *et al.*, 2011), and strain SA11 obtained from sheep's rumen (Kelly *et al.*, 2016), the latter being considered to belong to the new species of *E. maltosivorans* (Feng *et al.*, 2018). *E. limosum* and *E. maltosivorans* strains are capable of using a variety of C1 compounds, such as methanol, CO, as well as H_2 with CO_2, and their demethylating activity is high (Genthner *et al.*, 1981; DeWeerd *et al.*, 1988). These activities in the intestinal tract have been involved in co-degradation of dietary components such as pectin that generates methanol (Rode *et al.*, 1981). Moreover, dietary lignans and (iso)flavonoids that produce methoxylated aromatics can be converted by *E. limosum* strains into enterolactone and a range of other beneficial products (Jin *et al.*, 2007; Possemiers *et al.*, 2008; Struijs *et al.*, 2009). Similarly, vitamin B12 corrinoid-dependent TMA methyltransferases were recently identified in *E. limosum* and found to catalyze the demethylation of carnitine and betaine, thereby limiting the TMA formation and TMAO accumulation (Koeth *et al.*, 2013; Picking *et al.*, 2019; Kountz *et al.*, 2020). Based on their potential health promoting properties, *E. limosum*-related bacteria have been suggested to be among the next generation beneficial microbes (Kanauchi *et al.*, 2006), and bacteria related to *E. limosum* have been associated with longevity and health in a cohort of centenarians (Biagi *et al.*, 2010).

In the present study, we describe the complete genome sequence of the aforementioned *E. maltosivorans* YI^T, provide a detailed comparative genomic analysis, and use a proteome approach to identify the enzymes and pathways involved in acetogenesis (from H_2 and CO_2), butyrogenesis (from lactate and acetate and various sugars) and propionogenesis (from 1,2-PDO) as well as the conversion of quaternary amines (betaine, carnitine and choline), that is associated with the induction of unique TMA methyltransferases and proteins involved in the production of bacterial microcompartments.

Material and methods

Growth medium and conditions

Cultivation of *E. maltosivorans* YI^T (DSM 105863^T) was handled as previously described (Feng *et al.*, 2018). Briefly, it was grown based on anoxic basal medium (A. J M Stams *et al.*, 1993) supplemented with 1 g/L yeast extract and 20 mM of each substrate

separately. Eight different substrates were selected to conduct the comparative proteomics study for *E. maltosivorans*: homoacetogenic growth with H_2/CO_2 (80:20 v/v), butyrogenic growth with 20 mM lactate with 15 mM acetate, fermentation growth with 20 mM glucose or 20 mM maltose, propionogenic growth with 20 mM 1,2-PDO, and demethylate growth on either 20 mM carnitine, or betaine, or choline. Each condition was run in triplicates. For growth on carnitine, betaine, and choline (20 mM each), the growth medium was amended with 2,5 g/L peptone and 2,5 g/L yeast extract. Each condition was run in duplicates. Except otherwise indicated, cultures were incubated statically at 37ºC in the dark without shaking.

Genomic DNA preparation, assembly and annotation

Exponentially growing cells on maltose (50 ml) were harvested by centrifuging at 4°C for genomic DNA isolation. MasterPure Gram-positive DNA purification kit (Epicentre) was used to extract the genomic DNA of *E. maltosivorans* DSM 105863^T. The quality of the extracted DNA was measured using a NanoDrop 2000 spectrophotometer (Thermo Scientific, Waltham, USA). The genome was sequenced using both PacBio RSII instrument and Illumina. Both Illumina paired-end reads and PacBio subreads were used as input for the assembler spades (v.3.11.1) with a custom kmer setting of 21,31,51,81,91 and coverage cutoff set to auto. After removing scaffolds smaller than 500 bp, one scaffold was obtained of 43375050 bp (0 N's). Illumina paired-end reads were mapped back the assembly using bowtie2 (v2.3.3.1). The resulting sam files was converted with samtools (v1.3.1). The indexed bam file was used as in input for Pilon (v1.22) which resulted a 4337503 bp (N's) polished assembly. The complete genome sequence of *E. maltosivorans* YI^T (DSM 105863^T) was deposited at GenBank/EMBL-EBI under the accession number CP029487.1, and proteins were annotated by the NCBI Prokaryotic Genome Annotation Pipeline (Tatusova *et al.*, 2016; Haft *et al.*, 2018; Li *et al.*, 2021). The complete genomes of the three known *E. limosum* strains, including the type strain ATCC8486^T, strain KIST612 and strain SA11, were obtained from NCBI with accession numbers of CP019962.1, NC_014624.2 and CP011914.1, respectively.

Specific annotations

The core genome of the *E. maltosivorans* and *E. limosum* strains was identified using Spine and the pan-genome was identified using AGEnt (Ozer *et al.*, 2014). CRISPR genes of the four strains were annotated using CRISPRfinder (Grissa *et al.*, 2007). The CRISPRTarget tool identifies target phages using different databases and the search algorithm has its own

scoring system with a score of 20 which was kept as default minimum as suggested by the authors (Biswas *et al.*, 2013). Prophage sequences were detected using PHASTER (Arndt *et al.*, 2016). In general, if a given phage region's total score is < 70, it is recognized as incomplete; between 70 to 90, it is recognized as questionable; if > 90, it is intact. Genomic islands were identified using online IslandViewer version 4 (Bertelli *et al.*, 2017).

Proteomics

For proteomics analysis, *E. maltosivorans* cells cultivated with different substrates as described above were harvested at middle or late exponential growth phase by centrifugation for 20 min at 4700 g at 4 °C (Supplementary Figure 2). The pellets were washed with 1 ml PBS and immediately stored at -80 °C until protein extraction. In total, we conducted three sets of proteomic analyses, with the first set comparing homoacetogenic and butyrogenic growth to glucose fermentation in biological triplicates, the second comparing propionogenic growth to maltose fermentation in biological triplicates, and the last comparing growth with quaternary amines to glucose fermentation in biological duplicates.

To prepare the protein samples for the first set proteomes, an in-stage-tip sample preparation method was used (Kulak *et al.*, 2014). The harvested washed pellets were thawed on ice and 2 mg wet weight were transferred and resuspended in 0.5 ml of 100 mM Tris/HCl at pH8. The suspension was sonicated 6 times at 30% amplitude in cycles of 30 seconds pulse and 30 seconds rest on ice by a Branson sonifier SFX150 equipped with a 3 mm tip (Branson, Carouge, CH). Proteins in the supernatant were collected by centrifugation at 10000 g for 10 min at 4 °C and transferred to low binding Eppendorf microtubes. Disulphide bonds of the proteins were reduced by incubating in 20 mM dithiothreitol in a thermomixer at 500 rpm at 45 ºC for 15 min. When the mixture cooled down to room temperature, AcrylAmide was added up to 25 mM to alkylate the reduced cysteines in the dark at room temperature for 30 min. Followed by centrifugation at 14 000g for 2 min, 70 to 80 µl protein extract (ca 40 ug protein) was collected and loaded onto a C18 stage-tip using a double membrane (Empore C18, 3M), as described by Sánchez-Andrea *et al.*, (2020). After a clean-up with 150 µl 5% acetonitrile (AcNi) in 50 mM ammonium bicarbonate buffer (ABC), stage-tips were moved to clean 0.5 mL low binding microcentrifuge tubes and 500 ng of trypsin in 50 mM ABC was added on top to perform the enzymatic digestion of the proteins at room temperature overnight. The enzymatic digestion was stopped by adding 75 µl 0.1% formic acid and all liquid was eluted into the low binding tubes. In the end, hydrophobic peptides were eluted from the membrane

manually with 5 µl 50% AcNi/50% 0.1% formic acid. Finally, after drying most of the AcNi and water in a concentrator, the final volume was made up to 50 µl with 0.1% formic acid. The peptide samples were analyzed as described by Sánchez-Andrea *et al.*, (2020) using the same machine and setup. LCMS runs with all MSMS spectra obtained in first set proteome comparisons were analyzed with MaxQuant 1.6.0.1 as previous as well (Sánchez-Andrea *et al.*, 2020).

For the second and the third set proteomes, around 10 mg harvested pellets were thawed, resuspended into 100 mM Tris pH 8 and sonicated using the same procedure as described for the first set. After sonication, for the protein determination, samples were centrifuged at 10000 g for 10 min at 4 °C and the protein concentration was measured with Qubit™ Protein Assay Kit (Thermo Scientific, Waltham, MA). 40 µg protein of each (not centrifuged) sample was transferred to a 2 mL low binding tube. Proteins were reduced with 15 mM dithiotreitol (DDT) at 45 °C for 30 mins, unfolded with 6 M urea and alkylated with 20 mM AcrylAmide at 21 °C for 30 mins. The pH was adjusted to 7 with 10% Trifluoroacetic acid (TFA) and proteins were cleaned up by using a PAC method (Batth *et al.*, 2019) using speedbeads and washing the proteins with 1 ml 70% ethanol and then 1 ml 100% acetonitrile. Digestion was conducted with 100 µl 0.5 pg/µl trypsin in 50 mM ABC at room temperature overnight. To stop the digestion, 10% TFA in H_2O was added to the samples until the pH dropped to 3. After filtering the peptide samples, volumes were adjusted to 50 µl with 0.1% formic acid.

5 µl of peptide samples were loaded directly onto a 0.10 *250 mm ReproSil-Pur 120 C18-AQ 1.9 µm beads analytical column (prepared in-house) at a constant pressure of 825 bar (flow rate of circa 700 nl/min) with 1 ml/l HCOOH in water and eluted at a flow of 0.5 µl/min with a 50 min linear gradient from 9% to 34% acetonitril in water with 1 ml/l formic acid with a Thermo EASY nanoLC1000. An electrospray potential of 3 kV was applied directly to the eluent via a stainless-steel needle fitted into the waste line of the micro cross that was connected between the micro cross and the analytical column. Full scan positive mode FTMS spectra were measured between m/z 380 and 1400 on a Exploris 480 at resolution 60000. MS and MSMS AGC targets were set to 300 and 100% respectively or maximum ion injection times of 50 ms (MS) and 30 ms (MSMS) were used. HCD fragmented (Isolation width 1.2 m/z, 28% normalized collision energy) MSMS scans in a cycle time of 1.1 s were recorded for the most abundant 2-5+ charged peaks in data dependent mode (Resolution 15000, threshold 2e4, 15 s exclusion duration for the selected m/z +/- 10 ppm).

LCMS runs with all MSMS spectra obtained were analysed with MaxQuant 1.6.3.4 (Cox and Mann, 2008). For all three sets of proteome analysis, a *E. maltosivorans* sequence database (NCBI accession number 72721) was used together with a contaminants database that contains sequences of common contaminants including Trypsins (P00760, bovin and P00761, porcin) and human keratins (Keratin K22E (P35908), Keratin K1C9 (P35527), Keratin K2C1 (P04264) and Keratin K1CI (P35527)). Propionamide (C) set as a fixed modification, while variable modifications were set for Protein N-terminal Acetylation and M oxidation which were completed by non-default settings for de-amidation of N and Q, the maximum number of modifications per peptide was 5. The label-free quantification (LFQ) as well as the match between runs options were enabled. De-amidated peptides were allowed to be used for protein quantification and all other quantification settings were kept default. In MaxQuant, accepted were peptides and proteins with a false discovery rate (FDR) of less than 1% and proteins with at least 2 identified peptides of which at least one should be unique and at least one should be unmodified. Reversed hits were deleted from the MaxQuant output as well as all results showing a normalised LFQ value of 0 for both sample and control. The normal logarithm was taken from protein LFQ MS1 intensities as obtained from MaxQuant. Zero "Log LFQ" values were replaced by a value of 4.4 (A value slightly lower than the lowest measured value) to make sensible ratio calculations possible. Relative protein quantitation of the first and second set proteomes was done with Perseus by applying a two sample t-test using the "LFQ intensity" columns obtained with FDR set to 0.05 and S0 set to 1. Total non-normalised protein intensities corrected for the number of measurable tryptic peptides (intensity based absolute quantitation (iBAQ) intensity were, after taking the normal logarithm, used for plotting on the y-axis in a protein ratio versus abundance plot. All three mass spectrometry proteomics data have been deposited to the ProteomeXchange Consortium via the PRIDE (Vizcaíno *et al.*, 2016) partner repository with the dataset identifier PXD028586, PXD013114 and PXD028574.

Transmission Electron Microscopy

Biomass of *E. maltosivorans* YI^T grown with 1,2-PDO, betaine, or glucose were obtained by centrifugation (5 min, 4 ^{o}C at 14,000 g) from late exponential cultures. Biomass were resuspended and fixed in 1 mL 2.5% (v/v) glutaraldehyde in 0.1 M sodium cacodylate buffer (pH 7.2) for 1 h at room temperature. After rinsing in the same buffer, biomass was resuspended and incubated in 100 µl of 3% gelatin in 0.1 M phosphate at room temperature for 20 mins till gelatin solidified. The solidified specimens were incubated in 0.1 M sodium cacodylate buffer for 15 min at room temperature to become loose from tube wall. The

specimens were infiltrate by ethanol and were then embedded in resin for 8 hours at 70°C. Thin sections (<100 nm) of polymerized resin samples were obtained with microtomes. After staining with 2% (w/v) aqueous uranyl acetate, the samples were analyzed with a Jeol 1400 plus TEM.

Results and Discussion

Complete genome of *E. maltosivorans* YI^T and comparative genomics of prophages, CRISPR systems and relevant features

E. maltosivorans YI^T affiliates the *Eubacteriaceae* family of *Clostridium* cluster II, sharing highest 16S rRNA genes similarity to *E. limosum* SA11 (99.7%), *E. limosum* KIST612 (98.1%), *E. callanderi* AMC0717 (97.5%) and *E. limosum* ATCC 8486^T (97.3%), the latter being the type species of the *Eubacterium* genus (Wade, 2009) (Figure 1). The complete genome of *E. maltosivorans* YI^T consisted of a single circular chromosome of 4,337,501 bp with its general features being listed in Table 1. Many genomic features were shared with the related *E. limosum* strains ATCC 8486^T, KIST612 and SA11, for which complete genomes have been reported (Roh *et al.*, 2011; Kelly *et al.*, 2016; Song *et al.*, 2017).

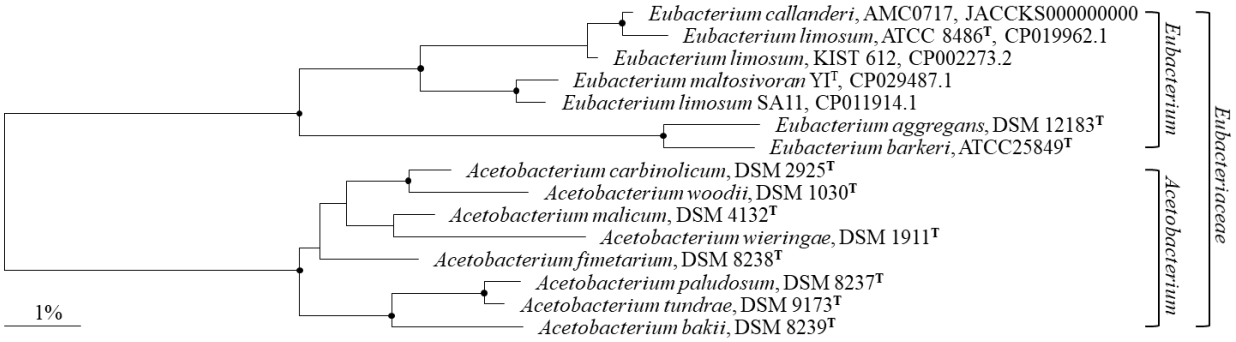

Figure 1. Phylogenetic affiliation of *E. maltosivorans* YI^T and related *E. limosum* strains. Neighbour-joining tree based on 16S rRNA gene sequence similarities calculated with Jukes–Cantor correction was adapted from Feng *et al.* (2018), with accession numbers of the deposited complete genomes of *E. maltosivorans* YI^T and related *E. limosum* and *E. callanderi* strains.

The genome of *E. maltosivorans* YI^T revealed 5 prophages sequences, of which 4 are intact and 1 is incomplete (Figure 2). The prophages in strain YI^T had similar G+C content: 47.70% (33.3 kb), 41.61% (38.1 kb), 44.95% (53 kb), and 48.59% (44.8 kb) for intact prophage one to four respectively; and 46.47% (22.9 kb) for the incomplete prophage (Fig. S1A). These prophages were unique as no sequences were shared with the single 58.8-kb prophage sequence with a reduced G+C content (40.86%) in strain SA11 that is closest related to strain YI^T (Fig.

S1B), indicating exposure to different prophages in human colon and in sheep rumen. In terms of prophage defense systems, both strains possessed CRISPR/Cas system in their genomes. Strain YI^T has one cluster of a 225 bp CRISPR array that contained a 30 bp long direct repeat (5-GTTGAAGCTTAACATGAGATGTATTTAAAT-3) with 3 spacers. Strain SA11 has a 2,328 bp CRISPR system with the same direct repeat with 35 spacers. No spacers were found to be shared between these two strains, indicating previous viral infections were different. Besides, strain SA11 has another 1,675 bp CRISPR array, which contained another 30 bp long repeat sequence (5-GTTGAAGTTTAACATGAGATGTATTTAAAT -3) with 25 spacers.

Table 1. General genome features of *E. maltosivorans* YI^T, *E. limosum* ATCC 8486^T, SA11, KIST612, and *E. callanderi* AMC0717. *mttB*: TMA methyltransferases

Strain	YI CP029487.1	SA11 CP011914.1	ATCC 8486^T CP019962.1	KIST612 CP002273.2	AMC0717 JACCKS000000000
Host	Human	Sheep	Human	Anaerobic digestor	Human colonic Mucosa
Genome size (bp)	4,337,501	4,150,332	4,422,837	4,316,707	4,327,770
GC content (%)	47.8	47.4	47.2	47.5	47.5
RNA	77	76	77	73	64
rRNA	16	16	17	16	11
tRNA	61	60	60	57	53
Prophage	5	1	4	4	1
No. Subsystems	351	347	354	358	245
No. CDs	4,227	4,044	4,303	4,284	4,539
No. *mttB* genes	41	39	42	33	31

The genome of *E. maltosivorans* is predicted to contain 41 *mttB* genes encoding TMA methyltransferases (MttB, COG05598), all of which are predicted to encode proteins in similar size of 458 to 487 amino acids with one exception of 54 amino acids. These *mttB* genes in *E. maltosivorans* clustered at 4 major locations in the genome, while in *E. limosum* strains they are more scattered (Figure 2). Similar to *E. limosum* strains, the *mttB* genes in *E. maltosivorans* are also often associated with genes for cobalamin B12-binding proteins, BCCT (betaine/carnitine/choline transporter) and MFS family transporters and GntR family transcriptional regulators (Kelly *et al.*, 2016; Picking *et al.*, 2019; Kountz *et al.*, 2020).

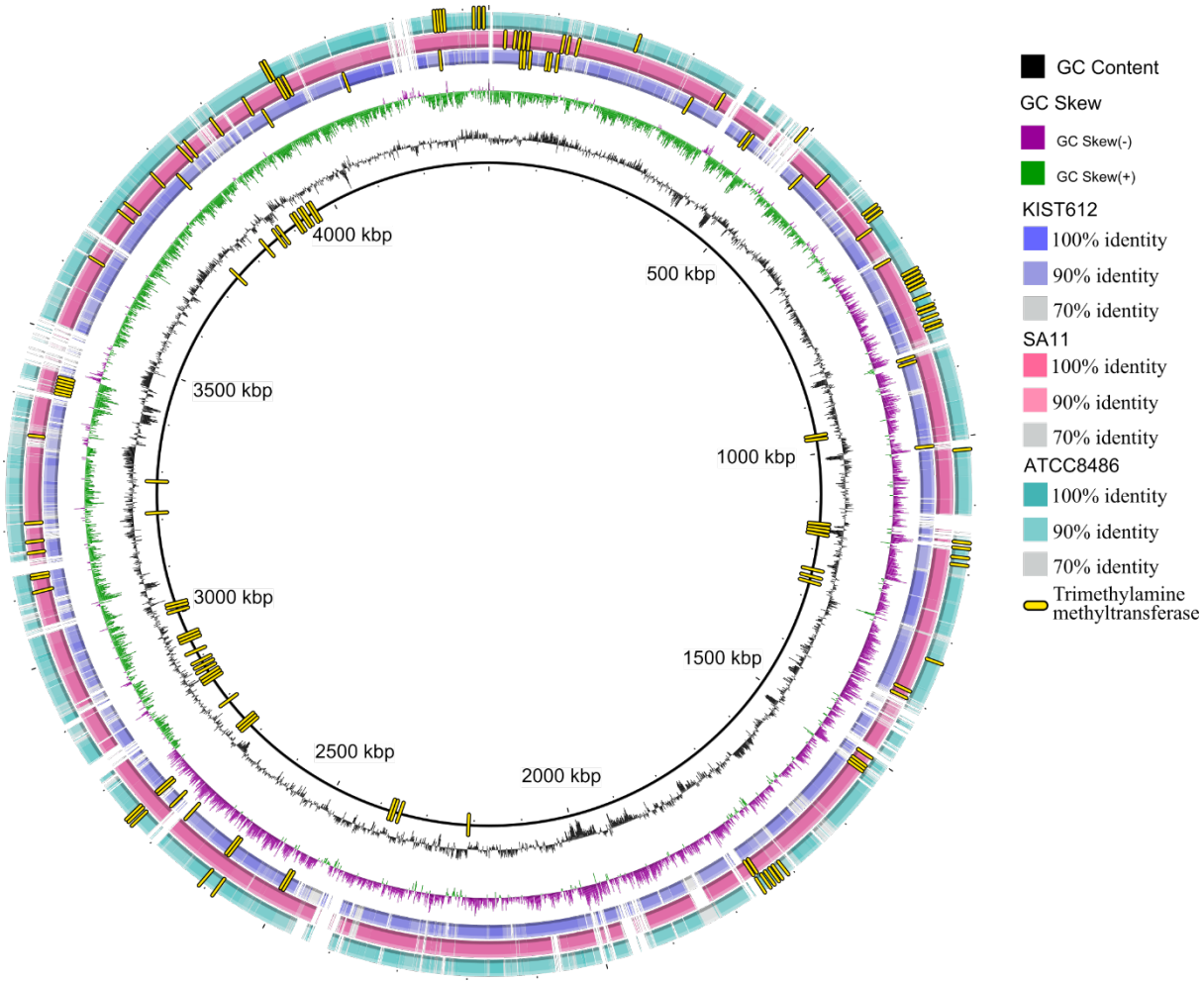

Figure 2. Genome map of *E. maltosivorans* YI^T compared to the close-related strain KIST612 (purple), SA11 (pink), and ATCC8486^T (green), with trimethylamine methyltransferases indicated in each strain (yellow).

Comparative proteomics of *E. maltosivorans* grown on different carbon sources

Since *E. maltosivorans* is highly versatile and capable of growing on a variety of different substrates (Feng *et al.*, 2018), we focused first on growth with H_2/CO_2 (further referred to as homoacetogenic growth) and lactate supplemented with acetate (further referred to as butyrogenic growth). Next, we tested growth of *E. maltosivorans* with 1,2-PDO (further referred to as propionogenic growth), as well as demethylation growth of quaternary amines including betaine, carnitine and choline. For this purpose, actively growing *E. maltosivorans* cells pre-cultured in glucose were washed and inoculated in basal medium containing either H_2/CO_2, 20 mM lactate plus 15 mM acetate, 20 mM glucose, or 20 mM 1,2-PDO. When strain YI^T was grown with 20 mM quaternary amines, an extra 2.5 g/l PEP was supplied in basal medium. The carbon recovery of homoacetogenic, butyrogenic and propionogenic growth were 57.1%, 88.2%, and 80.5% respectively, while that on its preferred substrate glucose was 72.8%

(Table 2). The missing carbon can be attributed to biomass production and intermediates that could not be detected by high-performance liquid chromatography at mid-log phase, such as amino acids.

Table 2: Substrate utilization and product formation by *E. maltosivorans* YI^T at the end exponential phase. Values are average of triplicates and their standard deviation. 1,2-PDO: 1,2-Propanediol.

	Consumption Substrate (mM)	Production (mM)					
		Acetate	Butyrate	Lactate	Formate	Propionate	Propanol
Glucose	11.6 ± 0.49	13.5 ± 1.16	0.6 ± 0.57	5.4 ± 1.10	5.1 ± 0.15	<0.1	<0.1
Lactate	9.3 ± 0.95	4.7 ± 0.77	3.8 ± 1.0	-	<0.1	-	-
H_2 (CO_2)	45.5 ± 0.85	6.5 ± 0.58	<0.1	<0.1	<0.1	-	-
1,2-PDO	17.5 ± 0.98	<0.1	<0.1	<0.1	<0.1	7.5 ± 0.63	6.6 ± 0.30

In order to study proteome dynamics of *E. maltosivorans* during growth on different substrates, we conducted three sets of proteomic analyses in eight growth conditions. The first was comparing homoacetogenic and butyrogenic growth to glucose fermentation, while the second was comparing propionogenic growth to maltose fermentation. To identify the potential role of MttB homologues in the butyrogenic conversion of quaternary amines, the third set of proteomes included *E. maltosivorans* cells grown on betaine, carnitine, choline and glucose. From a total of 4,227 protein coding sequences identified in the genome of *E. maltosivorans*, a collective of 1737 non-redundant proteins were identified in the aforementioned eight growth condition.

We observed the canonical proteins involved sin the WLP, the route from acetyl-CoA to butyrate and acetate, as well as acetyl-CoA synthase to be abundantly present in all the proteomes with very low fold-change values within them, suggesting that their corresponding genes are constitutively expressed. Moreover, we identified unique proteome dynamics associated to the growth with different carbon sources as discussed in detail below. Based on the metabolic profiles of the tested substrates, the genomic reconstruction and the results of the comparative proteogenomics experiments that are presented below, we generated a schematic overview of the (homo)acetogenic, propionogenic and butyrogenic conversions that will be discussed further (Figure 3).

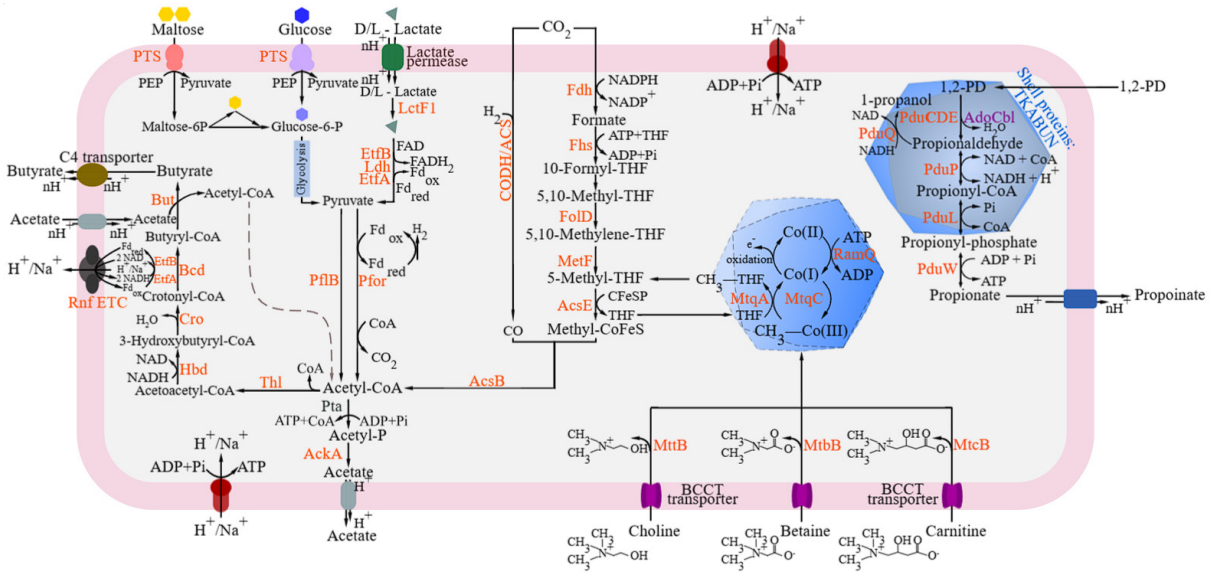

Figure 3. Schematic overview of the key metabolic features of *E. maltosivorans* based on genomic reconstruction and supported by proteome data. Proteins marked in blue are that detected in the proteome, while those in black are only identified in the genome but not detected in the proteome at any of the growth conditions. SCFA transporters most likely belong to the C4 TRAP family of transporters. The symport is with a proton and *n* indicates the number of protons transported across the cell membrane which may vary under various growth conditions. PTS: phosphoenolpyruvate-dependent sugar phosphotransferase system; Ldh: lactate dehydrogenase; EtfA/EtfB: electron transfer flavoprotein alpha/beta subunit; LctF1: lactate racemase; Pfor: pyruvate:ferredoxin oxidoreductase; PflB: Formate acetyltransferase; Pta: acetyl-CoA:phosphate acetyltransferase; Thl: thiolase; Hbd: 3-hydroxybutyryl-CoA dehydrogenase; Cro: crotonase; Bcd: butyryl-CoA dehydrogenase; But, butyryl-CoA:acetate CoA transferase; Fdh: Formate dehydrogenase; Fhs: formyl-THF synthetase; FolD: methylene-THF dehydrogenase; MetF: methylene-THF reductase; AcsE: methyltransferase; CODH: carbon monoxide dehydrogenase; ACS: CO dehydrogenase; AscB: acetyl-CoA synthase; MttB: TMA methyltransferases; MtbB: Betaine specific MttB; MtcB: carnitine specific MttB; MtqA: methylcorrinoid:THF methyltransferase; MtqC: corrinoid protein; RamQ: corrinoid activation enzyme; PduCDELPWQ: Propanediol utilization proteins; AdoCbl: adenosylcobalamin.

Proteomics-guided identification of the active DL-lactate utilization gene cluster and butyrogenic pathway in *E. maltosivorans*

Lactate is one of the most important metabolites for growth of anaerobic bacteria in the human intestinal environment (Duncan, *et al.*, 2004). It must be efficiently reused to avoid potential negative consequences, such as acidosis, neurotoxicity, and cardiac arrhythmia. During butyrogenic growth on lactate supplied with acetate, various proteins showed highly increased abundance (over 1000-fold as compared to homoacetogenic growth and glucose fermentation), including lactate dehydrogenase (Ldh, encoded by CPZ25_RS02230), electron transfer flavoprotein alpha subunit (EtfA, encoded by CPZ25_RS02225), ETF beta subunit (EtfB, encoded by CPZ25_RS02230), and lactate racemase (LctF1, encoded by

CPZ25_RS18455) (Figure 4A, Table S1). The lactate racemase LctF1 ensures both D- and L-lactate promoted growth of *E. maltosivorans*, which is in line with the substrate utilization since both DL-lactate were provided to strain YI. In the genome of *E. maltosivorans*, downstream of the *ldh* gene, there is a gene encoding a potential lactate permease (encoded by CPZ25_RS02235), the product of which was not detected in our current proteomic analysis, since it is a likely transmembrane protein. The organization of the DL-lactate utilization gene cluster of *lctABCDEFG* in strain YI is depicted in Figure 4B.

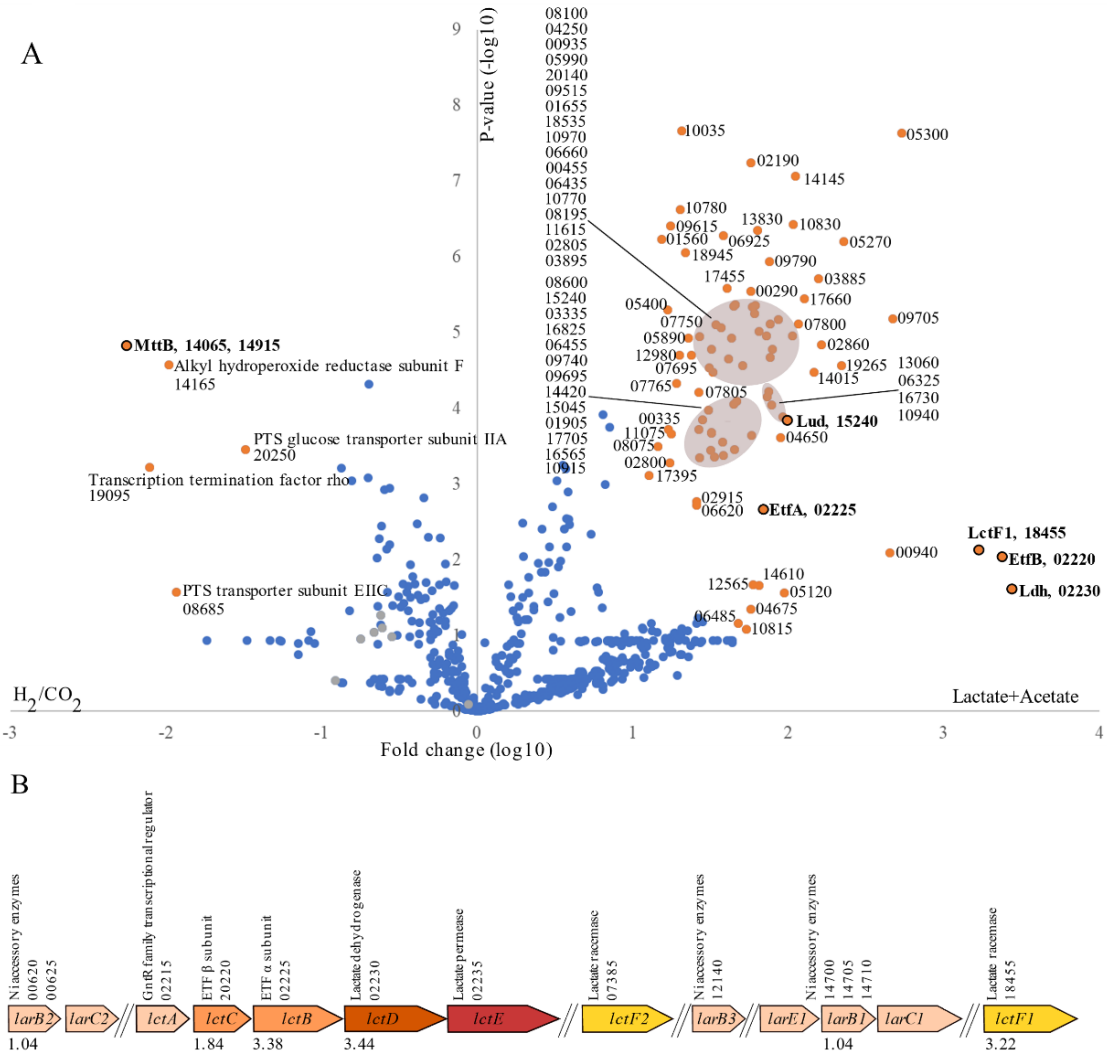

Figure 4. Differentially abundant proteins in *E. maltosivorans* cells grown on lactate/acetate and hydrogen (A) and organization of gene clusters involved in lactate utilization in the genome of *E. maltosivorans* (B). Proteins that are significantly different in abundance between the two conditions in the proteome are colored in orange, with the locus tags of the genes encoding for these proteins indicated. The locus tag for the genes encoded in *E. maltosivorans* starts with CPZ25_RS, which is omitted to avoid repetition in the figures. For clarity, proteins related to lactate utilization and the MttB are labelled in bold, and a complete list with product names for locus tags is given in Table S1. EtfA: electron transfer flavoprotein alpha; EtfB: electron transfer

Identification of the WLP in the proteome of *E. maltosivorans* YI^T and induction of two highly similar TMA methyltransferases

Hydrogen is a common gaseous microbial metabolite produced in the intestine through the fermentation of carbohydrates. CO_2 is also produced through a variety of decarboxylation reactions, notably from amino acid fermentations. Homoacetogenic bacteria can convert hydrogen together with CO_2 to acetate through WLP. Therefore, we sought to reconstruct the WLP in *E. maltosivorans* leading to the conversion of H_2/CO_2 to acetate.

The genes encoding proteins of the WLP in *E. maltosivorans* are mainly grouped in 3 clusters on the chromosome, consisting of a formate dehydrogenase cluster (CPZ25_RS17665-17675), a methyl (CPZ25_RS11820-11850) and a carbonyl branch (CPZ25_RS18530-18570) to form the central intermediate, acetyl-CoA (Supplementary Figure 3). All of the predicted genes involved in the WLP were detected in the current proteome study, except for MoeA (molybdenum cofactor guanylyltransferase, encoded by CPZ25_RS17670) and a formate dehydrogenase (Fdh) accessory protein (encoded by CPZ25_RS17675), indicating the activity of WLP in *E. maltosivorans*. However, most of the detected proteins were not higher produced in homoacetogenic growth, when compared with butyrogenic growth cells, suggesting constitutive expression of their genes (Tables S1 & S3). Remarkably, during growth on H_2/CO_2 two highly similar TMA methyltransferases (encoded by CPZ25_RS14065 and CPZ25_RS14915) were highly overproduced (over 150-fold change) as compared to growth on glucose or lactate and acetate (Figure 4A). These two TMA methyltransferases (considered as the MttB prototype) have an identical sequence and hence could not be distinguished from each other. Presently, it is not known whether these two TMA methyltransferases have a specific function in the homoacetogenic metabolism of *E. maltosivorans* strain YI^T.

Growth on maltose induces maltose-specific phosphotransferase and a set of internalin B-like proteins

Starch is a major source of energy in the human diet and is consumed in diverse forms. Resistant starch escapes digestion by glucoamylases in the upper GI tract and is degraded by the combined action of many gut bacteria in the colon, leading to beneficial impacts on colonic function and host health. Maltose is one of the by-products from the degradation of resistant starch that in the colon is mainly converted by *Ruminococcus bromii* (Ze *et al.*, 2012). The ability to utilize maltose is one of the differentiating features for *E. maltosivorans* in respect to

E. limosum. Therefore, we sought to identify the proteins involved in the metabolic pathway that converts maltose to acetate and butyrate by comparing the proteomes of *E. maltosivorans* grown on maltose and 1,2 PDO.

Genome analysis predicted that maltose uptake in strain YI^T depends on a maltose phosphoenolpyruvate phosphotransferase (Mal-PTS) system encoded by *malP* (CPZ25_RS08305). The phosphorylated maltose-6-phosphate is then degraded by a maltose-6-phosphate hydrolase (encoded by *malA*, CPZ25_RS08300) into glucose and glucose-6-phosphate, which both enter the glycolysis pathway and lead to production of acetate and butyrate. Lastly, there are two potential maltose operon regulators encoded by *malQ* and *malR* (CPZ25_RS08290 and CPZ25_RS08295, respectively) that may control the expression of the PTS genes and are located in the proximity of the genes for the maltose utilization cluster (Figure 5B).

The proteins encoded by the *malPQR* cluster of genes had significantly higher abundance in the proteome of cells grown on maltose compared to propionogenic growth (Figure 5A). Among these proteins, the products of *malR* and *malP* were uniquely detected in the cells grown with maltose, indicating that the Mal-PTS is specifical for transporting maltose. Remarkably, we also noticed that the products of genes closely located around the maltose utilization cluster were coordinately expressed and highly induced in the presence of maltose (Figure 5A). Among these genes, CPZ25_RS08280, CPZ25_RS08315, CPZ25_RS08325 and CPZ25_RS08330 encode large, over 1000 amino acid residue proteins. The protein products of CPZ25_RS08280, CPZ25_RS08325 and CPZ25_RS08330 share ~40% to 72% similarities to each other and their functions remain unknown although their genes were found to be conserved in all related *E. limosum* genomes. All proteins have signalP-predicted N-terminal signal sequences and those encoded by locus tags CPZ25_RS08315 and CPZ25_RS08320 have considerable similarity to internalin B, a well-studied *Listeria monocytogenes* surface protein involved in human cell binding (Parida *et al.*, 1998). Moreover, these both contain remnants of sortase recognition sequences in their C-terminus. Of note, the *E. maltosivorans* YI^T genome is predicted to encode two class B sortases (CPZ25_RS01590 and CPZ25_RS01785), a protein that is known to covalently couple this kind of proteins to the cell envelope (Ilangovan *et al.*, 2001; Marraffini *et al.*, 2006). Whether this is also the case with these internalin B-like proteins remains to be confirmed since cell-envelope binding usually precludes detection in the cytoplasmic proteome as we report here.

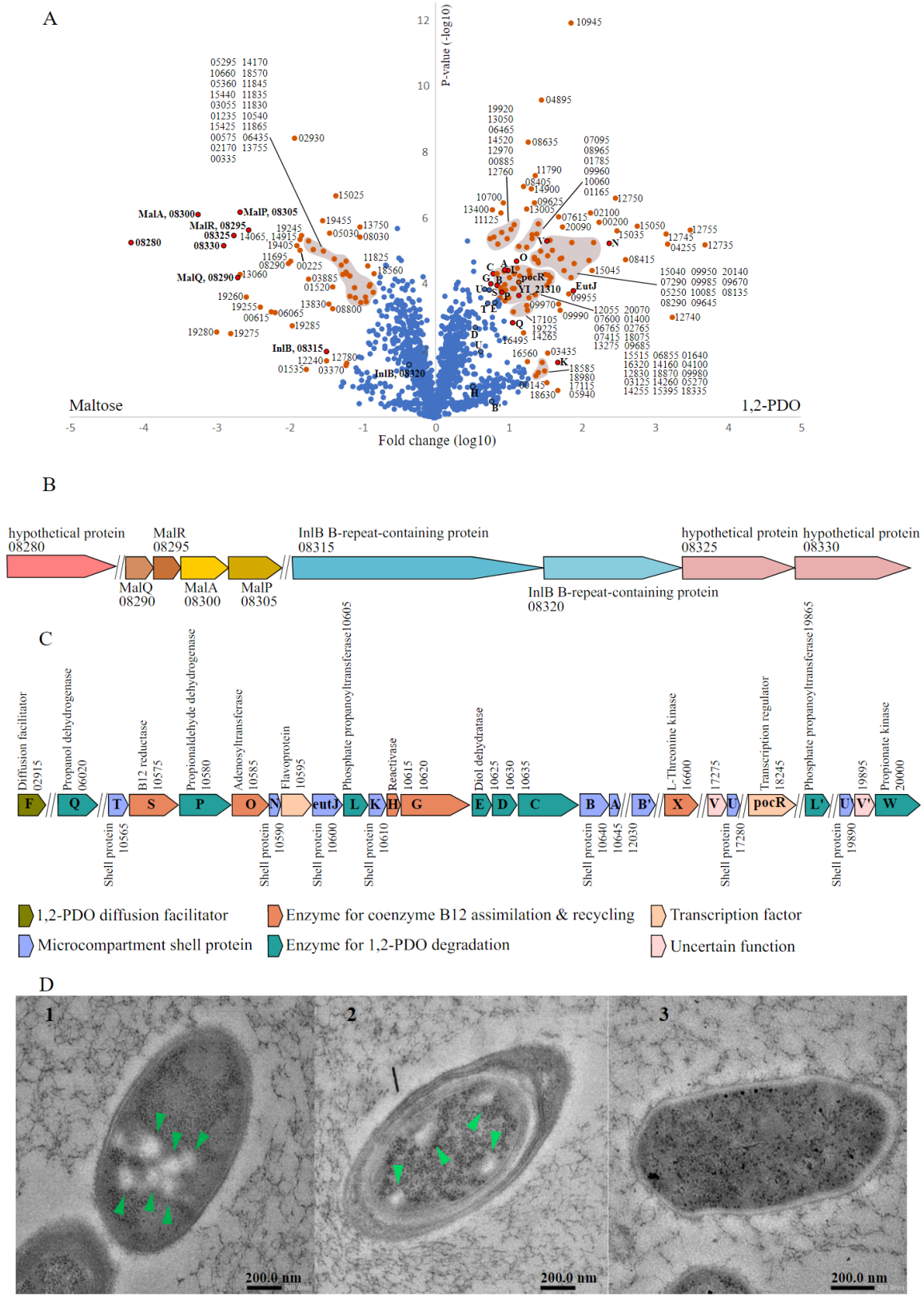

Figure 5. Comparative analysis of proteomics (A), prediction of gene clusters (B&C) and presence of BMCs (D) in *E. maltosivorans* grown on 1,2-PDO and maltose. A: Differentially abundant *E. maltosivorans* proteins in cells grown on 1,2-PDO versus on maltose. Proteins that are significantly different in abundance between the two conditions in the proteome are colored in orange, with the locus tags of the genes encoding for these proteins indicated. The locus tag

for the genes encoded in *E. maltosivorans* starts with CPZ25_RS, which is omitted to avoid repetition in the figures. For clarity, locus tags related with maltose utilization and microcompartments formation are labelled in bold, and a complete list with product names for locus tags is given in Table S4. B&C: Operon of the genes involved in maltose transportation and 1,2-PDO degradation in the genome of strain YI^T with color coded predicted functions. D: TEM visualization of microcompartments in *E. maltosivorans* strain YI^T when grown with 1,2-PDO (1), betaine (2) and negative control glucose (3). Green arrows point to microcompartments structures, with the black scale bars.

Growth on 1,2-PDO induces proteins involved in bacterial microcompartments

To further study the versatility of *E. maltosivorans*, we grew it on 1,2-PDO resulting in the production of equal amounts of propionate and 1-propanol (Fig. S4). Interestingly, we did not observe accumulation of intermediate propionaldehyde, which is known as a toxic compound to the cell. Therefore, we hypothesized that propionaldehyde could be sequestered within an organelle so-called a bacterial microcompartment (BMC) which is a distinct mechanism to avoid lethal effects while growing on 1,2-PDO or other substrates with toxic intermediates (Chowdhury *et al.*, 2014). This is in line with the detection of a total 27 *pdu* genes encoding BMC production and degradative enzymes in genome of *E. maltosivorans*, with 17 of which are closely located in a cluster. We found homologues of major (PduABB') and minor (PduKNTU) BMC shell proteins (Figure 5D1) This confirms earlier predictions for the presence of a PDU1 type BMC encoded by multiple loci in the genome of *E. limosum* KIST612 (Axen *et al.*, 2014).

Of note, a ethanolamine utilization (*eutJ*) homologue is located among the *pdu* cluster, which is a part of ethanolamine BMC and encodes a chaperone whose specific function is currently unknown (Kofoid *et al.*, 1999). When the proteome of 1,2-PDO-grown cells was compared with those grown on maltose, all these BMC shell proteins were detected at a significantly higher abundance and PduABKNU, as well as EutJ, were significantly overproduced (Figure 5A). The formation of BMCs during growth with 1,2-PDO was confirmed by analyzing cells grown on this substrate by transmission electron microscopy (TEM) and comparing these with cells grown on glucose (Figure 5D).

Growth on quaternary amines is associated with induction of bacterial microcompartments in *E. maltosivorans*

In our previous analysis we found that *E. maltosivorans* can grow on betaine (Feng *et al.*, 2018). To further test other quaternary amines, we grew *E. maltosivorans* on betaine,

carnitine, or choline (each 20 mM) on a medium with yeast extract and peptone (each 0.25 %). Compared to the negative control (without substrate), *E. maltosivorans* produced 5 mM and 8 mM acetate when grown on carnitine and betaine, respectively, and small amounts of butyrate productions (1-2 mM) was observed from both substrates (Fig. S5). However, choline did not generate these SCFA above background level but resting cells appeared to adapt to this substrate as evident from the determined proteome (see below).

Proteome analysis of *E. maltosivorans* grown on the quaternary amines and glucose detected 812 proteins with 420 as core proteins detected in all conditions. Importantly, 11 out of the 27 proteins encoded by the *pdu* cluster were detected to be higher expressed when *E. maltosivorans* was grown on quaternary amines than on glucose, especially the genes involved in cobalamin assimilation (encoded by *pduS*) and the formation of the BMC shells (encoded by *pduABN*, Table 3). Functional identification of BMCs was provided by TEM image analysis of *E. maltosivorans* cells grown on betaine that clearly revealed BMC structures that were similar in number and structure as those visible in cells grown on 1,2-PDO but absent in glucose-grown cells (Figure 5D2).The involvement of BMCs in the degradation of quaternary amines such as choline has been earlier established for *Desulfovibrio alaskensis, Proteus mirabilis* and an uropathogenic *Escherichia coli* (Kuehl *et al.*, 2014; Jameson *et al.*, 2016; Herring *et al.*, 2018). However, these bacteria all contain choline TMA lyase and its activating enzyme (CutCD) generate TMA and acetaldehyde. The BMCs are involved to sequester acetaldehyde to prevent toxicity, and subsequently metabolize acetaldehyde to ethanol and acetate (Herring *et al.*, 2018). On the other hand, the resulting TMA is excreted in the gut lumen and cannot be used as a nitrogen or carbon source by most of the gut microbes. TMA then can enter the bloodstream, and once transported to the liver it is converted to trimethylamine N-oxide (TMAO) predominantly by flavin monooxygenase 3. High serum levels of TMAO have been shown to promote formation of atherosclerotic plaques in a mouse model (Koay *et al.*, 2021). Furthermore, serum levels of TMAO were significantly correlated with the incidence of heart attack and stroke (Wang *et al.*, 2011). Moreover, it is a common uremic toxin (Velasquez *et al.*, 2016).In contrast to the TMA-producing species, *E. maltosivorans* deaminates betaine and other quaternary amines in a process that likely involves a BMC. Quaternary amines are thought to be actively transported into the cell by BCCT transporter family proteins that also likely export the generated deaminated products (Ziegler *et al.*, 2010). In addition, based on earlier discoveries in another strain (Müller *et al.*, 1981), recent studies have elucidated the biochemical pathway of quaternary amines in *E. limosum* ATCC 8486^T into acetate and

butyrate during demethylation of betaine, choline, and carnitine into dimethylglycine, dimethylethanolamine and norcarnitine, respectively (Müller *et al.*, 1981; Picking *et al.*, 2019; Kountz *et al.*, 2020). In this way, one of three methyl groups from quaternary amines is transferred to MtqC (a corrinoid protein), together with a cob(I)alamin by MttB homologs, forming methyl-Co(III)-MtqC. The N, N-dimethyl compound is thus produced and released. The methyl group is subsequently transferred to tetrahydrofolate (THF) by a methylcorrinoid:THF methyltransferase (MtqA). The resulting methyl-THF enters the WLP, leading to cell biomass, and acetate/butyrate and CO_2 production. Co(I) MtqC can be adventitiously oxidized to catalytically inactive cobalt (II), which is reduced to active cobalt (I) by the ATP and reducing power– dependent activity of RamQ (a corrinoid activation enzyme) (Picking *et al.*, 2019; Kountz *et al.*, 2020). Based on genomic reconstructions a similar pathway is expected to operate in *E. maltosivorans* (Figure 3). Moreover, the present proteomic and TEM data provide further support for the fact that BMCs play a role in this unique pathway, rationalize the observation that the WLP genes are rather constitutively expressed as needed for growth on quaternary amines, and explains the requirement for the high number of MttB homologs predicted from the genomes of *E. maltosivorans* and related species (Table 1; see below). In general, the BMCs are thought to protect the cell from toxic metabolic intermediates, prevent unwanted side reactions and may enhance flux through a multistep pathway (Kerfeld *et al.*, 2018). In absence of further data, we hypothesize that the role of a BMC in the demethylation of quaternary amines by *E. maltosivorans* may be to encapsulate the vitamin B12-depending demethylation cascade and contain the appropriate TMA methyltransferase within the BMC.

Table 3. Proteins involved in bacterial microcompartments in *E. maltosivorans* were higher expressed when grown with betaine (BE), carnitine (CA), and choline (CH) than with glucose (Glu). PD: Propanediol. The locus tag for the genes encoded in *E. maltosivorans* starts with CPZ25_RS, which is omitted to avoid repetition in the table.

Locus tag	Protein	Relative Protein abundance		
		BE vs Glu	CA vs Glu	CH vs Glu
10565	Polyhedral organelle shell protein PduT	2.7	3.4	1.9
10575	Cobalamin reducase, PduS	14.8	13.5	10.7
10580	Propionaldehyde dehydrogenase, PduP	2.4	3.2	2.5
10590	Shell protein, PduN	27.5	1.0	1.0
10620	Glycerol dehydratase reactivase subunit alpha	1.0	1.8	1.5
10625	PD dehydratase small subunit PduE	4.7	12.3	6.6
10630	PD dehydratase medium subunit PduD	5.4	12.3	4.3
10635	PD dehydratase large subunit PduC	9.1	13.2	9.1
10640	Microcompartment protein PduB	12.6	18.2	13.2
10645	Microcompartment protein PduA	6.2	6.5	2.3
19865	Phosphate propanoyl transferase, PduL	1.8	2.3	1.1

Table 4. Differential expression of 16 MttB homologs and other components of a corrinoid-dependent methyltransferase in *E. maltosivorans* strain YI^T when grown with betaine (BE), carnitine (CA), choline (CH) or glucose (Glu). MFS: major facilitator superfamily protein; RamQ: corrinoid activation enzyme; MtqA: methylcorrinoid:tetrahydrofolate methyltransferase; MtqC: a corrinoid protein. The locus tag for the genes encoded in *E. maltosivorans* starts with CPZ25_RS, which is omitted to avoid repetition in the table. Fold change induction was calculated by dividing the protein abundances in the different growth conditions.

Locus tag	Protein (potential function)	Fold change induction		
		BE vs Glu	CA vs Glu	CH vs Glu
04610	MttB protein	15.8	16.8	16.8
05865	betaine specific MttB protein	**114.5**	29.8	1.0
06255	MttB protein	33.9	6.6	0.7
12920	MttB protein	6.6	5.3	4.4
12935	MttB protein	60.3	19.1	1.0
13475	betaine specific MttB protein	**25.7**	1.0	1.0
13640	MttB protein	5.9	2.6	3.0
13755; 18250	betaine specific MttB protein	**1148.2**	3.2	17.2
14265	MttB protein	22.4	10.7	14.6
13805	carnitine specific MttB protein	1.0	**933.2**	1.0
14255	MttB protein	5.9	6.3	5.1
14915; 14065	carnitine specific MttB protein	3.1	**575.4**	9.6
17920	MttB protein	1.3	3.5	5.4
12890	choline specific MttB protein	1.0	1.0	**61.5**
11850	MtqA	5.6	2.2	0.9
13765	MFS transporter	70.8	1.0	1.0
14190	MtqC	0.5	0.04	0.0
18535	RamQ	4.2	1.8	0.9

Demethylation of quaternary amines is associated with induction of TMA methyltransferases in *E. maltosivorans*

Next, we focused on the expressed products of *mttB* genes in *E. maltosivorans* when induced by the growth with different quaternary amines and the other tested substrates (see Fig. 3). Among the total of 41 MttB homologs predicted by the genome of *E. maltosivorans*, 16 were detected to be present in the proteomes of cells grown on the quaternary amines. Of note, most of these detected MttB homologs were detected in the cells grown at all quaternary amines, except for protein products of CPZ25_RS12890 and CPZ25_RS13475, and CPZ25_RS13805, which was only detected when *E. maltosivorans* was grown on choline, betaine and carnitine, respectively (Table 4).

A recent proteome study of *E. limosum* grown on proline betaine showed high expression of only one of the MttB homologs, in line with earlier finding that this demethylating enzyme systems seem to be very specific (Muller *et al.*, 1981).The MttB enzymes catalyzed tetrahydrofolate methylation of proline betaine specifically, forming the key intermediate methyl-THF in the WLP (Picking *et al.*, 2019). Later, Kountz *et al.*, (2020) also revealed a carnitine specific MttB protein, namely MtcB, which catalyzes specifically L-carnitine demethylation. We found the homologs of MtpB and MtcB in the genome of *E. maltosivorans*, with 98.3% and 77.0% amino acid similarities (encoded by CPZ25_RS13805 and CPZ25_RS13245, respectively) to those in *E. limosum*. In addition, we identified MtqA and MtqC homologs in the genome of *E. maltosivorans*, sharing high similarity (>96% protein identity) to those of *E. limosum*.

In apparent contrast with the results obtained for *E. limosum* (Picking *et al.*, 2019; Kountz *et al.*, 2020), the *E. maltosivorans* proteome showed multiple overproduced MttB proteins for each of the quaternary amines betaine and carnitine as well as choline, though we only analyzed resting cells for the latter (Table 4). For instance, MttB homologues encoded by CPZ25_RS13805 and 18250 were >300 times higher produced when grown on betaine than when grown on carnitine, while MttB homologue encoded by CPZ25_RS13805 was >900 times overproduced when grown with carnitine than grown with betaine. Remarkably, although choline did not seem to support the growth of *E. maltosivorans*, the proteomes of the cells was affected, as one MttB homologue (encoded by CPZ25_RS12890) was uniquely produced when cells were incubated in the presence of choline. Based on our present proteome data, we hypothesize that candidate TMA methyltransferases specific for betaine are CPZ25_RS05865,

13475, 18250 and 13755, specific for carnitine are CPZ25_RS13805, 14065 and 14915, and CPZ25_RS12890 specific for choline.

To fully picture the 41 MttB homologues encoded by the genome of *E. maltosivorans*, a Maximum-likelihood phylogenetic tree was constructed (Figure 6). The amino acid sequence of these *E. maltosivorans* MttB proteins varied considerably, as when compared to the prototype MttB (CPZ25_RS14065 and 14915), these vary from 100% to approximately 27% in sequence identity. Through our current proteome and genome studies, we identified 16 active MttB homologues induced by growth or incubation with 3 different quaternary amines and proposed specific substrates for 8 MttB homologues. The substrates for the other MttB homologues in *E. maltosivorans* remain unknown but we speculate that these may be involved in growth on other C1 compounds like methanol, CO or formate. Moreover, these may be involved in the ability to demethylate other substrates such as dietary lignans and (iso)flavonoids, which have been linked to possible health benefits and longevity (Jin *et al.*, 2007; Possemiers *et al.*, 2008; Struijs *et al.*, 2009).

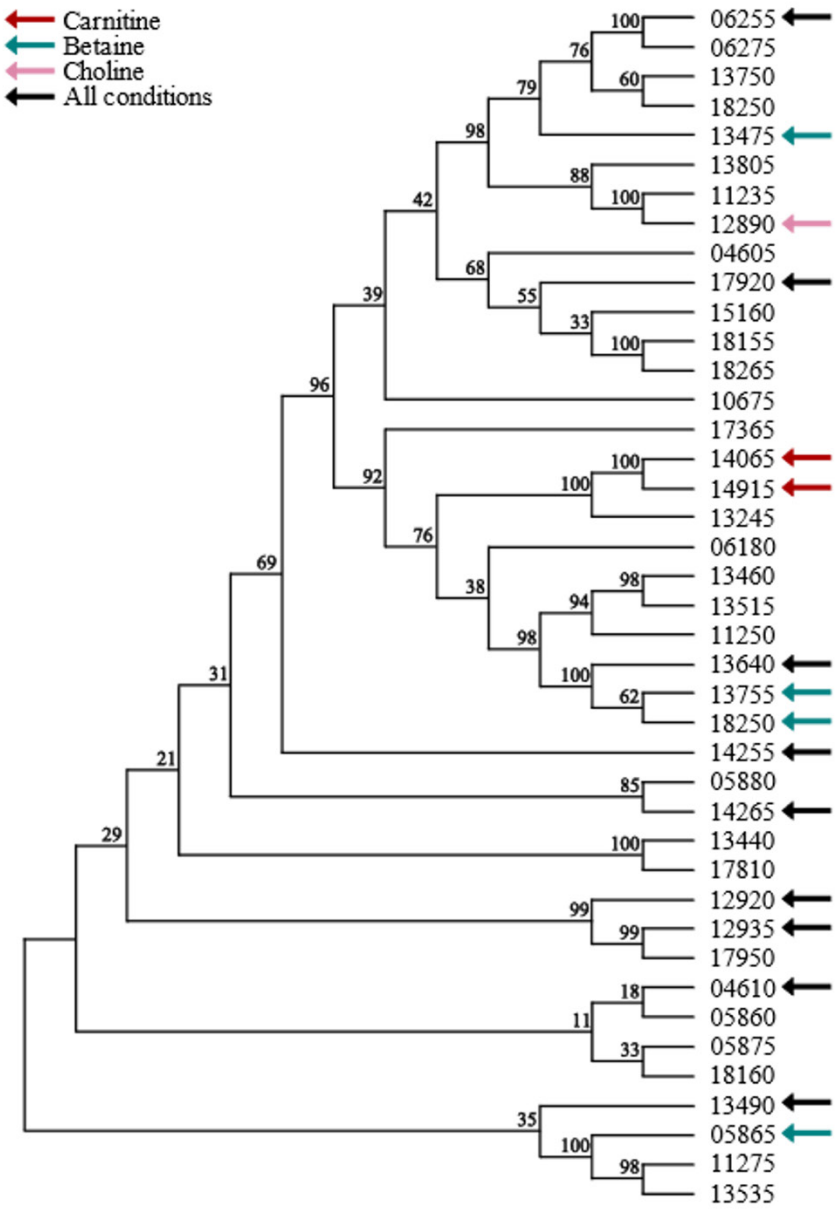

Figure 6. Maximum likelihood phylogenetic tree of 41 trimethylamine methyltransferase (MttB) homologues in *E. maltosivorans* YI^T. Label represents locus tag of the gene product, which in *E. maltosivorans* starts with CPZ25_RS. To avoid repetition of the prefix in the figure, the locus tags are represented only by the specific identifier. The numbers on branches represent the bootstrap values from 1000 replicates. The proteins detected in the proteomes described here are marked with arrows and the growth conditions are indicated.

Conclusions

Our genomic and proteomic analyses revealed key metabolic features of *E. maltosivorans* YI^T (Figure 2). *E. maltosivorans* has lactate utilization gene clusters, Ldh/Etf complex and butyryl-CoA dehydrogenase to convert low energy compounds D, L-lactate with acetate into butyrate. *E. maltosivorans* also catalyses the conversion of 1,2-PDO to propionate

and propanol and by proteome analysis and TEM, we confirmed that microcompartments were formed during the growth of *E. maltosivorans* with 1,2-PDO.

Genome analysis predicted *E. maltosivorans* YI^T to produce 41 trimethylamine methyltransferases (MttB). In our current proteome studies, 16 of these were detected when strain YI^T was grown with the quaternary amines betaine, carnitine and choline. In addition, 2 MttB proteins were produced when the cells were grown under homoacetogenic conditions. Substrate-specific MttB proteins for betaine, carnitine and choline were proposed based on the highly abundant protein products of *E. maltosivorans* compared to that grown with glucose. The deamination of betaine and other quaternary amines might also involve a microcompartment, possibly due to the vitamin B12-dependent nature of these MttB homologues. By this pathway, TMA production thus can be reduced in the human gut ecosystem and consequently leading to a lower TMAO level in the blood serum. The present study demonstrates that *E. maltosivorans* is highly versatile in converting low-energy fermentation end-products in the human gut into health-promoting SCFA and may be a useful therapeutic strain to prevent the production of the undesired TMAO.

Acknowledgments

We thank Jelmer Vroom and Iame Alves Guedes for assistant for the TEM pictures, as well as Dr. Sudarshan Shetty for useful suggestions on specific genome annotation. This work was supported by the SIAM Gravitation Grant 024.002.002 of the Netherlands Organization for Scientific Research.

Supplementary data

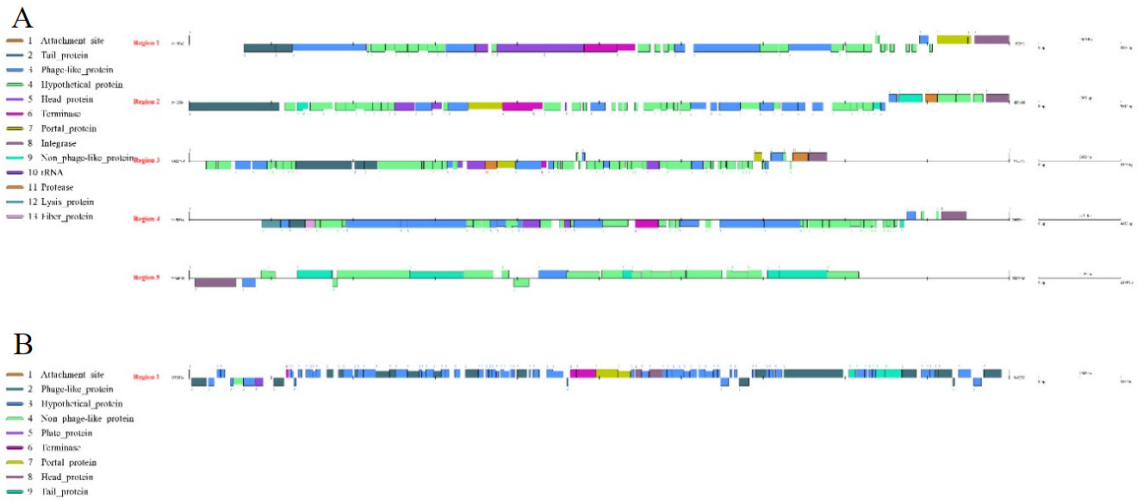

Supplementary Figure 1. Prophage genes detected in *E. maltosivorans* strain YI^T (A) and strain SA11 (B).

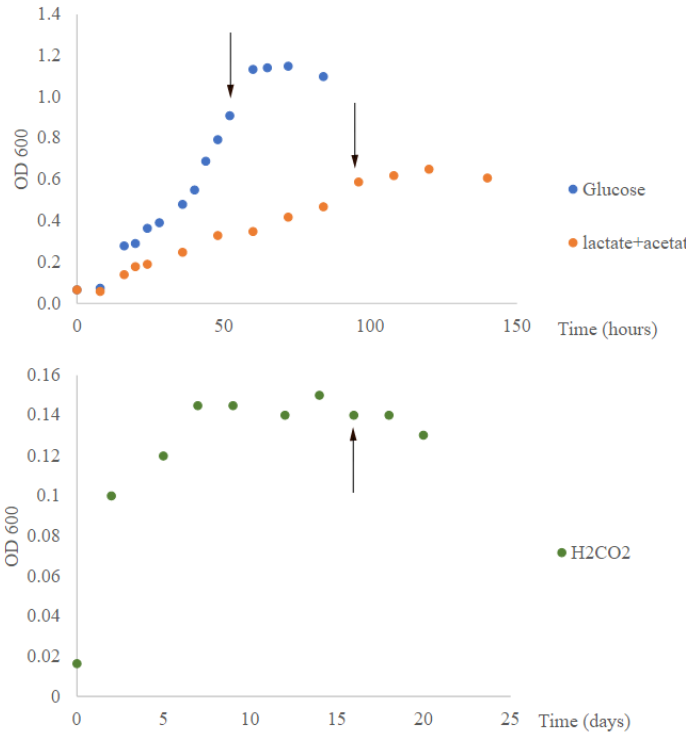

Supporting Figure 2: Growth curve of *E. maltosivorans* YI^T on different substrates (glucose; lactate+acetate; hydrogen+CO_2). Arrows indicate the sampling point of each growth condition.

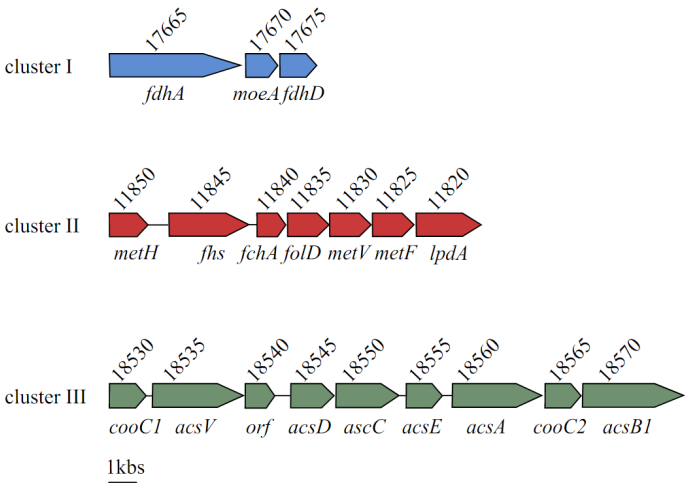

Supporting Figure 3. Gene clusters of Wood-Ljungdahl pathway in *E. maltosivorans* strain YI^T. The locus tag for the genes encoded in *E. maltosivorans* is CPZ25_RS*. To avoid repetition of the prefix in the tables, the locus tags are represented only by the specific identifier. Cluster I: the gene for formate dehydrogenase alpha subunit (*fdhA*) is organized together with the genes for a formate dehydrogenase accessory protein (*fdhD*) and a molybdenum cofactor guanylyltransferase (*moeA*); Cluster II: genes for methyltetrahydrofolate cobalamin methyltransferase (*metH*), formyl-THF synthetase (*fhs*), methenyl-THF cyclohydrolase (*fchA*), methylene-THF dehydrogenase (*folD*) and methylene-THF reductase (*metF*, *metV*) are organized together with the gene for a dihydrolipoyl dehydrogenase (*lpdA*). Cluster III: genes for the subunits of the CO dehydrogenase/acetyl CoA synthase complex consisting of CO dehydrogenase (*acsA*), acetyl-CoA synthase (*acsB1*), corrinoid-iron sulfur protein (*acsCD*) and methyltransferase (*acsE*) are organized together with two genes for a CODH nickel-insertion accessory protein (*cooC*) together with the genes for a corrinoid activation/regeneration protein (*acsV*) and a hypothetical protein (*orf*).

Table S1. Differentially expressed proteins in a pairwise comparison Lactate+Actate (butyrogenic growth) vs H_2+CO_2 (homoacetogenic growth). Positive values of the t-test difference (highlighted yellow) represent the proteins highly abundant in butyrogenic growth, while the negative values (highlighted orange) represent the proteins highly abundant in homoacetogenic growth. The locus tag for the genes encoded in *E. maltosivorans* is CPZ25_RS*. To avoid repetition of the prefix in the tables, the locus tags are represented only by the specific identifier. -Log p value represents -$\log_{10}$ transformed p-value from a pairwise two-tailed t-test comparing the two groups.

Locus Tag	Protein	-Log P value	Log10 Protein abundance (Lactate+Actate/ H_2+CO_2)
02230	Lactate dehydrogenase	1.6	3.4
02225	Electron transfer flavoprotein subunit alpha	2.0	3.4
18455	Nickel-dependent lactate racemase	2.1	3.2
05300	Alpha/beta hydrolase	7.6	2.7
09705	Aconitate hydratase	5.2	2.7
00940	Cyclase family protein	2.1	2.7
05270	OsmC family protein	6.2	2.4
19265	4Fe-4S dicluster domain-containing protein	4.6	2.3
02860	30S ribosomal protein S15	4.8	2.2
03885	Bifunctional 3,4-dihydroxy-2-butanone-4-phosphate synthase/GTP cyclohydrolase II	5.7	2.2

14015	PTS glucitol/sorbitol transporter subunit IIB	4.5	2.2
17660	Hypothetical protein	5.4	2.1
07800	DUF1667 domain-containing protein	5.1	2.1
14145	Helix-turn-helix transcriptional regulator	7.1	2.0
10830	Ribose 5-phosphate isomerase B	6.4	2.0
12605	Class I SAM-dependent methyltransferase	5.0	2.0
10940	Type 1 glutamine amidotransferase	3.8	2.0
05120	Nickel ABC transporter	1.6	2.0
16730	SEC-C domain-containing protein	3.9	2.0
04650	PTS glucitol/sorbitol transporter subunit IIB	3.6	2.0
09515	Rubrerythrin	5.2	1.9
06660	DNA-directed RNA polymerase subunit omega	4.8	1.9
06325	Lactoylglutathione lyase	4.0	1.9
01655	Response regulator transcription factor	5.1	1.9
00455	Nitroreductase family protein	4.7	1.9
09790	Adenylosuccinate synthase	5.9	1.9
13060	30S ribosomal protein S18	4.2	1.9
15240	Lactate utilization protein	4.2	1.9
10970	metal-dependent hydrolase	5.0	1.9
02220	Electron transfer flavoprotein subunit alpha	2.7	1.8
18535	DUF4445 domain-containing protein	5.0	1.8
14610	ABC transporter substrate-binding protein	1.7	1.8
13830	Hypothetical protein	6.4	1.8
05990	Citramalate synthase	5.4	1.8
20140	NAD(P)/FAD-dependent oxidoreductase	5.3	1.8
12565	ABC transporter substrate-binding protein	1.7	1.8
00935	4-hydroxythreonine-4-phosphate dehydrogenase PdxA	5.3	1.8
10915	Hypothetical protein	3.6	1.8
00290	sn-glycerol-1-phosphate dehydrogenase	5.5	1.8
02190	Mrp/NBP35 family ATP-binding protein	7.2	1.8
04675	Class II fructose-bisphosphate aldolase	1.3	1.8
10815	phospho-sugar mutase	1.1	1.7
03895	Bifunctional enzyme riboflavin biosynthesis protein RibD	4.6	1.7
06485	Serine-tRNA ligase	1.2	1.7
08600	Cysteine-tRNA ligase	4.1	1.7
04250	Amino acid-binding protein	5.4	1.7
14420	RpiB/LacA/LacB family sugar-phosphate isomerase	3.5	1.7
08100	Adenylosuccinate lyase	5.4	1.7
18980	MBL fold metallo-hydrolase	4.1	1.6
08195	N5-carboxyaminoimidazole ribonucleotide mutase	4.9	1.6
02805	UDP-glucose 4-epimerase GalE	4.6	1.6
17455	XTP/dITP diphosphatase	5.6	1.6
16565	Methylthioadenosine phosphorylase (MTAP)	3.4	1.6
06925	Antitoxin YefM	6.3	1.6
09695	dTDP-4-dehydrorhamnose reductase	3.6	1.6
10770	5'-methylthioadenosine/adenosylhomocysteine nucleosidase	5.1	1.6
06435	Transcriptional repressor	5.1	1.5
17705	Ribokinase	3.4	1.5
09685	dTDP-4-dehydrorhamnose 3,5-epimerase	4.5	1.5
07460	NAD(P)-binding domain-containing protein	3.7	1.5
11615	Helix-turn-helix transcriptional regulator	4.8	1.5
09740	Glucose-1-phosphate adenylyltransferase, GlgD subunit	3.7	1.5
13155	DNA polymerase III subunit beta	3.4	1.5
01360	Valine-tRNA ligase	4.5	1.5

03335	V-type ATP synthase subunit K	4.0	1.5
16825	STAS domain-containing protein	3.8	1.5
15045	L-fuculose-phosphate aldolase	3.3	1.4
07750	Hypothetical protein	5.0	1.4
06455	Insulinase family protein	3.7	1.4
07805	Chitobiase/beta-hexosaminidase C-terminal domain-containing protein	4.2	1.4
06620	Stk1 family PASTA domain-containing Ser/Thr kinase	2.7	1.4
02915	MIP family channel protein	2.8	1.4
07665	Response regulator transcription factor	4.7	1.4
05890	DUF362 domain-containing protein	4.9	1.4
18945	Glutamate-tRNA ligase	6.1	1.3
10035	Class I SAM-dependent methyltransferase	7.7	1.3
10780	Hypothetical protein	6.6	1.3
12980	Thioredoxin	4.7	1.3
07765	PTS-dependent dihydroxyacetone kinase phosphotransferase subunit DhaM	4.3	1.3
11075	Molecular chaperone HtpG	3.7	1.3
09615	Glycosyltransferase family 2 protein	6.4	1.2
02800	Nif3-like dinuclear metal center hexameric protein	3.3	1.2
00335	Hypothetical protein	3.7	1.2
05400	DUF896 domain-containing protein	5.3	1.2
01560	Hypothetical protein	6.2	1.2
08075	ABC transporter permease	3.5	1.2
17395	Dephospho-CoA kinase	3.1	1.1
20250	PTS transporter subunit EIIC	3.5	-1.5
08685	PTS transporter subunit EIIA	1.6	-1.9
14165	FAD-dependent oxidoreductase	4.6	-2.0
19095	Transcription termination factor Rho	3.2	-2.1
14065; 14915	trimethylamine methyltransferase	4.8	-2.3

Table S2. Differentially expressed proteins in a pairwise comparison Glucose vs Lactate+Actate (butyrogenic growth). Positive values of the t-test difference (highlighted yellow) represent the proteins highly abundant in glucose fermentation, while the negative values (highlighted orange) represent the proteins highly abundant in butyrogenic growth. The locus tag for the genes encoded in *E. maltosivorans* is CPZ25_RS*. To avoid repetition of the prefix in the tables, the locus tags are represented only by the specific identifier. -Log p value represents -$\log_{10}$ transformed p-value from a pairwise two-tailed t-test comparing the two groups.

Locus Tag	**Protein**	**-Log P value**	**Log10 Protein abundance (Glucose/Lactate+Actate)**
14160	Peroxiredoxin	4.8	2.9
13045	Pyridoxal 5'-phosphate synthase lyase subunit PdxS	4.2	2.5
06050	Flavodoxin	5.1	2.5
06065	Ferrous iron transport protein A	3.9	2.3
14165	FAD-dependent oxidoreductase	3.3	2.3
07620	Ferrous iron transporter B	4.2	2.2
02740	Cyclase family protein	4.4	2.2
17385	ABC transporter ATP-binding protein	3.9	2.0
03295	Argininosuccinate lyase	4.0	2.0
03315	Acetylglutamate kinase	5.3	2.0
20250	PTS transporter subunit EIIC	5.3	2.0
04400	V-type ATP synthase subunit B	3.9	2.0

19060	Alpha/beta hydrolase	6.6	2.0
20255	PRD domain-containing protein	6.3	2.0
17380	ABC transporter ATP-binding protein	5.1	1.9
02755	Uroporphyrinogen decarboxylase	4.9	1.8
03305	N-acetyl-gamma-glutamyl-phosphate reductase	6.9	1.8
00935	4-hydroxythreonine-4-phosphate dehydrogenase PdxA	5.4	-1.8
20140	NAD(P)/FAD-dependent oxidoreductase	5.3	-1.8
02230	Lactate dehydrogenase	5.3	-2.2
02220	Electron transfer flavoprotein subunit beta	2.6	-2.2
18455	Nickel-dependent lactate racemase	4.0	-2.4
02225	Electron transfer flavoprotein subunit alpha	2.6	-2.8

Table S3. Differentially expressed proteins in a pairwise comparison Glucose vs H_2+CO_2 (homoacetogenic growth). Positive values of the t-test difference (highlighted yellow) represent the proteins highly abundant in glucose fermentation, while the negative values (highlighted orange) represent the proteins highly abundant in homoacetogenic growth. The locus tag for the genes encoded in *E. maltosivorans* is CPZ25_RS*. To avoid repetition of the prefix in the tables, the locus tags are represented only by the specific identifier. -Log p value represents -$\log_{10}$ transformed p-value from a pairwise two-tailed t-test comparing the two groups.

Locus Tag	**Protein**	**-Log P value**	**Log10 Protein abundance (Glucose/H_2+CO_2)**
06070	hypothetical protein	4.8	2.9
00995	DUF1858 domain-containing protein	6.7	2.5
09705	Aconitase	6.6	2.4
05270	OsmC family protein	3.9	2.3
06065	Ferrous iron transport protein A	3.3	2.3
03310	Arginine biosynthesis bifunctional protein ArgJ	4.9	2.3
02860	30S ribosomal protein S15	3.9	2.3
14145	cro/c1-type helix-turn-helix domain	4.6	2.2
07620	Ferrous iron transporter B	4.4	2.2
02740	Cyclase family protein	3.9	2.2
10940	Glutamine amidotransferase	7.9	2.2
09790	Adenylosuccinate synthase	5.8	2.1
05990	Citramalate synthase	5.0	2.1
10830	Ribose 5-phosphate isomerase	6.9	2.1
12605	SAM-dependent methyltransferase	4.7	2.1
09560	P1 family peptidase	4.2	2.1
00455	Nitroreductase family protein	3.4	2.1
04400	V-type ATP synthase regulatory subunit B	6.6	2.0
18945	Glutamate-tRNA ligase	4.6	2.0
01360	Valine-tRNA ligase	7.6	1.9
17390	DNA polymerase I	6.2	1.9
03895	5-amino-6-(5-phosphoribosylamino)uracil reductase RibD	4.9	1.9
17420	Alcohol dehydrogenase, iron-type/glycerol dehydrogenase GldA	4.5	1.9
05970	Dihydroxy-acid dehydratase	1.2	1.9
08100	Adenylosuccinate lyase	9.2	1.9
13830	Hypothetical protein	5.2	1.9
07215	GTP cyclohydrolase I	3.7	1.9
09515	Rubrerythrin	5.0	1.9
19265	4Fe-4S ferredoxin-type iron-sulfur binding domain	6.3	1.9
04250	Amino acid-binding protein	4.5	1.9
06325	Glyoxalase I	6.7	1.9

12285	Hypothetical protein	3.9	1.9
05120	Solute-binding protein	1.5	1.9
10970	metal-dependent hydrolase	5.4	1.9
01655	Response regulator transcription factor	6.5	1.8
10770	Adenosylhomocysteine nucleosidase	6.2	1.8
02805	UDP-glucose 4-epimerase	4.5	1.8
13060	30S ribosomal protein S18	4.3	1.8
03305	N-acetyl-gamma-glutamyl-phosphate reductase	5.4	1.8
13090	Hypothesis protein	4.0	1.8
08195	5-(carboxyamino)imidazole ribonucleotide mutase	4.7	1.7
09685	dTDP-4-dehydrorhamnose 3,5-epimerase	4.1	1.7
01300	Acetyl-coa biotin carboxyl carrier protein	3.8	1.7
02190	Mrp/NBP35 family ATP-binding protein	3.9	1.7
14420	Galactose-6-phosphate isomerase subunit LacA	4.3	1.7
01305	Acetyl-coa carboxylase biotin carboxylase subunit	3.6	1.7
16565	MTAP family purine nucleoside phosphorylase	3.6	1.7
06925	Type II toxin-antitoxin system, antitoxin Phd/YefM	5.5	1.7
08600	Cysteine-tRNA ligase	7.7	1.7
10915	Hypothetical protein	3.5	1.7
16425	3-Dehydroquinate synthase, aroB	4.4	1.7
06455	Insulinase family protein	7.0	1.6
06485	Serine-tRNA ligase type1	1.1	1.6
09775	Transcription elongation factor GreA	4.2	1.6
07750	Hypothetical protein	4.6	1.6
08895	Fe-S cluster assembly scaffold protein NifU	4.2	1.6
08610	Hypothetical protein	3.8	1.6
09695	dTDP-4-dehydrorhamnose 3,5-epimerase	3.9	1.6
15140	Isoleucine-tRNA ligase	1.2	1.6
02915	Aquaporin family protein	1.5	1.6
00290	Glycerol 1-phosphate	4.4	1.6
02800	GTP cyclohydrolase 1 type 2/Nif3	3.4	1.5
08060	Dipeptide epimerase	1.3	1.5
07915	Transglutaminase domain-containing protein	1.3	1.5
08075	ABC transporter type 1	7.5	1.5
07800	Protein of unknown function DUF1667	5.8	1.5
14610	Nickel ABC transporter	1.4	1.5
17435	Glu-tRNAGln amidotransferase C subunit	5.4	1.5
09555	HAD family phosphatase	4.1	1.4
08885	Hypothetical protein	6.4	1.4
06435	Ferric uptake regulator	2.7	1.3
01560	Hypothetical protein	6.7	1.3
05300	Alpha/beta hydrolase	3.2	1.2
10035	SAM-dependent methyltransferase	6.6	1.2
07765	Phosphotransferase system, mannose-type IIA	3.9	1.1
05980	3-isopropylmalate dehydratase small subunit	3.7	1.1
07655	M23 family metallopeptidase	1.1	-1.6
07455	FGGY carbohydrate kinase	1.7	-1.8
19095	Rho factor	3.2	-2.1
14065; 14915	Trimethylamine methyltransferase	4.8	-2.3
10950	Hsp20	3.4	-2.3

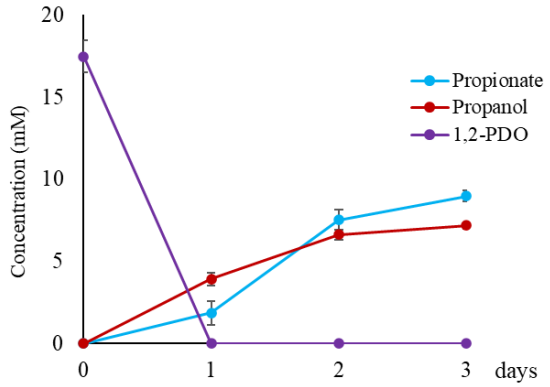

Supporting Figure 4. Metabolic end products of 1,2-Propendale (1,2-PDO) degradation by *E. maltosivorans* strain YI^T.

Table S4. Differentially expressed proteins in a pairwise comparison 1,2-PDO vs maltose. Positive values of the t-test difference (highlighted yellow) represent the proteins highly abundant in 1,2-PDO utilization growth, while the negative values (highlighted orange) represent the proteins highly abundant in maltose fermentation. The locus tag for the genes encoded in *E. maltosivorans* is CPZ25_RS*. To avoid repetition of the prefix in the tables, the locus tags are represented only by the specific identifier. -Log p value represents -log$_{10}$ transformed p-value from a pairwise two-tailed t-test comparing the two groups.

Locus Tag	Protein	-Log P value	Log10 Protein abundance (1,2-PDO/Maltose)
12735	Triose-phosphate isomerase	5.2	3.7
12755	Xylulose kinase	5.7	3.5
12740	YjbQ family protein	3.0	3.3
04255	Pyridoxamine 5-phosphate oxidase family protein	5.3	3.2
12745	Class II fructose-bisphosphate aldolase	5.6	3.2
15050	Class II aldolase/adducin family protein	5.8	2.8
08415	4Fe-4S dicluster domain-containing protein	4.8	2.6
15035	Carbohydrate kinase	5.6	2.5
12750	Ribulose-phosphate 3-epimerase	6.7	2.5
10590	Ethanolamine utilization protein EutN	5.3	2.4
00200	Putative DNA modification/repair radical SAM protein	5.9	2.2
15040	Dihydrofolate reductase	5.3	2.2
15045	L-fuculose-phosphate aldolase	4.4	2.1
02100	Anaerobic sulfite reductase subunit A	6.2	2.1
05250	Hypothetical protein	4.8	2.1
00960	Hypothetical protein	4.7	1.9
10600	Ethanolamine utilization protein EutJ	3.8	1.9
07290	DUF45 domain-containing protein	5.3	1.9
09985	Class II fructose-bisphosphate aldolase	4.3	1.9
10945	Diguanylate cyclase	12.0	1.9
09955	Deoxyribose-phosphate aldolase	3.8	1.8
09950	Carbohydrate kinase	4.5	1.8
09645	Undecaprenyl-phosphate glucose phosphotransferase	4.8	1.7
20090	Signal peptidase I	5.8	1.7
09990	Transaldolase	3.3	1.7
10085	(4Fe-4S)-binding protein	4.8	1.7
09970	Deoxyribose-phosphate aldolase	3.5	1.7
07615	Putative ABC transporter permease	6.1	1.7
10610	PduK BMC domain-containing protein	1.7	1.7
18630	50S ribosomal protein L33	0.8	1.7

08135	Tungsten ABC transporter substrate-binding protein	5.1	1.6
14160	Peroxiredoxin	4.2	1.6
17275	GTP-binding protein	5.4	1.6
06855	SOS response-associated peptidase	4.3	1.6
18870	RluA family pseudouridine synthase	4.1	1.6
03435	HD domain-containing protein	2.0	1.5
09670	ABC transporter ATP-binding protein	4.9	1.5
00145	Large conductance mechanosensitive channel protein MscL	1.1	1.5
16740	Hypothetical protein	5.3	1.5
14260	MFS transporter	4.0	1.5
14255	trimethylamine methyltransferase family protein	4.3	1.5
05940	Phosphate ABC transporter substrate-binding protein	1.4	1.5
17115	FAD-binding oxidoreductase	1.7	1.5
04895	Phospho-N-acetylmuramoyl-pentapeptide-transferase	9.6	1.5
20140	FAD/NAD(P)-binding oxidoreductase	5.0	1.4
09945	sn-glycerol-1-phosphate dehydrogenase	4.7	1.4
07095	Recombinase RecT	5.9	1.4
18980	MBL fold metallo-hydrolase	1.4	1.4
17410	DNA-binding response regulator	4.7	1.4
08965	Rhodanese-like domain-containing protein	5.6	1.4
18585	DUF3842 domain-containing protein	1.3	1.4
12830	N-acetyltransferase	3.7	1.4
11790	Demethoxyubiquinone hydroxylase family protein	7.3	1.4
10665	Cation-transporting P-type ATPase	4.8	1.4
09625	DUF2142 domain-containing protein	6.5	1.4
10030	ABC transporter substrate-binding protein	4.9	1.4
01785	Class B sortase	5.6	1.3
09960	Deoxyribose-phosphate aldolase	5.4	1.3
14900	Epoxyqueuosine reductase	6.9	1.3
16320	DNA-binding response regulator	4.2	1.3
09685	dTDP-4-dehydrorhamnose 3,5-epimerase	4.5	1.3
15515	YjbQ family protein	4.3	1.3
03125	ABC transporter ATP-binding protein	3.6	1.3
08635	ABC transporter ATP-binding protein	8.4	1.3
00360	Flavin reductase	1.2	1.3
17105	FAD-dependent oxidoreductase	3.2	1.3
10060	Potassium transporter Kup	5.2	1.3
16560	Cysteine hydrolase	1.7	1.3
19225	MarR family transcriptional regulator	3.4	1.2
13005	16S rRNA (cytidine(1402)-2-O)-methyltransferase	6.3	1.2
18105	Uma2 family endonuclease	1.0	1.2
14395	Metallophosphoesterase	1.0	1.2
08105	Pyridoxal phosphate-dependent aminotransferase	1.4	1.2
11785	Bacteriocin family protein	1.5	1.2
08405	GGDEF domain-containing protein	7.0	1.2
16495	ABC transporter ATP-binding protein	2.6	1.2
10930	Type IV pilus twitching motility protein PilT	1.2	1.2
19780	Magnesium-translocating P-type ATPase	1.4	1.2
06790	Hypothetical protein	1.4	1.2
09980	PHP domain-containing protein	4.3	1.2
19235	ABC transporter ATP-binding protein	1.0	1.2
04680	Sugar-binding transcriptional regulator	1.5	1.2
10595	Flavoprotein	3.7	1.1
01165	Hydroxyacid dehydrogenase	5.2	1.1
18245	pocR Transcription regulator	4.1	1.1
06675	Diaminopimelate epimerase	1.1	1.1
10585	Cob(I)yrinic acid a,c-diamide adenosyltransferase	4.7	1.1

15395	Hypothetical protein	4.5	1.1
00340	Hypothetical protein	1.1	1.1
01640	B12-binding domain-containing radical SAM protein	4.4	1.1
05270	OsmC family peroxiredoxin	3.9	1.1
17580	Magnesium transporter CorA family protein	1.4	1.1
14520	Hydantoinase/oxoprolinase family protein	5.8	1.1
06020	Hypothetical protein	2.9	1.1
14265	Trimethylamine methyltransferase family protein	3.2	1.1
18335	Holliday junction branch migration protein RuvA	3.9	1.1
12970	Thymidylate kinase	5.7	1.0
04100	DNA-binding response regulator	4.2	1.0
01400	Epoxyqueuosine reductase	3.6	1.0
10605	Phosphate propanoyltransferase	4.5	1.0
10120	Hypothetical protein	1.7	1.0
12760	MarR family transcriptional regulator	5.4	1.0
07415	Serine hydrolase	3.9	1.0
06765	Thiamine phosphate synthase	4.0	1.0
09400	Phage antirepressor protein	2.4	1.0
10645	Propanediol utilization microcompartment protein PduA	4.5	1.0
02765	Cyclase family protein	3.5	1.0
07600	Alanine/ornithine racemase family PLP-dependent enzyme	4.4	1.0
06355	Histidine phosphatase family protein	2.9	1.0
10700	tRNA (guanosine(46)-N7)-methyltransferase TrmB	6.5	0.9
00885	ABC transporter substrate-binding protein	5.6	0.9
11125	FMN-binding glutamate synthase family protein	6.2	0.9
10580	Aldehyde dehydrogenase EutE	3.8	0.9
13275	Phosphotransferase	3.9	0.9
20070	tRNA (guanosine(37)-N1)-methyltransferase TrmD	3.9	0.9
18075	1,2-diacylglycerol 3-glucosyltransferase	3.6	0.9
08540	SOS response-associated peptidase	3.5	0.9
05900	ABC transporter ATP-binding protein	3.4	0.9
14080	Cadmium-translocating P-type ATPase	2.3	0.9
06465	Hypothetical protein	5.3	0.9
18415	Hypothetical protein	3.5	0.9
10640	Propanediol utilization microcompartment protein PduB	4.5	0.9
12055	Glucose 1-dehydrogenase	4.4	0.9
10625	Propanediol dehydratase small subunit PduE	3.5	0.8
10635	Propanediol dehydratase large subunit PduC	4.4	0.8
19920	SsrA-binding protein SmpB	5.5	0.8
13400	MurR/RpiR family transcriptional regulator	6.3	0.8
13050	PLP-dependent aminotransferase family protein	5.4	0.8
12605	Class I SAM-dependent methyltransferase	3.5	-0.8
02035	4Fe-4S dicluster domain-containing protein	2.6	-0.8
11845	Formate--tetrahydrofolate ligase	3.8	-0.8
18560	Anaerobic CO dehydrogenase catalytic subunit	4.3	-0.8
02140	Non-ribosomal peptide synthetase	2.3	-0.9
18570	CO dehydrogenase complex subunit beta	4.0	-0.9
1182	5,10-methylenetetrahydrofolate reductase	4.6	-0.9
06435	Transcriptional repressor	3.5	-0.9
11820	Dihydrolipoyl dehydrogenase	3.7	-0.9
10035	Class I SAM-dependent methyltransferase	1.8	-1.0
08030	Hypothetical protein	5.5	-1.0
13755	Trimethylamine methyltransferase	3.5	-1.0
08810	Putative Ig domain-containing protein	1.9	-1.0
13750	Trimethylamine methyltransferase	5.8	-1.0

11915	Imidazole glycerol phosphate synthase subunit HisH	1.4	-1.0
16490	Hypothetical protein	1.4	-1.1
13305	FAD-binding protein	1.5	-1.1
10540	Hypothetical protein	3.6	-1.1
11835	Bifunctional 5,10-methylenetetrahydrofolate dehydrogenase	4.0	-1.1
11830	5,10-methylenetetrahydrofolate reductase	3.7	-1.2
02170	Xylulokinase	4.3	-1.2
00335	Hypothetical protein	4.4	-1.2
03370	Zinc-ribbon domain-containing protein	1.6	-1.2
01235	Xylulose kinase	4.8	-1.2
00575	PadR family transcriptional regulator	4.4	-1.2
12780	Hypothetical protein	1.6	-1.2
03335	V-type ATP synthase subunit K	1.1	-1.2
05985	3-isopropylmalate dehydratase large subunit	1.1	-1.3
15425	Transposase	4.3	-1.3
10915	Hypothetical protein	0.9	-1.3
03055	Methylated-DNA--[protein]-cysteine S-methyltransferase	4.6	-1.3
15025	Carbohydrate kinase	6.7	-1.4
15440	Hypothetical protein	4.8	-1.4
01520	Anthranilate synthase component I	4.0	-1.4
08800	Hypothetical protein	3.3	-1.4
05030	DegT/DnrJ/EryC1/StrS family aminotransferase	5.6	-1.4
13830	Hypothetical protein	3.4	-1.5
12240	DUF348 domain-containing protein	1.7	-1.5
08315	InlB B-repeat-containing protein	2.0	-1.5
05360	RnfABCDGE type electron transport complex subunit B	5.1	-1.5
19455	Cupin domain-containing protein	5.9	-1.5
10660	Biotin--[acetyl-CoA-carboxylase] ligase	5.1	-1.7
05295	Glycerate kinase	5.4	-1.7
03885	Bifunctional 3,4-dihydroxy-2-butanone-4-phosphate synthase	4.2	-1.7
01535	Indole-3-glycerol phosphate synthase TrpC	1.5	-1.7
19245	XRE family transcriptional regulator	5.5	-1.8
00225	Hypothetical protein	5.1	-1.8
14065; 14915	Trimethylamine methyltransferase	5.4	-1.8
19405	Hypothetical protein	5.2	-1.9
02930	PDZ domain-containing protein	8.5	-1.9
19285	4-hydroxybutyrate-acetyl-CoA CoA transferase	2.8	-2.0
11695	Hypothetical protein	4.7	-2.0
08290	Maltose operon regulators	4.7	-2.0
06065	Ferrous iron transport protein A	3.2	-2.2
00615	Hypothetical protein	3.2	-2.2
19255	Glu/Leu/Phe/Val dehydrogenase	3.3	-2.4
08295	Maltose operon regulators	5.7	-2.5
19260	ATP-binding protein	3.6	-2.6
08305	Maltose phosphoenolpyruvate phosphotransferase	6.2	-2.7
13060	30S ribosomal protein S18	4.3	-2.7
19270	3-methyl-2-oxobutanoate dehydrogenase subunit VorB	4.2	-2.7
08325	Hypothetical protein	5.5	-2.7
19275	2-oxoglutarate oxidoreductase	2.5	-2.8
08330	Hypothetical protein	5.2	-2.9
19280	2-oxoacid:ferredoxin oxidoreductase subunit gamma	2.6	-3.0
08300	Maltose-6-phosphate hydrolase	6.2	-3.2
08280	Hypothetical protein	5.3	-4.1

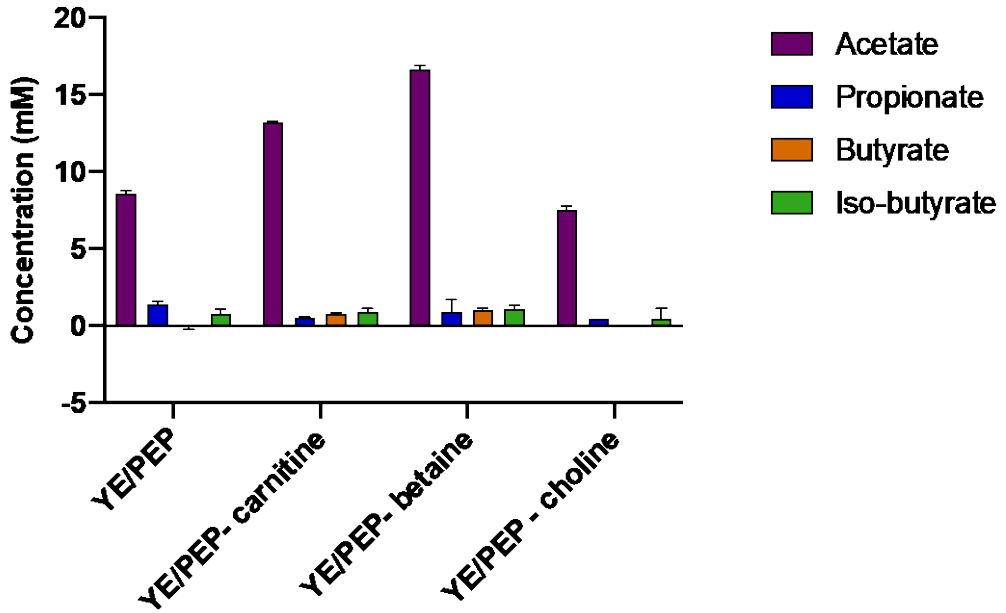

Supporting Figure 5. Short chain fatty acids produced by *E. maltosivorans* strain YI^T after 2 weeks incubation with 20 mM betaine, carnitine, or choline compared to grown with negative control (only supplemented with YE/PEP).

Chapter 5: *Sporobaculum desulfitilongum* gen. nov., sp. nov.: comparative genomics and proteomics of a novel sulfite-reducing and homoacetogenic member of the *Negativicutes* isolated from the human gut

Yuan Feng, Alfons J.M. Stams, Irene Sánchez-Andrea and Willem M. de Vos

Abstract

A novel spore-forming and anaerobic bacterium was isolated from a fecal sample of a healthy adult. The isolate, designated strain 2C^T was isolated performing sulfite reduction using pyruvate as substrate. Cells of strain 2C^T were long rods of typically 0.3 x 3 - 8 µm, but elongated to 30 - 40 µm under sulfite reduction conditions. Cells appeared singly and stained Gram-positive. Growth was observed within a temperature range of 30 to 45 °C (optimum, 35-37 °C), and a pH range of 6.0 to 8.0 (optimum 7.0-7.5). Strain 2C^T was able to respire with sulfite or thiosulfate, dimethyl sulfoxide and trimethylamine N-oxide while producing hydrogen sulfide, dimethyl sulfide and trimethylamine, respectively. Strain 2C^T did not show respiratory growth with sulfate, tetrathionate, nitrate or nitrite as electron acceptors.. Strain 2C^T showed acetogenic growth with H_2/CO_2 and was not able to ferment various sugars. The major cellular fatty acids of the isolate were $C_{16:0}$, $C_{16:1}$ *w9c* and $C_{14:0}$. The draft genome comprises 4.67 Mb with a G+C content of 43.6 mol% and is predicted to encode 5056 proteins. Based on the 16S rRNA gene sequence analysis, strain 2C^T shares highest similarity with *Lucifera butyrica* DSM 27520^T (92.5% rRNA gene identity), *Anaerospora hongkongensis* DSM 15969^T (90.6% rRNA gene identity) from the *Sporomusaceae* family (*Selenomonadales* order, *Negativicutes* class, *Bacillota* phylum).

Considering the distinctive physiological and phylogenetic characteristics of strain 2C^T (DSMZ= 116182^T, KCTC= 25735^T), it represents a new genus and species for which the name *Sporobaculum desulfitilongum* gen. nov., sp. nov., is proposed. Comparative proteogenomics of strain 2C^T grown on pyruvate alone or with additional sulfite or dimethylsulfoxide demonstrated an active dissimilatory sulfite reduction pathway with a special membrane complex for electron transfer.

Introduction

The human gut ecosystem can be viewed as an exquisite bioreactor in which commensal microbes collectively breakdown undigested food components and compounds released by the host, resulting in the production of a diverse range of metabolites that can have specific health effects. A key function of this microbial ecosystem is the fermentation of complex carbohydrates into short-chain fatty acids (SCFAs) such as acetate, propionate and butyrate. Extensive research has shown the impact of SCFAs on host physiology, highlighting their role in nourishing local gut epithelial cells and influencing metabolic pathways in distant organs including the liver, adipose tissue, muscles, and brain (Canfora et al., 2015; Dalile et al., 2019; Rastelli et al., 2019; de Vos et al., 2022).

In the last two decades, the sulfur metabolism of the gut ecosystem has gained increasing attention. Sulfur-containing metabolites play a vital role in human health: for instance amino acids such as methionine and cysteine serve as building blocks for the synthesis of proteins, and taurine functions for osmolyte regulation and bile acid conjugation (Nimni *et al.*, 2007). Like other higher animals, humans are unable to assimilate organic sulfur compounds from inorganic sulfur (Griffith, 1987; Francioso *et al.*, 2020). Therefore, acquiring organic sulfur through dietary sources is crucial. Methionine, cysteine, and taurine are the primary organic sulfur sources in food, found abundantly in animal and milk products, as well as certain plant-based foods, like wheat, rice, rapeseed, etc (Bos *et al.*, 2009). Inorganic sulfur compounds present in the gut, such as sulfate and sulfite, are mainly derived from their use as food preservatives and found in drinking water and beverages (Barton *et al.*, 2017). Additionally, endogenous sources of sulfur, including sulfated mucus and bile acids, are available for microbial metabolism in the gut. The human gut mucus layer, particularly in the distal colon, exhibits an increased sulfation pattern. Several intestinal mucin-degrading bacteria, such as *Akkermansia muciniphila*, many *Bacteroides* spp. and some *Bifidobacterium* spp., contain genomes that encode various sulfatases and can release sulfate when grown with mucin (Ottman *et al.*, 2017; Luis *et al.*, 2021). Bile acids are released into the duodenum after consumption of a meal to aid in the digestion of fats and fat-soluble nutrients. One fourth of the bile acids is conjugated with the sulfur-containing taurine, and bacterial bile salt hydrolases (BSH) can hydrolyse the amide bond, releasing taurine for further bacterial metabolism.

Although the amount and forms of sulfur from the human diet and endogenous sources vary considerably, there are numerous sulfur compounds available to gut microbiome, leading

in a reduced environment to the production of hydrogen sulfide (Carbonero, Benefiel, Alizadeh-Ghamsari, *et al.*, 2012). Among the sulfidogenic gut microbiomes, sulfate-reducing bacteria (SRB) performing dissimilatory sulfate reduction (DSR) have been extensively studied in the past two decades. SRB organic compounds (or hydrogen) as electron donors and sulfate as the terminal electron acceptor which is reduced to sulfite, then to Dsr-C trisulfite as an intermediates, and ultimately to sulfide. The dominant SRB in the gut ecosystem are *Desulfovibrio*, *Desulfotomaculum*, *Desulfobacter*, *Desulfomonas* and *Desulfobulbus* spp. (Carbonero, Benefiel, Alizadeh-Ghamsari, *et al.*, 2012).

It has been suggested that SRB contribute to intestinal gut disorders, since the H_2S produced is toxic and may induce bowel inflammation (Jia *et al.*, 2012; Figliuolo *et al.*, 2017). However, the role of SRB may be more subtle as sulfide is also a potent neurotransmitter and has signaling functions in the gut and the brain (Krueger *et al.*, 2010; Shefa *et al.*, 2018). A recent study differentiated between specific *Desulfovibrio* species and their differential association with disease (Singh *et al.*, 2023). Moreover, a recent human intervention with *D. piger,* one of the most abundant human commensal SRB, demonstrated its safety and a potential health benefit by sharing a symbiotic relationship between *Faecalibacterium prausnitzii* (Khan *et al.*, 2023). Other bacteria that reduce sulfite, but not sulfate, occur as well in the human gut. One such species is *Bilophila wadsworthia*, and high abundance of this sulfite reducer correlates with unhealthy conditions of the host including but not limited to obesity, systemic inflammation, cardiovascular disease (CVD), inflammatory bowel diseases (IBDs), irritable bowel syndrome (IBS) and autism spectrum disorder (Brahe *et al.*, 2015; Natividad *et al.*, 2018; Tabatabaei *et al.*, 2020; Kittana *et al.*, 2021).

Under stress conditions, the human gut produces inflammatory cytokines and other molecules that induce NADPH oxidase 1 in human colonic epithelial cells, leading to an increased amount of reactive oxygen species (ROS) (Yang *et al.*, 2007). The majority of these ROS carry unpaired electrons and free radicals that not only have antimicrobial activity but can also cause oxidation of metabolites present in the gut lumen. Consequently, dimethyl sulfide (DMS), TMA and thiosulfate are converted by oxidation into dimethyl sulfoxide (DMSO), trimethylamine N-oxide (TMAO) and tetrathionate (Paiva and Bozza, 2014; Stecher, 2015). These compounds were found to promote the population of oxygen-stress resistant pathogens like *E. coli* and *Salmonella* leading to a further tipping point and reduced diversity of gut microbiome (Zhu *et al.*, 2018).

In this work we isolated a novel sulfite-reducing human bacterial strain 2C^T and provided a phylogenetic, physiological and genomic analysis. It is capable of reducing sulfite and thiosulfate, but not sulfate. Moreover, it also reduced and grow on the potentially undesired DMSO and TMAO. Strain 2C^T (=DSMZ 116182^T = KCTC 25735^T) is considered to represent a new species of the novel genus *Sporobaculum* in *Sporomusaceae* family (*Selenomonadales* order, *Negativicutes* class, *Bacillota* phylum), for which the name *Sporobaculum desulfitilongum* gen. nov., sp. nov. is proposed.

Material and Methods

Source of the organisms and media preparation

A series of enrichment cultures aimed at discovering novel sulfidogenic bacteria were conducted using human fecal samples (approved by CCMO Netherlands, project ID: NL2907008109). Among these cultures, one exhibited notably high sulfide production with O_2-free basal medium supplemented with pyruvate and sulfite. This enrichment was selected to reveal its phylogenetic composition using 16S rRNA amplicon sequence analysis via a clone library. Detailed information regarding the enrichment setup and phylogenetic analysis were previously described (Feng *et al.*, 2017). The enriched bacterium, designated as strain 2C^T, belonged to the *Sporomusaceae* family of *Bacillota* phylum and showed limited (91%) 16S rRNA gene sequence similarity with that of known *Sporomusa* species. Strain 2C^T was isolated by performing pasteurization (in liquid media at 80 °C for 15 min), serial dilutions followed by 2 times streaking on agar plates (0.8% Agar noble, Difco), and a final serial dilution and growth with 10 µg/mL vancomycin. *Sporomusa sphaeroides* DSM 2875^T, *Anaerospora hongkongensis* DSM 15969^T and *Acetonema longum* DSM 6540^T were purchased from the German Collection of Microorganisms and Cell Cultures (DSMZ) (Braunschweig, Germany).

An O_2-free basal medium was prepared as previously described Stams *et al.*, (1993) and was supplemented with 0.5 g/L yeast extract; sodium sulfide was replaced by 0.5 g/L L-sodium cysteine as reducing agent. Cultures were incubated statically under 1.5 atm of N_2/CO_2 (80:20, v/v) and pH 7.2 at 37 °C. When the pH of the media needed to be modified, bicarbonate-buffer was removed and extra phosphate was added. The HCl and NaOH were used to adjust the pH to desired values before autoclaving. All solutions were heat-sterilized, except the vitamins solution which was filter-sterilized. Substrates were prepared in stocks of 1 M unless mentioned otherwise and added to the media at final concentrations ranging from 5 to 20 mM. Sodium

sulfite was prepared as a 250 mM stock solution in O_2-free demi water and filter-sterilized. When hydrogen was tested as a substrate, the headspace was exchanged to filter sterilized H_2/CO_2 (80:20, v/v).

Phenotypic characterization

Cell morphology, spore formation, and motility were examined by phase-contrast microscopy using a Leica DM2000 microscope (Leica Microsystems, Wetzlar, Germany). Scanning electron microscopy (SEM) was performed as previously described (Alphenaar *et al*., 1994) using a JEOL JSM-6480LV microscope (JEOL, Tokyo, Japan). Survival due to spore formation was checked after pasteurization by putting the cultivation bottle in 80°C water bath for 20 min. Gram-staining was performed according to the standard descriptions (Doetsch, 1981) and confirmed by checking reaction of cells with 3% (w/v) KOH. Catalase activity was determined by reaction with 3% (v/v) H_2O_2. Oxidase activity was tested with a fresh, filter sterilized 1% (w/v) tetramethyl-p-phenylenediamine solution (Sigma-Aldrich, St. Louis, MO, United States) in demi water. Idol and urease formation, gelatin and esculin hydrolysis were tested with API 20A (bioMérieux, France) in duplicate according to the manufacturer's instruction.

Growth experiments were conducted in triplicates and incubated up to 6 weeks. For physiological tests, strain $2C^T$ were cultivated in the basal medium containing 20 mM pyruvate and supplemented with 0.5 g/L of yeast extract. The temperature range and optimum for strain $2C^T$ were tested from 20 to 55 °C. The pH range and optimum were examined from 5.5 to 8.5, with intervals of 0.5 (including 7.2), at a constant temperature of 37 °C. Substrates for fermentative growth including sugars, organic acids, amino acids and sugar alcohols (Table 1) were tested in a final concentration of 20 mM. Negative controls without substrate were included. Electron acceptors were tested with in a final concentration of 10 mM, except otherwise indicated, included sulfate, thiosulfate, tetrathionate, sulfite (5 mM), DMSO, nitrate, nitrite (2 mM), and ferric iron. The electron donor remained consistent across all tested electron acceptors at 20 mM pyruvate.

Organic compounds were quantified by a Thermo Fisher Electron Spectra System high-performance liquid chromatograph (HPLC) equipped with an Agilent Metacarb 67H column and sulfuric acid (0.01 N) eluent at a flow rate of 0.8 mL min^{-1} at 45 °C. Gaseous compounds (H_2) were analyzed using a Shimadzu GC-2014 Gas Chromatograph equipped with a Molsieve

13X column. Nitrate, nitrite, sulfite, sulfate and thiosulfate were analysed using a Dionex 1000 ion chromatograph unit (Dionex) equipped with an IonPac AS17 Anion-Exchange column operating with a 0.1 mL min^{-1} flow rate at 30 °C. Sulfide production was measured by methylene-blue method (Cline, 1969). The amount of sulfide was determined by a spectrophotometer (U-1500, Hitachi, Japan) after the reaction was fully developed.

For membrane lipids fatty acids identification, strain $2C^T$ was grown on 20 mM pyruvate at 37 ºC for 5 days. *Sporomusa sphaeroides* DSM 2875^T, *Anaerospora hongkongensis* DSM 15969^T and *Acetonema longum* DSM 6540^T were grown in the same conditions for proper comparison. Cells were harvested, freeze dried and sent to the Deutsche Sammlung von Mikroorganismen und Zellkulturen (DSMZ, Braunschweig, Germany) for analysis.

Genomic DNA preparation, assembly, and annotation

Biomass of strain $2C^T$ grown with 20 mM pyruvate for 72 hours at 37 °C was harvested by centrifugation at 13000 g for 5 min at 4 °C. Genomic DNA was isolated by MasterPure™ (Epicentre, Madison, WI) and purified by Wizard® Genomic DNA Purification Kit (Promega) following the manufacturers' instructions. Illumina MiSeq and PacBio sequencing were performed at Novogene Biotechnology (Beijing, China). Both Illumina paired-end reads and PacBio subreads were used as input for the assembler spades (v.3.11.1) with a custom kmer setting of 21, 31, 51, 81, 91 and coverage cutoff set to auto. After removing scaffolds smaller than 500 bp, nine scaffold was obtained of 4,670,540 bp. Illumina paired-end reads were mapped back the assembly using bowtie2 (v2.3.3.1). The resulting sam files were converted with samtools (v1.3.1). The indexed bam file was used as in input for Pilon (v1.22) which resulted a polished assembly of a 4.6 Mb draft genome in 7 contigs. The assembled draft genome of strain $2C^T$ was annotated using the Semantic Annotation Platform with Provenance (SAPP) framework (Koehorst *et al.*, 2018). This framework consists of variety of tools, including Prodigal version 2.5 (Hyatt *et al.*, 2010), InterProScan 5RC7 (Jones *et al.*, 2014), tRNAscan-SE version 1.3.1 (Schattner *et al.*, 2005), RNAmmer version 1.2 (Lagesen *et al.*, 2007), and EnzDP (Feb-2016) for Enzyme Commission numbers (EC) prediction (N.-N. Nguyen *et al.*, 2015). The predicted EC's from EnzDP was used for KEGG (Kyoto Encyclopedia of Genes and Genomes) pathway analysis. CRISPR genes of strain $2C^T$ were annotated using CRISPRfinder (Grissa *et al.*, 2007). The CRISPRTarget tool identifies target phages using different databases and the search algorithm has its own scoring system with a score of 20 which was kept as default minimum as suggested by the authors (Biswas *et al.*,

2013). Prophage sequences were detected using PHASTER (Arndt *et al.*, 2016). In general, if a given phage region's total score is < 70, it is recognized as incomplete; between 70 to 90, it is recognized as questionable; if > 90, it is intact.

Phylogeny of strain 2C^T

The 16S rRNA gene sequence of strain 2C^T was obtained from the draft genome and deposited at GenBank under the accession number OR541985. To check whether there was any heterogeneity between 16S rRNA genes operons, a PCR amplicon of the 16S rRNA genes was sequenced by Sanger sequencing (performed by GATC Biotech, Germany). The 16S rRNA gene sequence of strain 2C^T was aligned with SILVA Incremental Aligner (SINA) (Pruesse *et al.*, 2012). The aligned sequence was merged with ARB program (Ludwig *et al.*, 2004) in a database (Ref NR 99, released 13.12.2017) of over 695,000 homologous prokaryotic 16S rRNA gene primary structures, and added by parsimony to the tree generated in the Living Tree Project (Yarza *et al.*, 2008, 2010). Phylogenetic reconstruction was performed by using the maximum likelihood (RaxML), neighbor-joining (with Jukes-Cantor correction) and maximum parsimony algorithms using different filters (termini, subact, none) as implemented in the ARB package. A consensus tree was generated with ARB v6.0 software. Pairwise comparison was performed taking into consideration the secondary structure of the 16S rRNA gene with the distance matrix method (similarity filter) implemented in ARB.

A maximum-likelihood phylogenomic tree of strain 2C^T and other closely related species in *Sporomusaceae* was constructed with IQ-TREE v1.6.12 (Nguyen *et al.*, 2015) from a filtered concatenated alignment of single-copy genes generated with GTDB-Tk v.1.0.2 (Chaumeil *et al.*, 2020). The LG+C40+F+R4 model was found to be the most optimal out of a wide selection of models with ModelFinder (Kalyaanamoorthy *et al.*, 2017). 1,000 ultra-fast bootstraps were performed to determine stability of the topology (Hoang *et al.*, 2018).

Comparative proteomics of strain 2C^T

Actively growing strain 2C^T was pre-cultured in medium with 20 mM pyruvate and inoculated (5%) in 120 mL of media in triplicates containing: 1) 20 mM pyruvate, 2) 20 mM pyruvate with 5 mM sulfite and 3) 20 mM pyruvate with 10 mM DMSO. Cells were harvested at mid-exponential phase. The samples were centrifuged at 4500 rpm for 20 min at 4°C. The cells and supernatant were stored immediately at -80 ºC until protein extraction. Collected cells were resuspended in 200 µL ice cold 100 mM Tris-HCl buffer (pH 8) and then centrifuged 1

min at 12 000g twice to make sure the medium was rinsed out. Protein extraction, trypsin digestion and elution, MS/MS analysis were the same as previously published (Feng *et al.*, 2022).

A strain 2C^T protein database was used together with a contaminants database that contains sequences of common contaminants including Trypsins (P00760, bovin and P00761, porcin) and human keratins (Keratin K22E (P35908), Keratin K1C9 (P35527), Keratin K2C1 (P04264) and Keratin K1CI (P35527). The "label-free quantification" as well as the "match between runs" options were enabled. De-amidated peptides were allowed to be used for protein quantification and all other quantification settings were kept default.

Filtering and further bioinformatic analysis of the MaxQuant/Andromeda workflow output and the analysis of the abundances of the identified proteins were performed with the Perseus 1.5.5.3 module (available at the MaxQuant suite). Accepted were peptides and proteins with a false discovery rate (FDR) of less than 1% and proteins with at least 2 identified peptides of which at least one should be unique and at least one should be unmodified. Missing data was imputed using random draws from a Gaussian distribution centered around a minimal value to control for proteins missing not at random (MNAR). Mostly, these proteins were potentially missed in one condition as a consequence of their intensities being below the detection limit. Relative protein quantitation of sample to control was done with Perseus by applying a two sample t-test using the "LFQ intensity" columns obtained with FDR set to 0.01 and S0 set to 1. Total non-normalized protein intensities corrected for the number of measurable tryptic peptides (intensity based absolute quantitation (iBAQ) intensity (Schwanhäußer, 2011), after taking the normal logarithm, used for plotting on the y-axis in a Protein ratio versus abundance plot. Lastly, nLC-MSMS system quality was checked with PTXQC (Bielow *et al.*, 2016) using the MaxQuant result files. Mass spectrometry proteomics data will be deposited to the ProteomeXchange Consortium via the PRIDE (Vizcaíno *et al.*, 2016) partner repository with the dataset.

Results and Discussion

Characterization of strain 2C^T

Cells of strain 2C^T were motile rods, 0.3-0.4 µm in width, 3 to 8 µm in length, appearing single, occasionally in pairs (Figure 1A). Cell chains were never observed. When strain 2C^T was grown with 5 mM sulfite along with 20 mM pyruvate, cells elongated to 30 to 40 µm

(Figure 1B). Several flagella were observed under scanning electron microscope in cells with terminal spores (Figure 1C). Colonies on agar were whitish, translucent and circular, about 1 mm diameter in size. Cells of strain 2C^T stained Gram-positive and reacted negatively with 3% (w/v) KOH. Strain 2C^T was both catalase and oxidase negative. Indole and urease formation were absent. Gelatin hydrolysis was positive but not esculin hydrolysis. After 20 min incubation in a water bath at 80 °C, cells formed spherical, terminal endospores (see Figure 1C). Extracellular vesicles were observed in stationary phase cultures. Temperature range for growth was 30-45 °C, with an optimum at 35-37 °C; pH range for growth was pH 6.0-8.0, but best within pH 7.0-7.5.

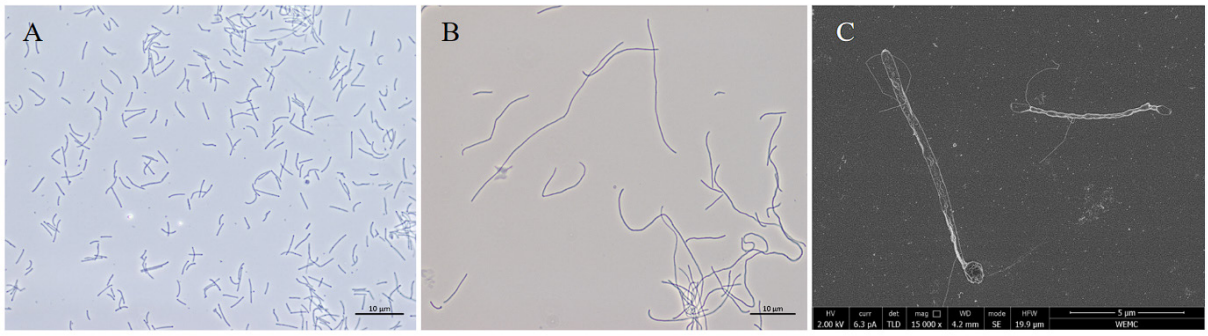

Figure. 1 Morphology of strain 2C^T. (A) Phase-contrast microphotographs of vegetative cells grown on 20 mM pyruvate. (B) Phase-contrast microphotographs of cells grown on 20 mM pyruvate and 5 mM sulfite. (C) Scanning electron microscopy image of strain 2C^T cell with sporangia in terminal position.

Phylogenetic position of strain 2C^T

Phylogenetically, strain 2C^T was placed within the reclassified *Sporomusaceae* family (*Selenomonadales* order, *Negativicutes* class), which was previously identified as *Selemonodales incertae sedis* 2 in the *Bacillota* phylum (Campbell *et al.*, 2015). The full 1336 bp 16S rRNA gene sequence, obtained from the draft genome, has been submitted to GenBank under accession number OR541985. Phylogenetic analysis showed that strain 2C^T shares highest levels of 16S rRNA gene similarity with *Lucifera butyrica* DSM 27520^T (92.5%), followed by 90.6% to *Anaerospora hongkongensis* DSM 15969^T, 90.3% to *Sporomusa sphaeroides* DSM 2875^T, 90.3% to *Methylomusa anaerophila* JCM 31821^T, and 90.0% to *Acetonema longum* DSM 6540^T (Figure 2A, Table S1). Notably, these similarity values fall below the threshold defined by Yarza *et al.* (2014), suggesting that strain 2C^T might potentially represent a novel genus. To further determine the phylogenetic position of strain 2C^T, a whole-genome tree was constructed for the 19 species belonging to *Sporomusaceae* and *Veillonellaceae* families (Figure 2B). Moreover, a pairwise average amino acid identity (AAI)

among these 20 species were calculated. In contrast with the 16S rRNA analysis, the whole genomic phylogenetic reconstruction shows that strain 2C^T separates from *Lucifera butyrica*, *Anaerospora hongkongensis,* and *Acetonema longum*, and forms a cluster with *Sporolituus thermophilus,* and *Thermosinus carboxydivorans*. (Table S2). This is in line with the AAI comparison results, where strain 2C^T shared highest AAI value to *Sporolituus thermophilus* (65.6%), *Thermosinus carboxydivorans* (65.4%), which fall within the threshold for genus-level differentiation (60-80%) (Luo *et al.*, 2014).

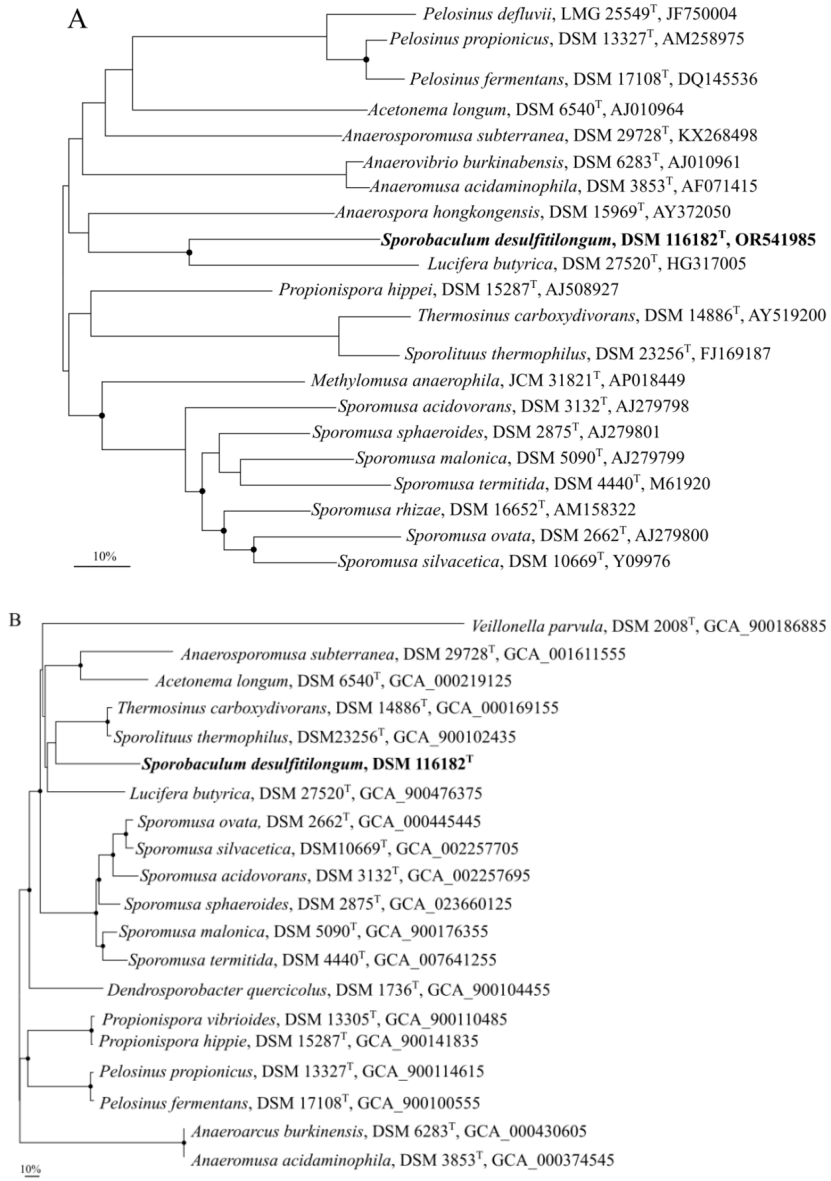

Figure 2. Phylogenetic reconstruction of strain 2C^T and related species in the *Sporomusaceae* family of the Firmicutes phylum. (A) Consensus tree based on 16S rRNA gene sequences (accession numbers are indicated), generated after applying the maximum likelihood, neighbor-joining and maximum parsimony algorithms implemented in the ARB package and based on 1000 replications. (B) Maximum-likelihood tree based on whole genomes from strain 2C^T and 19 related species for which genomes were available (see accession numbers). Bootstrap values

greater than 70% are indicated in solid cycles and bar indicates a 10% estimated sequence divergence for both trees.

Strain 2C^T shared common characteristics with other members of the *Sporomusaceae* family and a detailed comparison was made with the phylogenetically related species (Table 1). Like most species in *Sporomusaceae* family, strain 2C^T is strictly anaerobic, slightly curved, sporulating and motile. It is intriguing to notice that strain 2C^T and *Lucifera butyrica* are the only two isolates that showed a Gram-positive cell staining within the *Sporomusaceae* family. Although strain 2C^T shared the highest 16S rRNA gene similarity to *Lucifera butyrica*, it can be distinguished by its limited fermentative growth with carbohydrates. The ability to grow on C1 compounds, like CO_2 in the presence of H_2, is a property shared with strain 2C^T, *Lucifera butyrica*, *Acetonema longum* and many species in *Sporomusa* genus. While formate, methanol, butanol and betaine are fermented by virtually all *Sporomusa* species (with methanol and betaine supporting good growth), none of these substrates was utilized efficiently by strain 2C^T (Table 1).

Strain 2C^T was uncapable of sugar utilization, including glucose and fructose, which is another characteristic shared with *Anaerospora hongkongensis* and many *Sporomusa* species. Conversely, *Lucifera butyrica* and *Thermosinus carboxydovorans* showed rapid fermentative growth with different sugars. When growing with pyruvate, the predominant cellular fatty acids of strain 2C^T were C $_{16:0}$ (18.58 %), $C_{16:1}$ *w9c* (11.29 %) and C $_{14:0}$ (11.21 %). When growing with pyruvate, *Acetonema longum*, *Anaerospora hongkongensis* and *Sporomusa sphaeroides* had high abundant of $C_{16:1}$ *w9c* and Iso-$C_{13:0}$ 3OH. However, strain 2C^T uniquely showed high abundance of saturated straight-chain $C_{14:0}$ and $C_{16:0}$ under these conditions (Table S3). Finally, strain 2C^T can reduce sulfite, thiosulfate, DMSO and TMAO, a property which has not been shown to occur in any of the species of the genera *Sporomusa*, *Anaerospora* and *Acetonema*. These data demonstrate that the ecological, physiological and chemotaxonomical characteristics of previously strain 2C^T are different from those of phylogenetically related species that had been isolated. Based on the aforementioned genotypic and phenotypic traits, we propose that strain 2C^T represents a new species belonging to a novel bacterial genus, for which the name *Sporobaculum desulfitilongum* is proposed. Distinguishing features of strain 2C^T from related species are summarized in Table 1.

Table 1. Differential characteristics between strain 2C^T and its phylogenetically closest relatives.
+, positive; w, weak growth; -, negative. All strains were positive for aesculin hydrolysis. All strains were negative for urease and oxidase activity and for nitrate and sulfate reduction.1: Strain 2C^T, 2: *Lucifera butyrica* DSM 27520^T, 3: *Anaerospora hongkongensis* DSM 15969^T, 4: *Sporomusa sphaeroides* DSM 2875^T, 5: *Acetonema longum* strain DSM 6540^T, 6: *Sporolituus thermophilus* DSM 14886^T, 7: *Thermosinus carboxydivorans* DSM 23256^T. *Tested in this study.

Strain	1	2	3	4	5	6	7
Temp range/	30-45	25-40	37	15-45	19- 40	45-60	40-68
Optimum (°C)	35-37	37	ND	35-39	30-33	55	60
pH range/	6.0-8.0	3.5-7.0	ND	5.7-8.7	6.4-8.6	6.5-8.0	6.5-7.6
Optimum	7.0-7.5	5.5	ND	6.4-7.6	7.8	7.0	6.8–7.0
Gram staining	Positive	Positive	Negative	Negative	Negative	Negative	Negative
Size (µm)	0.3 -0.4 x 2-10	0.6 x 4-5	0.4-0.6 x 3.15-14.3	0.5-0.8 x 2-4	0.3-0.4 x 6-60	0.8-1.0 x 2-10	0.5 x 2.6-3
Spores	Yes	Yes	Yes	Yes	Yes	Yes	No
Substrates							
H_2/CO_2	+	-	-*	+	+	NT	NT
formate	-	-	-*	w	-	-	-
pyruvate	+	+	+*	+	+	-	+
lactate	-	-	+*	+	-	NT	-
glycerol	-	+	-*	+	-	-	
ethanol	-		-*	+	-	-	-
methanol	-	-	-*	+	-	NT	-
glucose	-	+	-*	-	+	-	+
xylose	-	+	-*	-	-	-	+
lactose	-	-	-*	-	-	-	+
fructose	-	-	w*	-	+	-	+
sucrose	-	-	-*	-	-	-	+
maltose	-	NT	w*	-	-	-	+
betaine	-	NT	-*	+	-	NT	NT
taurine	w	NT	-*	-*	NT	NT	NT
Electron Acceptors							
Sulfite	+	-	+	-	-*	+	-
Thiosulfate	+	+	NT	-	NT	+	-
TMAO	+	NT	NT	NT	NT	NT	NT
DMSO	+	+	-*	-*	-*	NT	NT

Genome properties of Strain 2C^T

The manually curated and annotated draft genome sequence of strain 2C^T comprised a chromosome of 4.67 Mbp with 46.3 mol% GC content. A total of 4,063 protein coding sequences were predicted as well as 91 tRNA, and18 rRNA genes (5 copies of 16S rRNA, 6 copies of 23S rRNA and 7 copies of 5S rRNA genes).

In the genome of strain 2C^T four prophage regions were identified: one with a size of 31 kb was intact and had an aberrant G+C content of 47.24%, while 3 others were incomplete with sizes of 10.6, 8.2 and 7.9 kb (Fig. S1). Strain 2C^T also contained a complete CRISPR/Cas system to defend against foreign DNA and a CRISPR array of a 1918 bp that contained a 37 bp long direct repeat (5-CTTTCAGTCTCCATTAATCGGAGAAGCTCAATGAAAC-3) with 25 spacers. Moreover, two potential CRISPRs were predicted, one cluster is of 107 bp containing a 24 bp long direct repeat (5-GGAAAAAAGTGATAGACCCAAGGC-3) with 1 spacer, and the other one is of 154 bp containing a 27 bp direct repeat (5-GGATACAGAGGGGGGGATACAGAGGAT-3) with 2 spacers.

As mobility was observes in strain 2C^T and the flagella visualized in SEM photos (Figure 1C), we examined the related genes in its genome. A set of genes encoding for the filament, the hook and the basal body of flagella were identified and are closely clustered from 2C_02861 to 2C_02886 (Figure 3), while genes encoding the flagellar motor stator protein A and B (MotAB, encoded by 2C_03431, 32) are located further downstream. It is noteworthy that strain 2C^T was found to possess *flgH* and *flgI*, which encode the major proteins for L-ring and P-ring of the flagellar basal body, respectively. The L- and P-ring are typical flagella structures found in Gram-negative bacteria, located in the outer membrane and periplasmic space. Furthermore, we investigated the genes involved in outer membrane biosynthesis. In Gram-negative bacteria, the outer membrane is predominantly composed of lipopolysaccharide (LPS), which has a tripartite structural organization consisting of lipid A, a core oligosaccharide region, and an O-specific polysaccharide chain or O-antigen (Whitfield and Trent, 2014). Essential gene clusters responsible for lipid A biosynthesis and heptose biosynthesis were identified in strain 2C^T (Table S3). Furthermore, heptosyltransferases I and II to form the complete lipid A-core, and O-antigen ligase to attach variety of polysaccharides to lipid A-core, were also identified in strain 2C^T (Table S3). Finally, the complete molecule of LPS is transferred to the outer membrane by the LPS transporting (LPT) protein complex (encoded by *lptABCDEFG*) (Sperandeo *et al.*, 2009), of which *lptD* and *lptE* were not identified in the

genome of strain 2C^T (Table S3). Considering the presence of identified outer membrane and LPS genes and the flagella structure, a double-membrane architecture structure is proposed although strain 2C^T stains Gram-positive (Figure 3).

Comparative proteomic analysis

Since strain 2C^T is capable of using sulfite and DMSO as terminal electron acceptors, we compared its proteome when grown under these two respiratory conditions with pyruvate as electron donor and under fermentative growth with pyruvate only. From a total of 4,063 protein coding sequences identified in the genome of strain 2C^T, 1,220 proteins were identified in the current study. A total of 682 proteins was detected in cultures grown with sulfite, 836 in cultures grown with DMSO, and 842 in pyruvate fermentation cultures with a core of 492 proteins produced at all the analyzed conditions. Besides the core, there were 31 extra proteins detected during both DMSO respiration and pyruvate fermentation conditions, while only one extra protein was detected solely in sulfite respiration condition (Table S4).

In a pairwise comparison (p value <0.01), 8 proteins showed significantly different abundance between sulfite-reducing and pyruvate cultures, 20 between sulfite-reducing and DMSO-reducing cultures and 23 between DMSO-reducing cultures and pyruvate-fermenting cultures. The complete lists of proteins with significantly different abundances in pairwise comparisons is given in Supporting Information (Tables S5–S7) and the most relevant are discussed below and used for the metabolic reconstruction (visualized in Figure 3).

Genomic and proteogenomic guided identification of sulfite metabolism in strain 2C^T

In classic sulfate-reducing bacteria like *D. desulfuricans*, sulfate is first activated with ATP to form adenosine phosphosulfate (APS) by sulfate adenylyltransferase (Sat). Thereafter, the activated sulfate in APS is reduced to sulfite by APS reductase, which consists of AprA and AprB subunits. AprAB receives the electrons from the Qmo (quinone-interacting membrane-bound oxidoreductase) ABC membrane complex, coupling in this way the electron flow between the quinone pool and the cytoplasm (Pires *et al.*, 2003). The genome of strain 2C^T does not encode for Sat, AprB, or the QmoABC complex genes, and consequently stain 2C^T cannot use sulfate as an electron acceptor.

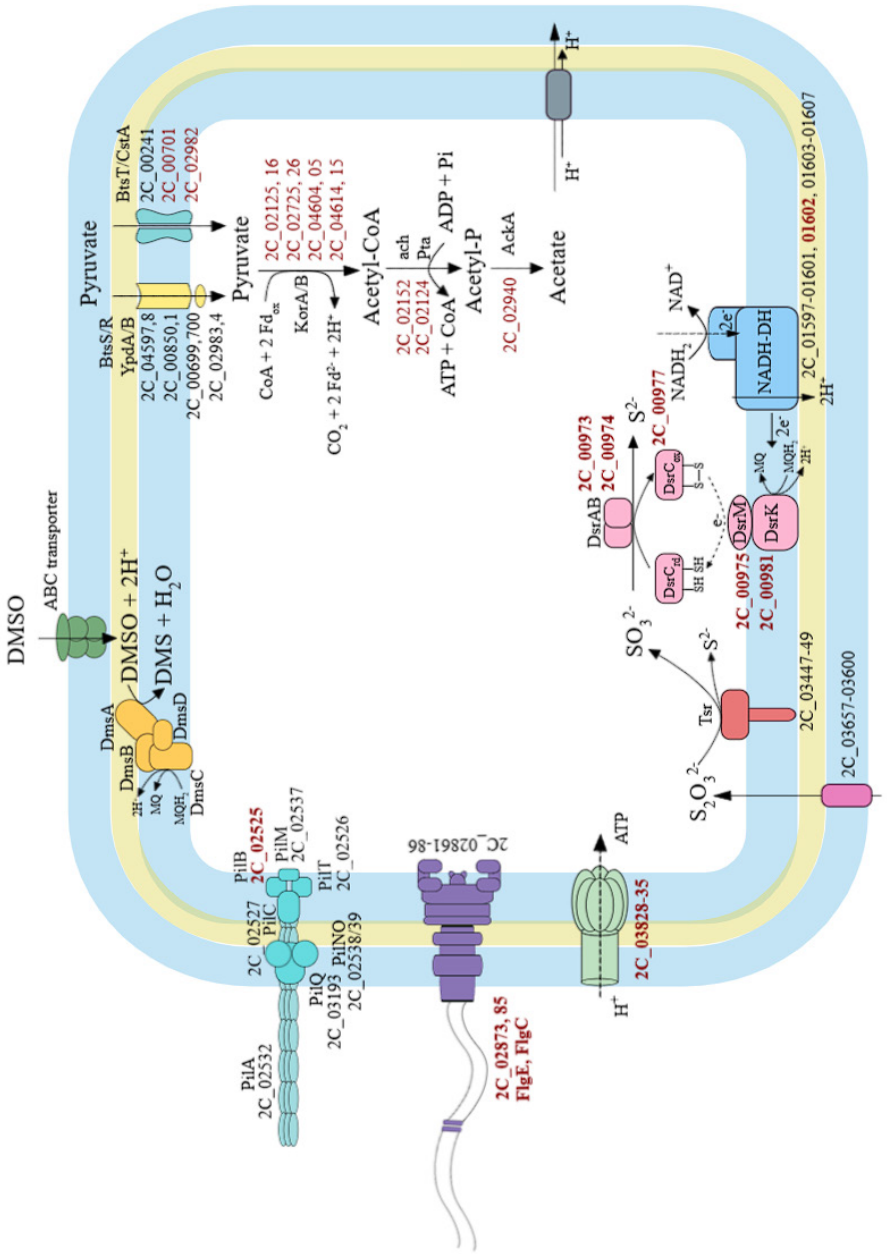

Figure 3. Metabolic reconstruction of the key metabolic features in *Sporobaculum desulfitilongum* strain 2C^T based on genomic predictions and supported by proteome data. As strain 2C^T belongs to the *Negativicutes order* and codes for LPS and other outer membrane components, a Gram-negative architecture is proposed. Gene loci marked in red are linked to genes that generated proteins detected in the proteome, while those in black are only identified in the genome but not detected in the proteome at any of tested growth conditions.

The canonical sulfidogenic process of sulfite reduction is known to be catalyzed by the dissimilatory sulfite reductase DsrAB in conjunction with DsrC, which coupling two and four electrons reduction, respectively. DsrC plays a crucial role by directly interacting with DsrAB, acting as a carrier for a partially reduced sulfur atom and forming a DsrC-trisulfide complex. At the membrane, the DsrC-trisulfide accepts electrons from the DsrMKJOP complex, undergoes further reduction, and is consequently released as hydrogen sulfide (Santos *et al.*, 2015). In general, Gram-negative SRB harbor the intact DsrMKJOP complex, while Gram-positive SRB contain the essential DsrMK components (Junier *et al.*, 2010). Regarding strain 2C^T, it is predicted to encode the essential dissimilatory sulfite reductase (DsrAB, encoded by 2C_00973 and 2C_00974), as well as DsrC (encoded by 2C_00977). Additionally, putative genes (2C_00975, 00981) encoding DsrM and DsrK subunits were located in close proximity to the dsrABC gene complex. Notably, genes encoding dsrJOP were absent in strain 2C^T, despite the proposed Gram-negative cell envelop. A similar situation has been reported in *Desulfurella amilsii*, where the Gram-negative SRB also possesses only the essential DsrMK components (Florentino *et al.*, 2017).

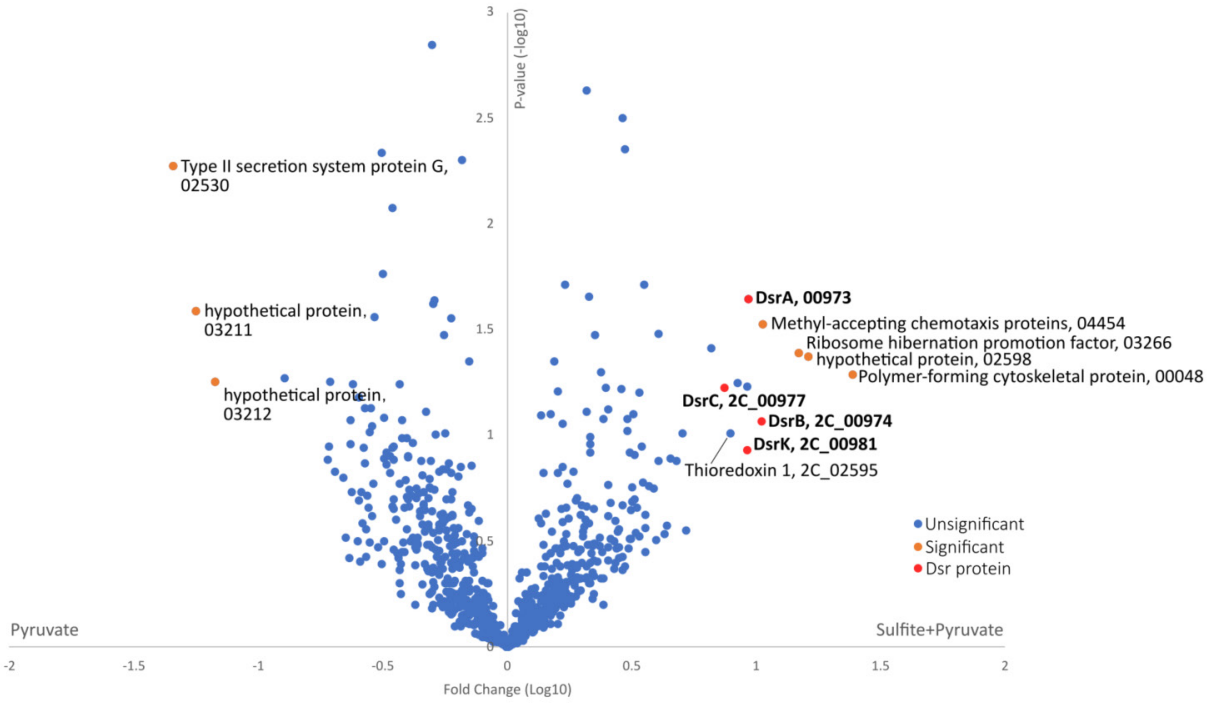

Figure 4. Differentially abundant proteins in *Sporobaculum desulfitilongum* strain 2C^T cells grown on sulfite/pyruvate and pyruvate. Proteins that are significantly different in abundance between the two conditions in the proteome are colored in orange, with the gene loci of the genes encoding for these proteins indicated. For clarity, proteins related to dissimilatory sulfite reduction (DSR) are labelled in bold. A complete list with product names for gene loci is given in Table S5.

Our comparative proteome analysis revealed notable differences in protein abundance between sulfite-reducing cultures and pyruvate cultures (Figure 4). Specifically, DsrAB and DsrC proteins showed approximately 10 times higher abundance in sulfite-reduction conditions compared to those in pyruvate cultures. (Figure 4). The DsrK was also found to be more abundant (9.2 times) in the proteome of sulfite reduction, while DsrM was not detected. Additionally, we detected a significantly higher levels of NADH-quinone oxidoreductase subunit I (encoded by 2C_01602, 10 times more abundant) in sulfite-reducing cells compared to DMSO-reducing cells. This observation strongly suggests that this NADH-quinone oxidoreductase (encoded by the gene loci 2C_01597-01607) is functional and involved in the electron transfer chain to cooperate with sulfite reduction (see the reconstructed sulfite reduction pathway in Figure 3).

Notably, we also observed an abundant production of thioredoxin (encoded by 2C_02595) and a protein product of a juxtaposed gene (2C_02598) with an unknown function in sulfite-reducing cultures. Specifically, the thioredoxin encoded by 2C_02595 was 7.9 and 6.8 times higher in sulfite-reducing cultures compared to pyruvate-fermenting and DMSO-reducing cultures, respectively. Similarly, the protein product of 2C_02598 was 16.3 and 1.9 times higher in sulfite-reducing cultures (Table S5). Domain analysis revealed that the protein encoded by 2C_02598 contains a redox-active disulfide domain and belongs to the iron-sulfur cluster repair protein (ScdA)-like superfamily, which was proposed to be involved in the repair of iron-sulfur clusters damaged by oxidative and nitrosative stress conditions in pathogens *Staphylococcus aureus* and *Neisseria gonorrhoeae* (Overton *et al.*, 2008). Thioredoxins are a class of small redox proteins that contain an active disulfide site with a CXXC motif (two cysteines separated by two amino acids XX) in their amino acid sequence, allowing thioredoxins to function as versatile protein disulfide oxidoreductases. Their activity is mediated through thiol-disulfide exchange reactions, which occur between the active site cysteines of the thioredoxins and the cysteines in the target protein (Bryk *et al.*, 2002). Thioredoxin genes are often regulated in response to external factors (Zeller and Klug, 2006). It has been suggested that thioredoxin plays a role in pathogen infection, such as in *Listeria monocytogenes*, *Helicobacter pylori*, and *Mycobacter tuberculosis*, by engaging in redox interactions against oxidative stress induced by diamide, hydrogen peroxide, and reactive oxygen or nitrogen species (Lu and Holmgren, 2014; Cheng *et al.*, 2017). Sulfite, being a reactive compound due to its unbound lone electron pair, acts as a potent reductant. Consequently, sulfite is toxic as it can cleave disulfide bonds, potentially modifying protein

structures and causing damage to nucleic acids and lipids in living organisms (Gunnison, 1981). It is tempting to speculate that the amount of this thioredoxin is increased to protect the cells from stress since strain 2C^T displayed robust growth in the presence of pyruvate and sulfite, resulting in the production of large amounts of sulfide and hence a low redox potential. Although thioredoxins primarily catalyze reductive reactions in the cytoplasm, it is also suggested that redox-active disulfides are highly dynamic and can be regulated by either oxidative or reductive changes in the local environment (Ladenstein and Ren, 2006; Bechtel and Weerapana, 2017). Therefore, based on our observations of high induced production of thioredoxin, along with the presence of the ScdA-like protein encoded by 2C_02598, we propose that these proteins may be involved in controlling the redox state of strain 2C^T during growth with reactive sulfite.

Proteogenomic guided identification of DMSO reduction in strain 2C^T

High concentrations of sulfide in gut lumen can initiate inflammation as it inhibits butyrate oxidation in colonocytes, damaging mucosal DNA and causing oxidation stress (Roediger *et al.*, 1993; Attene-Ramos *et al.*, 2010). To protect itself from the injurious effects of sulfide, the host mucosa can converts sulfide oxidizing it to thiosulfate (by sulfide-quinone reductase, persulfide dioxygenase, and sulfur transferase rhodanese), or to methanethiol (by S-methyltransferase) and then to DMS (Weiseger *et al.*, 1980; Hildebrandt and Grieshaber, 2008). Under inflammatory stress, ROS with antibacterial effects are produced by phagocytes and endothelial cells in the human colonic environment (Rizwan *et al.*, 2014). The active ROS can also oxidize gut lumen metabolites, leading to the productions of DMSO, TMAO and tetrathionate from DMS, TMA and thiosulfate, respectively (Paiva and Bozza, 2014; Stecher, 2015). Oxidative stress resistant pathogens like *E. coli* and *S. typhimurium* are capable of using these compounds as electron acceptors to promote their outgrowth, which leads to dysbiosis of gut microbiomes (Unden and Bongaerts, 1997; Winter *et al.*, 2011; Zeng *et al.*, 2017). Strain 2C^T also demonstrated the ability to use DMSO and TMAO as an electron acceptor, making it a potential competitor to *E. coli* and *S. typhimurium* under inflammatory colonic conditions.

In the current proteome study, protein products encoded by genes with gene loci 2C_00907, 00908, 03614, and 03615 were detected uniquely in DMSO growth condition, though these were not significantly higher induced compared to strain 2C^T cells growing under pyruvate fermentation and sulfite respiration conditions (Table 4). These proteins are highly homologous to those involved in the DMSO respiration system found in *E. coli*, consisting of

a molybdenum-containing active subunit DmsA, a 4Fe-4S ferredoxin-containing electron transport DmsB, a membrane anchor DmsC with several transmembrane helices, and a maturation chaperone protein DmsD (McEwan *et al.*, 2002) (Table 4). Hence, we assigned these genes as being involved in the DMSO reduction by strain 2C^T.

Table 4. Differential expression of dimethyl sulfoxide reductase (Dms) homologs in *S. desulfitilongum* strain 2C^T when grown with pyruvate, sulfite reduction or DMSO reduction cultures. Fold change induction was calculated by dividing the protein abundances in the different growth conditions.

Locus tag	Protein	Fold change induction	
		DMSO vs Pyruvate	DMSO vs Sulfite
2C_00907	DmsA1	4.6	4.6
2C_00908	DmsB1	4.6	4.6
2C_03614	DmsA2	2.4	2.4
2C_03615	DmsA3	2.8	2.8
2C_03616	DmsB2	1.8	2.4

Comparison of DMSO respiration genes of strain 2C^T and related species

Molybdenum oxidoreductases, utilizing molybdopterin as a cofactor, are crucial for electron transfer reactions in bacterial metabolic pathways. These proteins serve diverse roles, including functioning as nitrate reductases, formate dehydrogenases, sulfur, and N-oxide reductases (Wootton *et al.*, 1991). Notably, these proteins demonstrate sequence similarity among various prokaryotic oxidoreductases. For instance, DMSO and TMAO respiratory chains are usually categorized together, as they both consist of a molybdenum-containing subunit, a polyferredoxin-containing electron transfer subunit, and a membrane anchor subunit (McCrindle *et al.*, 2005). Extensive research has been conducted on DMSO and TMAO reductases in various microorganisms, such as *E. coli*, *Rhodobacter sphaeroides*, and *Shewanella oneidensis*. These studies have revealed mainly three different DMSO and TMAO respiratory chains, namely DmsABC in *E. coli*, Tor/Dor in *E. coli* and *R. sphaeroides*, and Dms/Cym-type in *Shewanella oneidensis* (McEwan *et al.*, 2002).

After examining the genome of strain 2C^T, we discovered in total four molybdopterin oxidoreductase respiration gene clusters scattered throughout its genome (Fig. 5). Three of these also encode complete DmsABC subunits, similar to that in *E. coli*. Two of these clusters (2C_00903-00911, and 2C_03614-03621) were assigned as DMSO reductases due to their identified function through the current proteome analysis. The genome of strain 2C^T did not contain genes for a TMAO respiratory chain which are typically associated with TMAO

reduction. Hence, it is likely that the observed TMAO reduction in strain 2C^T is carried out by one or more DMSO reductases since these are known to catalyze a wider range of S- and N-oxide substrates, while TMAO reductases specifically react with TMAO (Iobbi-Nivol *et al.*, 1996). To clarify, the other two molybdopterin oxidoreductase respiration gene clusters in strain 2C^T (2C_00268-00271 and 2C_00773-00774) were also assigned as DMSO reduction homologues for the following discussion, though their functions remain unrevealed.

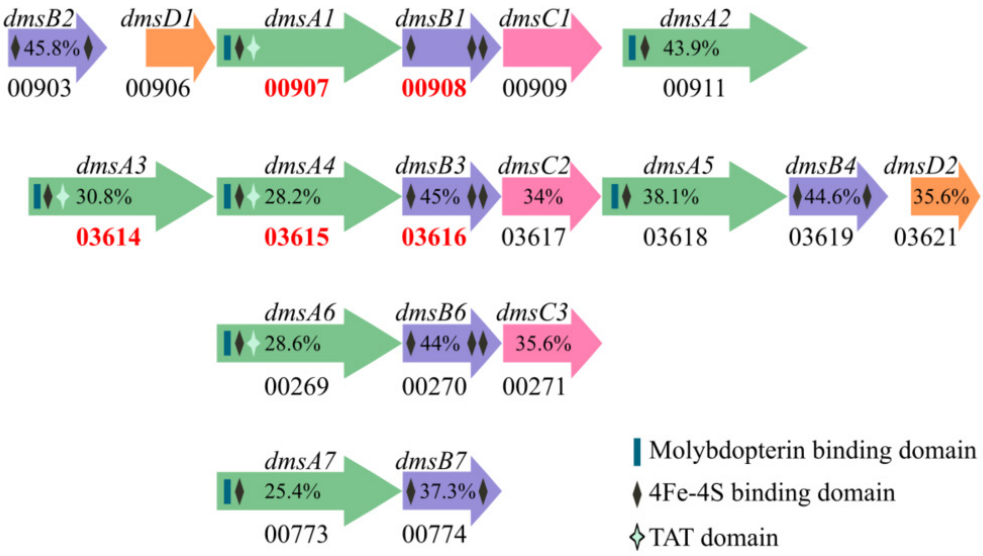

Figure 5. DMSO/TMAO reduction gene clusters in strain 2C^T. The identification was based on homology with molybdopterin binding domains and the presence of a TAT domain. Gene loci in bold red indicate that their protein products were more abundant in cells of strain 2C^T cells grown with DMSO than pyruvate.

The genome of strain 2C^T is predicted to encode a total of seven DmsA reductases, with varying lengths ranging from 677 to 813 amino acids. When compared to DmsA1 encoded by 2C_00907, the protein sequence similarity of these homologues ranges from 43.9% to 25.4%. All seven DmsA genes in strain 2C^T share similarities, as they all contain a molybdopterin binding domain and a putative 4Fe-4S cluster binding domain. Additionally, four of these genes are predicted to have a twin-arginine-motif (Tat system), indicating that these proteins are exported as metal-bound enzymes. An intriguing observation is that all three detected DmsA proteins in the current proteome study contain a TAT domain. A similar situation was recently reported in *Moorella thermoacetica*, which was predicted to encode three DsmA proteins with relatively low protein similarities of around 30% to each other. Remarkably, detailed transcription studies only showed expression in cells grown on DMSO of the genes for DsmA proteins with a TAT domain (Rosenbaum *et al.*, 2022). It has been established that all functional bacterial DMSO and TMAO reductases contain a TAT signal peptide in line with its secretion

as metal bound holoenzyme (McCrindle *et al.*, 2005). It was also suggested that putative DMSO reductases lacking such a sequence might instead be cytoplasmic biotin sulfoxide reductases (Gon *et al.*, 2000). These are likely not induced during growth on DMSO, hence explaining their absence from our current proteome analysis.

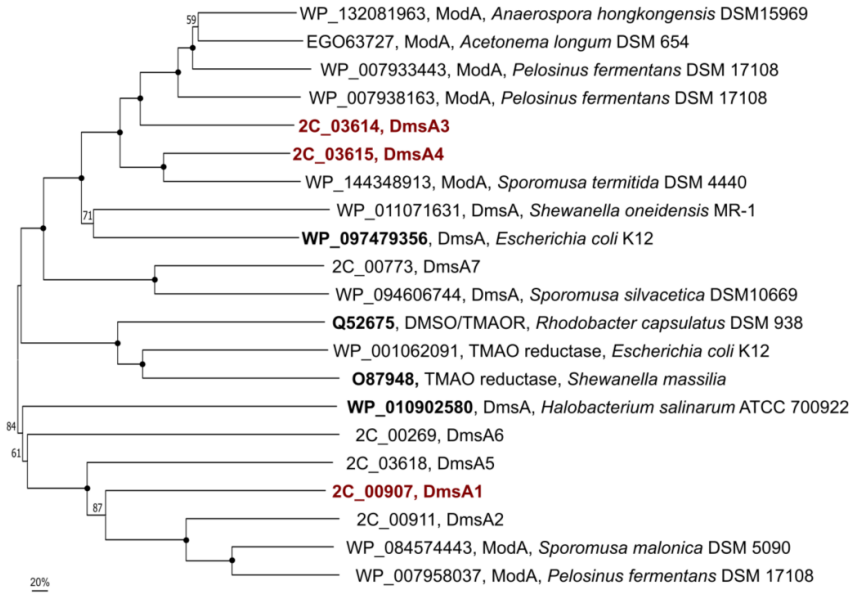

Figure 6. Maximum likelihood phylogenetic tree of the 7 DmsA homologs in strain 2C^T together with other molybdopterin-dependent oxidoreductases (ModA) in *Sporomusaceae* family, and reference DsmA or TMAO reductases in model organism (marked in bold black). Labels represent the NCBI protein accession number, protein function, taxonomic identity, and strain name. Bootstrap values from 1000 replicates higher than 95% are indicated by filled circles, and others by their number for clarity. Protein with accession number marked in bold red are DmsA detected in the current proteome of strain 2C^T.

Next, we conducted a search for homologous genes encoding molybdopterin-dependent oxidoreductases (ModA) within the genomes of bacteria closely related to strain 2C^T. A maximum likelihood phylogenetic tree was constructed with these ModA homologues in *Sporomusaceae* family, as well as from well-studied reference DmsA, TorA, DorA from aforementioned organisms (Fig. 6). We found homologues of ModA in *Anaerospora hongkongensis*, *Acetonema longum*, *Pelosinus fermentans*, and three *Sporomusa* species. However, in our current experiment where 10 mM DMSO was provided along with 20 mM pyruvate, *Anaerospora hongkongensis* and *Acetonema longum* did not show growth with DMSO reduction (Table 1). Furthermore, the ability to reduce DMSO has not been tested in *Sporomusa termitida*, *S. silvacetica*, and *S. malonica*, as these bacteria are primarily studied for their homoacetogenic properties. Therefore, gaining energy from both DMSO and TMAO reduction seems to be a unique metabolism in strain 2C^T. This study showed that the human

gut isolate 2C^T has a unique phylogenetic position and special metabolism that is not shared with its relatives as it is capable of reducing DMSO, TMAO, sulfite and thiosulfate together with pyruvate.

Description of *Sporobaculum* gen. nov.

Sporobaculum (Spo.ro.ba'cu.lum. Gr. fem. n. *spora*, spore; L. neut. n. *baculum*, small rod; N.L. neut. n. *Sporobaculum*, spore-bearing stick or rod)

Cells are spore-forming strictly anaerobic, motile, curved rods that stain Gram-positive. Catalase and oxidase activity were both negative while gelation hydrolysis was positive. Indole formation, urease activity and esculin hydrolysis were negative. neutrophilic The temperature range is 30-45 °C, with optimum 35-37 °C. The pH range is 6.0-8.0, with optimum 7.0-7.5. Does not utilize sugars for fermentative growth. The type species is *Sporobaculum desulfitilongum*.

Description of *Sporobaculum desulfitilongum* sp. nov.

Sporobaculum desulfitilongum (de.sul.fi.ti.lon'gum. L. pref. *de*, off, away; N.L. masc. n. sulfis -itis, sulfite; L. masc. adj. *longum*, long; N.L. neut. adj. *desulfitilongum*, reducing sulfite and long)

When growing with pyruvate, cells form thin, straight or slightly curved rods with rounded ends (0.3 x 5-8 μm). Acetate, H_2 and presumably CO_2 are produced during fermentative growth with pyruvate. The major cellular fatty acids of this isolate formed under such growth condition were C $_{16:0}$, $C_{16:1}\omega9c$ and C $_{14:0}$. When growing with pyruvate and sulfite cells are elongated to 30 to 50 μm. The isolate showed homoacetogenic growth with CO_2 and H_2. It does not use glucose, xylose, fructose, maltose, mannose, galactose, mannitol, lactose, raffinose, rhamnose, formate, glycerol, ethanol. It cannot respirate with sulfate, nitrite or nitrate. Strain 2C^T can use sulfite, thiosulfate as an electron donor with pyruvate to produce sulfide. It can reduce DMSO and TMAO to DSM and TMA. The G+C content of the genomic DNA is 46.3 mol%. The type strain is 2C^T (=DSM 116182^T, KCTC= 25735^T), isolated from human faeces.

Acknowledgements

We thank Bart Nijsse for genome assembly, Sjef Boeren for proteome analysis and Steven Aalvink for taking SEM photos.

Supplementary data

Table S1. Pairwise comparison of the 16S rRNA gene of *Sporobaculum desulfitilongum* with the closest isolates.

Type strains, accession numbers	Similarity (%)
Lucifera butyrica DSM 27520^T, HG317005	92.5
Anaerospora hongkongensis DSM 15969^T, AY372050	90.6
Sporomusa sphaeroides DSM 2875^T, AJ279801	90.3
Methylomusa anaerophila JCM 31821^T, AP018449	90.3
Acetonema longum DSM 6540^T, AJ010964	90.1
Sporomusa silvacetica DSM 10669^T, Y09976	90.0
Anaerosporomusa subterranea DSM 29728^T, KX268498	89.8
Sporomusa rhizae DSM 16652^T, AM158322	89.5
Propionispora hippei DSM 15287^T, AJ508927	89.5
Anaeromusa acidaminophila DSM 3853^T, AF071415	89.3
Anaeroarcus burkinensis DSM 6283^T, AJ010961	89.2
Sporomusa malonica DSM 5090^T, AJ279799	89.2
Sporomusa ovata DSM 2662^T, AJ279800	89.1
Sporomusa acidovorans DSM 3132^T, AJ279798	89.0
Sporolituus thermophilus DSM 23256^T	88.7
Sporomusa termitida DSM 4440^T, FJ169187	88.6
Pelosinus fermentans DSM 17108^T, DQ145536	88.3
Thermosinus carboxydivorans DSM 14886^T, AY519200	88.3
Pelosinus fermentans DSM 17108^T, DQ145536	87.8
Pelosinus delfuvii LMG 25549^T, JF750004	87.5

Table S2. AAI similarities (%) among the closest isolates in *Sporomusaceae* family to *Sporobaculum desulfitilongum*.

Type strains, accession numbers	AAI Similarity (%)
Sporolituus thermophilus, GCA_900102435	65.6
Thermosinus carboxydivorans, GCA_000169155	65.4
Sporomusa malonica, GCA_900176355	63.4
Anaerosporomusa subterranea, GCA_001611555	62.4
Sporomusa termitida, GCA_007641255	61.9
Sporomusa sphaeroides, GCA_023660125	61.4
Sporomusa silvacetica, GCA_002257705	61.1
Sporomusa acidovorans, GCA_002257695	61.1
Lucifera butyrica, GCA_900476375	61.0
Sporomusa ovata, GCA_000445445	60.6
Dendrosporobacter quercicolus, GCA_900104455	60.4
Pelosinus fermentans, GCA_900100555	60.3
Pelosinus propionicus, GCA_900114615	59.5
Acetonema longum, GCA_000219125	59.4
Propionispora hippie, GCA_900141835	59.1
Propionispora vibrioides, GCA_900110485	58.9
Anaeromusa acidaminophila, GCA_000374545	56.0
Anaeroarcus burkinensis, GCA_000430605	55.9
Veillonella parvula, GCA_900186885	47.5

Table S3. Relative abundance (% of total) of cellular fatty acids of *Sporobaculum desulfitilongum* strain 2C^T and its phylogenetic closest relatives growing on pyruvate.

Fatty acids	Strain 2C^T	*Sporomusa sphaeroides*	*Acetonema longum*	*Anaerospora hongkongensis*
Saturated straight-chain				
$C_{10:0}$	2.38	0.38	3.24	0.69
$C_{11:0}$	1.46	0.77		
$C_{12:0}$	6.26			
$C_{13:0}$	0.22			
$C_{14:0}$	**11.21**	0.71	2.06	1.51
$C_{15:0}$	1.62	0.52	0.08	0.36
$C_{16:0}$	**18.58**	5.78	6.47	7.81
$C_{17:0}$	0.34	0.43		0.14
$C_{18:0}$	1.24	0.71	0.80	1.03
$C_{19:0}$				
Unsaturated straight-chain				
$C_{14:1}$ *w5c*			0.44	
$C_{15:1}$ *w8c*	0.84	1.67	0.31	1.50
$C_{15:1}$ *w6c*		0.23		
$C_{16:1}$ *w9c*	**11.29**	**12.81**	**18.16**	**21.14**
$C_{16:1}$ *w7c*		6.51	**9.16**	5.55
$C_{16:1}$ *w5c*		0.13	0.09	0.15
Iso $C_{17:1}$ *w10c*	1.57			**9.32**
Iso $C_{17:1}$ *w9c*		0.15	**9.30**	
$C_{17:1}$ *w9c*				0.56
$C_{17:1}$ *w8c*	1.06	3.71	0.42	1.03
$C_{17:1}$ *w6c*				0.86
$C_{18:1}$ *w9c*	2.10	3.11	8.44	3.85
$C_{18:1}$ *w7c*	0.33	1.48	2.97	1.58
$C_{18:1}$ *w5c*				
$C_{20:1}$ *w7c*				
Hydroxy acids				
$C_{10:0}$ *3OH*			0.07	
$C_{11:0}$ *3OH*	-	0.10		0.08
Iso-$C_{11:0}$ *3OH*		0.26	0.07	0.07
$C_{12:0}$ *2OH*	0.14		0.27	0.14
$C_{12:0}$ *3OH*	**6.08**	2.69	**10.62**	**7.85**
$C_{12:1}$ *3OH*		0.11		
$C_{13:0}$ *2OH*		0.09		0.17
$C_{13:0}$ *3OH*				
Iso-$C_{13:0}$ *3OH*	**7.57**	**14.62**	**10.41**	**19.97**
$C_{14:0}$ *3OH*	**8.99**		0.82	
$C_{15:0}$ *3OH*	-			
Iso-$C_{16:0}$ *3OH*	0.14			
Saturated branched-chain				
Iso-$C_{11:0}$	1.27	**9.54**	**9.79**	4.86
Anteiso- $C_{11:0}$		0.12		
Iso-$C_{12:0}$	0.19			

Iso-$C_{13:0}$	0.57			
Anteiso- $C_{13:0}$	0.09			
Iso-$C_{15:0}$	4.66	3.48	1.30	2.70
Iso-$C_{15:1}$ *F*			1.81	0.76
Anteiso- $C_{15:0}$	0.12			0.14
Iso-$C_{16:0}$	0.07			
Iso-$C_{17:0}$	0.51	2.75	0.76	2.13
Anteiso- $C_{17:0}$				0.13
Iso-$C_{20:0}$				
Unsaturated branched-chain				
$C_{12:0}$ *ALDE?*	**9.05**	-		
Anteiso- $C_{17:1}$		2.84		

Supplementary Figure 1. Prophage genes detected in *Sporobaculum desulfitilongum* strain 2C^T.

Table S3. Lipid A biosynthetic genes (*lpx*), heptose biosynthetic genes (*gmh*), lipopolysaccharide transporting (LPT) protein complex (*lpt*) and other lipopolysaccharide related gene clusters in *Sporobaculum desulfitilongum* (gene loci start with 2C_). MsbA: ATP-dependent lipid A-core flippase; WaaA: 3-deoxy-D-manno-octulosonic acid transferase; *WaaC: heptosyltransferases I; WaaF: heptosyltransferases II; WaaL: O-antigen ligase;* RfaQ: lipopolysaccharide core heptosyltransferase

Gene	locus	Gene	locus	Gene	locus
lpxA	03789	*gmhA*	03125	*lptA*	03777
lpxB	03787	*gmhB*	03128	*lptB*	03776
lpxC	03791	*gmhC*	03126	*lptC*	03778
lpxD	03797	*gmhD*	03127	*lptD*	-
lpxI	03788	*waaC*	03121; 03440	*lptE*	-
lpxK	03784	*waaF*	03122; 03129	*lptF/G*	03775
lpxL	03795	*waaL*	02139; 03133	*rfaQ*	03121, 03122
lpxM	03779				
msbA	03786				
waaA	03785				

Table S4. Unique proteins detected per condition analysed. The locus tag for the genes encoded in strain $2C^T$ is 2C_*. To avoid repetition of the prefix in the tables, the locus tags are represented only by the specific identifier.

Condition	Locus Tag	Protein
10 mM pyruvate	00118	methyl-accepting chemotaxis protein
	00179	AAA proteins
	00315	TRAP transporter substrate-binding protein
	00376	DUF2088 domain-containing protein
	00687	DNA-binding response regulator
	00831	DEAD-box ATP-dependent RNA helicase CshA
	01025	DNA-directed RNA polymerase subunit delta
	01170	Hypothetical protein
	01175	AmmeMemoRadiSam system protein A
	01381	pyridoxine/pyridoxal/pyridoxamine kinase
	02204	efflux RND transporter periplasmic adaptor subunit
	02554	GTP cyclohydrolase I FolE2
	02607	UDP-N-acetylmuramoyl-tripeptide—D-alanyl-D-alanine ligase
	02689	Ribulose-phosphate 3-epimerase
	02787	DUF3870 domain-containing protein
	02858	Chemotaxis protein-glutamate methylesterase
	02876	flagellar hook-length control protein FliK
	03055	Metalloprotease TldD/PmbA
	03087	Single-stranded-DNA-specific exonuclease RecJ
	03101	SpoIID/LytB domain-containing protein
	03111	SpoIIE family protein phosphatase
	03460	Sodium-translocating pyrophosphatase
	03447	thiosulfate reductase PhsA
	03511	HlyD family secretion protein
	03630	Indolepyruvate oxidoreductase subunit IorB
	03775	YjgP/YjgQ family permease
	03810	Peptidase S55, SpoIVB
	04059	Uracil-DNA glycosylase
	04437	DUF896 domain-containing protein
	04461	Molybdopterin biosynthesis protein
	04531	NADH:flavin oxidoreductase/NADH oxidase
10 mM pyruvate + 5 mM DMSO	00043	[FeFe] hydrogenase H-cluster maturation GTPase HydF
	00054	Glutamate synthase
	00056	FAD-dependent oxidoreductase
	00062	ABC transporter ATP-binding protein
	00134	Tetratricopeptide repeat protein
	00388	Hypothetical protein
	00658	type I restriction-modification system subunit M
	00905	Hypothetical protein
	00907	Dimethyl sulfoxide reductase DmsA
	00908	Dimethyl sulfoxide reductase DmsB

	00939	Methyl-accepting chemotaxis protein
	00953	2-dehydropantoate 2-reductase
	01001	2-isopropylmalate synthase
	01343	Tryptophan synthase subunit beta
	01378	NADH:flavin oxidoreductase
	01623	Imidazole glycerol phosphate synthase subunit HisF
	01639	AAA family ATPase
	01864	Polyamine aminopropyltransferase
	02256	Citrate lyase subunit beta
	02257	Citrate lyase subunit alpha
	02310	ArsB/NhaD family transporter
	02422	HlyC/CorC family transporter
	02647	ABC transporter substrate-binding protein
	03125	D-sedoheptulose 7-phosphate isomerase
	03614	Dimethyl sulfoxide reductase DmsA
	03615	Dimethyl sulfoxide reductase DmsA
	03671	Cysteine synthase A
	03684	Acetolactate synthase large subunit
	03786	Lipid A export permease/ATP-binding protein MsbA
	04170	Hypothetical protein
	04381	Alpha/beta-type small acid-soluble spore protein
10 mM pyruvate + 5 mM sulfite	03389	Efflux RND transporter periplasmic adaptor subunit

Table S5. Differentially expressed proteins in a pairwise comparison Sulfite + Pyruvate vs Pyruvate. Positive values of the t-test difference (highlighted yellow) represent the proteins highly abundant in sulfite respiration, while the negative values (highlighted orange) represent the proteins highly abundant in pyruvate fermentation. -Log p value represents $-\log_{10}$ transformed p-value from a pairwise two-tailed t-test comparing the two groups.

Locus Tag	**Protein**	**-Log P value**	**Log Protein abundance** (Sulfite+Pyruvate / Pyruvate)
00048	Polymer-forming cytoskeletal protein	1.2	1.4
00973	Sulfite reductase, dissimilatory-type subunit alpha	1.6	0.97
02598	DUF1858 domain-containing protein	1.4	1.2
03266	Ribosome-associated translation inhibitor RaiA	1.4	1.2
04454	Methyl-accepting chemotaxis sensory transducer	1.5	1.0
02530	Prepilin-type N-terminal cleavage/methylation domain-containing protein	2.3	-1.3
03211	DUF1659 domain-containing protein	1.6	-1.3
03212	DUF2922 domain-containing protein	1.3	-1.2

Table S6. Differentially expressed proteins in a pairwise comparison DMSO + Pyruvate vs Pyruvate. Positive values of the t-test difference (highlighted yellow) represent the proteins highly abundant in sulfite respiration, while the negative values (highlighted orange) represent the proteins highly abundant in pyruvate fermentation. -Log p value represents $-\log_{10}$ transformed p-value from a pairwise two-tailed t-test comparing the two groups.

Locus Tag	**Protein**	**-Log P value**	**Log Protein abundance (DMSO**+Pyruvate / Pyruvate**)**
00048	Polymer-forming cytoskeletal protein	1.7	1.2
00054	Glutamate synthase	1.8	1.1
00055	4Fe-4S binding protein	2.2	0.9
00056	FAD-dependent oxidoreductase	1.7	0.9
00057	ABC transporter substrate-binding protein	3.7	1.6
01329	CoA transferase	2.2	1.0
01937	NADP-dependent malic enzyme	2.2	1.2
02154	Cobalamin B12-binding domain-containing protein	1.5	1.1
02257	Citrate lyase alpha subunit	2.4	1.4
02453	Sulfur carrier protein ThiS adenylyltransferase ThiF	3.4	0.8
02454	Thiamine phosphate synthase	2.8	1.1
02647	ABC transporter substrate-binding protein	3.0	1.5
02702	Inosine-5′-monophosphate dehydrogenase	1.6	1.1
03266	Ribosome-associated translation inhibitor RaiA	1.9	1.0
04017	ABC transporter substrate-binding protein	3.4	1.8
04581	Glutamine synthetase	2.2	1.4
00945	2-hydroxyacid dehydrogenase-like protein	3.9	-0.9
01025	DNA-directed RNA polymerase subunit delta	4.1	-0.9
02530	Prepilin-type N-terminal cleavage/methylation domain-containing protein	2.5	-1.2
02544	efflux transporter, RND family, MFP subunit	4.0	-1.1
03211	DUF1659 domain-containing protein	1.2	-1.1
03212	DUF2922 domain-containing protein	3.2	-1.9
03865	50S ribosomal protein L31	3.0	-0.9

Table S7. Differentially expressed proteins in a pairwise comparison DMSO+Pyruvate vs Sulfite+Pyruvate. Positive values of the t-test difference (highlighted yellow) represent the proteins highly abundant in sulfite respiration, while the negative values (highlighted orange) represent the proteins highly abundant in pyruvate fermentation. -Log p value represents $-\log_{10}$ transformed p-value from a pairwise two-tailed t-test comparing the two groups.

Locus Tag	**Protein**	**-Log P value**	**Log Protein abundance (**DMSO+Pyruvate / Sulfite+Pyruvate**)**
04017	ABC transporter substrate-binding protein	2.5	1.8
00057	ABC transporter substrate-binding protein	3.0	1.5
04581	Glutamine synthetase	1.7	1.1
01937	NADP-dependent malic enzyme	2.7	1.0

00055	4Fe-4S binding protein	2.3	1.0
02647	ABC transporter substrate-binding protein	2.0	1.0
02473	HDIG domain-containing protein	1.5	1.0
04497	ABC transporter substrate-binding protein	2.0	1.0
00849	Di- and tricarboxylate transporter	3.4	1.0
00577	Aminomethyl-transferring glycine dehydrogenase subunit GcvPA	2.4	1.0
01872	Lactate utilization protein	1.7	0.9
02257	Citrate lyase alpha subunit	2.9	0.9
02153	Methylmalonyl-CoA mutase family protein	2.1	0.9
04612	Glu/Leu/Phe/Val dehydrogenase	1.8	0.9
02544	efflux transporter, RND family, MFP subunit	3.4	-0.9
04454	Methyl-accepting chemotaxis sensory transducer	1.9	-0.9
04366	Penicillin-binding protein 1A	2.1	-1.0
03389	Efflux RND transporter periplasmic adaptor subunit	3.2	-1.0
00945	2-hydroxyacid dehydrogenase-like protein	3.7	-1.0
01472	Molybdopterin molybdotransferase MoeA	1.4	-1.0
01602	NADH-quinone oxidoreductase subunit I	1.6	-1.0

Chapter 6: General discussion and concluding remarks

The ongoing process of urbanization and the widespread consumption of highly processed, energy-dense foods are thought to have contributed to the emergence of chronic metabolic and inflammatory disorders such as Inflammatory Bowel Disease (IBD) including ulcerative colitis (UC) and Crohn's disease (CD), Irritable Bowel Syndrome (IBS), Colon Rectal Cancer (CRC), and cardiometabolic conditions like Type 2 Diabetes (T2D) or CardioVascular Disease (CVD). These health challenges have become prevalent among a significant population in both developed and developing countries. The human gut microbiome, a dynamic system composed by trillions of micro-organisms, maintains constant interactions with the host and plays a crucial role in both health and disease. In patients with IBD or IBS, the gut microbiome often exhibits a higher composition of sulfate-reducing bacteria (SRB), accompanied by increased fecal sulfide production. Similarly, individuals with CVD commonly display elevated levels of trimethylamine N-oxide (TMAO) in their arteries, and its precursor is the gut microbiome metabolite trimethylamine (TMA) (Wang *et al.*, 2011). Nevertheless, the cause-and-effect relationships behind these associations remain uncertain.

The objective of this thesis is to delve into the anaerobic conversion of sulfur-containing compounds and trimethylamine within the human gut. Initiated by a classic enrichment experiment using human stool samples, our research aimed to explore the diversity of bacteria either sulfidogenic or related with the human gut sulfur cycle. Two novel bacteria, *Eubacterium maltosivorans* and *Sporobaculum desulfitilongum* were isolated in this thesis and they were thoroughly characterised and studied at omic level. The main findings of this research are presented and discussed here within the rapidly advancing realm of the human gut microbiome, providing insights into potential future approaches and opportunities within this field of study.

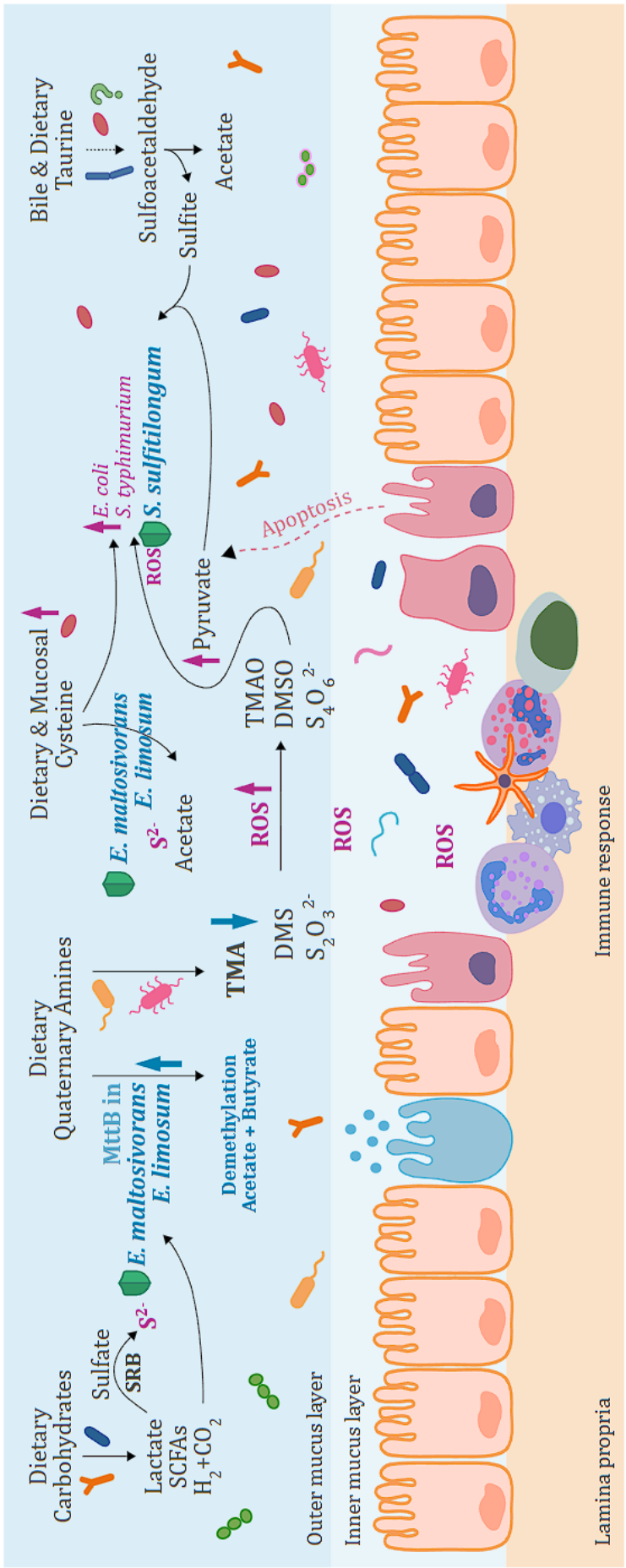

Figure 1. Overview featuring novel gut bacteria *Eubacterium maltosivorans* and *Sporobaculum desulfitilongum* involved in sulfur and trimethylamine (TMA) metabolism. TMA is converted to TMAO in the liver by hepatic flavin monooxygenase 3. High TMAO concentration in blood leads to increased risk of cardiovascular disease, atherosclerosis, and chronic kidney disease. *E. maltosivorans* and *E. limosum* mitigate TMA formation by demethylating quaternary amines, producing beneficial acetate and butyrate. *E. maltosivorans* tolerates high sulfide concentration (5 mM), potentially influencing gut microbiome deviations in specific pathological conditions. In inflammatory conditions, NADPH oxidase induction in human colonic epithelial cells leads to elevated reactive oxygen species (ROS) levels, oxidizing gut lumen metabolites (DMS, thiosulfate, TMA) to DMSO, tetrathionate, and TMAO. These compounds promote pathogen proliferation like *E. coli* and *Salmonella*. *S. desulfitilongum* can reduce DMSO and TMAO in the presence of pyruvate, potentially outcompeting pathogens and establishing a niche in inflammation or infection conditions.

1. *E. maltosivorans*: a versatile probiotic candidate

E. maltosivorans was enriched from a culture supplied with 20 mM lactate plus 5 mM sulfite where sulfide was produced at levels up to 5 mM (**Chapter 2**). This novel species was comprehensively characterized, and its draft genome was sequenced and annotated (**Chapter 3)**. *E. maltosivorans* YI^T combines many important and beneficial metabolisms in a single strain, including homoacetogenic, butyrogenic and propionogenic growth. Moreover, it exhibits the capability to utilize maltose, setting it apart from its closely related species *E. limosum*. To gain deeper insights into the metabolic pathways of *E. maltosivorans*, global expressed proteome data was used for reconstructing the beneficial pathways aforementioned that were summarized in a metabolic model (**Chapter 4**). In addition, the comparative proteomics performed in **Chapter 4** led to the identification of proteins involved in 1,2-propanediol (1,2-PD) utilization, vitamin B12 biosynthesis, and quaternary amines demethylation – the processes were predicted to take partially place within Bacterial MicroCompartments (BMC) as these were visualized by electron microscopy while the BMC proteins were induced. Through a comparative analysis of genomes between *E. limosum* and *E. maltosivorans* (**Chapter 4**), it was revealed that these two species share numerous key beneficial metabolic features. In the subsequent discussion, we will dive into the potential of both *E. maltosivorans* and *E. limosum* as promising next-generation probiotics, with a focus on our isolate.

1.1 Lactate utilization with butyrogenic growth

For anaerobic fermentation of lactate, it is necessary to cope with the energetically unfavourable oxidation of lactate to pyruvate (see below Reaction 1) (Weghoff *et al.*, 2015). As first described for *Acetobacterium woodi*, this energy barrier can be partially overcome by a unique electron confurcation complex formed by lactate dehydrogenase (LDH) and electron-transferring flavoprotein (EtfAB) (Weghoff *et al.*, 2015). Proteome data indicate this complex to be induced in *E. maltosivorans* and engages only with the reduced ferredoxin (Fd^{2-}), which has a more reduced potential, thus overcoming the original endergonic reaction (see below Reaction 2) (Weghoff *et al.*, 2015). Another electron confurcation complex with butyryl-CoA dehydrogenase in *E. maltosivorans* ensures butyrogenic growth from acetate. This *E. maltosivorans* gene cluster *lct*, which is also conserved in *E. limosum*, was explained with detail in **Chapter 4**. Till date, only a few bacteria residing in the human intestinal tract are known to utilize both D- and L-lactate for butyrate production, which includes *Anaerostipes caccae*,

Anaerostipes rhamnosivorans, *Anaerobutyricum soehngenii* and *Anaerobutyricum halii* (Shetty *et al.*, 2020; Louis *et al.*, 2022).

$Lactate + NAD^+ \rightarrow Pyruvate + NADH^+$ $\Delta G^{0'} = +25$ kJ/mol Reaction 1

$Lactate + Fd^{2-} + 2\ NAD^+ \rightarrow Pyruvate + Fd + 2\ NADH$ $\Delta G^{0'} = -9.5$ kJ/mol Reaction 2

Lactate is produced by lactic acid bacteria such as lactobacilli, streptococci and bifidobacteria through fermentation. In healthy individuals, colonic lactate is usually not accumulated (Louis *et al.*, 2022). Whereas in IBD patients, an increased abundance of lactic acid bacteria accompanied with a decreased butyrogenic bacteria, and an elevated fecal lactate levels were reported (Wang *et al.*, 2014). Furthermore, recent studies have detected increased luminal L-lactate during colon inflammation, potentially supporting the fitness of pathogenic *E. coli* and *Salmonella* (Gillis *et al.*, 2018; Taylor *et al.*, 2022). *E. maltosivorans*, produces butyrate and acetate from both D,L-lactate, hence it may be one of the candidates for challenging the dysbiosis caused by lactate accumulation.

1.2 *E. maltosivorans* can tolerate high sulfide concentration.

E. maltosivorans, although not a sulfidogenic bacterium, displays unique sulfur metabolism traits by demonstrating a robust growth when enriched with a sulfide concentration of 5 mM (**Chapter 2**). Healthy colons typically contain 1.0 to 2.4 mM of sulfide, while elevated sulfide levels have been observed in inflamed ones. Elevated sulfide concentrations adversely affect colonic epithelial cells, colonocyte metabolism, and disrupt the gut mucus layer (**Chapter 1**). Furthermore, sulfide toxicity extends to commensal bacteria by inducing oxidative damage and reducing glutathione level, which result in lipid peroxidation and DNA damage (Fu *et al.*, 2018; Mendes *et al.*, 2021). It has been reported that *Desulfovibrio piger*, one of the most abundant colonic sulfate-reducing bacteria (SRB), showed reduced growth and sulfate reduction rates when exposed to sulfide concentrations exceeding 4 mM (Kushkevych, Dordević, *et al.*, 2019). Several *Lactobacillus* species which are commonly regarded as probiotics, exhibit significantly lower tolerance to sulfide. For instance, *L. reuteri* showed no growth after 24 hours of incubation with 1.4 mM of sulfide, while *L. plantarum* and *L. fermentum* displayed no growth with 0.6 mM (Kushkevych, Kotrsová, *et al.*, 2019).

In a lactate-competition experiment involving butyrogenic bacteria (*Anaerostipes caccae* and *Anaerobutyricum halii*) and sulfidogenic *D. piger*, the growth of *D. piger* remained

unaffected in the co-culture with either *Anaerostipes caccae* or *Anaerobutyricum halii* (Marquet *et al.*, 2009). However, the growth of both butyrogenic bacteria was hindered, resulting in reduced butyrate production. This suggested that lactate could promote the growth of *D. piger*, leading to increased sulfide production in the presence of sulfate. Moreover, this outcome might also be attributed to the cytotoxic effect of the produced sulfide (~1.3 mM) on the tested butyrogenic bacteria, although specific sulfide toxicity data are unavailable.

Given that *E. maltosivorans* displaces a lactate-utilising ability and high sulfide tolerance, it could gain a survival edge in environments with elevated luminal sulfide concentrations. Consequently, it may contribute to modulating gut microbiome deviations under specific pathological conditions, such as IBS or IBD.

1.3 *E. maltosivorans* and *E. limosum* provide alternative pathway to degrade quaternary amines and avoid the production of TMA

Quaternary amines are commonly present in various components of human diets. Carnitine is found in red meat, while choline and betaine are present in both plant-based and animal-derived foods. Within the human gastrointestinal tract, these quaternary amines can undergo degradation by many intestinal species, resulting in the production of TMA (Fig. 1). Yet the main intestinal TMA-producing bacteria still need to be identified and further studied *in vitro*. In-depth computational studies have focused on three key enzymes involved in TMA production: choline-TMA lyase (CutC), carnitine oxygenase (CntA) and betaine reductase (GrdH). Bacteria carrying the *cutC* and *grdH* are prevalent across various bacteria species, in particular *Clostridium* XIVa strains and *Eubacterium* sp. strain AB3007. Conversely, *cntA* comprised sequences primarily linked to *Escherichia* (Rath *et al.*, 2017).

The produced TMA is absorbed by epithelium cells and enters the bloodstream. Within the liver, TMA is oxidized to TMA N-oxide (TMAO). Elevated levels of serum TMAO have been associated with the initiation of atherosclerosis, heightened incidence of adverse cardiovascular events, vascular inflammation, as well as increased risks of colorectal and liver cancers, and mortality in kidney disease patients (Missailidis *et al.*, 2016; Liu *et al.*, 2018; Jalandra *et al.*, 2021). Moreover, a study investigating the diet-gut microbiota-TMAO axis within a German population-based cohort (n = 425) revealed significant correlations between the abundances of two bacterial TMA-forming genes (*cntA* and *cutC*) and plasma TMAO levels. The study also identified a strong association between advancing age and TMAO levels (Rath

et al., 2021). The high demethylation activity of *E. limosum* (and potentially *E. maltosivorans*) provides an alternative pathway to degrade quaternary amines leading to the formation of N,N-dimethyl compounds instead of TMA. Consequently, these *Eubacterium* might offer a natural mechanism to regulate overall TMA production by the gut microbiota, as well as the abundance of TMA-producing bacteria (Figure 2).

The rich reservoir of methyltransferase family proteins (MttB) was first reported in *E. limosum* SA11 by Kelly *et al.,* (2016), but a deep analysis was not performed. Later studies have further revealed *E. limosum* to be a specialist in degrading various quaternary amines, with four substrate-specific MttB proteins were assigned to demethylate one -CH_3 from betaine, choline, carnitine and γ-butyrobetaine leading to the production of the corresponding N,N-dimethyl compounds (Picking *et al.*, 2019; Kountz *et al.*, 2020; Ellenbogen *et al.*, 2021). In **Chapter 4**, we reported the unusually abundant *mttB* gene homologs encoded in *E. maltosivorans* YI^T and related species through a comparative genome analysis (31 to 42 homologs in different strains). Through the proteome approach, we tried to link these unusually abundant MttB to potential functions in *E. maltosivorans* (**Chapter 4**). We observed that 16 products of *mttB* gene homologs were more abundant in the proteomes of *E. maltosivorans* grown with quaternary amines (betaine, choline, and carnitine) than in cells grown with maltose (**Chapter 4**). Notably, 9 of these products were consistently present across all quaternary amine growth conditions, while 7 were specifically elevated depending on the substrate. This result is different than that of the previous studies on *E. limosum*, in which only one MttB protein was proposed for each tested quaternary amines. This difference can be explained by the fact that *E. maltosivorans* and *E. limosum* are two distinct species, despite sharing several physiological similarities.

A blastp search revealed that most of the *mttB* genes exhibited high similarity within other *Eubacterium* species including *E. callanderi*, *E. barkeri* and *E. aggregans*. A few *mttB* genes in *E. maltosivorans* also share high similarity (>40% amino acid similarity) to those in *Acetobacterium*, *Sporomusa*, *Desulfitobacterium*, *Ruminococcus* and *Oscillospiraceae*. Future functional characterization of the numerous MttB homologs encoded by *E. maltosivorans* and *E. limosum* may provide us further insight into the potential benefits of these organisms for human health enhancement.

1.4 Versatile metabolic of *E. maltosivorans* and *E. limosum*

The versatile characteristics of *E. maltosivorans* and *E. limosum* enable these potentially next generation beneficial bacteria to adapt their metabolism according to substrate availability. In a cohort study of 40 infants, the interaction among different lactate-utilizing bacteria was studied (Pham *et al.*, 2017). Several lactate utilizers were recovered from faecal samples of the infants, including the butyrate producing *E. limosum*, and the propionate and hydrogen producing *Veillonella ratti*. In individual cultures grown with D,L-lactate, *V. ratti* exhibited a higher growth rate than *E. limosum*, accompanied by significant hydrogen accumulation. When *E. limosum* and *V. ratti* were co-cultured with D,L-lactate, hydrogen accumulation notably reduced by two-fold compared to *V. ratti* monoculture. The qPCR and HPLC data further exposed that in co-culture, *V. ratti* had 100 times higher copy numbers than *E. limosum*, and butyrate production was absent (Pham *et al.*, 2017). This suggested that, rather than relying on lactate utilization, *E. limosum* ensured its growth by shifting to a homoacetogenic growth, consuming the hydrogen produced by *V. ratti*. This decrease in hydrogen accumulation could potentially yield beneficial effects, such as reducing colic development in infants.

2. *S. desulfitilongum* has the potential to establish a niche amid inflammatory conditions

From the enrichment experiment described in **Chapter 2**, we achieved the successful isolation of a sulfite-reducing strain, named *Sporobaculum desulfitilongum*, which belongs to the *Sporomusaceae* family. While it did not display fermentative growth with sugars, it showed significant growth on pyruvate. Moreover, *S. desulfitilongum* displayed the ability to reduce sulfite, thiosulfate, DMSO, and TMAO when pyruvate was available (**Chapter 5**).

Pyruvate is a crucial primary metabolite and serves as a junction point for various metabolic pathways in both prokaryotes and eukaryotes. Although present in low concentrations, pyruvate has been measured in human fecal samples. However, due to differences in sample perpetration and measurement techniques, reported pyruvate concentrations in the literature have shown inconsistency in healthy individuals (0.5 or 3 μmol/g wet feces) (Huda-Faujan *et al.*, 2010; Gardana *et al.*, 2017). Furthermore, elevated pyruvate concentrations have been detected in the fecal samples of patients with UC and CD compared to healthy controls with levels of 12.9, 2.1, and 0.5 μmol/g wet feces, respectively (Takaishi *et al.*, 2008). The phenomenon of pyruvate overflow, observed in fast-growing bacteria under nutrient-rich conditions where the production of pyruvate exceeds its

consumption rate, results in its accumulation in the media (Paczia *et al.*, 2012; Salar-García *et al.*, 2017; Ma *et al.*, 2019). It remains uncertain whether a similar phenomenon occurs in the human gut environment, considering that excreted pyruvate can be rapidly consumed by other bacteria. However, given the measured low pyruvate concentrations in fecal samples, it is plausible to assume the existence of a pyruvate overflow and re-uptake mechanism within the gut lumen. This pyruvate overflow induced cross-feeding hypothesis in the gut environment has also been proposed by other researchers (Morita *et al.*, 2019; Tremblay *et al.*, 2021).

Pyruvate is an excellent metabolite to support the bacterial growth. Several systems have been identified for pyruvate transport, categorized into substrate-specific pyruvate transporters (BtsT, CstA and YhjX in *E. coli* and *Salmonella typhimurium*), and monocarboxylate transporters with a broader substrate specificity including pyruvate (Jolkver *et al.*, 2009; Kreth *et al.*, 2013; Charbonnier *et al.*, 2017). The genome of *S. desulfitilongum* harbors seven substrate-specific pyruvate transporter gene homologs. In the comparative proteome study described in **Chapter 5**, two of these pyruvate transporter homologs to CstA were detected. Since pyruvate was the growth substrate at all conditions (pyruvate, pyruvate/sulfite, and pyruvate/DMSO), these two protein products did not exhibit significant differences. However, both pyruvate transporter proteins were higher induced in pyruvate culture. The protein product of 2C_00701 displayed 1.3- and 1.6-times higher expression in the pyruvate culture than in the pyruvate/sulfite and pyruvate/DMSO cultures, respectively, while that of 2C_02982 exhibited approximately 3-fold increase than in cells grown with pyruvate/sulfite.

Inflammatory conditions in the human gut trigger the production of inflammatory cytokines and other molecules, leading to the activation of NADPH oxidase 1 in colonic epithelial cells, subsequently resulting in increased reactive oxygen species (ROS) production. Pyruvate possesses the ability to scavenge one of these common ROS, hydrogen peroxide, through nonenzymatic decarboxylation (Giandomenico *et al.*, 1997; Singh *et al.*, 2022). Considering the elevated levels of pyruvate observed in faecal samples from individuals experiencing inflammation (Takaishi *et al.*, 2008; Huda-Faujan *et al.*, 2010), it is tempting to speculate that a heightened pyruvate overflow may act as an antioxidant defence mechanism. The exceeding pyruvate could benefit the fitness of pathogens like *Salmonella typhimurium* (Anderson *et al.*, 2021; Paulini *et al.*, 2022), trigger biofilm formation in *Staphylococcus aureus* and *Clostridioides difficile* (Wishart *et al.*, 2018; Tremblay *et al.*, 2021), and induce virulence factor in pathogens like *Listeria monocytogene*s, and *Vibrio parahaemolyticus* (Schär *et al.*,

2010; Xie *et al.*, 2019). Notably, ROS induction further promotes the oxidation of common gut lumen metabolites like sulfide, thiosulfate, DMS, and TMA, transforming them into tetrathionate, DMSO, and TMAO, respectively. Importantly, these compounds have been found to boost the fitness of *Salmonella typhimurium* (Anderson *et al.*, 2021; Paulini *et al.*, 2022). Lastly, inflammatory, or infectious conditions often lead to increased apoptotic cell death, releasing pyruvate into the gut lumen (Anderson *et al.*, 2021). This release might potentially foster a cycle that amplifies pathogen proliferation.

The comparative proteome study described in **Chapter 5** unveiled the identification of two overproduced thioredoxin-like proteins in *S. desulfitilongum* under sulfite reduction growth conditions. Prior research suggests that thioredoxin contributes to pathogen infection by participating in the scavenging of ROS, playing a crucial role in maintaining intracellular redox status (Lu and Holmgren, 2014; Cheng *et al.*, 2017; Yang *et al.*, 2019). Armed with its dedicated pyruvate uptake system, the ability to reduce thiosulfate, DMSO, and TMAO, and the production of thioredoxin-like protein, *S. desulfitilongum* might establish a niche under conditions of inflammation or infection by competing with the pathogens.

3. Bacterial sulfidogenic metabolism of cysteine is overestimated and understudied

Both inorganic and organic sulfur compounds relevant to human nutrition and physiology were provided to the enrichment as electron acceptor, or a carbon source for fermentative growth (**Chapter 2)**. One noteworthy discovery was the potential significance of cysteine as a source of colonic sulfide production. Cysteine metabolism in bacteria is not a novel subject. Its significance in the synthesis of various molecules, such as glutathione, Coenzyme A, iron-sulfur clusters, and in transsulfuration is well recognized (Osman *et al.*, 1997). The predominant sulfidogenic cysteine metabolic pathway, described as cysteine desulfhydration, deamination, or fermentation in literature has been described in **Chapter 1**. The dedicated anaerobic cysteine catabolic enzymes in both *S. typhimurium* and *E. coli* were recently identified and designated as CyuA, CyuP, and CyuR (Loddeke *et al.*, 2017).

In **Chapter 2**, our primary discovery emphasized cysteine degradation as a prominent sulfidogenic process. Additionally, several studies also highlighted cysteine as a main driver for colonic bacterial sulfide production (Hale *et al.*, 2018; Yao *et al.*, 2018). Given its sulfidogenic nature, bacterial cysteine degradation has received considerable attention in the context of various diseases, including IBD, IBS, and CRC (Blachier *et al.*, 2019; Teigen *et al.*,

2019; Walker and Schmitt-Kopplin, 2021). In a recent metagenomic data mining study, more than 15 cysteine enzymes from 5 different pathways were collectively taken into account, leading to the identification of diverse cysteine degradation pathways distributed across 13 phyla and 141 genera (Wolf *et al.*, 2022). However, this seemingly extensive representation of sulfidogenic cysteine metabolism could be an overestimation, as it accounted in both cysteine transsulfuration and secondary cysteine metabolic enzymes.

Sulfide is indeed formed from cysteine by the action of enzymes like cystathionine-β-lyase (CBS) or cystathionine-γ-lyase (CSE) in transsulfuration pathway. However, transsulfuration is tightly controlled with the metabolic demands of the cell. Several enzymes in *E. coli* indeed exhibit desulfhydration activities, such as tryptophanase (TnaA), 3-mercaptopyruvate sulfurtransferase (MstA or SseA), cystathionine β-lyases (MetC or MalY), and cysteine synthase (CysK and CysM). However, their total activity (27 nmol min^{-1} mg $protein^{-1}$ at 37 °C) is significantly lower than that of cysteine desulfhydrase in *S. typhimurium* (260 nmol min^{-1} mg $protein^{-1}$ at 23 °C) (Kredich *et al.*, 1972; Awano *et al.*, 2005). This was underscored by a recent study where a *ΔcyuA* mutant *E. coli* failed to produce sulfide when provided with 1 mM cysteine, while the *cyuA*$^{+}$ *E. coli* yielded up to 70 μM sulfide. When the cysteine amount was elevated to 5 mM, *ΔcyuA* mutant *E. coli* showed sulfide production which was slower and less compared to *cyuA*$^{+}$ strain (Zhou and Imlay, 2022). These results suggest that secondary cysteine metabolic enzymes do not act as primary drivers of sulfide production, regardless of whether cysteine concentrations are low or high. Moreover, multiple studies have found that *ΔcyuA* and *ΔcyuR* mutants of both *S. typhimurium* and *E. coli* were sensitive to exogenous cysteine (2 mM and 5 mM, respectively), resulting in longer lag phase and lower cell density (Oguri *et al.*, 2012; Shimada *et al.*, 2016; Loddeke *et al.*, 2017; Zhou and Imlay, 2022).

Cysteine catabolism has gathered significant attention, but with a primarily focus on pathogenic bacteria or bacteria associated with adverse symptoms, such as *Clostridium difficile*, *Fusobacterium polymorphum* (Dubois *et al.*, 2016; Basic *et al.*, 2017). Another pathogen *Klebsiella*, which is commonly mentioned in its potential cysteine degradation property, was tested with 0.63 mM cysteine as it is an essential nutrient for the growth of certain strains (McIver and Tapsall, 1988). Overall, it appears that physiological examinations of cysteine catabolism with a specific focus on commensal gut microbiota remain limited.

The study of human gut microbiome cysteine catabolism holds significance for several reasons. First, despite the efficient protein digestion and absorption in ileum, a notable amount of undigested or partially digested protein reaches the colon (Beaumont *et al.*, 2017). Depending on diet, protein quantities entering the large intestine can range from 3 g/day on a protein-free diet to 17 g/day on a moderately high-protein intake (including vegan or plant-based diet) or western diets (Yao *et al.*, 2016). Second, after digested from protein, or mucin in the anoxic gut lumen, free cysteine can stay as it is. Conversely under aerobic conditions, two cysteine molecules can undergo oxidative cross-linking to form cystine. Third, free amino acids are not well absorbed by the mammalian colonic mucosa (van der Wielen *et al.*, 2017). The presence of proteins and hence cysteine in the colon and their utilization by gut microbiota is evidenced by the abundance of lysine-degrading and butyrate-producing bacteria (Bui *et al.*, 2020). Lastly, investigating the potential of non-harmful or non-pathogenic gut microbiota capable of cysteine catabolism offers the opportunity to counteract the growth and activity of potential pathogens. *E. maltosivorans* and *E. limosum* release sulfide when cysteine was provided as the sole carbon source (**Chapter 3**). With the ability to cope with high sulfide discussed in the previous section, *E. maltosivorans* might be able to mitigate pathogenic activity within the gut environment, promoting overall gut health and stability.

4. The special, one and only *Bilophila wadsworthia*

Bilophila, though not the central focus at the onset of my thesis activities, threaded its way through my research. This genus appeared from the first enrichment experiment, as it was highly enriched in sulfite reduction, and taurine degradation coupled with pyruvate enrichments for both healthy and IBS donors (**Chapter 2**). Over the course of this thesis, several rounds of enrichment experiments were conducted with the aim of isolating novel *Bilophila* or taurine-utilizing organisms from various faecal samples. The findings from these experiments, however, were not incorporated into the thesis chapters, given that the majority of the enriched OTUs exhibited very high (>99%) similarity of their 16S rRNA gene sequences to that of the *B. wadsworthia* type strain. Upon revisiting these results, we began to ponder why taurine is so difficult to degrade anaerobically and why *Bilophila* excels in thriving with taurine.

4.1 The solutions to degrade taurine by bacteria

Taurine features a thermodynamically stable bond between carbon and sulfur (Liebman, 1991). This is due to the relatively similar electronegativities of carbon (2.55) and sulfur (2.58),

resulting in a tight and slightly polar connection which makes C-sulfonates less susceptible to decompose. In general, there are two approaches to metabolize taurine (Fig. 2). The first way is to directly break the inert C-S bond in taurine by taurine dioxygenase (TauD) found in *E. coli* with the presence of oxygen and 2-oxoglutarate, which allows *E. coli* to utilise sulfite for assimilation (Eichhorn *et al.*, 1997). The second catabolic pathway is to first deaminate taurine, achieved either through taurine dehydrogenase with cytochrome *c* in aerobic and anaerobic bacteria, or via the taurine-pyruvate transaminase (Tpa) coupled with alanine dehydrogenase (Ald) in only anaerobic bacteria (Cook and Denger, 2002). The produced sulfoacetaldehyde, which possesses a highly polarized carbon-oxygen double bond (C=O) with a less stable C-S bond than that in taurine, will undergo different desulfonation processes.

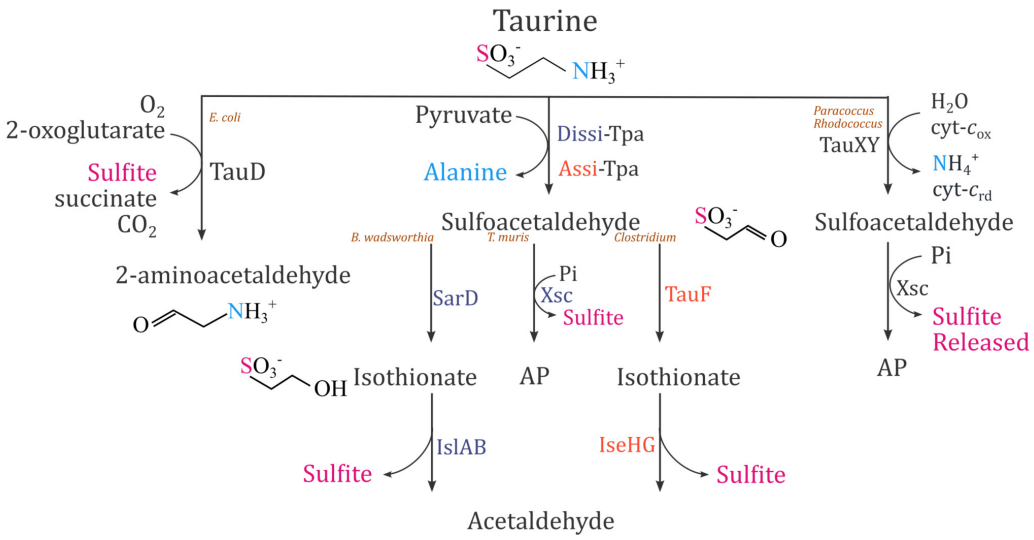

Figure 2. Bacterial taurine metabolism pathways. TauD: Alpha-ketoglutarate-dependent taurine dioxygenase; Dissi: dissimilatory; Assi: assimilatory; Tpa: Taurine-pyruvate aminotransferase; SarD and TauF: sulfoacetaldehyde reductase; IslAB and IseHG: isethionate-sulfite lyase; TauXY: Putative taurine dehydrogenase; Xsc: Sulfoacetaldehyde acetyltransferase.

4.2 What makes *B. wadsworthia* a specialist to utilise taurine?

Firstly, *B. wadsworthia* possesses a Tpa for dissimilatory growth. Taurine degradation, including both dissimilate and assimilate growth, has been studied in anaerobic bacteria across various environments, ranging from freshwater and marine habitats, sewage digesters, to the human gut. Assimilatory taurine utilization was observed in several *Clostridium* species with up to 100 µM taurine supplied (Chien *et al.*, 1995; Xing, Wei, Zhou, *et al.*, 2019). Notably, *B. wadsworthia*, along with environmental bacteria *Desulfonispora thiosulfatigenes*, and *Desulforhopalus singaporensis* use taurine as their sole carbon source (Denger *et al.*, 1999; Lie *et al.*, 1999). While similar reactions are expected in assimilatory and dissimilatory growth

involving taurine, distinct enzymes might arise due to varying substrate affinities, with dissimilatory reactions having higher *Km* values in the mM range and assimilatory reactions having lower *Km* values in the μM range. This distinction is evident as the assimilatory Tpa in *C. pasteurianum* and *C. beijerinckii* shares ~33% protein identity with that in *B. wadsworthia*, while dissimilatory Tpa in *D. thiosulfatigenes* and *D. singaporensis* shows ~55% protein identity.

The Tpa enzyme functions as the gatekeeper enzyme for taurine degradation. TPA is a pyridoxal phosphate-dependent belonging to the omega-amino acid--pyruvate aminotransferase group utilizing pyruvate exclusively as the amino acceptor (Yonaha *et al.*, 1977). A BLASTp search of Tpa from *B. wadsworthia* (Swiss-Prot entry Q9APM5) yielded matches with >70% protein similarity primarily with uncultured *Bilophila* sp., *Desulfovibrio* sp., *Mailhella* sp., and the isolate *Desulfobulbus oralis*. These metagenome data originated from the human gut, wastewater, natural environments, and ruminants. Protein similarity ranging from 70% to 50% mainly corresponds to aerobic and anaerobic bacteria from environmental habitats like freshwater, marine water, and sediments. At around 50% protein similarity, BLASTp results indicate matches to general aminotransferases or proteins in the aspartate aminotransferase family.

Moreover, *B. wadsworthia* encodes a glycyl radical enzyme (GRE) IslA to cleave the C-S bond from isethionate which is reduced from sulfoacetaldehyde, which is equivalent to IseG in *C. butyricum*. GREs employ protein-centered radical intermediates in catalysis, functioning exclusively under strict anaerobic conditions. Together with a partner activating enzyme from the radical SAM family, a vital glycine-centered radical is installed posttranslationally, insuring intricate C-C, C-O, C-N and the recently discovered C-S bond cleavages (Backman *et al.*, 2017; Peck *et al.*, 2019). Furthermore, the kinetics of IseG in the taurine-assimilating *C. butyricum* differs significantly from that of dissimilating IslA in *D. desulfuricans* (K_m = 6.73 ± 0.46 mM *vs.* K_m = 44.8 ± 3.5 mM) (Xing, Wei, Hua, *et al.*, 2019). Lastly, the C-S cleavage from isethionate leads to the generation of potentially toxic sulfite and acetaldehyde. The thriving of *B. wadsworthia* on taurine is further enhanced by two additional reasons, as it demonstrates the ability to create BMCs that capsulate the toxic acetaldehyde until it is oxidized to acetate, and *B. wadsworthia* is capable of sulfite reduction, thereby generating ATP.

Overall, genes related to dissimilatory taurine degradation seem like a trick kept in sulfate- or sulfite-reducing bacteria. However, the presence of all these unique and key enzymes encoded in its genome might suggest a pathogenic feature of *B. wadsworthia*, especially since taurine is present in high concentrations (2-20 mM) in various human tissues. A potential pathobiont function of *B. wadsworthia* has been described in mice experiments (Z. Feng *et al.*, 2017).

4.3 Taurine degradation in *S. desulfitilongum*

During *S. desulfitilongum* characterization, this isolate showed weak growth on taurine and utilised up to 2 mM taurine from an initial concentration of 20 mM during a 14-days incubation period (**Chapter 5**). A detailed analysis of its genome showed that *S. desulfitilongum* lacks the gene for a typical dissimilatory Tpa protein with high similarity to that of *B. wadsworthia*, however, 3 aminotransferases showing 30% protein similarity have been identified. Furthermore, no dedicated sulfoacetaldehyde reductase was found in strain 2C but an aldehyde-alcohol dehydrogenase. Interestingly, strain 2C possesses two genes annotated as choline trimethylamine-lyase and GRE, which showed relatively high identity to the IslA in *B. wadsworthia*. This is in line with the bioinformatics search in the paper where IslA was first identified, the choline trimethylamine-lyase form the closest cluster with IslA in *B. wadsworthia* (Peck *et al.*, 2019). Putting these together it seems likely that strain 2C could assimilate taurine.

Furthermore, marine strain *Paracoccus denitrificans* PD1222 is able to grow with taurine and releasing sulfite and sulfate to the media (Felux *et al.*, 2013) (pathway summarised in Figure 2). If a similar taurine pathway is also present in the gut environment, *S. desulfitlongum* could form a cross-feeding interaction by reducing sulfite released from taurine (Figure 1).

4.4 Is *B. wadsworthia* the only specialist to degrade taurine in the gut?

The answer remained to be yes until not long ago. *Taurinivorans muris*, represents the type strain of a novel genus in the family *Desulfovibrionaceae* of the phylum *Desulfobacterota*, was isolated from mouse gut and demonstrated taurine-respiring growth (Ye *et al.*, 2023). The taurine-respiration pathway in *T. muris* differs to that in *B. wadsworthia*, as sulfite is directly released from sulfoacetaldehyde catalysed by a sulfoacetaldehyde acetyltransferase (Xsc) instead of being reduced to isethionate as found in *B. wadsworthia* (Figure 2). The released

sulfite is further reduced to sulfide as *T. muris* harbors the classic dissimilatory sulfite reducing gene cluster (Ye *et al.*, 2023). However, *B. wadsworthia* is still the dominant taurine-respiring kind in the human gut ecosystem (Ye *et al.*, 2023). Notably, a recent metagenomic study focused on the chicken gut has introduced a novel *Bilophila* species, *Bilophila faecipullorum* (Gilroy, 2021), yet its ability to degrade taurine is upon testing after achieving the isolate.

Culturomics and metagenomics

Enrichment and isolation threaded throughout the course of this research. We undertook enrichments using diverse faecal donors and a wider array of sulfur compounds, such as tetrathionate, thiosulfate, and cysteate, serving as electron acceptors. Most of the results have been summarized here and detailed in the **Chapter 2**, **4** and **5**. Nonetheless, within one of these enrichments *Desulfovibrio* spp., *Oscillobacter* spp., and uncharacterized *Ruminococcoceae* appeared to be co-enriched. Despite their presence, these microorganisms were not dominantly enriched, and attempts at isolation through dilution and plating strategies did not yield success. Often identified in molecular microbial studies, these organisms are referred to as the "core microbiota". However, due to the lack of physiological data of these uncultured species, specific substrates and targeted strategies for their enrichment and isolation remain unknown.

Metagenomic analyses could provide valuable insights for bringing uncultured microbes into cultivation. High-quality assembled metagenomic data from enrichment cultures offer opportunities for gene-targeted isolation, antibiotic resistance gene exploration, and culture media optimization. Emerging reports demonstrated successful isolation of novel species constituting a minor portion of the microbial community in various environments using these strategies based on metagenomic insights (Karnachuk et al., 2021; Lapidus and Korobeynikov, 2021; Zhang et al., 2021; Rubin et al., 2022).

Isolation is not always essential for addressing specific research questions. Metagenomic or metatranscriptomic approaches offer insights into the genetic content, functional potential, and gene expression profiles of entire microbial communities without necessitating the isolation of individual microbes. These methods enable researchers to study the collective activities of diverse microorganisms within complex microbial communities. While data-mining studies present a rapid and cost-effective alternative to wet-lab experiments, the labor-intensive nature of cultivation raises questions about its worthiness, particularly considering claims of functional redundancy in the gut microbiome. However, there are

compelling arguments that support the need for isolating and characterizing gut isolates, the more so as the predictive capacity of genome-based approaches is still limited.

The need for isolation varies based on specific research objectives and should be guided by well-defined reasons aligned with those goals. On the contrast, while genome-based insights are valuable, they require validation through physiological experiments, underscoring the importance of experimental validation. *S. desulfitilongum* stands as a good example. Despite its genomic capacity for complete glycolysis enzymes, various sugar transporters, and lactate dehydrogenase, our characterization in **Chapter 5** highlighted growth solely with pyruvate. Similarly, *E. maltosivorans* showcases a distinctive story through its abnormal abundance of MttB, where 41 MttB homologs share protein sequence identities ranging from 100% to approximately 27%. Though comparative genoproteomic analysis (**Chapter 4**), 16 MttB were functional when with four different quaternary amines. Surprisingly, the substrate specificity of MttB did not appear to correlate with the protein similarities.

In considering sulfate reduction in the human gut, *Desulfovibrio* stands as the most abundant genus of sulfate-reducing bacteria (SRB), frequently associated with chronic diseases like IBD and IBS due to its high prevalence (Figliuolo *et al.*, 2017; Dordević *et al.*, 2021). A recent study discerned specific *Desulfovibrio* species and their distinct associations with certain diseases, owing to a handful of evidence from *in vitro* studies (Singh *et al.*, 2023). Furthermore, a recent human intervention involving *D. piger*, one of the most prevalent human commensal SRB, demonstrated its safety and potential health benefits through a symbiotic relationship with *Faecalibacterium prausnitzii* (Khan *et al.*, 2023). These significant outcomes were only feasible due to the isolation and cultivation of these specific strains.

“Our understanding of the microbes residing within our bodies and their effect on our health is limited by our ability to identify the microbial content. The two main paths to microbial research are either through marker genes, such as the 16S ribosomal RNA genes, or through reference alignment of shotgun read sequencing. In both cases, the broad genetic contents of each microbe is deduced from what is known about its genome." as stated by Leviatan *et al.* (2022). To address this limitation, a deliberate integration of culturomics with metagenomics could offer enhanced resolutions at the 16S rRNA gene level and expanded reference protein sequences. This combined approach may enable a more comprehensive understanding of ecosystem-level processes, community structures, and functional relationships among different microbial taxa.

Concluding remarks

Sulfur metabolism is a crucial metabolism for humans and their gut microbiome. This thesis started with an enrichment experiment with human fecal samples, through which we identified key players of microbial sulfur metabolism. Via this enrichment process, we successfully isolated, characterized, sequenced, and analyzed the genomes of two novel bacteria: *E. maltosivorans* and *S. desulfitilongum*. Moreover, we elucidated their distinctive metabolic pathways by means of comparative proteomic studies.

Over the past two decades, the field of gut microbiota has made significant strides, largely propelled by advancements in omics technologies. While high throughput sequencing greatly enhances the depth and resolution of genome and metagenome data, and computational analysis facilitates the prediction of protein functions, progress in understanding the metabolic functions of the human gut microbiome remains relatively slow compared to the volume of generated sequencing data. This prompts a pressing need to address the gap in our understanding of uncultured bacteria by isolating novel bacterial strains and more importantly, understanding their physiological traits, which is the core objective of this thesis. To fulfil this objective, it is crucial to explore the uncultured microorganisms across diverse geographical populations. This exploration can be achieved by integrating state-of-the-art culturomics with omics technologies.

Appendices

References

Abayakoon, P., Jin, Y., Lingford, J.P., Petricevic, M., John, A., Ryan, E., et al. (2018) Structural and biochemical insights into the function and evolution of sulfoquinovosidases. *ACS Cent Sci* **4**: 1266–1273.

Adams, J.M. and Capecchi, M.R. (1966) N-formylmethionyl-sRNA as the initiator of protein synthesis. *Proc Natl Acad Sci* **55**: 147–155.

Adsit Jr, F.G., Randall, T.A., Locklear, J., and Kurtz, D.M. (2022) The emergence of the tetrathionate reductase operon in the *Escherichia coli*/*Shigella* pan-genome. *Microbiologyopen* **11**: e1333.

Ahlman, B. (1993) The content of free amino acids in the human duodenal mucosa. *Clin Nutr* **12**: 266–271.

Ahuja, V. and Tandon, R.K. (2010) Inflammatory bowel disease in the Asia–Pacific area: a comparison with developed countries and regional differences. *J Dig Dis* **11**: 134–147.

Alnouti, Y. (2009) Bile acid sulfation: A pathway of bile acid elimination and detoxification. *Toxicol Sci* **108**: 225–246.

Ananieva, O., Nilsson, I., Vorobjova, T., Uibo, R., and Wadstrom, T. (2002) Immune responses to bile-tolerant *Helicobacter* species in patients with chronic liver diseases, a randomized population group, and healthy blood donors. *Clin Diagn Lab Immunol* **9**: 1160–1164.

Anderson, C.J., Medina, C.B., Barron, B.J., Karvelyte, L., Aaes, T.L., Lambertz, I., et al. (2021) Microbes exploit death-induced nutrient release by gut epithelial cells. *Nature* **596**: 262–267.

Andreesen, J.R. (1994) Glycine metabolism in anaerobes. *Antonie Van Leeuwenhoek* **66**: 223–237.

De Angelis, M., Curtin, A.C., McSweeney, P.L.H., Faccia, M., and Gobbetti, M. (2002) *Lactobacillus reuteri* DSM 20016: purification and characterization of a cystathionine γ-lyase and use as adjunct starter in cheesemaking. *J Dairy Res* **69**: 255–267.

Antonelli, M., Benedetti, B., Cavaliere, C., Cerrato, A., La Barbera, G., Montone, C.M., et al. (2019) Enrichment procedure based on graphitized carbon black and liquid chromatography-high resolution mass spectrometry for elucidating sulfolipids composition of microalgae. *Talanta* **205**: 120162.

Arndt, D., Grant, J.R., Marcu, A., Sajed, T., Pon, A., Liang, Y., and Wishart, D.S. (2016) PHASTER: a better, faster version of the PHAST phage search tool. *Nucleic Acids Res* **44**: W16–W21.

Attene-Ramos, M.S., Wagner, E.D., Gaskins, H.R., and Plewa, M.J. (2007) Hydrogen sulfide induces direct radical-associated DNA damage. *Mol cancer Res* **5**: 455–459.

Attene-Ramos, M.S., Wagner, E.D., Plewa, M.J., and Gaskins, H.R. (2006) Evidence that hydrogen sulfide is a genotoxic agent. *Mol cancer Res* **4**: 9–14.

Attene-Ramos, M.S., Nava, G.M., Muellner, M.G., Wagner, E.D., Plewa, M.J., and Gaskins, H.R. (2010) DNA damage and toxicogenomic analyses of hydrogen sulfide in human intestinal epithelial FHs 74 Int cells. *Environ Mol Mutagen* **51**: 304–314.

Auch, A.F., Jan, M., Klenk, H.P., and Göker, M. (2010) Digital DNA-DNA hybridization for microbial species delineation by means of genome-to-genome sequence comparison. *Stand Genomic Sci* **2**: 117–134.

Awano, N., Wada, M., Mori, H., Nakamori, S., and Takagi, H. (2005) Identification and functional analysis of *Escherichia coli* cysteine desulfhydrases. *Appl Environ Microbiol* **71**: 4149–4152.

Axen, S.D., Erbilgin, O., and Kerfeld, C.A. (2014) A taxonomy of bacterial microcompartment loci constructed by a novel scoring method. *PLoS Comput Biol* **10**: e1003898.

Baars, E.K. (1930) Over Sulphatreductie door Bacterien Dissertation. *WD Meinema, NV, Delft, Holl*.

Bachmann, O., Juric, M., Seidler, U., Manns, M.P., and Yu, H. (2011) Basolateral ion transporters involved in colonic epithelial electrolyte absorption, anion secretion and cellular homeostasis. *Acta Physiol* **201**: 33–46.

Backman, L.R.F., Funk, M.A., Dawson, C.D., and Drennan, C.L. (2017) New tricks for the glycyl radical enzyme family. *Crit Rev Biochem Mol Biol* **52**: 674–695.

Baliou, S., Adamaki, M., Ioannou, P., Pappa, A., Panayiotidis, M.I., Spandidos, D.A., *et al.* (2021) Protective role of taurine against oxidative stress. *Mol Med Rep* **24**: 1–19.

Barcenilla, A., Pryde, S.E., Martin, J.C., Duncan, S.H., Stewart, C.S., Henderson, C., and Flint, H.J. (2000) Phylogenetic Relationships of Butyrate-Producing Bacteria from the Human Gut.

Baron, E.J., Summanen, P., Downes, J., Roberts, M.C., Wexler, H., and Finegold, S.M. (1989)

Bilophila wadsworthia, gen. nov. and sp. nov., a unique gram-negative anaerobic rod recovered from appendicitis specimens and human faeces. *Microbiology* **135**: 3405–3411.
Barton, L.L., Ritz, N.L., Fauque, G.D., and Lin, H.C. (2017) Sulfur cycling and the intestinal microbiome. *Dig Dis Sci* **62**: 2241–2257.
Basic, A., Blomqvist, M., Dahlén, G., and Svensäter, G. (2017) The proteins of *Fusobacterium* spp. involved in hydrogen sulfide production from L-cysteine. *BMC Microbiol* **17**: 1–10.
Batth, T.S., Tollenaere, M.X., Rüther, P., Gonzalez-Franquesa, A., Prabhakar, B.S., Bekker-Jensen, S., *et al*. (2019) Protein aggregation capture on microparticles enables multipurpose proteomics sample preparation. *Mol Cell Proteomics* **18**: 1027–1035.
Bauchart-Thevret, C., Stoll, B., and Burrin, D.G. (2009) Intestinal metabolism of sulfur amino acids. *Nutr Res Rev* **22**: 175–187.
Beaumont, M., Portune, K.J., Steuer, N., Lan, A., Cerrudo, V., Audebert, M., et al. (2017) Quantity and source of dietary protein influence metabolite production by gut microbiota and rectal mucosa gene expression: a randomized, parallel, double-blind trial in overweight humans. *Am J Clin Nutr* **106**: 1005–1019.
Bechtel, T.J. and Weerapana, E. (2017) From structure to redox: The diverse functional roles of disulfides and implications in disease. *Proteomics* **17**: 1600391.
Beijerinck, M.W. (1895) Über Spirillum desulfuricans als ursache von sulfatreduktion. *Zentralblatt Bakteriol* **1**: 1–9.
Benning, C. (1998) Biosynthesis and function of the sulfolipid sulfoquinovosyl diacylglycerol. *Annu Rev Plant Biol* **49**: 53–75.
Bensid, A., El Abed, N., Houicher, A., Regenstein, J.M., and Özogul, F. (2022) Antioxidant and antimicrobial preservatives: Properties, mechanism of action and applications in food–a review. *Crit Rev Food Sci Nutr* **62**: 2985–3001.
Benson, A.A., Daniel, H., and Wiser, R. (1959) A sulfolipid in plants. *Proc Natl Acad Sci* **45**: 1582–1587.
Bertelli, C., Laird, M.R., Williams, K.P., Simon Fraser University Research Computing Group, Lau, B.Y., Hoad, G., et al. (2017) IslandViewer 4: expanded prediction of genomic islands for larger-scale datasets. *Nucleic Acids Res* **45**(W1): W30–W35.
den Besten, G., van Eunen, K., Groen, A.K., Venema, K., Reijngoud, D.-J., and Bakker, B.M. (2013) The role of short-chain fatty acids in the interplay between diet, gut microbiota, and host energy metabolism. *J Lipid Res* **54**: 2325–2340.
Biagi, E., Nylund, L., Candela, M., Ostan, R., Bucci, L., Pini, E., et al. (2010) Through ageing, and beyond: Gut microbiota and inflammatory status in seniors and centenarians. *PLoS One* **5**: e10667.
Bielow, C., Mastrobuoni, G., and Kempa, S. (2016) Proteomics Quality Control: Quality Control Software for MaxQuant Results. *J Proteome Res* **15**: 777–787.
Biswas, A., Gagnon, J.N., Brouns, S.J.J., Fineran, P.C., and Brown, C.M. (2013) CRISPRTarget: bioinformatic prediction and analysis of crRNA targets. *RNA Biol* **10**: 817–827.
Blachier, F., Beaumont, M., and Kim, E. (2019) Cysteine-derived hydrogen sulfide and gut health: a matter of endogenous or bacterial origin. *Curr Opin Clin Nutr Metab Care* **22**: 68–75.
Blachier, F., Davila, A.-M., Mimoun, S., Benetti, P.-H., Atanasiu, C., Andriamihaja, M., *et al*. (2010) Luminal sulfide and large intestine mucosa: friend or foe? *Amino Acids* **39**: 335–347.
Borriello, S.P. and Owen, R.W. (1982) The metabolism of lithocholic acid and lithocholic acid-3-α-sulfate by human fecal bacteria. *Lipids* **17**: 477–482.
Bos, C., Huneau, J., and Gaudichon, C. (2009) Sulfur amino acids contents of dietary proteins: daily intakes and requirement. *Glutathione sulfur Amin acids Hum Heal Dis John Wiley Sons Inc New Jersey* 21–33.
Bourriaud, C., Robins, R.J., Martin, L., Kozlowski, F., Tenailleau, E., Cherbut, C., and Michel, C. (2005) Lactate is mainly fermented to butyrate by human intestinal microfloras but inter-individual variation is evident. *J Appl Microbiol* **99**: 201–212.
Brahe, L.K., Le Chatelier, E., Prifti, E., Pons, N., Kennedy, S., Hansen, T., et al. (2015) Specific gut microbiota features and metabolic markers in postmenopausal women with obesity. *Nutr Diabetes* **5**: e159–e159.
Brosnan, J.T. and Brosnan, M.E. (2006) The Sulfur-Containing Amino Acids: An Overview. *The*

Journal of nutrition **136**: 1636S-1640S.
Brown, J.M. and Hazen, S.L. (2014) Meta-organismal nutrient metabolism as a basis of cardiovascular disease. *Curr Opin Lipidol* **25**: 48.
Bryk, R., Lima, C.D., Erdjument-Bromage, H., Tempst, P., and Nathan, C. (2002) Metabolic enzymes of mycobacteria linked to antioxidant defense by a thioredoxin-like protein. *Science* **295**: 1073–1077.
Bui, T.P.N., Troise, A.D., Nijsse, B., Roviello, G.N., Fogliano, V., and de Vos, W.M. (2020) *Intestinimonas*-like bacteria are important butyrate producers that utilize Nε-fructosyllysine and lysine in formula-fed infants and adults. *J Funct Foods* **70**: 103974.
Bunker, G.C. (1936) Water Supply Problems in the Tropics of Spanish America. *New Engl Wafer Work Ass J* **50**: 1–104.
Burg, M.B. and Ferraris, J.D. (2008) Intracellular organic osmolytes: function and regulation. *J Biol Chem* **283**: 7309–7313.
Burrichter, A., Denger, K., Franchini, P., Huhn, T., Müller, N., Spiteller, D., and Schleheck, D. (2018) Anaerobic degradation of the plant sugar sulfoquinovose concomitant with H_2S production: *Escherichia coli* K-12 and *Desulfovibrio* sp. strain DF1 as co-culture model. *Front Microbiol* **9**: 2792.
Burrichter, A.G., Dörr, S., Bergmann, P., Haiß, S., Keller, A., Fournier, C., et al. (2021) Bacterial microcompartments for isethionate desulfonation in the taurine-degrading human-gut bacterium Bilophila wadsworthia. *BMC Microbiol* **21**:1–16.
Calero, C.D.Q., Rincón, E.O., and Marqueta, P.M. (2020) Probiotics, prebiotics and synbiotics: useful for athletes and active individuals? A systematic review. *Benef Microbes* **11**: 135–149.
Camilleri, M. (2022) Bile acid detergency: Permeability, inflammation, and effects of sulfation. *Am J Physiol Liver Physiol* **322**: G480–G488.
Campbell, C., Adeolu, M., and Gupta, R.S. (2015) Genome-based taxonomic framework for the class *Negativicutes*: division of the class *Negativicutes* into the orders *Selenomonadales* emend., *Acidaminococcales* ord. nov. and *Veillonellales* ord. nov. *Int J Syst Evol Microbiol* **65**: 3203–3215.
Canfora, E.E., Jocken, J.W., and Blaak, E.E. (2015) Short-chain fatty acids in control of body weight and insulin sensitivity. *Nat Rev Endocrinol* **11**: 577–591.
Cannon, R.J. and Ho, C.T. (2018) Volatile sulfur compounds in tropical fruits. *J food drug Anal* **26**: 445–468.
Carbonero, F., Benefiel, A.C., Alizadeh-Ghamsari, H.A., and Gaskins, H.R. (2012) Microbial pathways in colonic sulfur metabolism and links with health and disease. *Front Physiol* **3**: 448.
Carbonero, F., Benefiel, A.C., and Gaskins, H.R. (2012) Contributions of the microbial hydrogen economy to colonic homeostasis. *Nat Rev Gastroenterol Hepatol* **9**: 504–518.
CATO, E.P., HOLDEMAN, L. V, and Moore, W.E.C. (1981) Designation of *Eubacterium limosum* (Eggerth) prévot as the type species of *Eubacterium* request for an opinion. *Int J Syst Evol Microbiol* **31**: 209–210.
Chambers, E.S., Viardot, A., Psichas, A., Morrison, D.J., Murphy, K.G., Zac-Varghese, S.E.K., *et al*. (2015) Effects of targeted delivery of propionate to the human colon on appetite regulation, body weight maintenance and adiposity in overweight adults. *Gut* **64**: 1744–1754.
Chang, I.-S., Kim, D.H., Kim, B.H., Shin, P.K., Yoon, J.H., Lee, J.S., and Park, Y.H. (1997) Isolation and identification of carbon monxide utilzing anaerobe, *Eubacterium limosum* KIST612. *Microbiol Biotechnol Lett* **25**: 1–8.
Charbonnier, T., Le Coq, D., McGovern, S., Calabre, M., Delumeau, O., Aymerich, S., and Jules, M. (2017) Molecular and physiological logics of the pyruvate-induced response of a novel transporter in *Bacillus subtilis*. *MBio* **8**: 10–1128.
Chassard, C., Dapoigny, M., Scott, K.P., Crouzet, L., Del'Homme, C., Marquet, P., et al. (2012) Functional dysbiosis within the gut microbiota of patients with constipated-irritable bowel syndrome. *Aliment Pharmacol Ther* **35**: 828–838.
Chaumeil, P.-A., Mussig, A.J., Hugenholtz, P., and Parks, D.H. (2020) GTDB-Tk: a toolkit to classify genomes with the Genome Taxonomy Database. **36**:1925–1927.
Cheng, C., Dong, Z., Han, X., Wang, H., Jiang, L., Sun, J., *et al*. (2017) Thioredoxin A is essential for motility and contributes to host infection of *Listeria monocytogenes* via redox interactions.

Front Cell Infect Microbiol **7**: 287.
Cheng, S., Sinha, S., Fan, C., Liu, Y., and Bobik, T.A. (2011) Genetic analysis of the protein shell of the microcompartments involved in coenzyme B12-dependent 1, 2-propanediol degradation by *Salmonella*. *J Bacteriol* **193**: 1385–1392.
Chesney, R.W. (1985) Taurine: its biological role and clinical implications. *Adv Pediatr* **32**: 1–42.
Chien, C., Leadbetter, E.R., and Godchaux, W. (1995) Sulfonate-sulfur can be assimilated for fermentative growth. *FEMS Microbiol Lett* **129**: 189–193.
Chowdhury, C., Sinha, S., Chun, S., Yeates, T.O., and Bobik, T.A. (2014) Diverse bacterial microcompartment organelles. *Microbiol Mol Biol Rev MMBR* **78**: 438.
Chun, J., Oren, A., Ventosa, A., Christensen, H., Arahal, D.R., da Costa, M.S., et al. (2018) Proposed minimal standards for the use of genome data for the taxonomy of prokaryotes. *Int J Syst Evol Microbiol* **68**: 461–466.
Cline, J.D. (1969) Spectrophotometric determination of hydrogen sulfide in natural waters. *Limnol Oceanogr* **14**: 454–458.
Cook, A.M. and Denger, K. (2002) Dissimilation of the C_2 sulfonates. *Arch Microbiol* **179**: 1–6.
Cox, J. and Mann, M. (2008) MaxQuant enables high peptide identification rates, individualized ppb-range mass accuracies and proteome-wide protein quantification. *Nat Biotechnol* **26**: 1367–1372.
Craciun, S. and Balskus, E.P. (2012) Microbial conversion of choline to trimethylamine requires a glycyl radical enzyme. *Proc Natl Acad Sci* **109**: 21307–21312.
Croix, J.A., Carbonero, F., Nava, G.M., Russell, M., Greenberg, E., and Gaskins, H.R. (2011) On the relationship between sialomucin and sulfomucin expression and hydrogenotrophic microbes in the human colonic mucosa. *PLoS One* **6**: e24447.
D'Amore, T., Di Taranto, A., Berardi, G., Vita, V., Marchesani, G., Chiaravalle, A.E., and Iammarino, M. (2020) Sulfites in meat: Occurrence, activity, toxicity, regulation, and detection. A comprehensive review. *Compr Rev Food Sci Food Saf* **19**: 2701–2720.
Dalile, B., Van Oudenhove, L., Vervliet, B., and Verbeke, K. (2019) The role of short-chain fatty acids in microbiota-gut-brain communication. *Nat Rev Gastroenterol Hepatol* **16**: 461–478.
Deleu, S., Machiels, K., Raes, J., Verbeke, K., and Vermeire, S. (2021) Short chain fatty acids and its producing organisms: An overlooked therapy for IBD? *EBioMedicine* **66**: 103293.
Demarquoy, J., Georges, B., Rigault, C., Royer, M.-C., Clairet, A., Soty, M., et al. (2004) Radioisotopic determination of L-carnitine content in foods commonly eaten in Western countries. *Food Chem* **86**: 137–142.
Denger, K., Stackebrandt, E., and Cook, a M. (1999) *Desulfonispora thiosulfatigenes* gen. nov., sp. nov., a taurine-fermenting, thiosulfate-producing anaerobic bacterium. *Int J Syst Bacteriol* **49** : 1599–1603.
Denger, K., Weiss, M., Felux, A.-K., Schneider, A., Mayer, C., Spiteller, D., *et al*. (2014) Sulphoglycolysis in *Escherichia coli* K-12 closes a gap in the biogeochemical sulphur cycle. *Nature* **507**: 114–117.
Deplancke, B. and Gaskins, H.R. (2001) Microbial modulation of innate defense: goblet cells and the intestinal mucus layer. *Am J Clin Nutr* **73**: 1131S-1141S.
Devkota, S., Wang, Y., Musch, M.W., Leone, V., Fehlner-Peach, H., Nadimpalli, A., *et al*. (2012) Dietary-fat-induced taurocholic acid promotes pathobiont expansion and colitis in *Il*10-/-mice. *Nature* **487**: 104–108.
DeWeerd, K.A., Saxena, A., Nagle Jr, D.P., and Suflita, J.M. (1988) Metabolism of the 18O-methoxy substituent of 3-methoxybenzoic acid and other unlabeled methoxybenzoic acids by anaerobic bacteria. *Appl Environ Microbiol* **54**: 1237–1242.
Doetsch, R.N. (1981) Determinative methods of light microscopy. *Man methods Gen Bacteriol* 21–33.
Dordević, D., Jančíková, S., Vítězová, M., and Kushkevych, I. (2021) Hydrogen sulfide toxicity in the gut environment: Meta-analysis of sulfate-reducing and lactic acid bacteria in inflammatory processes. *J Adv Res* **27**: 55–69.
Dubois, T., Dancer-Thibonnier, M., Monot, M., Hamiot, A., Bouillaut, L., Soutourina, O., *et al*. (2016) Control of *Clostridium difficile* physiopathology in response to cysteine availability. *Infect Immun* **84**: 2389–2405.
Duncan, S.H., Louis, P., and Flint, H.J. (2004) Lactate-utilizing bacteria, isolated from human feces,

that produce butyrate as a major fermentation product. *Appl Environ Microbiol* **70**: 5810–5817.
Egan, M., Jiang, H., O'Connell Motherway, M., Oscarson, S., and van Sinderen, D. (2016) Glycosulfatase-encoding gene cluster in *Bifidobacterium breve* UCC2003. *Appl Environ Microbiol* **82**: 6611–6623.
Eggerth, A.H. (1935) The Gram-positive non-spore-bearing anaerobic bacilli of human feces. *J Bacteriol* **30**: 277–299.
Eichhorn, E., van der Ploeg, J.R., Kertesz, M.A., and Leisinger, T. (1997) Characterization of α-ketoglutarate-dependent taurine dioxygenase from *Escherichia coli*. *J Biol Chem* **272**: 23031–23036.
Ellenbogen, J.B., Jiang, R., Kountz, D.J., Zhang, L., and Krzycki, J.A. (2021) The MttB superfamily member MtyB from the human gut symbiont *Eubacterium limosum* is a cobalamin-dependent γ-butyrobetaine methyltransferase. *J Biol Chem* **297**: 101327.
European Food Safety Authority (2016) Scientific Opinion on the re-evaluation of sulfur dioxide (E 220), sodium sulfite (E 221), sodium bisulfite (E 222), sodium metabisulfite (E 223), potassium metabisulfite (E 224), calcium sulfite (E 226), calcium bisulfite (E 227) and potassium bisulfite. *Efsa J* **14**: 4438.
Fan, Y. and Pedersen, O. (2021) Gut microbiota in human metabolic health and disease. *Nat Rev Microbiol* **19**: 55–71.
Fava, F. and Danese, S. (2011) Intestinal microbiota in inflammatory bowel disease: friend of foe? *World J Gastroenterol WJG* **17**: 557.
Felux, A.-K., Denger, K., Weiss, M., Cook, A.M., and Schleheck, D. (2013) *Paracoccus denitrificans* PD1222 utilizes hypotaurine via transamination followed by spontaneous desulfination to yield acetaldehyde and, finally, acetate for growth. *J Bacteriol* **195**: 2921–2930.
Felux, A.-K., Spiteller, D., Klebensberger, J., and Schleheck, D. (2015) Entner–Doudoroff pathway for sulfoquinovose degradation in *Pseudomonas putida* SQ1. *Proc Natl Acad Sci* **112**: E4298–E4305.
Feng, Y., Bui, T.P.N., Stams, A.J.M., Boeren, S., Sánchez-Andrea, I., and de Vos, W.M. (2022) Comparative genomics and proteomics of *Eubacterium maltosivorans*: functional identification of trimethylamine methyltransferases and bacterial microcompartments in a human intestinal bacterium with a versatile lifestyle. *Environ Microbiol* **24**: 517–534.
Feng, Y., Stams, A.J.M., Sánchez-Andrea, I., and De Vos, W.M. (2018) *Eubacterium maltosivorans* sp. nov., a novel human intestinal acetogenic and butyrogenic bacterium with a versatile metabolism. *Int J Syst Evol Microbiol* **68**: 3546–3550.
Feng, Y., Stams, A.J.M., de Vos, W., and Sánchez-Andrea, I. (2017) Enrichment of sulfidogenic bacteria from the human intestinal tract. *FEMS Microbiol Lett* **364**: fnx028.
Feng, Z., Long, W., Hao, B., Ding, D., Ma, X., Zhao, L., and Pang, X. (2017) A human stool-derived *Bilophila wadsworthia* strain caused systemic inflammation in specific-pathogen-free mice. *Gut Pathog* **9**: 1–10.
Figliuolo, V.R., Dos Santos, L.M., Abalo, A., Nanini, H., Santos, A., Brittes, N.M., et al. (2017) Sulfate-reducing bacteria stimulate gut immune responses and contribute to inflammation in experimental colitis. *Life Sci* **189**: 29–38.
Finkelstein, J.D. (1990) Methionine metabolism in mammals. *J Nutr Biochem* **1**: 228–237.
Finkelstein, J.D. and Martin, J.J. (2000) Homocysteine. *Int J Biochem Cell Biol* **32**: 385–389.
Fite, A., Macfarlane, G.T., Cummings, J.H., Hopkins, M.J., Kong, S.C., Furrie, E., and Macfarlane, S. (2004) Identification and quantitation of mucosal and faecal desulfovibrios using real time polymerase chain reaction. *Gut* **53**: 523–529.
Flint, H.J., Scott, K.P., Louis, P., and Duncan, S.H. (2012) The role of the gut microbiota in nutrition and health. *Nat Rev Gastroenterol Hepatol* **9**: 577–589.
Florentino, A.P., Brienza, C., Stams, A.J.M., and Sánchez-Andrea, I. (2016) *Desulfurella amilsii* sp. nov., a novel acidotolerant sulfur-respiring bacterium isolated from acidic river sediments. *Int J Syst Evol Microbiol* **66**: 1249–1253.
Florentino, A.P., Stams, A.J.M., and Sánchez-Andrea, I. (2017) Genome sequence of *Desulfurella amilsii* strain TR1 and comparative genomics of desulfurellaceae family. *Front Microbiol* **8**: 222.
Florentino, A.P., Weijma, J., Stams, A.J.M., and Sánchez-Andrea, I. (2015) Sulfur reduction in acid

rock drainage environments. *Environ Sci Technol* **49**: 11746–11755.
Florin, T.H.J., Neale, G., Goretski, S., and Cummings, J.H. (1993) The sulfate content of foods and beverages. *J food Compos Anal* **6**: 140–151.
Francioso, A., Baseggio Conrado, A., Mosca, L., and Fontana, M. (2020) Chemistry and biochemistry of sulfur natural compounds: Key intermediates of metabolism and redox biology. *Oxid Med Cell Longev* **2020**: 2020.
Fraser, R.D.B., MacRae, T.P., Sparrow, L.G., and Parry, D.A.D. (1988) Disulphide bonding in α-keratin. *Int J Biol Macromol* **10**: 106–112.
Fritz, G., Büchert, T., Huber, H., Stetter, K.O., and Kroneck, P.M.H. (2000) Adenylylsulfate reductases from archaea and bacteria are 1: 1 αβ-heterodimeric iron–sulfur flavoenzymes–high similarity of molecular properties emphasizes their central role in sulfur metabolism. *Febs Lett* **473**: 63–66.
Froese, D.S., Fowler, B., and Baumgartner, M.R. (2019) Vitamin B12, folate, and the methionine remethylation cycle–biochemistry, pathways, and regulation. *J Inherit Metab Dis* **42**: 673–685.
Frommeyer, B., Fiedler, A.W., Oehler, S.R., Hanson, B.T., Loy, A., Franchini, P., *et al*. (2020) Environmental and intestinal phylum firmicutes bacteria metabolize the plant sugar sulfoquinovose via a 6-deoxy-6-sulfofructose transaldolase pathway. *IScience* **23**: 101510.
Fu, L.H., Wei, Z.Z., Hu, K.D., Hu, L.Y., Li, Y.H., Chen, X.Y., *et al*. (2018) Hydrogen sulfide inhibits the growth of *Escherichia coli* through oxidative damage. *J Microbiol* **56**: 238–245.
Fukuda, K., Hirai, Y., Yoshida, H., Nakajima, T., and Usui, T. (1982) Free amino acid content of lymphocytes nd granulocytes compared. *Clin Chem* **28**: 1758–1761.
Funabashi, M., Grove, T.L., Wang, M., Varma, Y., McFadden, M.E., Brown, L.C., et al. (2020) A metabolic pathway for bile acid dehydroxylation by the gut microbiome. *Nature* **582**: 566–570.
Gardana, C., Del Bo, C., and Simonetti, P. (2017) Validation and application of an ultrahigh-performance liquid chromatographic-Orbitrap mass spectrometric method for the simultaneous detection and quantification of volatile and non-volatile organic acids in human faecal samples. *J Pharm Biomed Anal* **141**: 46–51.
Genthner, B.R., Davis, C.L., and Bryant, M.P. (1981) Features of rumen and sewage sludge strains of *Eubacterium limosum*, a methanol- and H_2-CO_2-utilizing species. *Appl Environ Microbiol* **42**: 12–19.
Giandomenico, A.R., Cerniglia, G.E., Biaglow, J.E., Stevens, C.W., and Koch, C.J. (1997) The importance of sodium pyruvate in assessing damage produced by hydrogen peroxide. *Free Radic Biol Med* **23**: 426–434.
Gibson, G.R., Macfarlane, G.T., and Cummings, J.H. (1988) Occurrence of sulphate-reducing bacteria in human faeces and the relationship of dissimilatory sulphate reduction to methanogenesis in the large gut. *J Appl Bacteriol* **65**: 103–111.
Gibson, J.A., Sladen, G.E., and Dawson, A.M. (1976) Protein absorption and ammonia production: the effects of dietary protein and removal of the colon. *Br J Nutr* **35**: 61–65.
Gibson, R., Macfarlane, G., and Cummings, J. (1993) Leading article: Sulphate reducing bacteria and hydrogen metabolism in the human. *Gut* **34**: 437–439.
Gijs, L., Perpete, P., Timmermans, A., and Collin, S. (2000) 3-Methylthiopropionaldehyde as precursor of dimethyl trisulfide in aged beers. *J Agric Food Chem* **48**: 6196–6199.
Gillis, C.C., Hughes, E.R., Spiga, L., Winter, M.G., Zhu, W., de Carvalho, T.F., *et al*. (2018) Dysbiosis-associated change in host metabolism generates lactate to support *Salmonella* growth. *Cell Host Microbe* **23**: 54–64.
Gish, W. and States, D.J. (1993) Identification of protein coding regions by database similarity search. *Nat Genet* **3**: 266–272.
Gon, S., Patte, J.C., Méjean, V., and Iobbi-Nivol, C. (2000) The torYZ (yecK bisZ) operon encodes a third respiratory trimethylamine N-oxide reductase in *Escherichia coli*. *J Bacteriol* **182**: 5779–5786.
Gould, G.W. and Russell, N.J. (2003) Sulfite. In *Food preservatives*. Springer, pp. 85–101.
Griffith, O.W. (1987) Mammalian sulfur amino acid metabolism: an overview. *Methods Enzymol* **143**: 366–376.
Grimble, R.F. (2006) The effects of sulfur amino acid intake on immune function in humans. *J Nutr* **136**: 1660S-1665S.

Grissa, I., Vergnaud, G., and Pourcel, C. (2007) CRISPRFinder: a web tool to identify clustered regularly interspaced short palindromic repeats. *Nucleic Acids Res* **35**: W52–W57.
Gum, J.R., Hicks, J.W., Toribara, N.W., Rothe, E.M., Lagace, R.E., and Kim, Y.S. (1992) The human MUC2 intestinal mucin has cysteine-rich subdomains located both upstream and downstream of its central repetitive region. *J Biol Chem* **267**: 21375–21383.
Gunnison, A.F. (1981) Sulphite toxicity: a critical review of *in vitro* and *in vivo* data. *Food Cosmet Toxicol* **19**: 667–682.
Guzior, D.V. and Quinn, R.A. (2021) Microbial transformations of human bile acids. *Microbiome* **9**: 1–13.
Haft, D.H., DiCuccio, M., Badretdin, A., Brover, V., Chetvernin, V., O'Neill, K., *et al*. (2018) RefSeq: an update on prokaryotic genome annotation and curation. *Nucleic Acids Res* **46**: D851–D860.
Hale, V.L., Jeraldo, P., Mundy, M., Yao, J., Keeney, G., Scott, N., et al. (2018) Synthesis of multi-omic data and community metabolic models reveals insights into the role of hydrogen sulfide in colon cancer. *Methods* **149**: 59–68.
Hamer, H.M., Jonkers, D., Venema, K., Vanhoutvin, S., Troost, F.J., and Brummer, R.J. (2008) Review article: The role of butyrate on colonic function. *Aliment Pharmacol Ther* **27**: 104–119.
Hansen, J., Bruun, S. V, Bech, L.M., and Gjermansen, C. (2002) The level of *MXR1* gene expression in brewing yeast during beer fermentation is a major determinant for the concentration of dimethyl sulfide in beer. *FEMS Yeast Res* **2**: 137–149.
Hanson, B.T., Dimitri Kits, K., Löffler, J., Burrichter, A.G., Fiedler, A., Denger, K., *et al*. (2021) Sulfoquinovose is a select nutrient of prominent bacteria and a source of hydrogen sulfide in the human gut. *ISME J* **15**: 2779–2791.
Herring, T.I., Harris, T.N., Chowdhury, C., Mohanty, S.K., and Bobik, T.A. (2018) A bacterial microcompartment is used for choline fermentation by *Escherichia coli* 536. *J Bacteriol* **200**: e00764-17.
Hildebrandt, T.M. and Grieshaber, M.K. (2008) Three enzymatic activities catalyze the oxidation of sulfide to thiosulfate in mammalian and invertebrate mitochondria. *FEBS J* **275**: 3352–3361.
Hilton, B.L. and Oleszkiewicz, J.A. (1988) Sulfide-induced inhibition of anaerobic digestion. *J Environ Eng* **114**: 1377–1391.
Hiniker, A. and Bardwell, J.C.A. (2004) *In vivo* substrate specificity of periplasmic disulfide oxidoreductases. *J Biol Chem* **279**: 12967–12973.
Hinnebusch, B.F., Meng, S., Wu, J.T., Archer, S.Y., and Hodin, R.A. (2002) The effects of short-chain fatty acids on human colon cancer cell phenotype are associated with histone hyperacetylation. *J Nutr* **132**: 1012–1017.
Hoang, D.T., Chernomor, O., Von Haeseler, A., Minh, B.Q., and Vinh, L.S. (2018) UFBoot2: improving the ultrafast bootstrap approximation. *Mol Biol Evol* **35**: 518–522.
Holmén Larsson, J.M., Karlsson, H., Sjövall, H., and Hansson, G.C. (2009) A complex, but uniform *O*-glycosylation of the human MUC2 mucin from colonic biopsies analyzed by nanoLC/MS^n. *Glycobiology* **19**: 756–766.
Hove, H. and Mortensen, P.B. (1995) Colonic lactate metabolism and D-lactic acidosis. *Dig Dis Sci* **40**: 320–330.
Hove, H., Nordgaard-Andersen, I., and Mortensen, P.B. (1994) Effect of lactic acid bacteria on the intestinal production of lactate and short-chain fatty acids, and the absorption of lactose. *Am J Clin Nutr* **59**: 74–79.
Huda-Faujan, N., Abdulamir, A.S., Fatimah, A.B., Anas, O.M., Shuhaimi, M., Yazid, A.M., and Loong, Y.Y. (2010) The impact of the level of the intestinal short chain fatty acids in inflammatory bowel disease patients versus healthy subjects. *Open Biochem J* **4**: 53–58.
Huijghebaert, S., Parmentier, G., and Eyssen, H. (1984) Specificity of bile salt sulfatase activity in man, mouse and rat intestinal microflora. *J Steroid Biochem* **20**: 907–912.
Hyatt, D., Chen, G.L., LoCascio, P.F., Land, M.L., Larimer, F.W., and Hauser, L.J. (2010) Prodigal: prokaryotic gene recognition and translation initiation site identification. *BMC Bioinformatics* **11**: 1–11.
Ijssennagger, N., van der Meer, R., and van Mil, S.W.C. (2016) Sulfide as a mucus barrier-breaker in inflammatory bowel disease? *Trends Mol Med* **22**: 190–199.
Ilangovan, U., Ton-That, H., Iwahara, J., Schneewind, O., and Clubb, R.T. (2001) Structure of sortase,

the transpeptidase that anchors proteins to the cell wall of *Staphylococcus aureus*. *Proc Natl Acad Sci* **98**: 6056–6061.
Iobbi-Nivol, C., Pommier, J., Simala-Grant, J., Méjean, V., and Giordano, G. (1996) High substrate specificity and induction characteristics of trimethylamine-N-oxide reductase of *Escherichia coli*. *Biochim Biophys Acta (BBA)-Protein Struct Mol Enzymol* **1294**: 77–82.
Irimura, T., Wynn, D.M., Hager, L.G., Cleary, K.R., and Ota, D.M. (1991) Human colonic sulfomucin identified by a specific monoclonal antibody. *Cancer Res* **51**: 5728–5735.
Irmler, S., Raboud, S., Beisert, B., Rauhut, D., and Berthoud, H. (2008) Cloning and characterization of two *Lactobacillus casei* genes encoding a cystathionine lyase. *Appl Environ Microbiol* **74**: 99–106.
Jacobsen, J.G. and Smith, L.H. (1968) Biochemistry and physiology of taurine and taurine derivatives. *Physiol Rev* **48**: 424–511.
Jalandra, R., Dalal, N., Yadav, A.K., Verma, D., Sharma, M., Singh, R., *et al*. (2021) Emerging role of trimethylamine-N-oxide (TMAO) in colorectal cancer. *Appl Microbiol Biotechnol* **105**: 7651–7660.
Jameson, E., Fu, T., Brown, I.R., Paszkiewicz, K., Purdy, K.J., Frank, S., and Chen, Y. (2016) Anaerobic choline metabolism in microcompartments promotes growth and swarming of *Proteus mirabilis*. *Environ Microbiol* **18**: 2886–2898.
Janaky, R., Ogita, K., Pasqualotto, B.A., Bains, J.S., Oja, S.S., Yoneda, Y., and Shaw, C.A. (1999) Glutathione and signal transduction in the mammalian CNS. *J Neurochem* **73**: 889–902.
Janeiro, M.H., Ramírez, M.J., Milagro, F.I., Martínez, J.A., and Solas, M. (2018) Implication of trimethylamine N-oxide (TMAO) in disease: potential biomarker or new therapeutic target. *Nutrients* **10**: 1398.
Jew, S., AbuMweis, S.S., and Jones, P.J.H. (2009) Evolution of the human diet: linking our ancestral diet to modern functional foods as a means of chronic disease prevention. *J Med Food* **12**: 925–934.
Jia, W., Whitehead, R.N., Griffiths, L., Dawson, C., Bai, H., Waring, R.H., *et al*. (2012) Diversity and distribution of sulphate-reducing bacteria in human faeces from healthy subjects and patients with inflammatory bowel disease. *FEMS Immunol Med Microbiol* **65**: 55–68.
Jiang, J., Chan, A., Ali, S., Saha, A., Haushalter, K.J., Lam, W.L.M., *et al*. (2016) Hydrogen sulfide–mechanisms of toxicity and development of an antidote. *Sci Rep* **6**: 20831.
Jin, J.S., Zhao, Y.F., Nakamura, N., Akao, T., Kakiuchi, N., and Hattori, M. (2007) Isolation and characterization of a human intestinal bacterium, *Eubacterium* sp. ARC-2, capable of demethylating arctigenin, in the essential metabolic process to enterolactone. *Biol Pharm Bull* **30**: 904–911.
Jolkver, E., Emer, D., Ballan, S., Krämer, R., Eikmanns, B.J., and Marin, K. (2009) Identification and characterization of a bacterial transport system for the uptake of pyruvate, propionate, and acetate in *Corynebacterium glutamicum*. *J Bacteriol* **191**: 940–948.
Jones, B. V, Begley, M., Hill, C., Gahan, C.G.M., and Marchesi, J.R. (2008) Functional and comparative metagenomic analysis of bile salt hydrolase activity in the human gut microbiome. *Proc Natl Acad Sci* **105**: 13580–13585.
Jones, P., Binns, D., Chang, H.Y., Fraser, M., Li, W., McAnulla, C., *et al*. (2014) InterProScan 5: genome-scale protein function classification. *Bioinformatics* **30**: 1236–1240.
Junier, P., Junier, T., Podell, S., Sims, D.R., Detter, J.C., Lykidis, A., et al. (2010) The genome of the Gram-positive metal- and sulfate-reducing bacterium *Desulfotomaculum reducens* strain MI-1. *Environ Microbiol* **12**: 2738–2754.
Kadokura, H., Tian, H., Zander, T., Bardwell, J.C.A., and Beckwith, J. (2004) Snapshots of DsbA in action: detection of proteins in the process of oxidative folding. *Science* **303**: 534–537.
Kalisch, B., Dörmann, P., and Hölzl, G. (2016) DGDG and glycolipids in plants and algae. *Lipids plant algae Dev* 51–83.
Kalyaanamoorthy, S., Minh, B.Q., Wong, T.K.F., Von Haeseler, A., and Jermiin, L.S. (2017) ModelFinder: fast model selection for accurate phylogenetic estimates. *Nat Methods* **14**: 587–589.
Kanauchi, O., Fukuda, M., Matsumoto, Y., Ishii, S., Ozawa, T., Shimizu, M., et al. (2006) *Eubacterium limosum* ameliorates experimental colitis and metabolite of microbe attenuates

colonic inflammatory action with increase of mucosal integrity. *World J Gastroenterol WJG* **12**: 1071.

Karnachuk, O.V., Lukina, A.P., Kadnikov, V.V, Sherbakova, V.A., Beletsky, A.V, Mardanov, A.V, and Ravin, N.V (2021) Targeted isolation based on metagenome-assembled genomes reveals a phylogenetically distinct group of thermophilic spirochetes from deep biosphere. *Environ Microbiol* **23**: 3585–3598.

Karu, N., Deng, L., Slae, M., Guo, A.C., Sajed, T., Huynh, H., *et al*. (2018) A review on human fecal metabolomics: methods, applications and the human fecal metabolome database. *Anal Chim Acta* **1030**: 1–24.

Katoh, T., Maeshibu, T., Kikkawa, K., Gotoh, A., Tomabechi, Y., Nakamura, M., *et al*. (2017) Identification and characterization of a sulfoglycosidase from *Bifidobacterium bifidum* implicated in mucin glycan utilization. *Biosci Biotechnol Biochem* **81**: 2018–2027.

Kelly, D.P. (1999) Thermodynamic aspects of energy conservation by chemolithotrophic sulfur bacteria in relation to the sulfur oxidation pathways. *Arch Microbiol* **171**: 219–229.

Kelly, W.J., Henderson, G., Pacheco, D.M., Li, D., Reilly, K., Naylor, G.E., *et al*. (2016) The complete genome sequence of *Eubacterium limosum* SA11, a metabolically versatile rumen acetogen. *Stand Genomic Sci* **11**: 26.

Kerfeld, C.A., Aussignargues, C., Zarzycki, J., Cai, F., and Sutter, M. (2018) Bacterial microcompartments. *Nat Rev Microbiol* **16**: 277–290.

Kessler, D. (2006) Enzymatic activation of sulfur for incorporation into biomolecules in prokaryotes. *FEMS Microbiol Rev* **30**: 825–840.

Khan, M.T., Dwibedi, C., Sundh, D., Pradhan, M., Kraft, J.D., Caesar, R., et al. (2023) Synergy and oxygen adaptation for development of next-generation probiotics. *Nature* **620**: 381–385.

Kimura, H., Shibuya, N., and Kimura, Y. (2012) Hydrogen sulfide is a signaling molecule and a cytoprotectant. *Antioxid Redox Signal* **17**: 45–57.

Kittana, M., Ahmadani, A., Al Marzooq, F., and Attlee, A. (2021) Dietary fat effect on the gut microbiome, and its role in the modulation of gastrointestinal disorders in children with autism spectrum disorder. *Nutrients* **13**: 3818.

Kivenson, V. and Giovannoni, S.J. (2020) An expanded genetic code enables trimethylamine metabolism in human gut bacteria. *Msystems* **5**: e00413-e00420.

Klampfer, L., Huang, J., Sasazuki, T., Shirasawa, S., and Augenlicht, L. (2003) Inhibition of interferon γ signaling by the short chain fatty acid butyrate. *Mol Cancer Res* **1**: 855–862.

Klein, E. (1908) On the nature and causes of taints in miscured hams. *Lancet* **174**: 1832–1834.

Koay, Y.C., Chen, Y.C., Wali, J.A., Luk, A.W.S., Li, M., Doma, H., *et al*. (2021) Plasma levels of trimethylamine-N-oxide can be increased with 'healthy' and 'unhealthy' diets and do not correlate with the extent of atherosclerosis but with plaque instability. *Cardiovasc Res* **117**: 435–449.

Koehorst, J.J., van Dam, J.C.J., Saccenti, E., Martins dos Santos, V.A.P., Suarez-Diez, M., and Schaap, P.J. (2018) SAPP: functional genome annotation and analysis through a semantic framework using FAIR principles. *Bioinformatics* **34**: 1401–1403.

Koeth, R.A., Levison, B.S., Culley, M.K., Buffa, J.A., Wang, Z., Gregory, J.C., et al. (2014) γ-butyrobetaine is a proatherogenic intermediate in gut microbial metabolism of L-carnitine to TMAO. *Cell Metab* **20**: 799–812.

Koeth, R.A., Wang, Z., Levison, B.S., Buffa, J.A., Org, E., Sheehy, B.T., *et al*. (2013) Intestinal microbiota metabolism of L-carnitine, a nutrient in red meat, promotes atherosclerosis. *Nat Med* **19**: 576–585.

Kofoid, E., Rappleye, C., Stojiljkovic, I., and Roth, J. (1999) The 17-gene ethanolamine (*eut*) operon of *Salmonella typhimurium* encodes five homologues of carboxysome shell proteins. *J Bacteriol* **181**: 5317.

Körber, T.T., Frantz, N., Sitz, T., Abdalla, M.A., Mühling, K.H., and Rohn, S. (2022) Alterations of content and composition of individual sulfolipids, and change of fatty acids profile of galactolipids in lettuce plants (*Lactuca sativa* L.) grown under sulfur nutrition. *Plants* **11**: 1342.

Kountz, D.J., Behrman, E.J., Zhang, L., and Krzycki, J.A. (2020) MtcB, a member of the MttB superfamily from the human gut acetogen *Eubacterium limosum*, is a cobalamin-dependent carnitine demethylase. *J Biol Chem* **295**: 11971–11981.

Kowlgi, N.G. and Chhabra, L. (2015) D-lactic acidosis: an underrecognized complication of short bowel syndrome. *Gastroenterol Res Pract* **2015**: 476215.
Kredich, N.M., Keenan, B.S., and Foote, L.J. (1972) The purification and subunit structure of cysteine desulfhydrase from *Salmonella typhimurium*. *J Biol Chem* **247**: 7157–7162.
Kreth, J., Lengeler, J.W., and Jahreis, K. (2013) Characterization of pyruvate uptake in *Escherichia coli* K-12. *PLoS One* **8**: e67125.
Krueger, D., Foerster, M., Mueller, K., Zeller, F., Slotta-Huspenina, J., Donovan, J., *et al*. (2010) Signaling mechanisms involved in the intestinal pro-secretory actions of hydrogen sulfide. *Neurogastroenterol Motil* **22**: 1224-e320.
Kuehl, J. V, Price, M.N., Ray, J., Wetmore, K.M., Esquivel, Z., Kazakov, A.E., *et al*. (2014) Functional genomics with a comprehensive library of transposon mutants for the sulfate-reducing bacterium *Desulfovibrio alaskensis* G20. *MBio* **5**: e01041–14.
Kulak, N.A., Pichler, G., Paron, I., Nagaraj, N., and Mann, M. (2014) Minimal, encapsulated proteomic-sample processing applied to copy-number estimation in eukaryotic cells. *Nat Methods* **11**: 319–324.
Kushkevych, I., Cejnar, J., Treml, J., Dordević, D., Kollar, P., and Vítězová, M. (2020) Recent advances in metabolic pathways of sulfate reduction in intestinal bacteria. *Cells* **9**: 698.
Kushkevych, I., Dordević, D., and Vítězová, M. (2019) Toxicity of hydrogen sulfide toward sulfate-reducing bacteria *Desulfovibrio piger* Vib-7. *Arch Microbiol* **201**: 389–397.
Kushkevych, I., Kotrsová, V., Dordević, D., Buňková, L., Vítězová, M., and Amedei, A. (2019) Hydrogen sulfide effects on the survival of lactobacilli with emphasis on the development of inflammatory bowel diseases. *Biomolecules* **9**: 752.
Ladenstein, R. and Ren, B. (2006) Protein disulfides and protein disulfide oxidoreductases in hyperthermophiles. *FEBS J* **273**: 4170–4185.
Lagesen, K., Hallin, P., Rødland, E.A., Stærfeldt, H.H., Rognes, T., and Ussery, D.W. (2007) RNAmmer: consistent and rapid annotation of ribosomal RNA genes. *Nucleic Acids Res* **35**: 3100–3108.
Laidlaw, S.A., Grosvenor, M., and Kopple, J.D. (1990) The taurine content of common foodstuffs. *J Parenter Enter Nutr* **14**: 183–188.
Lampreia, J., Pereira, A.S., and Moura, J.G. (1994) Adenylylsulfate reductases from sulfate-reducing bacteria. *Methods Enzymol* **243**: 241–260.
Lapidus, A.L. and Korobeynikov, A.I. (2021) Metagenomic data assembly–the way of decoding unknown microorganisms. *Front Microbiol* **12**: 613791.
Laue, H., Friedrich, M., Ruff, J., and Cook, A.M. (2001) Dissimilatory sulfite reductase (desulfoviridin) of the taurine-degrading, non-sulfate-reducing bacterium *Bilophila wadsworthia* RZATAU contains a fused DsrB-DsrD subunit. *J Bacteriol* **183**: 1727–1733.
Leavitt, W.D., Venceslau, S.S., Pereira, I.A.C., Johnston, D.T., and Bradley, A.S. (2016) Fractionation of sulfur and hydrogen isotopes in *Desulfovibrio vulgaris* with perturbed DsrC expression. *FEMS Microbiol Lett* **363**: fnw226.
Lee, H., Kho, H.-S., Chung, J.W., Chung, S.C., and Kim, Y.K. (2006) Volatile sulfur compounds produced by *Helicobacter pylori*. *J Clin Gastroenterol* **40**: 421–426.
Lefebvre, P., Cariou, B., Lien, F., Kuipers, F., and Staels, B. (2009) Role of bile acids and bile acid receptors in metabolic regulation. *Physiol Rev* **89**: 147–191.
Leviatan, S., Shoer, S., Rothschild, D., Gorodetski, M., and Segal, E. (2022) An expanded reference map of the human gut microbiome reveals hundreds of previously unknown species. *Nat Commun* **13**: 3863.
Levine, J., Ellis, C.J., Furne, J.K., Springfield, J., and Levitt, M.D. (1998) Fecal hydrogen sulfide production in ulcerative colitis. *Am J Gastroenterol* **93**: 83–87.
Li, W., O'Neill, K.R., Haft, D.H., DiCuccio, M., Chetvernin, V., Badretdin, A., *et al*. (2021) RefSeq: expanding the Prokaryotic Genome Annotation Pipeline reach with protein family model curation. *Nucleic Acids Res* **49**: D1020–D1028.
Libiad, M., Vitvitsky, V., Bostelaar, T., Bak, D.W., Lee, H.J., Sakamoto, N., *et al*. (2019) Hydrogen sulfide perturbs mitochondrial bioenergetics and triggers metabolic reprogramming in colon cells. *J Biol Chem* **294**: 12077–12090.
Lie, T.J., Clawson, M.L., Godchaux, W., and Leadbetter, E.R. (1999) Sulfidogenesis from 2-

aminoethanesulfonate (taurine) fermentation by a morphologically unusual sulfate-reducing bacterium, *Desulforhopalus singaporensis* sp. nov. *Appl Environ Microbiol* **65**: 3328–3334.
Liebman, J.F. (1991) Thermochemistry of sulphonic acids and their derivatives. *Sulphonic Acids, Esters their Deriv* 283–321.
Liu, J., Wei, Y., Lin, L., Teng, L., Yin, J., Lu, Q., *et al*. (2020) Two radical-dependent mechanisms for anaerobic degradation of the globally abundant organosulfur compound dihydroxypropanesulfonate. *Proc Natl Acad Sci* **117**: 15599–15608.
Liu, Z.Y., Tan, X.Y., Li, Q.J., Liao, G.C., Fang, A.P., Zhang, D.M., *et al*. (2018) Trimethylamine N-oxide, a gut microbiota-dependent metabolite of choline, is positively associated with the risk of primary liver cancer: a case-control study. *Nutr Metab* **15**: 1–9.
Loddeke, M., Schneider, B., Oguri, T., Mehta, I., Xuan, Z., and Reitzer, L. (2017) Anaerobic cysteine degradation and potential metabolic coordination in *Salmonella enterica* and *Escherichia coli*. *J Bacteriol* **199**: 10–1128.
Lopetuso, L.R., Scaldaferri, F., Petito, V., and Gasbarrini, A. (2013) Commensal *Clostridia*: leading players in the maintenance of gut homeostasis. *Gut Pathog* **5**: 23.
Loubinoux, J., Jaulhac, B., Piemont, Y., Monteil, H., and Le Faou, A.E. (2003) Isolation of sulfate-reducing bacteria from human thoracoabdominal pus. *J Clin Microbiol* **41**: 1304–1306.
Louis, P., Duncan, S.H., Sheridan, P.O., Walker, A.W., and Flint, H.J. (2022) Microbial lactate utilisation and the stability of the gut microbiome. *Gut Microbiome* **3**: e3.
Louis, P. and Flint, H.J. (2017) Formation of propionate and butyrate by the human colonic microbiota. *Environ Microbiol* **19**: 29–41.
Lu, J. and Holmgren, A. (2014) The thioredoxin antioxidant system. *Free Radic Biol Med* **66**: 75–87.
Lück, E. and Jager, M. (1997) Sulfur dioxide. In *Antimicrobial food additives*. Springer, pp. 102–115.
Ludwig, W., Strunk, O., Westram, R., Richter, L., Meier, H., Yadhukumar, A., *et al*. (2004) ARB: A software environment for sequence data. *Nucleic Acids Res* **32**: 1363–1371.
Luis, A.S., Jin, C., Pereira, G.V., Glowacki, R.W.P., Gugel, S.R., Singh, S., et al. (2021) A single sulfatase is required to access colonic mucin by a gut bacterium. *Nature* **598**: 332–337.
Luo, C., Rodriguez-r, L.M., and Konstantinidis, K.T. (2014) MyTaxa: an advanced taxonomic classifier for genomic and metagenomic sequences. *Nucleic Acids Res* **42**: e73–e73.
Ma, W., Liu, Y., Lv, X., Li, J., Du, G., and Liu, L. (2019) Combinatorial pathway enzyme engineering and host engineering overcomes pyruvate overflow and enhances overproduction of N-acetylglucosamine in *Bacillus subtilis*. *Microb Cell Fact* **18**: 1–12.
Magee, E.A., Richardson, C.J., Hughes, R., and Cummings, J.H. (2000) Contribution of dietary protein to sulfide production in the large intestine: an *in vitro* and a controlled feeding study in humans. *Am J Clin Nutr* **72**: 1488–1494.
Malekzadeh, M.M., Vahedi, H., Gohari, K., Mehdipour, P., Sepanlou, S.G., Ebrahimi Daryani, N., *et al*. (2016) Emerging epidemic of inflammatory bowel disease in a middle income country: a nation-wide study from Iran. *Arch Iran Med* **19**: 2–15.
Marciano, F. and Vajro, P. (2017) Oxidative stress and gut microbiota. In *Gastrointestinal tissue*. Elsevier, Chapter **8**: 113–123.
Marquet, P., Duncan, S.H., Chassard, C., Bernalier-Donadille, A., and Flint, H.J. (2009) Lactate has the potential to promote hydrogen sulphide formation in the human colon. *FEMS Microbiol Lett* **299**: 128–134.
Marraffini, L.A., Dedent, A.C., and Schneewind, O. (2006) Sortases and the art of anchoring proteins to the envelopes of gram-positive bacteria. *Microbiol Mol Biol Rev* **70**: 192–221.
Masten Rutar, J., Jagodic Hudobivnik, M., Nečemer, M., Vogel Mikuš, K., Arčon, I., and Ogrinc, N. (2022) Nutritional quality and safety of the *Spirulina* dietary supplements sold on the Slovenian Market. *Foods* **11**: 849.
McCrindle, S.L., Kappler, U., and McEwan, A.G. (2005) Microbial dimethylsulfoxide and trimethylamine-N-oxide respiration. *Adv Microb Physiol* **50**: 147-201e.
McEwan, A.G., Ridge, J.P., McDevitt, C.A., and Hugenholtz, P. (2002) The DMSO reductase family of microbial molybdenum enzymes; molecular properties and role in the dissimilatory reduction of toxic elements. *Geomicrobiol J* **19**: 3–21.
McGorrin, R.J. (2011) The significance of volatile sulfur compounds in food flavors: An overview. *Volatile sulfur Compd food* **1068**: 3–31.

McIver, C.J. and Tapsall, J.W. (1988) Characteristics of cysteine-requiring strains of *Klebsiella* isolated from urinary tract infections. *J Med Microbiol* **26**: 211–215.
Medani, M., Collins, D., Docherty, N.G., Baird, A.W., O'Connell, P.R., and Winter, D.C. (2011) Emerging role of hydrogen sulfide in colonic physiology and pathophysiology. *Inflamm Bowel Dis* **17**: 1620–1625.
Mendes, S.S., Miranda, V., and Saraiva, L.M. (2021) Hydrogen sulfide and carbon monoxide tolerance in bacteria. *Antioxidants* **10**: 729.
Michigami, Y. and Ueda, K. (1994) Sulphite stabilizer in ion chromatography. *J Chromatogr A* **663**: 255–258.
Mimoun, S., Andriamihaja, M., Chaumontet, C., Atanasiu, C., Benamouzig, R., Blouin, J.M., *et al*. (2012) Detoxification of H_2S by differentiated colonic epithelial cells: implication of the sulfide oxidizing unit and of the cell respiratory capacity. *Antioxid Redox Signal* **17**: 1–10.
Missailidis, C., Hällqvist, J., Qureshi, A.R., Barany, P., Heimbürger, O., Lindholm, B., *et al*. (2016) Serum trimethylamine-N-oxide is strongly related to renal function and predicts outcome in chronic kidney disease. *PLoS One* **11**: e0141738.
Módis, K., Coletta, C., Erdélyi, K., Papapetropoulos, A., and Szabo, C. (2013) Intramitochondrial hydrogen sulfide production by 3-mercaptopyruvate sulfurtransferase maintains mitochondrial electron flow and supports cellular bioenergetics. *FASEB J* **27**: 601–611.
Moore, J., Babidge, W., Millard, S., and Roediger, W. (1998) Colonic luminal hydrogen sulfide is not elevated in ulcerative colitis. *Dig Dis Sci* **43**: 162–165.
Moore, J.W., Babidge, W., Millard, S., and Roediger, W.E. (1997) Effect of sulphide on short chain acyl-CoA metabolism in rat colonocytes. *Gut* **41**: 77–81.
Moore, W.E.C. and Cato, E.P. (1965) Synonymy of *Eubacterium limosum* and *Butyribacterium rettgeri*: *Butyribacterium limosum* comb. nov. *Int J Syst Evol Microbiol* **15**: 69–80.
Moore, W.E.C., Johnson, J.L., and Holdeman, L. V (1976) Emendation of *Bacteroidaceae* and *Butyrivibrio* and descriptions of *Desulfomonas* gen. nov. and ten new species in the genera *Desulfomonas*, *Butyrivibrio*, *Eubacterium*, *Clostridium*, and *Ruminococcus*. *Int J Syst Evol Microbiol* **26**: 238–252.
Morita, N., Umemoto, E., Fujita, S., Hayashi, A., Kikuta, J., Kimura, I., et al. (2019) GPR31-dependent dendrite protrusion of intestinal $CX3CR1^+$ cells by bacterial metabolites. *Nature* **566**: 110–114.
Mortensen, P.B. and Clausen, M.R. (1996) Short-chain fatty acids in the human colon: relation to gastrointestinal health and disease. *Scand J Gastroenterol* **31**: 132–148.
Mountfort, D.O., Grant, W.D., Clarke, R., and Asher, R.A. (1988) *Eubacterium callanderi* sp. nov. that demethoxylates O-methoxylated aromatic acids to volatile fatty acids. *Int J Syst Bacteriol* **38**: 254–258.
Müller, E., Fahlbusch, K., Walther, R., and Gottschalk, G. (1981) Formation of N, N-dimethylglycine, acetic acid, and butyric acid from betaine by *Eubacterium limosum*. *Appl Environ Microbiol* **42**: 439–445.
Muñoz-Tamayo, R., Laroche, B., Walter, É., Doré, J., Duncan, S.H., Flint, H.J., and Leclerc, M. (2011) Kinetic modelling of lactate utilization and butyrate production by key human colonic bacterial species. *FEMS Microbiol Ecol* **76**: 615–624.
Mustafa, A.K., Gadalla, M.M., Sen, N., Kim, S., Mu, W., Gazi, S.K., et al. (2009) H_2S signals through protein S-sulfhydration. *Sci Signal* **109**: 1259–1268.
Nakamura, N., Lin, H.C., McSweeney, C.S., Mackie, R.I., and Gaskins, H.R. (2010) Mechanisms of microbial hydrogen disposal in the human colon and implications for health and disease. *Food Sci Technol* **1**: 363–395.
Natividad, J.M., Lamas, B., Pham, H.P., Michel, M.L., Rainteau, D., Bridonneau, C., *et al*. (2018) *Bilophila wadsworthia* aggravates high fat diet induced metabolic dysfunctions in mice. *Nat com* **9**:2802.
Nava, G.M., Carbonero, F., Croix, J.A., Greenberg, E., and Gaskins, H.R. (2011) Abundance and diversity of mucosa-associated hydrogenotrophic microbes in the healthy human colon. *ISME J* **6**: 57–70.
Nguyen, L.-T., Schmidt, H.A., Von Haeseler, A., and Minh, B.Q. (2015) IQ-TREE: a fast and effective stochastic algorithm for estimating maximum-likelihood phylogenies. *Mol Biol Evol*

32: 268–274.
Nguyen, N.-N., Srihari, S., Leong, H.W., and Chong, K.-F. (2015) EnzDP: Improved enzyme annotation for metabolic network reconstruction based on domain composition profiles. *J Bioinform Comput Biol* **13**: 1543003.
Nimni, M.E., Han, B., and Cordoba, F. (2007) Are we getting enough sulfur in our diet? *Nutr & Metab* **4**: 1–12.
Northfield, T.C. and McColl, I. (1973) Postprandial concentrations of free and conjugated bile acids down the length of the normal human small intestine. *Gut* **14**: 513–518.
Nugent, R. (2008) Chronic diseases in developing countries: health and economic burdens. *Ann N Y Acad Sci* **1136**: 70–79.
Oguri, T., Schneider, B., and Reitzer, L. (2012) Cysteine catabolism and cysteine desulfhydrase (CdsH/STM0458) in *Salmonella enterica* Serovar Typhimurium. *J Bacteriol* **194**: 4366–4376.
Osman, L.P., Mitchell, S.C., and Waring, R.H. (1997) Cysteine, its metabolism and toxicity. *Sulfur reports* **20**: 155–172.
Ottman, N., Davids, M., Suarez-Diez, M., Boeren, S., Schaap, P.J., Martins dos Santos, V.A.P., *et al*. (2017) Genome-scale model and omics analysis of metabolic capacities of *Akkermansia muciniphila* reveal a preferential mucin-degrading lifestyle. *Appl Environ Microbiol* **83**: e01014-17.
Overton, T.W., Justino, M.C., Li, Y., Baptista, J.M., Melo, A.M.P., Cole, J.A., and Saraiva, L.M. (2008) Widespread distribution in pathogenic bacteria of di-iron proteins that repair oxidative and nitrosative damage to iron-sulfur centers. *J Bacteriol* **190**: 2004–2013.
Ozer, E.A., Allen, J.P., and Hauser, A.R. (2014) Characterization of the core and accessory genomes of *Pseudomonas aeruginosa* using bioinformatic tools Spine and AGEnt. *BMC Genomics* **15**: 1–17.
Paczia, N., Nilgen, A., Lehmann, T., Gätgens, J., Wiechert, W., and Noack, S. (2012) Extensive exometabolome analysis reveals extended overflow metabolism in various microorganisms. *Microb Cell Fact* **11**: 1–14.
Paiva, C.N. and Bozza, M.T. (2014) Are reactive oxygen species always detrimental to pathogens? *Antioxid Redox Signal* **20**: 1000–1037.
Parcell, S. (2002) Sulfur in human nutrition and applications in medicine. *Altern Med Rev* **7**: 22–44.
Parida, S.K., Domann, E., Rohde, M., Müller, S., Darji, A., Hain, T., et al. (1998) Internalin B is essential for adhesion and mediates the invasion of *Listeria monocytogenes* into human endothelial cells. *Mol Microbiol* **28**: 81–93.
Paulini, S., Fabiani, F.D., Weiss, A.S., Moldoveanu, A.L., Helaine, S., Stecher, B., and Jung, K. (2022) The biological significance of pyruvate sensing and uptake in *Salmonella enterica* Serovar Typhimurium. *Microorganisms* **10**: 1751.
Peck, S.C., Denger, K., Burrichter, A., Irwin, S.M., Balskus, E.P., and Schleheck, D. (2019) A glycyl radical enzyme enables hydrogen sulfide production by the human intestinal bacterium *Bilophila wadsworthia*. *Proc Natl Acad Sci* **116**: 3171–3176.
Peng, Y., Leung, H.C.M., Yiu, S.M., and Chin, F.Y.L. (2012) IDBA-UD: A *de novo* assembler for single-cell and metagenomic sequencing data with highly uneven depth. *Bioinformatics* **28**: 1420–1428.
Pequegnat, B., Sagermann, M., Valliani, M., Toh, M., Chow, H., Allen-Vercoe, E., and Monteiro, M.A. (2013) A vaccine and diagnostic target for *Clostridium bolteae*, an autism-associated bacterium. *Vaccine* **31**: 2787–2790.
Pereira, I.A.C., Ramos, A.R., Grein, F., Marques, M.C., da Silva, S.M., and Venceslau, S.S. (2011) A comparative genomic analysis of energy metabolism in sulfate reducing bacteria and archaea. *Front Microbiol* **2**: 69.
Pham, V.T., Lacroix, C., Braegger, C.P., and Chassard, C. (2017) Lactate-utilizing community is associated with gut microbiota dysbiosis in colicky infants. *Sci Rep* **7**: 1–13.
Picking, J.W., Behrman, E.J., Zhang, L., and Krzycki, J.A. (2019) MtpB, a member of the MttB superfamily from the human intestinal acetogen *Eubacterium limosum*, catalyzes proline betaine demethylation. *J Biol Chem* **294**: 13697–13707.
Picton, R., Eggo, M.C., Merrill, G.A., Langman, M.J.S., and Singh, S. (2002) Mucosal protection against sulphide: importance of the enzyme rhodanese. *Gut* **50**: 201–205.

Pires, R.H., Lourenço, A.I., Morais, F., Teixeira, M., Xavier, A. V, Saraiva, L.M., and Pereira, I.A.C. (2003) A novel membrane-bound respiratory complex from *Desulfovibrio desulfuricans* ATCC 27774. *Biochim Biophys Acta (BBA)-Bioenergetics* **1605**: 67–82.

Pires, R.H., Venceslau, S.S., Morais, F., Teixeira, M., Xavier, A. V, and Pereira, I.A.C. (2006) Characterization of the *Desulfovibrio desulfuricans* ATCC 27774 DsrMKJOP complex a membrane-bound redox complex involved in the sulfate respiratory pathway. *Biochemistry* **45**: 249–262.

Podolsky, D.K. and Isselbacher, K.J. (1983) Composition of human colonic mucin. Selective alteration in inflammatory bowel disease. *J Clin Invest* **72**: 142–153.

Poloni, S., Blom, H.J., and Schwartz, I.V.D. (2015) Stearoyl-CoA desaturase-1: is it the link between sulfur amino acids and lipid metabolism? *Biology (Basel)* **4**: 383–396.

Possemiers, S., Rabot, S., Espín, J.C., Bruneau, A., Philippe, C., González-Sarrías, A., *et al*. (2008) *Eubacterium limosum* activates isoxanthohumol from hops (*Humulus lupulus* L.) into the potent phytoestrogen 8-prenylnaringenin *in vitro* and in rat intestine. *J Nutr* **138**: 1310–1316.

Prideaux, L., Kamm, M.A., De Cruz, P.P., Chan, F.K.L., and Ng, S.C. (2012) Inflammatory bowel disease in Asia: a systematic review. *J Gastroenterol Hepatol* **27**: 1266–1280.

Pruesse, E., Peplies, J., and Glöckner, F.O. (2012) SINA: accurate high-throughput multiple sequence alignment of ribosomal RNA genes. *Bioinformatics* **28**: 1823–1829.

Pujari, R. and Banerjee, G. (2021) Impact of prebiotics on immune response: from the bench to the clinic. *Immunol Cell Biol* **99**: 255–273.

Qin, J., Li, R., Raes, J., Arumugam, M., Burgdorf, K.S., Manichanh, C., *et al*. (2010) A human gut microbial gene catalogue established by metagenomic sequencing. *Nature* **464**: 59–65.

Quast, C., Pruesse, E., Yilmaz, P., Gerken, J., Schweer, T., Yarza, P., *et al*. (2012) The SILVA ribosomal RNA gene database project: improved data processing and web-based tools. *Nucleic Acids Res* **41**: D590–D596.

Rajilić-Stojanović, M., Shanahan, F., Guarner, F., and de Vos, W.M. (2013) Phylogenetic analysis of dysbiosis in ulcerative colitis during remission. *Inflamm Bowel Dis* **19**: 481–488.

Rajilić-Stojanović, M. and de Vos, W.M. (2014) The first 1000 cultured species of the human gastrointestinal microbiota. *FEMS Microbiol Rev* **38**: 996–1047.

Rastelli, M., Cani, P.D., and Knauf, C. (2019) The gut microbiome influences host endocrine functions. *Endocr Rev* **40**: 1271–1284.

Rath, S., Heidrich, B., Pieper, D.H., and Vital, M. (2017) Uncovering the trimethylamine-producing bacteria of the human gut microbiota. *Microbiome* **5**: 1–14.

Rath, S., Rox, K., Kleine Bardenhorst, S., Schminke, U., Dörr, M., Mayerle, J., *et al*. (2021) Higher trimethylamine-N-oxide plasma levels with increasing age are mediated by diet and trimethylamine-forming bacteria. *Msystems* **6**: e00945-21.

Rath, S., Rud, T., Karch, A., Pieper, D.H., and Vital, M. (2018) Pathogenic functions of host microbiota. *Microbiome* **6**: 1–13.

Rey, F.E., Gonzalez, M.D., Cheng, J., Wu, M., Ahern, P.P., and Gordon, J.I. (2013) Metabolic niche of a prominent sulfate-reducing human gut bacterium. *Proc Natl Acad Sci U S A* **110**: 13582–13587.

Rhem, H.J. (1964) Microbial inhibition in foods. *Microb Inhib food action, use Nat Occur Microb Inhib foods* 105–115.

Rho, J., Wright, D.P., Christie, D.L., Clinch, K., Furneaux, R.H., and Roberton, A.M. (2005) A novel mechanism for desulfation of mucin: identification and cloning of a mucin-desulfating glycosidase (sulfoglycosidase) from *Prevotella* strain RS2. J Bacteriol **187**: 1543–1551.

Richter, M. (2013) Functional diversity of organic molecule enzyme cofactors. *Nat Prod Rep* **30**: 1324–1345.

Richter, M. and Rosselló-Móra, R. (2009) Shifting the genomic gold standard for the prokaryotic species definition. *Proc Natl Acad Sci* **106**: 19126–19131.

Ridlon, J.M., Kang, D.J., and Hylemon, P.B. (2006) Bile salt biotransformations by human intestinal bacteria. *J Lipid Res* **47**: 241–59.

Ridlon, J.M., Kang, D.J., Hylemon, P.B., and Bajaj, J.S. (2014) Bile acids and the gut microbiome. *Curr Opin Gastroenterol* **30**: 332–8.

Rizwan, S., ReddySekhar, P., and MalikAsrar, B. (2014) Reactive oxygen species in inflammation

and tissue injury. *Antioxid Redox Signal* **20**: 1126–1167.
Robbe, C., Capon, C., Maes, E., Rousset, M., Zweibaum, A., Zanetta, J.P., and Michalski, J.C. (2003) Evidence of regio-specific glycosylation in human intestinal mucins: presence of an acidic gradient along the intestinal tract. *J Biol Chem* **278**: 46337–46348.
Rode, L.M., Genthner, B.R.S., and Bryant, M.P. (1981) Syntrophic association by cocultures of the methanol-and CO_2-H_2-utilizing species *Eubacterium limosum* and pectin-fermenting *Lachnospira multiparus* during growth in a pectin medium. *Appl Environ Microbiol* **42**: 20–22.
Rodriguez-R, L. and Konstantinidis, K. (2016) The enveomics collection : a toolbox for specialized analyses of microbial genomes and metagenomes. *Peer J Prepr* **4**: e1900v1.
Roe, D.A. and Weston, M.O. (1965) Potential significance of free taurine in the diet. *Nature* **205**: 287–288.
Roediger, W.E.W., Duncan, A., Kapaniris, O., and Millard, S. (1993) Reducing sulfur compounds of the colon impair colonocyte nutrition: implications for ulcerative colitis. *Gastroenterol* **104**: 802–809.
Roh, H., Ko, H.-J., Kim, D., Choi, D.G., Park, S., Kim, S., *et al*. (2011) Complete genome sequence of a carbon monoxide-utilizing acetogen, *Eubacterium limosum* KIST612. *J Bacteriol* **193**: 307–308.
Rosenbaum, F.P., Poehlein, A., Daniel, R., and Müller, V. (2022) Energy-conserving dimethyl sulfoxide reduction in the acetogenic bacterium *Moorella thermoacetica*. *Environ Microbiol* **24**: 2000–2012.
Rubin, B.E., Diamond, S., Cress, B.F., Crits-Christoph, A., Lou, Y.C., Borges, A.L., *et al*. (2022) Species-and site-specific genome editing in complex bacterial communities. *Nat Microbiol* **7**: 34–47.
Salar-García, M.J., Bernal, V., Pastor, J.M., Salvador, M., Argandoña, M., Nieto, J.J., *et al*. (2017) Understanding the interplay of carbon and nitrogen supply for ectoines production and metabolic overflow in high density cultures of *Chromohalobacter salexigens*. *Microb Cell Fact* **16**: 1–12.
Sánchez-Andrea, I., Guedes, I.A., Hornung, B., Boeren, S., Lawson, C.E., Sousa, D.Z., *et al*. (2020) The reductive glycine pathway allows autotrophic growth of *Desulfovibrio desulfuricans*. *Nat Commun* **11**: 5090.
Santos, A.A., Venceslau, S.S., Grein, F., Leavitt, W.D., Dahl, C., Johnston, D.T., and Pereira, I.A.C. (2015) A protein trisulfide couples dissimilatory sulfate reduction to energy conservation. *Science* **350**: 1541–1545.
Scanlan, P.D., Shanahan, F., and Marchesi, J.R. (2009) Culture-independent analysis of desulfovibrios in the human distal colon of healthy, colorectal cancer and polypectomized individuals. *FEMS Microbiol Ecol* **69**: 213–221.
Schär, J., Stoll, R., Schauer, K., Loeffler, D.I.M., Eylert, E., Joseph, B., et al. (2010) Pyruvate carboxylase plays a crucial role in carbon metabolism of extra- and intracellularly replicating *Listeria monocytogenes*. *J Bacteriol* **192**: 1774–1784.
Schattner, P., Brooks, A.N., and Lowe, T.M. (2005) The tRNAscan-SE, snoscan and snoGPS web servers for the detection of tRNAs and snoRNAs. *Nucleic Acids Res* **33**: W686–W689.
Schicho, R., Krueger, D., Zeller, F., Von Weyhern, C.W.H., Frieling, T., Kimura, H., *et al*. (2006) Hydrogen sulfide is a novel prosecretory neuromodulator in the Guinea-pig and human colon. *Gastroenterology* **131**: 1542–1552.
Schiff, J.A. and Fankhauser, H. (1981) Assimilatory sulfate reduction. In *Biology of inorganic nitrogen and sulfur*. Springer, pp. 153–168.
Schmitt, E., Coureux, P.D., Monestier, A., Dubiez, E., and Mechulam, Y. (2019) Start codon recognition in eukaryotic and archaeal translation initiation: a common structural core. *Int J Mol Sci* **20**: 939.
Schouten, C. (1946) The role of sulphur bacteria in the formation of the so-called sedimentary copper ores and pyritic ore bodies. *Econ Geol* **41**: 517–538.
Schroeder, B.O. (2019) Fight them or feed them: how the intestinal mucus layer manages the gut microbiota. *Gastroenterol Rep* **7**: 3–12.
Schugar, R.C. and Brown, J.M. (2015) Emerging roles of Flavin Monooxygenase 3 (FMO3) in cholesterol metabolism and atherosclerosis. *Curr Opin Lipidol* **26**: 426.

Schuller-Levis, G.B. and Park, E. (2003) Taurine: new implications for an old amino acid. *FEMS Microbiol Lett* **226**: 195–202.
Schwanhäußer, B. (2011) Global analysis of cellular protein dynamics by pulse-labeling and quantitative mass spectrometry. (Doctoral dissertation, Humboldt-Universität zu Berlin).
Sen, C.K. (2001) Cellular thiols and redox-regulated signal transduction. *Curr Top Cell Regul* **36**: 1–30.
Shefa, U., Kim, M.S., Jeong, N.Y., and Jung, J. (2018) Antioxidant and cell-signaling functions of hydrogen sulfide in the central nervous system. *Oxid Med Cell Longev* **2018**: 1873962.
Shetty, S.A., Boeren, S., Bui, T.P.N., Smidt, H., and de Vos, W.M. (2020) Unravelling lactate-acetate and sugar conversion into butyrate by intestinal Anaerobutyricum and Anaerostipes species by comparative proteogenomics. *Environ Microbiol* **22**: 4863–4875.
Shimada, T., Tanaka, K., and Ishihama, A. (2016) Transcription factor DecR (YbaO) controls detoxification of L-cysteine in *Escherichia coli*. *Microbiology* **162**: 1698–1707.
da Silva, S.M., Venceslau, S.S., Fernandes, C.L., Valente, F.M., and Pereira, I.A. (2008) Hydrogen as an energy source for the human pathogen *Bilophila wadsworthia*. *Antonie Van Leeuwenhoek* **93**: 381–390.
Singh, S.B., Carroll-Portillo, A., and Lin, H.C. (2023) *Desulfovibrio* in the Gut: The Enemy within? *Microorganisms* **11**: 1772.
Singh, V., Ahlawat, S., Mohan, H., Gill, S.S., and Sharma, K.K. (2022) Balancing reactive oxygen species generation by rebooting gut microbiota. *J Appl Microbiol* **132**: 4112–4129.
Skerman, V., McGowan, V., and Sneath, P. (1980) Approved lists of bacterial names. *Med J Aust* **2**: 3–4.
Sleator, R.D. and Hill, C. (2002) Bacterial osmoadaptation: the role of osmolytes in bacterial stress and virulence. *FEMS Microbiol Rev* **26**: 49–71.
Smith, E.A. and Macfarlane, G.T. (1997) Dissimilatory amino acid metabolism in human colonic bacteria. *Anaerobe* **3**: 327–337.
Smith, M.E., Bekker, M.Z., Smith, P.A., and Wilkes, E.N. (2015) Sources of volatile sulfur compounds in wine. *Aust J Grape Wine Res* **21**: 705–712.
Song, Y., Shin, J., Jeong, Y., Jin, S., Lee, J.K., Kim, D.R., *et al*. (2017) Determination of the genome and primary transcriptome of syngas fermenting *Eubacterium limosum* ATCC. *Sci Rep* **7**: 13694.
Speciale, G., Jin, Y., Davies, G.J., Williams, S.J., and Goddard-Borger, E.D. (2016) YihQ is a sulfoquinovosidase that cleaves sulfoquinovosyl diacylglyceride sulfolipids. *Nat Chem Biol* **12**: 215–217.
Sperandeo, P., Dehò, G., and Polissi, A. (2009) The lipopolysaccharide transport system of Gram-negative bacteria. *Biochim Biophys Acta* **1791**: 594–602.
Spitze, A.R., Wong, D.L., Rogers, Q.R., and Fascetti, A.J. (2003) Taurine concentrations in animal feed ingredients; cooking influences taurine content. *J Anim Physiol Anim Nutr* **87**: 251–262.
Stach, K., Stach, W., and Augoff, K. (2021) Vitamin B6 in health and disease. *Nutrients* **13**: 3229.
Stackebrandt, E. and Ebers, J. (2006) Taxonomic parameters revisited: tarnished gold standards. *Microbiol today* **33**: 152–155.
Stams, A. J M, Van Dijk, J.B., Dijkema, C., and Plugge, C.M. (1993) Growth of syntrophic propionate-oxidizing bacteria with fumarate in the absence of methanogenic bacteria. *Appl Environ Microbiol* **59**: 1114–1119.
Stecher, B. (2015) The roles of inflammation, nutrient availability and the commensal microbiota in enteric pathogen infection. *Microbiol Spectr* **3**: 297–320.
Stewart, J.A., Chadwick, V.S., and Murray, A. (2006) Carriage, quantification, and predominance of methanogens and sulfate-reducing bacteria in faecal samples. *Lett Appl Microbiol* **43**: 58–63.
Struijs, K., Vincken, J., and Gruppen, H. (2009) Bacterial conversion of secoisolariciresinol and anhydrosecoisolariciresinol. *J Appl Microbiol* **107**: 308–317.
Sturman, J.A. (1993) Taurine in development. *Physiol Rev* **73**: 119–147.
Sturman, J.A. and Hayes, K.C. (1980) The biology of taurine in nutrition and development. In *Advances in nutritional research*. Springer, pp. 231–299.
Subramaniam, S. and Fletcher, C. (2018) Trimethylamine N-oxide: breathe new life. *Br J Pharmacol* **175**: 1344–1353.
Sundaravelu, N., Sangeetha, S., and Sekar, G. (2021) Metal-catalyzed C–S bond formation using

sulfur surrogates. *Org Biomol Chem* **19**: 1459–1482.
Suzuki, I. (1999) Oxidation of inorganic sulfur compounds: chemical and enzymatic reactions. *Can J Microbiol* **45**: 97–105.
Szabo, C., Ransy, C., Módis, K., Andriamihaja, M., Murghes, B., Coletta, C., *et al*. (2014) Regulation of mitochondrial bioenergetic function by hydrogen sulfide. Part I. Biochemical and physiological mechanisms. *Br J Pharmacol* **171**: 2099–2122.
Tabatabaei, M., Dehvari, A., Geramizadeh, B., and Niakan, M.H. (2020) Probable role of *Bilophila wadsworthia* in appendicle infection. *Med Lab J* **14**: 29–35.
Takaishi, H., Matsuki, T., Nakazawa, A., Takada, T., Kado, S., Asahara, T., *et al*. (2008) Imbalance in intestinal microflora constitution could be involved in the pathogenesis of inflammatory bowel disease. *Int J Med Microbiol* **298**: 463–472.
Tatusova, T., DiCuccio, M., Badretdin, A., Chetvernin, V., Nawrocki, E.P., Zaslavsky, L., *et al*. (2016) NCBI prokaryotic genome annotation pipeline. *Nucleic Acids Res* **44**: 6614–6624.
Taylor, S.J., Winter, M.G., Gillis, C.C., Silva, L.A. da, Dobbins, A.L., Muramatsu, M.K., *et al*. (2022) Colonocyte-derived lactate promotes *E. coli* fitness in the context of inflammation-associated gut microbiota dysbiosis. *Microbiome* **10**: 1–17.
Teigen, L.M., Geng, Z., Sadowsky, M.J., Vaughn, B.P., Hamilton, M.J., and Khoruts, A. (2019) Dietary factors in sulfur metabolism and pathogenesis of ulcerative colitis. *Nutrients* **11**: 931.
Thompson, M.C., Crowley, C.S., Kopstein, J., Bobik, T.A., and Yeates, T.O. (2014) Structure of a bacterial microcompartment shell protein bound to a cobalamin cofactor. *Acta Crystallogr Sect F Struct Biol Commun* **70**: 1584–1590.
Timmers, P.H.A., Gieteling, J., Widjaja-Greefkes, H.C.A., Plugge, C.M., Stams, A.J.M., Lens, P.N.L., and Meulepas, R.J.W. (2015) Growth of anaerobic methane-oxidizing archaea and sulfate-reducing bacteria in a high-pressure membrane capsule bioreactor. *Appl Environ Microbiol* **81**: 1286–1296.
Tindall, B.J., Rosselló-Móra, R., Busse, H.J., Ludwig, W., and Kämpfer, P. (2010) Notes on the characterization of prokaryote strains for taxonomic purposes. *Int J Syst Evol Microbiol* **60**: 249–266.
Tremaroli, V. and Bäckhed, F. (2012) Functional interactions between the gut microbiota and host metabolism. *Nature* **489**: 242–249.
Tremblay, Y.D.N., Durand, B.A.R., Hamiot, A., Martin-Verstraete, I., Oberkampf, M., Monot, M., and Dupuy, B. (2021) Metabolic adaption to extracellular pyruvate triggers biofilm formation in *Clostridioides difficile*. *ISME J* **15**: 3623–3635.
Unden, G. and Bongaerts, J. (1997) Alternative respiratory pathways of *Escherichia coli*: energetics and transcriptional regulation in response to electron acceptors. *Biochimica et biophysica acta* **1320**: 217–234.
Vasoo, S., Mason, E.L., Gustafson, D.R., Cunningham, S.A., Cole, N.C., Vetter, E.A., *et al*. (2014) *Desulfovibrio legallii* prosthetic shoulder joint infection and review of antimicrobial susceptibility and clinical characteristics of *Desulfovibrio* infections. *J Clin Microbiol* **52**: 3105–3110.
Velasquez, M.T., Ramezani, A., Manal, A., and Raj, D.S. (2016) Trimethylamine N-oxide: the good, the bad and the unknown. *Toxins* **8**: 326.
Vijay, A. and Valdes, A.M. (2022) Role of the gut microbiome in chronic diseases: a narrative review. *Eur J Clin Nutr* **76**: 489–501.
Vizcaíno, J.A., Csordas, A., Del-Toro, N., Dianes, J.A., Griss, J., Lavidas, I., *et al*. (2016) 2016 update of the PRIDE database and its related tools. *Nucleic Acids Res* **44**: D447–D456.
de Vos, W.M. and Nieuwdorp, M. (2013) A gut prediction. *Nature* **498**: 48–49.
de Vos, W.M., Tilg, H., Van Hul, M., and Cani, P.D. (2022) Gut microbiome and health: Mechanistic insights. *Gut* **71**: 1020–1032.
Wade, W.G. (2009) Genus I. *Eubacterium* Prévot 1938,. *Bergey's Man Syst Bacteriol* **3**: 865–890.
Walker, A. and Schmitt-Kopplin, P. (2021) The role of fecal sulfur metabolome in inflammatory bowel diseases. *Int J Med Microbiol* **311**: 151513.
Wang, W., Chen, L., Zhou, R., Wang, X., Song, L., Huang, S., *et al*. (2014) Increased proportions of *Bifidobacterium* and the *Lactobacillus* group and loss of butyrate-producing bacteria in inflammatory bowel disease. *J Clin Microbiol* **52**: 398–406.

Wang, Z., Klipfell, E., Bennett, B.J., Koeth, R., Levison, B.S., Dugar, B., *et al*. (2011) Gut flora metabolism of phosphatidylcholine promotes cardiovascular disease. *Nature*.

Warren, Y. a., Tyrrell, K.L., Citron, D.M., and Goldstein, E.J.C. (2006) *Clostridium aldenense* sp. nov. and *Clostridium citroniae* sp. nov. isolated from human clinical infections. *J Clin Microbiol* **44**: 2416–2422.

Weghoff, M.C., Bertsch, J., and Müller, V. (2015) A novel mode of lactate metabolism in strictly anaerobic bacteria. *Environ Microbiol* **17**: 670–677.

Weiseger, R.A., Pinkus, L.M., and Jakoby, W.B. (1980) Thiol-S-methyltransferase: suggested role in detoxification of intestinal hydrogen sulphide. *Biochem Pharmacol* **29**: 2885–2887.

Wheeler, P.R., Coldham, N.G., Keating, L., Gordon, S. V, Wooff, E.E., Parish, T., and Hewinson, R.G. (2005) Functional demonstration of reverse transsulfuration in the *Mycobacterium tuberculosis* complex reveals that methionine is the preferred sulfur source for pathogenic mycobacteria. *J Biol Chem* **280**: 8069–8078.

Whitfield, C. and Trent, M.S. (2014) Biosynthesis and export of bacterial lipopolysaccharides. *Annu Rev Biochem* **83**: 99–128.

van der Wielen, N., Moughan, P.J., and Mensink, M. (2017) Amino acid absorption in the large intestine of humans and porcine models. *J Nutr* **147**: 1493–1498.

Williamson, M.A. and Rimstidt, J.D. (1992) Correlation between structure and thermodynamic properties of aqueous sulfur species. *Geochim Cosmochim Acta* **56**: 3867–3880.

Wilson, K., Mudra, M., Furne, J., and Levitt, M. (2008) Differentiation of the roles of sulfide oxidase and rhodanese in the detoxification of sulfide by the colonic mucosa. *Dig Dis Sci* **53**: 277–283.

Winter, S.E. and Bäumler, A.J. (2011) A breathtaking feat: to compete with the gut microbiota, *Salmonella* drives its host to provide a respiratory electron acceptor. *Gut Microbes* **2**: 58–60.

Winter, S.E., Lopez, C.A., and Bäumler, A.J. (2013) The dynamics of gut-associated microbial communities during inflammation. *EMBO Rep* **14**: 319–327.

Winter, S.E., Winter, M.G., Ave, O.S., Ca, D., and Butler, B.P. (2011) Gut inflammation provides a respiratory electron acceptor for *Salmonella*. **467**: 426–429.

Wishart, D.S., Feunang, Y.D., Marcu, A., Guo, A.C., Liang, K., Vázquez-Fresno, R., *et al*. (2018) HMDB 4.0: the human metabolome database for 2018. *Nucleic Acids Res* **46**: D608–D617.

Wolf, P.G., Cowley, E.S., Breister, A., Matatov, S., Lucio, L., Polak, P., *et al*. (2022) Diversity and distribution of sulfur metabolic genes in the human gut microbiome and their association with colorectal cancer. *Microbiome* **10**: 1–16.

Wong, J.M.W., de Souza, R., Kendall, C.W.C., Emam, A., and Jenkins, D.J.A. (2006) Colonic health: fermentation and short chain fatty acids. *J Clin Gastroenterol* **40**: 235–243.

Wootton, J.C., Nicolson, R.E., Cock, J.M., Walters, D.E., Burke, J.F., Doyle, W.A., and Bray, R.C. (1991) Enzymes depending on the pterin molybdenum cofactor: sequence families, spectroscopic properties of molybdenum and possible cofactor-binding domains. *Biochim Biophys Acta* **1057**: 157–185.

Worden, J.A. and Stipanuk, M.H. (1985) A comparison by species, age and sex of cysteinesulfinate decarboxylase activity and taurine concentration in liver and brain of animals. *Comp Biochem Physiol Rev* **82**: 233–239.

Wright, D.P., Rosendale, D.I., and Roberton, A.M. (2000) *Prevotella* enzymes involved in mucin oligosaccharide degradation and evidence for a small operon of genes expressed during growth on mucin. *FEMS Microbiol Lett* **190**: 73–79.

Wu, G. (2009) Amino acids: Metabolism, functions, and nutrition. *Amino Acids* **37**: 1–17.

Wu, G. (2020) Important roles of dietary taurine, creatine, carnosine, anserine and 4-hydroxyproline in human nutrition and health. *Amino Acids* **52**: 329–360.

Wu, J.-Y. and Prentice, H. (2010) Role of taurine in the central nervous system. *J Biomed Sci* **17**: 1–6.

Xie, T., Pang, R., Wu, Q., Zhang, J., Lei, T., Li, Y., et al. (2019) Cold tolerance regulated by the pyruvate metabolism in *Vibrio parahaemolyticus*. *Front Microbiol* **10**: 178.

Xing, M., Wei, Y., Hua, G., Li, M., Nanjaraj Urs, A.N., Wang, F., *et al*. (2019) A gene cluster for taurine sulfur assimilation in an anaerobic human gut bacterium. *Biochem J* **476**: 2271–2279.

Xing, M., Wei, Y., Zhou, Y., Zhang, J., Lin, L., Hu, Y., and Hua, G. (2019) Radical-mediated CS bond cleavage in C2 sulfonate degradation by anaerobic bacteria. *Nat Commun* **10**: 1–11.

Yang, D., Elner, S.G., Bian, Z.-M., Till, G.O., Petty, H.R., and Elner, V.M. (2007) Pro-inflammatory cytokines increase reactive oxygen species through mitochondria and NADPH oxidase in cultured RPE cells. *Exp Eye Res* **85**: 462–472.

Yang, D., Liu, X., Xu, W., Gu, Z., Yang, C., Zhang, L., *et al*. (2019) The *Edwardsiella piscicida* thioredoxin-like protein inhibits ASK1-MAPKs signaling cascades to promote pathogenesis during infection. *PLoS Pathog* **15**: e1007917.

Yao, C.K., Muir, J.G., and Gibson, P.R. (2016) Insights into colonic protein fermentation, its modulation and potential health implications. *Aliment Pharmacol Ther* **43**: 181–196.

Yao, C.K., Rotbart, A., Ou, J.Z., Kalantar-Zadeh, K., Muir, J.G., and Gibson, P.R. (2018) Modulation of colonic hydrogen sulfide production by diet and mesalazine utilizing a novel gas-profiling technology. *Gut Microbes* **9**: 510–522.

Yarza, P., Ludwig, W., Euzéby, J., Amann, R., Schleifer, K.H., Glöckner, F.O., and Rosselló-Móra, R. (2010) Update of the All-Species Living Tree Project based on 16S and 23S rRNA sequence analyses. *Syst Appl Microbiol* **33**: 291–299.

Yarza, P., Richter, M., Peplies, J., Euzeby, J., Amann, R., Schleifer, K.H., *et al*. (2008) The All-Species Living Tree project: a 16S rRNA-based phylogenetic tree of all sequenced type strains. *Syst Appl Microbiol* **31**: 241–250.

Yarza, P., Yilmaz, P., Pruesse, E., Glöckner, F.O., Ludwig, W., Schleifer, K.H., *et al*. (2014) Uniting the classification of cultured and uncultured bacteria and archaea using 16S rRNA gene sequences. *Nat Rev Microbiol* **12**: 635–645.

Ye, H., Borusak, S., Eberl, C., Krasenbrink, J., Weiss, A.S., Chen, S.C., *et al*. (2023) Ecophysiology and interactions of a taurine-respiring bacterium in the mouse gut. *Nat Commun* **14**: 5533.

Yonaha, K., Toyama, S., Yasuda, M., and Soda, K. (1977) Properties of crystalline ω-amino acid: pyruvate aminotransferase of *Pseudomonas* sp. F–126. *Agric Biol Chem* **41**: 1701–1706.

Zachmann, M., Tocci, P., and Nyhan, W.L. (1966) The occurrence of γ-aminobutyric acid in human tissues other than brain. *J Biol Chem* **241**: 1355–1358.

Zdych, E., Peist, R., Reidl, J., and Boos, W. (1995) MalY of *Escherichia coli* is an enzyme with the activity of a beta CS lyase (cystathionase). *J Bacteriol* **177**: 5035–5039.

Ze, X., Duncan, S.H., Louis, P., and Flint, H.J. (2012) *Ruminococcus bromii* is a keystone species for the degradation of resistant starch in the human colon. *ISME J* **6**: 1535–1543.

Zeisel, S.H., Mar, M.H., Howe, J.C., and Holden, J.M. (2003) Concentrations of choline-containing compounds and betaine in common foods. *J Nutr* **133**: 1302–1307.

Zeller, T. and Klug, G. (2006) Thioredoxins in bacteria: functions in oxidative stress response and regulation of thioredoxin genes. *Naturwissenschaften* **93**: 259–266.

Zeng, M.Y., Inohara, N., and Nuñez, G. (2017) Mechanisms of inflammation-driven bacterial dysbiosis in the gut. *Mucosal Immunol* **10**: 18–26.

Zhang, J., Liu, Y.X., Guo, X., Qin, Y., Garrido-Oter, R., Schulze-Lefert, P., and Bai, Y. (2021) High-throughput cultivation and identification of bacteria from the plant root microbiota. *Nat Protoc* **16**: 988–1012.

Zhou, Y. and Imlay, J.A. (2022) *Escherichia coli* uses a dedicated importer and desulfidase to ferment cysteine. *MBio* **13**: e02965.

Zhu, W., Winter, M.G., Byndloss, M.X., Spiga, L., Duerkop, B.A., Hughes, E.R., *et al*. (2018) Precision editing of the gut microbiota ameliorates colitis. *Nature* **553**: 208–211.

Zhu, Y., Jameson, E., Crosatti, M., Schäfer, H., Rajakumar, K., Bugg, T.D.H., and Chen, Y. (2014) Carnitine metabolism to trimethylamine by an unusual Rieske-type oxygenase from human microbiota. *Proc Natl Acad Sci* **111**: 4268–4273.

Ziegler, C., Bremer, E., and Krämer, R. (2010) The BCCT family of carriers: from physiology to crystal structurem *Mol Microbiol* **78**:13–34.

Ziegler, E.E. and Filer Jr, L.J. (1996) Present knowledge of nutrition. *International Life Sciences Institute*.

ZoBell, C.E. (1946) Marine microbiology. A monograph on hydrobacteriology. *Mar Microbiol A Monogr hydrobacteriology*.

Zommiti, M., Feuilloley, M.G.J., and Connil, N. (2020) Update of probiotics in human world: a nonstop source of benefactions till the end of time. *Microorganisms* **8**: 1907.

Summary

The primary objective of this thesis is to explore the anaerobic conversion of sulfur-containing compounds and trimethylamine within the human gut. **Chapter 1** presents a literature review summarizing the current state of knowledge regarding human gut bacteria and their involvement in sulfur and trimethylamine metabolism.

Enrichment experiments were conducted to explore sulfidogenic bacteria within the human intestinal tract. Fecal samples from a healthy individual and another diagnosed with irritable bowel syndrome were used for enrichment, employing sulfate or sulfite as electron acceptors along with various electron donors. Additionally, organic sulfur compounds like ox-bile, taurine, and cysteine were included to facilitate respiration or fermentation growth. This research described in **Chapter 2** unveiled that sulfite reduction and cysteine degradation were the primary sulfidogenic processes in the gut microbiome, and the most abundantly enriched bacteria belonged to *Bilophila* and genera within *Clostridium* cluster XIVa. Moreover, two novel bacterial strains were isolated, with strain 2C identified as a novel sulfite reducer, and strain YI as a novel fermentative bacterium capable of tolerating high concentrations of both sulfite and sulfide (both at 5 mM).

In **Chapter 3**, a comprehensive examination of the morphological, biochemical and physiological properties of the isolate led to the description of *Eubacterium maltosivorans* YI^T. This bacterium demonstrated homoacetogenic growth with CO_2 and CO with H_2. Additionally, it displays fermentative capabilities with a range of monomeric sugars and disaccharides, including maltose, yielding acetate and butyrate as primary end products. It also can generate beneficial butyrate and propionate from low energy compounds, as it shows butyrogenic growth from lactate and acetate and propionogenic growth from 1,2-propanediol. Lastly, *E. maltosivorans* exhibits the ability to deaminate quaternary amines (e.g., betaine, carnitine, and choline), resulting in acetate and butyrate production, consequently mitigating the formation of undesirable trimethylamine.

Chapter 4 presents an in-depth analysis through comparative genomic and proteomic studies conducted on *E. maltosivorans*. Its complete genome was sequenced, annotated, and compared with closely related *Eubacterium limosum* species. Both species possess a rich reservoir of methyltransferase family proteins (MttB). Differential proteomics was employed to get insight into the versatile metabolism of *E. maltosivorans*. This strategy identified the

active lactate dehydrogenase, electron-transferring proteins EtfA and EtfB in *E. maltosivorans* to cope with the endergonic lactate oxidation. A complete *lctABCDEF* cluster was identified in this bacteria. Furthermore, during deamination growth with tested quaternary amines (betaine, carnitine, and choline), *E. maltosivorans* abundantly produced a set of 16 TMA methyltransferases. Moreover, the synthesis of proteins related to bacterial microcompartments suggests their potential involvement in the vitamin B12-dependent deamination of these quaternary amines.

In **Chapter 5**, the characterization of *Sporobaculum desulfitilongum* $2C^T$ gen. nov., sp. nov. is described. *S. desulfitilongum* does not utilize various sugars. Sulfite, DMSO and TMAO reduction coupled with pyruvate support great growth of *S. desulfitilongum*, but it cannot reduce sulfate, thiosulfate nor sulfur. Proteome studies identified active sulfite reduction pathway, and pyruvate specific transporters in *S. desulfitilongum*.

Chapter 6 provides a summary of the research, discussing the role of newly isolated anaerobes in sulfur metabolism and shedding light on trimethylamine metabolism insights garnered from this thesis.

List of publications

Y. Feng[1], T. P. N. Bui[1,2], A. J. M. Stams[1,3], S. Boeren[4], I. Sánchez-Andrea[1], W. M. de Vos[1,5] (2022) Comparative genomics and proteomics of *Eubacterium maltosivorans:* Functional identification of trimethylamine methyltransferases and bacterial microcompartments in a human intestinal bacterium with a versatile lifestyle. *Environmental Microbiology* **24(1)**: 517-534.

Y. Feng[1], A. J. M. Stams[1,3], I. Sánchez-Andrea[1], W. M. de Vos[1,5] (2018) *Eubacterium maltosivorans* sp. nov., a novel human intestinal acetogenic and butyrogenic bacterium with a versatile metabolism. *International journal of systematic and evolutionary microbiology* **68**: 3546-3550

Y. Feng[1], A. J. M. Stams[1,3], W. M. de Vos[1,5], I. Sánchez-Andrea[1] (2017) Enrichment of sulfidogenic bacteria from the human intestinal tract. *FEMS Microbiology Letters* **364**: fnx028.

Manuscripts in preparation

A. Beau[6], J. Natividad[7], B. Benoit[6], P. Delerive[7], S. Duboux[8], **Y. Feng**[8], …L. Koppe[6,9]. A specifically designed synbiotic reduces uremic toxin generation via gut microbiota modulations and improves kidney function in experimental chronic kidney disease. Manuscript submitted to *Kidney International*.

Y. Feng[1], A. J. M. Stams[1,3], I. Sánchez-Andrea[1] and W. M. de Vos[1,5]. *Sporobaculum desulfitilongum* gen. nov., sp. nov.: comparative genomics and proteomics of a novel sulfite-reducing and homoacetogenic member of the *Negativicutes* isolated from the human gut.

1. Laboratory of Microbiology, Wageningen University and Research, The Netherlands.
2. Caelus Pharmaceuticals, Amsterdam, The Netherlands.
3. Centre of Biological Engineering, IBB - Institute for Biotechnology and Bioengineering, University of Minho, Portugal.
4. Laboratory of Biochemistry, Wageningen University and Research, The Netherlands.
5. Human Microbiome Research Program, Faculty of Medicine, University of Helsinki, Finland.
6. CarMeN laboratory, INSERM, INRAE, Claude Bernard Lyon 1 University, Pierre Bénite, France.
7. Nestle Health Science, Lausanne, Switzerland
8. Nestlé Research, Lausanne, Switzerland
9. Dept of Nephrology and Nutrition, Centre Hospitalier Lyon Sud

Acknowledgement

"*When I was a child, luxury was fur coats, evening dresses, and villas by the sea. Later on, I thought it meant leading the life of an intellectual. Now I feel that it is also being able to live out a passion for a man or a woman.*"

—Annie Ernaux, Simple Passion

Luxury holds different meanings for different individuals, and it can change for the same person over time. For a long time, luxury for me included delicate clothing, a beach house, working in a leading company with a fancy title and having free time to travel around the globe. During the pandemic, being able to go back to my parents in China was an unrealistic luxury. Upon finishing my thesis, I realized that completing this 'marathon' with the support from three responsible and responsive scientists was a luxury. And my luxury was extended to a great many people—for your support, collaborations, and knowledge, as well as your company.

I would like to thank **Willem**, **Fons** and **Irene** for accepting me as a PhD student to explore the interplay between the microbiome, nutrition, and health with a focus on understanding the bacterial physiology. Throughout my PhD contract, all of you provided quality supervision, guidance, and training. Your support has extended beyond my time at Wageningen, lasting for years after my departure.

Willem, this thesis would not have been accomplished without you. Your consistent check-ins over the years were invaluable. Each interaction with you left me feeling encouraged, reassured, and not alone in navigating the challenges of writing. Discussions about research with you were not only encouraging but also deeply inspiring. Through your guidance, we found out the interesting features of *E. maltosivorans* and writing Chapter 4 with you allowed me to experience the joy of wrapping up and presenting a compelling scientific story. Beyond the scientific training I received from you, the personal lessons were equally profound. Despite your full agenda, you were always on time for meetings and prompt in responding to emails. As a VVIP in the field of microbiology, your humility and commitment to equality are truly admirable. Your robust, clear and efficient style of work has set a model for my career.

Fons, thank you for encouraging me to write and send you one page each day, with the added motivation of a bottle of Swiss white wine if I fail. You always responded quickly with critical comments when I sent my manuscripts, even though I probably owe you a vineyard plus a winery. Thank you for coming to the lab and had meeting with me during my revisit to Wageningen in 2023. I appreciate your efforts in selecting the defense day and keeping track of the submission deadline for me, and I am sincerely thankful for your support and contributions.

Irene, congratulations in advance on the graduation of all your students from MicFys! You are a sharp scientist, a caring and patient supervisor, and a warm mother of two kids. Balancing these diverse responsibilities is challenging, yet you thrived in each role. Thank you for providing comments of my last chapter so robustly despite the challenges of your move. I truly think you possess a magic brush for polishing writing. After relocate several sections in Chapter 4 upon your suggestions, the storyline became clearer. This modification together with

contributions from Willem and Fons, resulted in a direct approval from the reviewers for publication.

Nam, thank you for your contributions in further exploring the versatile character of *E. maltosivorans*. Your commitment to conducting additional growth tests and proteomic analysis within strict and limited working hours during pandemic is truly commendable. Thank you also for sharing your deep knowledge in butyrate-producing bacteria. **Sjef**, you were always available and prompt whenever I had proteomics questions. I highly appreciated your contributions. **Ton van Gelder**, thank you for testing and troubleshooting with Dionex. Your work has played a crucial role in the quantification of sulfite, sulfate, thiosulfate, tetrathionate, DMSO, and TMAO for my thesis. It was also a pleasure to share the office with you, and having conversations about weather forecast and your brewing experiment. **Anja**, you are always so kind, helpful and patient. Thank you for handling paperwork for all foreign PhD students, including me, and also for once again managing my documents for the short revisit to the lab in 2023.

Anna F, Daan and **Lot**, I enjoyed your company in the sulfur family. All of you are persistent and curious scientists, and your achievements have also motivated me. Conversations with you have always been easy, warm, and supportive. **Anna**, reconnecting with you was a great pleasure. I recall your acknowledgment for your thesis in 2017, about telling your grandpa how far you've come, and it's heartening to see you continue to achieve a life you enjoy. I am truly happy for you. **Daan**, I can finally make the joke that I am DONE too! **Lot**, others see you as an assistance professor (congratulations!), in my eyes you are the same warm girl.

Ivette, my PhD first aid, you became my 'The Book of Answers' when I lacked fellow PhDs to discuss administration details. Your support and patience made the final steps of my PhD remarkably smooth. **Iame**, a special thanks for processing and delivering my samples during the stressful pandemic period. Upon my return to Wageningen in 2023, you generously lent me your spare bike, which saved me a significant amount of commuting time and greatly enhanced my mobility. **Max**, thank you for delivering my package to the culture collection.

Diana, thank you for welcoming my short revisit to the lab in 2023. Your voluntary extension of my wur account was immensely helpful. It granted me access to literature and ensured the smooth submission of my thesis. Your leadership maintains a dynamic and inclusive MicFys team. **Emilie**, **Lucas**, **Anna D**, **Tom Schonewille**, **Reinier**, and **Ivette**, it was a delightful summer sharing the office with you. **Anna D**, bumping into you again in the lab was unexpected, but what a small world! Talking with you are always straightforward and enjoyable. **Yehor**, **Anca**, **Maaike** and **Isabelle**, big thanks for the help in the lab; your introduction and assistance made my lab work easier. I'd like to extend my appreciation to **Timon** (for the BBQ), **Adrian** and **Siebe** (for the chats and laughs).

The **Laboratory of Microbiology** stands as a warm multicultural family with many generous hearts. Immersing myself in this inclusive, open, and accepting atmosphere provided me with invaluable experiences beyond scientific training. I enjoyed the Lab BBQs, Lab Trips, Christmas dinners, girls' dinners, and PhD trip with colleagues from **MolEco**, **BacGen** and **SSB**.

The MicFysers of my time —**Peer**, **Nam**, **Susakul**, **Michael**, **Anna F**, **Vicente**, **Lara**, **Samet**, **Monika**, **Jueeli**, **Monir**, **Nikolas S**, **Cata**, **Nico**, **Martijn**, **Daan**, **Lot**, **Sara**, **Ivette**, **Nohemi**, **Irene**, **Cristina**, **Caroline** and **Diana** — it was a pleasure to have each of you on my journey. Our MicFys meetings were filled with critical comments and constructive suggestions, while our MicFys dinners brought cultural delights and personal stories to the table.

A heartfelt thanks to colleagues and friends in **MolEco**, **BacGen** and **SSB**. **Siavash**, **Floor**, **Teresita**, **Romy**, **Lennart**, **Johanna**, **Yannis**, **Prokopis**, **Menia**, **Emmy**, **Nico C**, **Hauke**, **Detmer**, **Clara**, **Erwin**, **Joyshree**, **Prarthana**, **Teunke**, **Ioannis**, **Wen**, **Ruben**, **Niru**, **Kal**, **Rob**, **Linde**, **Maria**, and the list goes on. Thank you all for being there, for your assistance, questions and suggestions, the enjoyable dinners and chats, and sharing a drink or two.

My lab work could have been impossible without the support, assistance, and teaching from the technical team. Thank you **Steven**, **Ineke** (since my master thesis), **Merlijn**, **Sjon**, **Tom van der Weijer**, **Philippe**, and **Wim**. I highly appreciate your efforts in keeping the lab facilities and samples well-organized. Thanks to your dedication, even after 5 years of leaving Wageningen, I managed to locate my well-labelled treasure box containing strain 2C in the -80°C freezer and successfully revive it.

I would give my special thanks to **Jueeli**, **Sudarshan**, and **Alex U** for the fun and chill times we shared during our early days as new, naive PhDs, especially for the dinners and movie nights. **Johanna**, I had many enjoyable activities and parties with you, and I appreciate your relaxing and calm company. Thanks to the Greater China gang in MIB, **Loo Wee**, **Yue**, **Ying**, **Yifan**, **Jie**, **Peng**, **Caifang**, **Chen Z**, and **Dailing**. We not only can enjoy food, laughter, and cultural festivals together, but I deeply appreciate knowing that each of you can be counted on in any emergency situation.

A special acknowledgment goes to the beautiful and cheerful Hispanic group, **Javi**, **Cata**, **Nohemi**, **Ivette**, **Sara**, **Nico**, **Irene**, **Teresita**, and **Juanan**. You brought so many positive vibes both in the lab and after work. Thank you for the encouraging words, great food, wins, hugs and reorganizations. **Cata** and **Javi**, or *batman* and *bastardo*, thanks for your company during the latter part of my PhD journey in Wageningen. Your humour and your attitude of not taking life too serious have definitely eased my stress and depressions. **Cata**, thanks for all the supportive and understanding talks. I am more than happy to see the two of you have built a beautiful family over these years!

Xiaoqian and **Tim**, thanks for accepting my stay in Wageningen back in 2018. On behalf of Baillou, I pass her appreciation for how you and **Molly** took wonderful care of **Inti**. The same compliment goes to **Maarten**, for being a responsible father for **Zaza**. **Bart**, **Arwa**, **Siri**, and **Fady**, I enjoy the company of your family. Thank you for the great food and insightful talks. I extend my great appreciation to **Sara** and **Sven**, along with the lovely **Chalotte** and **Oscar**, for accepting me, twice, to stay at your place for weeks when I was back to Wageningen. Your support made my stay 100 times more convenient and economical. **Sven**, your photos have definitely captured treasurable moments for so many of us, and we all appreciated that.

Dorett and **Basti**, having your thoughtful and punctual spirits as my paranymphs is like having a double set of parachutes. The kickstart meeting for Yuan's defense, initiated by my paranymphs in early January, confirmed my excellent choices. **Dorett**, our friendship started with finding the best coffee on the Wageningen campus, and I am grateful that it has endured through our moves. I appreciate you hosting me for a two-week writing retreat at your place, with unlimited supply of tasty coffee. The change of environment and having a close friend to share my thoughts were invaluable during that time. A big thanks to your assistance in checking my English and attending to small details in important documents. **Basti**, you have a crowded schedule of social life, yet you still pay great and close attention to your friends, despite the physical distance. Thank you for your countless help in bioinformatics, for checking the genome assembly (thanks to **Bart** as well), and for promptly answering my questions. I appreciate your responsiveness in sending me papers upon request. You are a truly dependable friend! It was nice to have you both as part of my Wageningen life, and having you as my **paranymphs** added a great closure.

Beyond the life in Wageningen, I also met a group of fabulous people whose support I consider precious to my PhD journey. **Hanne**, thank you for unlocking me from the hardships of thesis writing, with delicious food and uplifting company. **一星、春月、玥玥、娟姐、纪元**和**杜博文**，谢谢你们在我痛苦的论文写作之路上，听我抱怨并用美食和陪伴给予我快乐。谢谢我在国内长久以来的好朋友**刘一婷**、**靳桢**、**朱玥**和**柳莹**，即使隔着时差和屏幕，与你们聊天也让我感觉近在咫尺。**晓楠**、**李洵**，有幸能在一众中国硕士留学生中和你们成为非常好的朋友，留在荷兰的你们是我想要回去看看的原因之一。

Je tiens à remercier mes amis Montains, **Julie**, **Dane**, **Greg** x2, **Sarah**, **David**, **Julia**, **Arnaud**, **Aline**, **Aurélien, Diane, Xavier**, **Alban** et **Marine**. Benoit et moi sommes ravis d'avoir partagé tous ces moments et notamment avec vous lors des en été et à Noël. **Julie** et **Marine**, merci pour les discussions enrichissantes, pour votre support émotionnel, et ces bon moments au sport. **David**, merci pour ton excellent soutien dans ma recherche d'emploi. Merci à la famille **Sahli** pour leur apport régulier de leur délicieuse bolognaise et champignons sous toute formes de **Hans**, merci pour les petites conversations me permettant de pratiquer mon français avec **Chantal** et **Eléonore**. Quel plaisir de pouvoir se balader dans ce magnifique jardin avec sa vue pittoresque sur le lac et les montagnes. Ce seront toujours des souvenirs inoubliables pour moi.

Annie et **Thierry**, je vous considère tous les deux comme faisant partie de ma famille. Les célébrations de Noël avec vous, **Benoit**, **Cyril** et **Mila** ont créé une atmosphère familiale sincère qui allait au-delà des aspects religieux et commerciaux de la fête aux yeux d'une Chinoise. Merci d'avoir supporté mon comportement de princesse au fil des ans, et je suis reconnaissante de vous avoir auprès de moi. **Annie**, merci pour la délicieuse cuisine et l'aide à la couture. **Thierry**, merci pour ton dévouement à toujours vouloir aider. Tout particulièrement merci à toi et à **Clément** d'avoir fait le déplacement depuis la France, tout spécialement pour déménager de Wageningen à Lausanne. **Annie** et **Thierry** sachez que je vous porte au fond de mon cœur.

Benoit, thank you for your presence and support over the years. We've had our ups and downs, and I feel fortunate that we've made it through together. I appreciate your understanding during my less hardworking and cheerful moments. Thank you for supporting me in your own way

without adding pressure, allowing me to slowly complete my thesis worry-free. I appreciate you making adjustments to many aspects of your life, including but not limited to being more punctual, making plans for activities, learning to make Chinese food and learning Chinese. And to further encourage you, I will write the remaining part in Chinese. 你是个非常善良、真诚、有钻研精神的人，透过你的角度，我也了解到了更丰富多元的世界，谢谢你的陪伴和付出。最后想告诉你，你包的饺子很好看。**Baillou**, my stubborn cute-face cat, aka chouchou mao, thank you for showing your soft belly and giving me kisses every time I give you pâté. I accept that you prefer daddy over me.

最后要写给我的最最亲爱的**妈妈爸爸**。从我选择出国读硕士，到决定留下读博士，再到换一个国家开始工作生活，你们不仅给予了我经济上的支持，更珍贵的是你们的理解，和即使不理解时的包容和接受，特别是妈妈。我非常感谢你们让我有机会体验更多的世界。**妈妈**，你的圆融，善良，耐心，和保持学习的态度是我的榜样。谢谢**翘翘**，**小橘子**和**聚宝**对爸爸妈妈的陪伴。谢谢如同家人的**阿姨**、**叔叔**、**孙麟**和**小融融**。

Now, if you were to ask what luxury means to me, I'd say it's finishing a milestone in my life and starting a new chapter with a light and content heart.

祝大家健康平安

冯媛

Yuan Feng

Wageningen, 20 March, 2024

About the author

Yuan Feng, written as 冯媛 in Chinese, was born on 6th April, 1989, in Nanyang, Henan province, China. She started her bachelor's degree in Animal Sciences at Southwest University, Chongqing, China, in 2006. After completing her degree in 2010, Yuan pursued an eight-month internship at Chia Tai Co. Ltd..

Yuan moved to the Netherlands in 2011 to pursue her master's studies, specializing in Animal Nutrition at the Department of Animal Sciences at Wageningen University. In her master thesis, Yuan explored the relationship between hindgut microbiota and growth performances in poultry, with manipulations on protein sources, butyric acid supplement, and diet structures. This thesis, which was co-supervised by the Department of Animal Sciences and Microbiology, introduced Yuan to the captivating interplay between the microbiome, nutrition, and health. This experience further provided her with the opportunity to do her Ph.D. project from 2014 to 2018, co-supervised by Prof. Willem de Vos, Prof. Fons Stams, and Dr. Irene Sánchez-Andrea, in which she explored novel bacteria related to sulfur and trimethylamine metabolism in the human gut microbiome.

In 2019, Yuan relocated to Switzerland, and from 2019 to 2020 had a role as Associate Specialist in the Technical Microbiology team of Nestlé Research, where she gained experience in prototyping novel food applications with probiotics.

At the moment, Yuan lives in Lausanne, Switzerland and is exploring options for future challenges.

Netherlands Research School for the
Socio-Economic and Natural Sciences of the Environment

D I P L O M A

for specialised PhD training

The Netherlands research school for the
Socio-Economic and Natural Sciences of the Environment
(SENSE) declares that

Yuan Feng

born on 6th of April 1989 in Henan, China

has successfully fulfilled all requirements of the
educational PhD programme of SENSE.

Wageningen, 20th of March 2024

SENSE coordinator PhD education	The SENSE Director
Dr Ir Peter Vermeulen	Dr Jampel Dell'Angelo

The SENSE Research School declares that **Yuan Feng** has successfully fulfilled all requirements of the educational PhD programme of SENSE with a work load of 50.4 EC, including the following activities:

SENSE PhD Courses

- Environmental research in context (2015)
- Research in context activity: Co-organised a 2-day Summer School for SIAM project (2017)

Other PhD and Advanced MSc Courses

- The Intestinal Microbiome and Diet in Human and Animal Science, VLAG (2014)
- Microbial physiology, Wageningen University (2014)
- Bioinformation Technology, Wageningen University (2015)
- SIAM metagenomics course, Nijmegen University (2016)
- SIAM Summer School, Royal Institute for Sea Research (2016)
- Proteomics, VLAG (2017)

Management and Didactic Skills Training

- Board member of SIAM council (2017)
- Teaching practicals for the BSc course "Microbial Physiology" (MIB-20306) (2015 -2018)
- Teaching in the BSc course "Metabolic Engineering" (2017-2018)
- Supervising MSc student with thesis entitled "Characterization of a novel acetogenic bacterium isolated from human faecal sample" (2017)
- Supervising MSc student with thesis entitled "Isolation and characterization of novel sulfidogenic bacteria from the human gastrointestinal tract" (2018)

Oral Presentations

- *Sulfur metabolism in the human gut microbiota.* SENSE PhD trip "Microbiology and SSB in USA" 11th-22nd May 2015, Californian, USA
- *Pitch: Fecal enrichments reveal novel sulfite reducer in the human intestinal tract.* Microbiology Centennial Symposium, 20 October 2017, Wageningen, The Netherlands

The doctoral study program was supported by the Netherlands Ministry of Education, Culture and Science and the Netherlands Organization for Scientific Research through the Soehngen Institute of Anaerobic Microbiology (SIAM) gravitation grant 024.002.002

Financial support from the Laboratory of Microbiology (Wageningen University) for printing this thesis is gratefully acknowledged.

Cover design: Yuan Feng | Fei Wang
Printing: ProefschriftMaken | www.proefschriftmaken.nl